Analysis of growth dynamics of Mediterranean bioenergy crops

Sotiris V. Archontoulis

Thesis committee

Thesis supervisor
Prof. dr. ir. P.C. Struik
Professor of Crop Physiology, Wageningen University, the Netherlands

Thesis co-supervisors:
Prof. dr. N.G. Danalatos
Professor of Agronomy and Applied Crop Physiology, University of Thessaly, Greece

Dr. X. Yin
Assistant professor, Centre for Crop Systems Analysis, Wageningen University

Other members:
Prof. dr. ir. L.E.M. Marcelis, Wageningen University, the Netherlands
Prof. dr. S.D. Koutroubas, Democritus University of Thrace, Greece
Dr. N.P.R. Anten, Utrecht University, the Netherlands
Dr. S. Amaducci, Università Cattolica del Sacro Cuore, Piasenza, Italy

Analysis of growth dynamics of Mediterranean bioenergy crops

Sotiris V. Archontoulis

Thesis
submitted in fulfilment of the requirements for the degree of doctor
at Wageningen University
by the authority of the Rector Magnificus,
Prof. dr. M.J. Kropff,
in the presence of the
Thesis Committee appointed by the Academic Board
to be defended in public
on Monday 3 Oct 2011
at 4 p.m. in the Aula.

Abstract

Archontoulis S.V., 2011. Analysis of growth dynamics of Mediterranean bioenergy crops. Doctorate Thesis, Wageningen University, Wageningen, the Netherlands, with English and Dutch summaries, 235 pp.

In spite of the rapidly growing bioenergy production worldwide, there is lack of field experience and experimental data on the cultivation of bioenergy crops. This study aims to advance crop management operations and modelling studies by providing essential information on phenology, agronomy and crop physiology of three Mediterranean bioenergy crops: *Helianthus annuus* (sunflower), *Hibiscus cannabinus* (kenaf) and *Cynara cardunculus* (cynara). These crops cover a wide range of bio-industrial applications and fit into different cropping strategies. For these crops, we identified the most important knowledge gaps and performed a series of field experiments to fill some of those, particularly for cynara.

Information on phenology and seed yield potential for cynara was missing mainly due to its complex inflorescence structure. This thesis codifies and describes cynara's phenological growth stages according to the universal BBCH coding system. This scale can be used by everyone involved in the production of this crop under all circumstances. In addition, we present a robust allometric model for estimating seed yield under diverse management and environmental conditions. Inputs to the model are two easily quantifiable inflorescence traits: total weight and number of seed-bearing heads per unit area.

Additionally, this thesis investigates factors at leaf, canopy and crop level that determine biomass production for all tested crops and provides key parameters for crop growth modelling. Leaf photosynthesis and respiration rates in response to light, temperature and leaf nitrogen were quantified. Based on such data, a biochemical model for C_3 leaf photosynthesis and an empirical model for respiration were parameterized and validated. Then, to upscale these rates from the leaf to the canopy level, light- and nitrogen extinction coefficients over time and in response to water availability were determined in detail. It was shown that the light extinction coefficient changes under water stress conditions and time of year, while leaf nitrogen only shows a strong vertical distribution within crop canopy during the mid-season. Relevant agronomic data, such as biomass production over time and leaf area index in response to management practices, are also presented for the three crops.

This thesis contributes to the general objective of gaining more insight into bioenergy production from crop species. The findings can help farmers, researchers and modellers to better evaluate agricultural land uses and to improve biomass quantity and quality. Among the studied species, the perennial cynara shows the greatest potential for energy production in the Mediterranean region because a significant part of the production is achieved in the winter–spring period relying on natural rainfall.

Key words: cynara, kenaf, sunflower, phenology, agronomy, crop physiology, modelling, biomass production, crop growth, growth stages, BBCH code, seed yield, oil/seed ratio, leaf area index, leaf nitrogen, light and nitrogen extinction coefficients, photosynthesis, respiration, respiration acclimation, bioenergy, Greece, Mediterranean region.

Dedicated to my parents

(*Αφιερώνεται στους γονείς μου*)

Preface

This thesis is a step towards understanding bio-energy production from crop species. The research idea was formulated during my MSc studies on crop science, which after almost five years of work on literature review, field and laboratory experimentation, data analysis, and results presentation, yielded this thesis. Many people contributed to this thesis, directly or indirectly, to whom I would like to express my sincere gratefulness.

Firstly, I am heavily indebted to all my supervisors (Picture 1) for their overall contribution and especially to Professors dr. Paul Struik and dr. Nicholas Danalatos who created funds for this study.
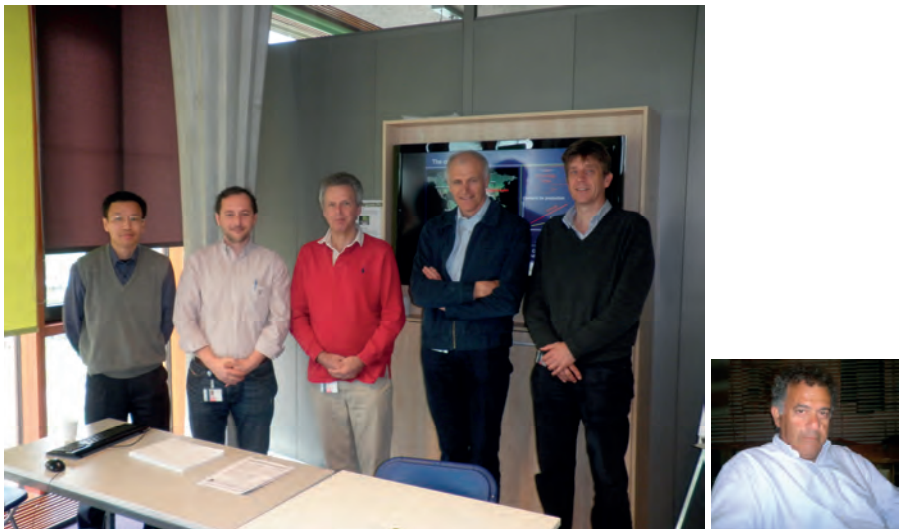
Picture 1: PhD project team, direction from left to right: Xinyou Yin, Sotiris Archontoulis, Paul Struik, Jan Vos, Lammert Bastiaans, and Nicholas Danalatos. They all deserve to be acknowledged for their roles, but Wageningen University rules do not allow to have them all as (co-)promotors.

I am deeply grateful to my promotor and main supervisor Prof. dr. Paul Struik for his excellent guidance during this PhD study. Working with Paul (since 2005 including MSc studies) I learned that I must look after every detail; to be precise and concrete. Paul's detailed comments in my draft manuscripts improved considerably my ability to write scientific papers while his overall efforts guaranteed high quality of this thesis. Paul, thank you for your prompt –always within few hours!– and very informative responses to all my queries, for editing the manuscripts,

for your helpful suggestions during our project meetings, for your wise advices about my future career and also for your worthy letters on getting fellowships and solving administrative issues. It was a great honour and pleasure to be member of your group, and I honestly wish to work with you again in the future!

I am really thankful to my co-promotor and supervisor Prof. dr. Nicholas Danalatos for his overall input and drive from my BSc towards the PhD studies. I am working with Nicholas since 2000 and I consider him as my "big brother" because he was always next to me, any time of the day, providing ample scientific knowledge and vital advices for my life. Nicholas thanks for your friendship, for your critical comments and views on my research work, for our discussions which were always a continuous source of inspiration for me and also for your motivation to continue my MSc and PhD studies at Wageningen University. Now I can realize the value of your advice!

Dr. Jan Vos, Dr. Xinyou Yin and Dr. Lammert Bastiaans, the co-supervisors from CSA, had a vital role in this PhD project and I am very indebted to them.

Dr. Jan Vos was my first teacher at Wageningen University and I learned a lot from his very interesting lectures in the 'Crop Ecology' course. Jan was instrumental in the crop physiological meta-analysis of the data. Jan, thanks for your challenging suggestions during our project meetings, for your very helpful comments on my draft manuscripts and especially for your key-words (e.g. BBCH). Sometimes it took me hours or days to interpret those, but once I did, the papers were easier formulated. Jan, I am not going to forget that in modern life every split second counts!

Dr. Xinyou Yin research work inspired me. Actually, much of my research was designed to feed his crop model (GECROS). Working with Xinyou I learned to seek for biological answers, to develop biologically meaningful parameters and I advanced my skills in modelling. Xinyou, thanks for your stimulating ideas which were very useful for setting up the experimental plan and for analysing the datasets, and for your valuable comments on the draft manuscripts. Without your help, I would have never been able to go so deeply into the understanding and modelling of photosynthesis. Xinyou, I wish to see GECROS running for bioenergy crops soon!

The contribution of dr. Lammert Bastiaans during the initial phases of my PhD was dominant because he taught me how to put my ideas in a logical and appropriate order. This is the root for a good research, perhaps sounds easy but it is not. Lammert, thanks also for your positive and very helpful comments during our team meetings and on my draft manuscripts.

Contents

Chapter 1

General introduction

Abstract

This chapter provides an overview of renewable energy sources, with particular emphasis on bioenergy production. Options to increase bioenergy production from plants are addressed and knowledge gaps are highlighted. The aim of the thesis, the methodological framework and an overall thesis structure are outlined in this chapter.

Drivers for renewable energy production

By 2050, the world population is likely to be 9.1 billion, the atmospheric CO_2 concentration 550 ppm, the ozone concentration 60 ppb, the climate warmer by *ca* 2°C (Jaggard *et al.*, 2010) and the fossil fuel reserves most likely will be depleted (Saidur *et al.*, 2011a). This indicates that measures must be taken to satisfy future population needs, i.e. increase food and energy production, and to protect our environment. So far, energy has received the most attention. This is because: (1) fossil fuels – oil, coal-lignite and natural gas – currently dominate the world energy economy, covering more than 80% of the total primary energy supply worldwide (Fig. 1.1a; Heinimo & Junginger, 2009); (2) energy consumption is increasing much faster than the increase in population (Hein, 2005; Sims *et al.*, 2006); (3) energy use is by far the most important source of environmental pollution, i.e. oil and gas fired power stations contributed almost 60% to greenhouse gas emissions in EU-27 in 2007 (Eurostat, 2010); (4) there is a desire to reduce dependency on fossil fuel imports, i.e. in 2007 55% of the total energy consumed in the EU-27 was imported, and it was predicted that this could rise to 70% if measures were not taken to increase domestic energy supplies (Eurostat, 2010; Magar *et al.*, 2011); and (5) the political cost of the high oil prices and the saturated markets for the agri-products (Ohlrogge *et al.*, 2009; Banse *et al.*, 2011).
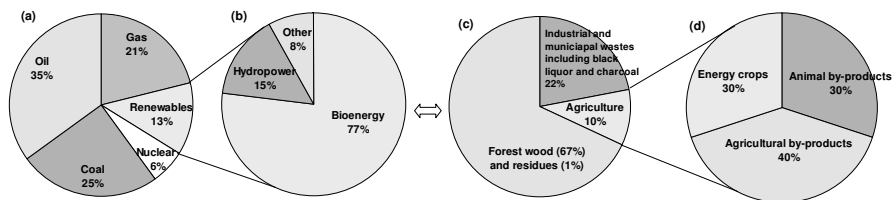
Figure 1.1: Panels *a* and *b* illustrate the breakdown of the primary energy sources (oil, coal, gas, nuclear and renewable) and of the renewable energy sources (biomass, hydropower, and others including geothermal, wind and solar energy), respectively. Panel *c* illustrates the different biomass sources for bioenergy production and panel *d* indicates the contribution of energy crops to bioenergy production. Data are retrieved from IEA Bieonergy (2009) and refer to global level (2005/2006).

Favourable policies and international climate agreements (e.g. Kyoto Protocol) promoted a rapid growth of renewable energy sources over the last decade (see an overview by Lychnaras & Scneider, 2011). For instance, the latest EU directive (2009/28/EC) highlighted: (1) raise the share of renewable energy to 20%; (2) increase the level of liquid biofuels in transport sector to 10% by 2020 (in addition to liquid biofuels, renewable electricity for trains and electric cars will be

taken into account); (3) reduce greenhouse gas emissions by at least 20% compared to 1990; and (4) improve energy efficiency by 20%.

These targets had a strong impact on society. Indeed, over the last decade, scientific research on renewable energy (particularly bioenergy) increased exponentially (Fig. 1.2; and Romo-Fernandez *et al.*, 2011), investors tremendously increased the number of energy processing plants (AEBIOM, 2008), and farmers incorporated bioenergy cultivations into their farms (Christou *et al.*, 2010). However, currently the contribution of renewable energies to total energy supply is still small (Fig. 1.1a), although trends show a stable annual increase (Eurostat, 2010).

The world's current total primary energy supply is about 510 EJ per year (1 EJ=10^{18} Joule) and expected to reach 600–1000 EJ by 2050 (IEA Bioenergy 2009; IEA, 2010). Renewable energy sources accounted for 13% (60 EJ) of this (Fig. 1.1a). In EU-27, primary energy production totalled 849.6 million *toe* (tonnes of oil equivalent) in 2007 (1 *toe* = 48.87 GJ; 1 GJ =10^9 Joule) (Eurostat, 2010). In Europe, production of renewable energy sources accelerated (Table 1.1), with biomass to be the most important source (Fig. 1.1b; Table 1.1).
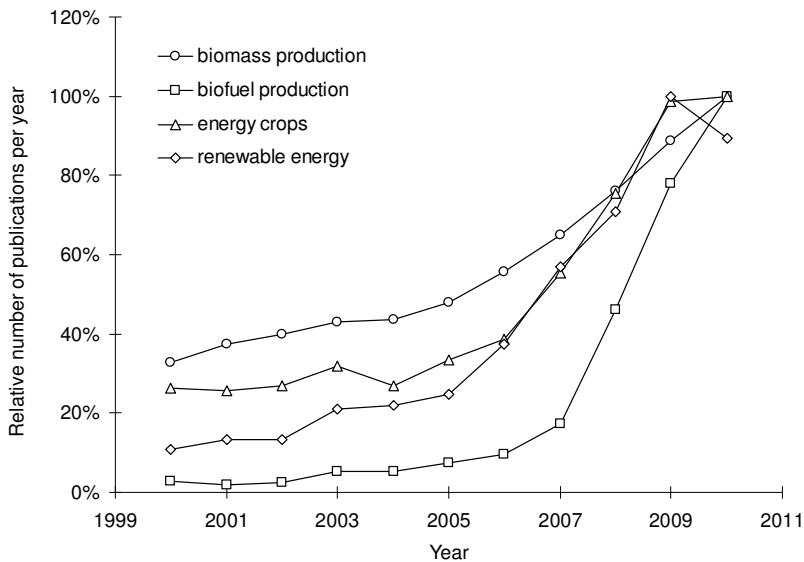
Figure 1.2: Relative number of publications per year found in ISI Web of knowledge (assessed on 2nd of May 2011) using the following keywords: biomass production, biofuel production, energy crops and renewable energy. The corresponding total number of publications appeared for the above keywords were 40440, 2205, 3684 and 14681, respectively. Relative values (%) calculated by dividing the actual year value with the maximum value for each keyword.

Table 1.1: Primary production and distribution of renewable energies in EU countries

	Production (1000 *toe*[1])		Share of total, 2007 (%)				
	1997	2007	Solar energy	Biomass & waste	Geothermal energy	Hydropower energy	Wind energy
EU-27	92390	138831	0.9	69.3	4.2	19.2	6.5
Belgium	633	1273	0.4	93.4	0.2	2.6	3.3
Bulgaria	488	995	–	71.5	3.3	24.8	0.4
Germany	7712	28121	2.1	78.7	0.4	0.1	19.3
Greece	1340	1677	9.5	67.0	0.8	6.4	12.1
Spain	6737	10288	1.3	52.4	0.1	23.2	23.0
France	17646	18645	0.2	70.2	0.7	27.1	1.9
Italy	8412	11901	0.5	30.9	42.0	23.7	2.9
Netherlands	1547	2496	0.9	86.9	–	0.4	11.9
Austria	5985	7839	1.4	56.5	0.4	39.5	2.2
Finland	6752	8589	0.0	85.6	0.0	14.2	0.2
Sweden	13774	15639	0.1	62.8	0.0	36.4	0.8
UK	2071	4368	1.1	78.5	0.0	10.0	10.4

(source: Eurostat, 2010)

Energy from biomass

Globally, bioenergy represented 10.4% (50 EJ or 1023 million *toe*) of the world primary energy use in 2005/2006 (Sims *et al.*, 2006; IEA Bioenergy, 2009; Yusuf *et al.*, 2011).

The total biomass production possible is debatable, with estimates up to 700 EJ, but in most cases between 150 and 500 EJ per year, indicating that plants are grossly under-explored (Jurginger *et al.*, 2006; Tilman *et al.*, 2006; de Vries *et al.*, 2007; Campbell *et al.*, 2008; Dornburg et al., 2008; Wise *et al.*, 2009; Haberl *et al.*, 2010; Beringer *et al.*, 2011). Residues from forests and agricultural and other organic wastes can provide 50–150 EJ per year, while the remaining would come from energy crops, surplus forest growth, and increased agricultural productivity (IEA Bioenergy, 2009; see also Table 2 in Heinimo & Junginger, 2009). By including production constrains like irrigation water, sustainability criteria and impact of climate change on crop production, Beringer *et al.* (2011) recently estimated global biomass production potentials as moderate as 126 to 216 EJ by 2050. Bioenergy crops comprised 15 to 27% of this potential.

In EU-27, biomass accounted for 70% of the renewable energy production or 11.3% of total primary energy production in 2007 (Table 1.1). In US, biomass

---

[1] *toe* = tonnes of oil equivalent. 1 *toe* = 48.87 GJ = 48.87 × 10^9 Joule

accounted for 50% of the renewable energies in 2009 (Boundy *et al.*, 2010). Based on present technological achievements, bioenergy has the following advantages compared to other renewable energies:

$\Rightarrow$ biomass raw materials come in a wide range of forms (crops, trees, residues, organic waste and animal manure) which are abundant in most parts of the world while wastes will always exist (EUR 21350, 2005; Saidur *et al.*, 2011b);

$\Rightarrow$ biomass is a versatile fuel that can be converted using existing technology to different types of fuels like solid, liquid and gaseous, satisfying different needs;

$\Rightarrow$ all products that currently results from the processing of petrochemicals can be produced from biomass feedstock (Sims *et al.*, 2006; Christou *et al.*, 2010; Yusuf *et al.*, 2011);

$\Rightarrow$ bioenergy is recognized as being carbon-neutral, significantly reducing the amount of carbon dioxide in the atmosphere compared with burning fossil fuels (Menichetti & Otto, 2009; Magar *et al.*, 2011). For instance, net carbon emissions from generation of a unit of bioenergy are 10 to 20 times lower than emissions from fossil fuel-based generations (Sims *et al.*, 2006);

$\Rightarrow$ bioenergy production and processing promotes regional economic development for farmers and society with alternative new employment positions;

$\Rightarrow$ bioenergy promotes energy stability (reduced dependence on short-term weather changes compared to wind and photovoltaic systems);

$\Rightarrow$ biomass has fewer problems with energy storage compared to wind and photovoltaic systems (Saidur *et al.*, 2011b)

$\Rightarrow$ biomass plantations, if managed well, may actually increase biodiversity (Semere & Slater, 2007; Baum *et al.*, 2009) and soil qualities (Tilman *et al.*, 2006), at least on previously degraded land. Sims *et al.* (2006) provided a list with additional social, environmental, and economic benefits of bioenergy.

On the other hand there are some concerns about bioenergy. This is because biomass plantations require land, water and nutrients. If not managed correctly, the large-scale cultivation of biomass plantations and a substantial utilization of residues from agriculture and forestry, may increase greenhouse gas emissions, environmental degradation, and may introduce new risks for food security (Beringer *et al.*, 2011). For example the water requirements of energy derived from biomass is about 70 to 400 times more than those for energy derived from fossil fuels, wind and sun (Gerben-Leenes *et al.*, 2008). More than 90% of the water needed is used in the production while a small amount is used in the processing of biomass (Berndes, 2002; De Fraiture & Berndes, 2009).

Table 1.2: Meteorological characteristics of five climatic zones and possible energy crops including short rotation coppice (SRC) of trees for Europe (adapted from Krasuska *et al.*, 2010)

Climatic zone	Rainfall (mm)		Temperature (°C)		Months
	Oct–Apr	May–Sep	Min	Max	Temp < 0°C
Nemoral [a]	309.8	310.8	2.4	9.3	4.6
Continental [b]	380.9	393.4	4.2	13.1	4.1
Atlantic [c]	662.1	393.7	5.4	12.4	1.1
Lusitanian [d]	851.5	321.7	8.4	17.4	0.0
Mediterranean [e]	474.0	166.3	9.7	19.4	0.2

Table 1.2 continued

Climate zone	EU country [f]	Energy crops and SRC (alphabetical order)
Nemoral	EE, FI, LV, LT, PL, SE	flax, poplar, rapeseed, reed canary grass, willow
Continental	AT, BE, BG, CZ, DK, DE, HU, LT, LU, PL, RO, SK	flax, maize, miscanthus, poplar, rapeseed, sorghum, sugarbeet, sunflower, willow
Atlantic	DK, DE, IE, NL, UK, BG, FR,	flax, hemp, miscanthus, poplar, rapeseed, sugarbeet, switchgrass, willow
Lusitanian	FR, PT, ES	eucalyptus, hemp, maize, miscanthus, poplar, rapeseed, sorghum, soybean, sugarbeet, sunflower, willow
Mediterranean	FR, GR, IT, PT, ES	cynara, ethiopian mustard, eucalyptus, flax, giant reed, kenaf, maize, miscanthus, poplar, rapeseed, safflower, sorghum, soybean, sugarbeet, sunflower

[a]: Nemoral covers the lowlands and undulating plains of south Scandinavia and the north-west of the Russian Plain including the Baltic countries.

[b]: Continental is mostly on the plains and lowlands of central and eastern Europe and uplands and low mountains of the Balkan peninsula, lowlands, valleys and mountain peripheries on the middle- and lower-Danube Plains, and the Black Sea.

[c]: Atlantic covers Britain, Ireland, western coast of Scandinavia, and lowlands and plains of Jutland, north and west Germany, north and central France, Belgium, and the Netherlands.

[d]: Lusitanian covers from west Atlantic coast of France to the North Atlantic coast of Spain and the North Atlantic coast of Portugal.

[e]: Mediterranean covers the whole Mediterranean basin

[f]: EE = Estonia, FI = Finland, LV = Latvia, LT = Lithuania, PL = Poland, SE = Sweden, AT = Austria, BE = Belgium, BG = Bulgaria, CZ = Czech Republic, DK = Denmark, DE = Germany, HU = Hungary, RO = Romania, SK = Slovak Republic, IE = Ireland, NL = Netherlands, UK = United Kingdom, FR = France, PT = Portugal, ES = Spain, GR = Greece, IT = Italy

Biomass sources and biofuel types

There are three main sources of biomass: (1) the purpose-grown energy crops and trees; (2) harvest and process residues from forest and agriculture; and (3) organic wastes including animal manure and municipal wastes.

Biomass can be converted by a variety of processes to a wide range of products: (1) solid biofuel including chips, pellets and briquettes; (2) liquid biofuel including bioethanol and biodiesel; (3) gaseous biofuel (biogas); and other bio-products like bio-plastics, lubricants, etc. In literature the terms bioenergy and biofuel are misused (Karp & Shield, 2008). In this thesis, bioenergy is a generic term that includes all types of biofuels, while the term biofuel with the word solid or liquid or gaseous in front refers to a specific bioenergy product.

Solid biofuels are mainly used for heating and power generation, liquid biofuels for transportation, and gaseous biofuels for all. However, use of solid biofuel in transport sector is currently possible (viz. electrical trains and cars; Ohlrogge *et al.*, 2009).

Energy crops and short rotation forestry

Presently energy derived from dedicated bioenergy crops is small (Fig. 1.1c, d), but in future years is expected to make up most of the total biomass potential. The choice for the most suitable energy crop to grow is complex and relies on many factors like soil-climate conditions (e.g. Table 1.2), market availability, harvesting and transportation issues, etc. Below, I categorize energy crops and short rotation trees in six major categories based on structural composition, conversion technology and bioenergy use:

(1) Woody lignocellulosic plants like poplar, willow and eucalyptus for production of wood-chips, pellets or bioethanol based on 2nd generation crop/fuel chains[2];

(2) Herbaceous lignocellulosic plants like miscanthus, switchgrass, cynara, fibre sorghum, and kenaf for production of agro-pellets, biogas or bioethanol based on 2nd generation crop/fuel chain;

---

[2] First, second and third generation biofuels are crop/fuel chains based on existing (from sugar, starch and oil crops), developing (from lignocellulosic feedstock) and on emerging / future conversion technologies (including hydrogen production from biomass or biodegradable waste), respectively. Source: Karp & Shield *et al.*, 2008.

(3) Oil crops like rapeseed, oil palm, sunflower and soybean for biodiesel production based on 1st generation crop/fuel chain and agro-pellets production by using crop residues;

(4) Sugar crops like sugarcane, sweet sorghum and sugarbeet for bioethanol production based on 1st or 2nd generation crop/fuel chain;

(5) Starch crops like wheat, rye, triticale and maize for agro-pellets using crop residues and bioethanol production based on 1st generation crop/fuel chains;

(6) Leguminous plants and grasses can be processed together with manure or waste to produce biogas for heat, electricity or fuel.

Some energy crops are multi-purposed with various applications (e.g. *Cynara cardunculus*). In EU, bioenergy production from crop species initiated with the utilization of the traditional annual crops like rapeseed, wheat, barley and maize, for liquid biofuels. However, recent studies indicated that (1) practices to convert food-product carbohydrates or plant oils into ethanol and biodiesel have only limited, if any, capabilities to curb emissions (Crutzen *et al.*, 2008; Fargione *et al.*, 2008); (2) direct competition with food production for the most fertile lands (Searchinger *et al.*, 2008; Melillo *et al.*, 2009; Lapola *et al.*, 2010); and (3) lower benefits compared to perennial crops (e.g. miscanthus, willow) in terms of production costs, agrochemical and fertilizer inputs, adaptability and productivity in low fertile soils, and carbon sequestration (Venturi & Venturi, 2003; Lemus & Lal, 2005; Sartori *et al.*, 2006; Sims *et al.*, 2006; Beringer *et al.*, 2011).

At a global level, sugarcane, oil palm, rapeseed, and to a much lower extent miscanthus, poplar, willow and eucalyptus comprise the dominant energy cultivations. In EU-27, rapeseed is the leading crop for biodiesel production (followed by sunflower), while miscanthus, willow and poplar are currently used for solid or gaseous biofuels production (Christou *et al.*, 2010). Of course there are several other crops that are currently tested at a large scale, e.g. cynara (Gominho *et al.*, 2011).

Harvest and process residues from agriculture and forestry

Direct use of forest trees or indirect use of forest residues constitutes the major source for solid biofuel production (e.g. wood-pellets; Fig. 1.1c). In general, the demand for wood-pellets has increased considerably in recent years, e.g. pellet consumption in Sweden increased by 240% from 1997 to 2006, causing shortage of the "traditional" raw materials such as sawdust and wood shavings, indicating therefore a need for further exploitation of the agricultural residues and/or crops (Nilsson *et al.*, 2011).

Organic wastes

Municipal and industrial solid and liquid wastes comprise a supplementary but significant source of biomass (~22%; Fig. 1.1c). Approximately each EU citizen produces on average 500 kg of municipal waste per year, which yields 225 million tonnes of municipal waste per year (EUR 21350, 2005). Typically, municipal waste has a heating value of 8–12 MJ kg^{-1}, meaning that from one tonne of municipal waste 2 GJ electricity can be produced, which should not be neglected.

Solid biofuels: chips, pellets and briquettes

In the EU-27, primary energy production from solid biomass yielded 69 million *toe* in 2008, increased by 48% since 1995, i.e. the year in which the European White Paper on renewable energies was adopted (Christou *et al*., 2010). In 2008, more than 440 pellet plants were operated in Europe. Its number is increasing continually due to the dynamic market development, while its production capacity is 7.5 million tonnes of pellets per year, providing therefore a reliable renewable energy supply (AEBIOM, 2008). The energy content of wood pellets is about 17 GJ per tonne dry biomass having a density of 650 kg m^{-3}. To replace oil, one needs about three times its volume in pellets.

Liquid biofuels: biodiesel and bioethanol

Transport biofuels (bioethanol ~21 MJ L^{-1} and biodiesel ~34 MJ L^{-1}) are currently the fastest growing modern bioenergy sector, receiving a lot of public attention. Presently, they represent 1.5% of total road transport fuel consumption and 2% of bioenergy (IEA Bioenergy, 2009). However, to meet the demand for road transport fuel, biofuel production is expected to increase by a factor 10 to 20 by 2030, which corresponds to a 6–8% average annual growth rate (IEA Bioenergy, 2009). There are also different views, i.e. biofuels can make only a modest contribution to future transport sector (~10%; Connor & Hernandez, 2009).

In EU-27 liquid biofuels contributed 12 million *toe* to bioenergy (~13%) in 2008 and showed a remarkable growth rate over the last decade (Eurostat, 2010). Biodiesel represented 79.5% of biofuels dedicated to transport (2.6% of total transport fuel; Fischer *et al*., 2010a), far ahead from bioethanol (19.3%). For biodiesel, rapeseed is the principal feedstock followed by sunflower, while some 120 biodiesel plants are currently operating in Europe (Christou *et al*., 2010). For bioethanol cereals (~70% in 2008) and to a lesser extent sugar crops are currently used in Europe.

Gaseous biofuels: biogas

Biogas is produced from a variety of organic wastes, including plant straw, through gasification. Chemically biogas comprises a mixture of hydrocarbons (mainly methane) and other gases (Yuan *et al.*, 2008). In EU-27 biogas production contributed 7.5 million *toe* (~7.8%) to bioenergy in 2008 (Eurostat, 2010). Biogas has a calorific value 6 kWh m^{-3} (1 kWh = 3.6 MJ) that corresponds to about half a litre of diesel oil.

Bioproducts

Any consideration of biomass for energy purposes would be incomplete without a reference to its use for non-energy products. All products that currently result from the processing of petrochemicals can be produced from biomass feedstock (Sims *et al.*, 2006). These include traditional plant-based products like oils, starch, textiles, pharmaceutical products (vaccines) or others like lubricants, polymers additives, high matrix composites, biodegradable plastics, paints, surfactants, etc. Christou *et al.*, 2010). Sims *et al.* (2006) put forward the view that energy crops may become more economic if high value products are first extracted from the plants and the remaining are used for lower value energy production.

Options to increase bioenergy production

To meet ambitious future targets, energy production from all renewable sources must increase further. In terms of bioenergy, it was estimated that about 230–250 million *toe* are needed for Europe by 2020 (Ragwitz *et al.*, 2005; AEBIOM, 2010; Christou *et al.*, 2010). This means that bioenergy production should more than double in the following 13 years (from 96.2 million *toe* in 2007; Table 1.1). A key question addressed in several studies is how bioenergy production can be increased in an economical and sustainable manner without causing major distortions in the food, feed and other markets (Connor & Hernandez, 2009; Christou *et al.*, 2010; Krasuska *et al.*, 2010; Beringer *et al.*, 2011; Mueller *et al.*, 2011).

In previous sections of this chapter, all possible biomass sources for energy production were reviewed and their potentials were given. It became clear that forest wood and wood residues (sawdust, wood shavings) that presently comprise the major bioenergy contributor (Fig. 1.1c; AEBIOM, 2008) have already reached a near saturation point (Nilsson *et al.*, 2011). Thus options to further explore wood will probably no longer yield much gain. On the other hand there are reports indicating that there are large amounts of unexplored biomass, e.g. tree pruning, but in those cases exploitation is constrained by logistical issues. Municipal and industrial wastes comprise an important source (Fig. 1.1c) but

options to increase bioenergy from wastes are through better utilization efficiency.

Obviously, a substantial increase in bioenergy must come from agricultural crops and residues, which at present have a small contribution (Fig. 1.1c and d; Heinimo & Junginger, 2009) but a large potential (see earlier section). A number of reasons including public acceptability, food security, and agronomic and ecological issues were responsible for the low contribution of energy crops so far. However, as mentioned earlier, the favourable policies, the high oil prices, the saturated markets for the agro-products (Banse *et al*., 2011) and the rapid growth of the international bioenergy trade and market (AEBIOM, 2008; Saidur *et al*., 2011a) helped to overcome many issues. In a recent survey (Magar *et al*., 2011), it was found that bioenergy is viewed quite favourably in the EU and bioenergy use is publicly accepted.

Options to increase bioenergy production from agriculture are: to increase crop area and/or crop yields and to employ more efficient extraction and conversion methods, i.e. second or third generation crop/fuel chains. The global Scientific Committee on Problems of the Environment (SCOPE) announced that countries can find solutions, but at a global level, expansion of bioenergy production from agriculture must be achieved in the context of a 50% increase in food production by 2030 (Connor & Hernandez, 2009). This means that a sustainable increase in bioenergy production must come firstly from a greater productivity of the existing arable land and secondly by increasing crop land. This view is also supported by many others, while for example Karp & Shield (2008) stated that it will be a challenge to elevate energy crop yields further; unlike the yield advances in food crops, this increase must be achieved without significantly increasing the input requirements.

Another way to increase bioenergy consumption in EU-27 is by increasing modern biofuel imports but this is not a viable option. At global level, to achieve bioenergy targets in the longer term, government policies and industrial efforts need to be directed at increasing biomass yield levels and modernising agriculture in regions such as Africa, and Latin America, thus directly increasing global food production and the resources available for biomass utilization (IEA Bioenergy, 2009).

Expansion in crop land: Europe

In the EU approximately 150 million ha are covered by forests and some 180 million ha are devoted to agricultural activities (60% arable crops). Finding land for growing energy crops is an important issue, but not as catastrophic as has been presented by the media. Cultivation of non-food crops like cotton, flax, hemp, etc., has a long tradition in Europe and sometimes occupied considerable

areas of land. In recent years, the surplus of food production drove policy-makers to support set-aside policies, i.e. in 2001 some 5.7 million ha of crop land was left fallow (EUR 21350, 2005).

According to Krasuska *et al*. (2010) up to 13.2 million ha (~7.3% of EU crop land) have not been used for food or feed production over the period 2003–2007 (the 80% of this land was fallow land). The same authors estimated that some 20.3 million ha (theoretical area) could be available for cultivation of non-food crops (including bioenergy) in Europe by the year 2020. In 2008, some 3 million ha (~1.6% of EU crop land) of energy crops were grown in EU-27. Obviously, this proportion was not enough to have any effect on food production or prices (see additional arguments by Mueller *et al*., 2011).

Future projection studies indicated that in order for Europe to reach 2020 targets, the area devoted to energy crops should expand to 18–25 million ha (~12% of EU crop land; approximately 15 million ha crops for biodiesel; 5 million ha for biogas and 5 million ha for solid biofuel; EEA, 2006; Jossart, 2009; Ozdemir *et al*., 2009; AEBIOM, 2010; Christou *et al*., 2010). Other studies predicted that this area will need to be 20.5 million ha by 2020 and 26.3 million ha by 2030 (Krasuska *et al*., 2010) or 44–53 million ha by 2030 (Fischer *et al*., 2010b). Although above estimates gave a preliminary indication about the future land use, they were based on limited information regarding the crops' adaptability and productivity issues and on a number of unwarranted assumptions (e.g. effects of climate on crop production). Nevertheless, all agreed that central and eastern European countries like Bulgaria, Poland, Romania and the Czech Republic will play a very significant role in the near future (van Dam *et al*., 2008).

Improve energy crop yields

To improve biomass yields, combined efforts should be made from different research areas such as biotechnology, genetics, agronomy, and engineering. Progress so far is extremely slow because the importance of energy crops was underestimated in previous years (EUR, 2006). Dedicated energy crops are largely undomesticated (have not undergone the centuries of improvement that characterize major food crops) with large yield variability (Zegada-Lizarazu *et al*., 2010). This indicates that large gains can be expected over the next few decades via breeding programmes, e.g. long-term breeding of switchgrass in US has produced large yield gains (Sims *et al*., 2006). Some of the preferable traits for improvement are: radiation interception; photosynthesis, light, water and nutrient use efficiencies; etc. (Sims *et al*., 2006; Karp & Shield, 2008). Emerging advanced approaches, like new biotechnological routes with genetically modified plants and/or a systems biology approach can also help in improving yields. Currently such information exists only for poplar.

Another way to explore further and improve yields of energy crops is by using crop simulation models, via the selection of the best management techniques and the identification of the most suitable areas for cultivation. Such models are powerful tools for investigating potential and actual growth under different conditions. A number of growth models have been developed for annual and perennial crops (van Ittersum *et al*., 2003; Yin & van Laar, 2005; see also Table 5 in Karp & Shield, 2008), which vary in their degree of empiricism and number of parameters affecting yield. Empirical models are very useful in helping to predict yield at different sites. However, from the viewpoint of target traits process-based models are more informative. If models are robust and their parameters characterize genotypes, the models can be used to test different hypotheses concerning the importance of altering different traits. In this context, more research on agronomy and crop physiology is needed to parameterize these models for new energy crops (Karp & Shield, 2008). The recent crop growth model for miscanthus is a good example (Hastings *et al*., 2009).

Given that the data accumulated so far are still not enough to allow yield improvements in short-term through biotechnology and genetics, use of crop models seems a viable option in finding short-term solutions. Moreover, for the perennial crops which are considered as the most promising for bioenergy it will take several years for a new improvement to be realized by using genetic approaches (Connor & Hernandez, 2009). Improvements in mechanization of energy crops will also improve yields because at present there are large yield gaps between attainable and harvestable biomass for the majority of energy crops.

Employing second generation technologies

Introduction of the second generation crop/fuel chains (lignocellulosic biomass to fuel) into commercial scale is expected after 2015–2020 (Ragauskas *et al*., 2006; Duer & Christensen, 2010).

Problem statement

As discussed in previous sections of this chapter, in the near-future new energy crops will be included in the cropping systems while the production area of other crops will expand further to meet targets for bioenergy production. However, it is generally recognized that in spite of the fast bioenergy growth worldwide due to favourable policies, there is a lack of strong data to support this growth. This limitation is particularly noticeable for the agronomy and crop physiology of new energy crops (EUR, 2006; Sims *et al*., 2006; Karp & Shield, 2008; Connor & Hernandez, 2009; Krasuska *et al*., 2010; Zegada-Lizarazu *et al*., 2010; Banse *et al*., 2011). This kind of information is needed to provide farmers with new

perspectives and options to diverse farming activities; researchers to select appropriate species/genotypes for specific regions; and modellers to better evaluate future land use including food, fibre, feed and fuel crops. Recently, Beringer *et al*. (2011) stated that assessments of global bioenergy potentials suffer inherently from a lack of data and limited field experience from bioenergy cultivations. Obviously data from different regions with different soil-climatic conditions and on different cropping systems should emerge. In line with the general objective, I chose the Mediterranean region and three bioenergy crops to provide such information.

Currently, experience with large scale bioenergy plantations is limited to sugarcane and rapeseed. Lignocellulosic bioenergy plantations are sporadic (e.g. willow, poplar, miscanthus) or are still in experimental basis (e.g. sorghum, cynara) and it is debatable whether yield levels observed at controlled test sites are transferable to large areas with less favourable climate, soil and management conditions (Beringer *et al*., 2011). This indicates a further need to accumulate more agronomic knowledge in order to optimize their production, both quantitatively and qualitatively, and to integrate them into traditional cropping systems (Zedada-Lizarazu *et al*., 2010).

On the other hand, in order to interpret biomass production in relation to genotype × management × environment interactions, advances in crop physiology should also be obtained. For instance, studies on leaf/canopy photosynthesis or base temperature for plant growth, which comprise fundamental aspects in crop science, can hardly be found in literature for dedicated energy crops. The importance of such information is vital given also that crop production is directly linked to climatic variables, such as CO_2, radiation and temperature, which are expected to change. The lack of such data is because studies on energy crops were initiated only recently (Fig. 1.2) and were focused at crop level adaptability and productivity issues.

To speed up our understanding on energy crops and to design or improve production systems, future studies should aim to enhance physiological understandings of their growth and development dynamics. Such understanding will help generate parameters for use in generic crop growth models (see earlier section). Later, by combining such models with soil maps, more reliable assessments of regional and global bioenergy potentials (and greenhouse gas emissions from agriculture) are possible.

Mediterranean region

Each country has to make its own contribution to the overall bioenergy target. In this thesis, I focus on the Mediterranean region where suitable bioenergy plantations have yet to be formulated, in contrast to central and northern

European where such cultivations exist (e.g. rapeseed). Irrigation water, the most limiting factor of crop production in the Mediterranean region, brings another important issue for consideration.

Selected crop species

There are several candidate species for bioenergy production in Mediterranean countries (Table 1.2). In this thesis, I study *Helianthus annuus* (sunflower), *Hibiscus cannabinus* (kenaf) and *Cynara cardunculus* (cynara or cardoon) because these crops cover a wide range of bio-industrial applications, fit into different cropping strategies (short or long growing periods, cultivation with or without irrigation, etc.) and because previous studies have shown promising results in terms of their production potential.

Sunflower is an annual C_3 oil crop for biodiesel production, the second most important "biodiesel" crop in Europe. Earlier studies showed that sunflower can reach high seed yield up to 5.5 t ha^{-1}, with an oil/seed content of 44% (Danalatos *et al*., 2004, 2005).

Kenaf is an annual C_3 fibre crop with viable bio-products for the industry (e.g. Alexopoulou *et al*., 2005; Ardente *et al*., 2008) and lignocellulosic biomass for energy production. Stem comprises the commercial product with yields of 10 to 20 t dry matter ha^{-1} (Danalatos & Archontoulis, 2010).

Cynara is a perennial C_3 herb with annual cycles that can be used for combined heat and electricity production, for biodiesel production (from seeds) or for bioethanol production (lignocellulosic biomass). Cynara is propagated by seeds, grown as rainfed during autumn-winter-spring periods, and harvested dry during summer time achieving biomass yields from 6 to 30 t dry matter ha^{-1} y^{-1} (Fernández *et al*., 2006; Danalatos, 2008).

Objectives

The goal of this study is to enhance agronomic and crop physiological information for sunflower, kenaf and cynara needed for improved crop management and for initiating modelling studies exploring the potential role of these crops as suppliers of biomass for energy production in Mediterranean environments. For this, studies on phenology, biomass yields, crop growth, canopy profiles of light and nitrogen, and leaf gas exchange rates were scheduled. Among selected crops considerable less information was available in literature for cynara; while given its perennial character and advantages in terms of water saving, more effort will be put on it. For these crops, we identified the most important knowledge gaps and performed a series of field experiments to fill some of those, particularly for cynara. The specific objectives were:

⇒ To define phenological growth stages of *Cynara cardunculus* (Chapter 2);

⇒ To develop a robust and easily applicable methodology to estimate seed yields of *Cynara cardunculus* and to explore its yielding potential (Chapter 3);

⇒ To investigate temporal dynamics in the vertical distributions of light and nitrogen in canopies of cynara, kenaf and sunflower in relation to water stress (Chapter 4);

⇒ To quantify photosynthesis and respiration parameters for sunflower, kenaf and cynara (Chapter 5);

⇒ To explore growth and biomass accumulation over time for sunflower, kenaf and cynara in relation to management practices in Greece (Chapter 6).

Methodological framework

This thesis is mainly based on experimental field work, data analysis and modelling. Three major field experiments were set up in central Greece (Palamas, 39°25′N, 22°05′E) in 2007, 2008 and 2009. Each experiment (same design) represented one crop. The experimental design was a split–plot in four blocks. Main factor comprised the irrigation application at two levels (fully irrigated and water stressed) and the sub-factor was nitrogen application at three levels (0, 80 and 160 kg N ha^{-1}). Crops were grown in different sections of the same field. The soil at the site was a deep, fertile loamy, with moderately shallow groundwater table (Aquic Xerofluvent; USDA, 1975).

Additionally in the same field, several supplementary plots with sunflower and kenaf crops were sown at different dates each year. This aimed to determine phenological events particularly for the kenaf crop, which is a short-day crop in terms of its response to photoperiod, and secondly for gas exchange measurements in order to assess leaves with different leaf age. All supplementary plots were irrigated. For cynara additional measurements were taken from several other fields that were located some 5–100 km from the main site (see Chapter 3).

The experimental protocol consisted of the following measurements per crop and per year: (1) destructive harvests at frequent time intervals to determine growth rates, biomass accumulation, leaf area index, specific leaf area, nitrogen concentrations and biomass partitioning over time; (2) midday measurements of light penetration at several insertion points within crop canopies and at different times; (3) day- and night-time gas exchange measurements at different crop

stages; (4) frequent assessments of phenological events (e.g. flowering) and of leaf water potential. Full meteorological data and canopy temperatures at different insertion heights and at different crop stages were also recorded on a hourly basis. The experimental protocol, measurements and data analysis were designed in such a way in order to parameterize later the dynamic crop growth model GECROS (Yin & van Laar, 2005). Data from experiments conducted on sunflower and kenaf in 2006 were included in the analyses of the data generated in this project.

It should also be mentioned that the present thesis only includes part of the data accumulated in all these years; the remaining data are currently analyzed and will be published soon elsewhere. For instance, parameterization of GECROS model for the studied bioenergy crops is in process.

Outline of the thesis

This thesis consists of seven chapters (Fig. 1.3). Chapter 1 (this chapter) provides an update on bioenergy production and shows the importance of energy crops. Knowledge gaps are identified, while a list of objectives and the way to deal with them is also presented. Chapter 2 deals with crop phenology and describes growth stages of the perennial *Cynara cardunculus* using a universal coding system, the BBCH code. Chapter 3 provides an allometric model to predict *Cynara cardunculus* seed yield and reports attainable seed and biomass yields from 16 field experiments. Chapters 4 and 5 provide ecophysiological parameters for use in crop models and vital information for researchers to interpret biomass formation for any environment. Light and nitrogen extinction coefficients as well as photosynthetic and respiration rates are provided for sunflower, kenaf and cynara. Chapter 6 is a collection of annual studies describing crop growth and biomass accumulation in relation to management practices. Chapter 7 (General discussion) provides a synthesis of the results reported in previous chapters and discusses the overall contribution of this thesis.
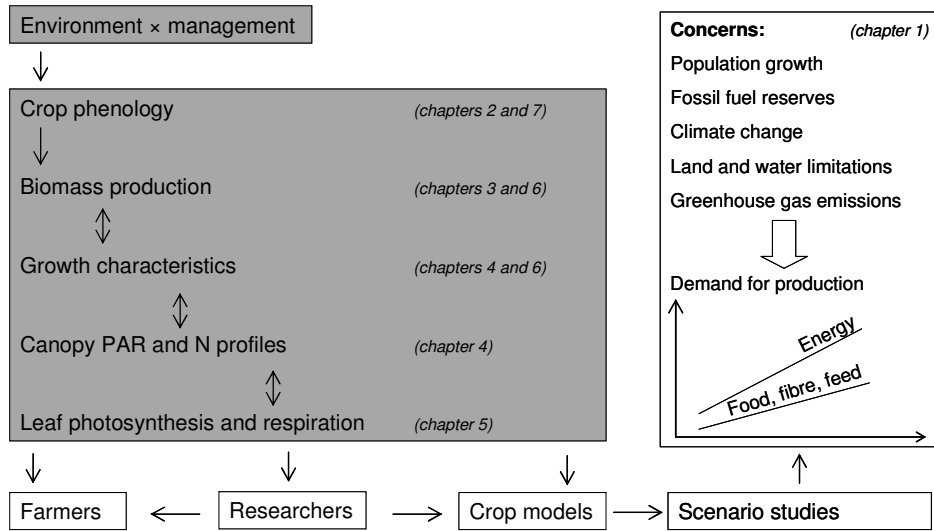
Figure 1.3: Schematic thesis outline. Grey boxes represent research undertaken and analyzed in this thesis. Combined with the white boxes a view on how to deal with future demands as well as the potential contribution of this thesis is illustrated. Concerns about energy security and environmental protection as well as present and future status of bioenergy production from plants are reviewed in Chapter 1. Different kinds of arrows indicate information flow.

Chapter 2

Phenological growth stages of *Cynara cardunculus*: codification and description according to the BBCH scale

Abstract

Cynara cardunculus is a herbaceous perennial crop known from ancient times. During the last three decades this thistle has intensively been researched and recently became a commercial crop for biofuel production. As there is an increasing need for more information on this crop, we present here the phenological growth stages based on the Biologische Bundesanstalt, Bundessortenamt, CHemische Industrie (BBCH) scale and its associated decimal code. Nine principal growth stages have been defined and each principal stage has been subdivided into secondary growth stages. Descriptive keys with illustrations are also provided. A practical use of the scale is proposed, with particular reference to harvest time and management treatments. This scale aims to support farmers and researchers to efficiently plan management practices and experimental treatments.

Introduction

Knowledge of crop phenology is central in plant-related sciences. It comprises: (a) a useful tool for scheduling management applications (e.g. irrigation, fertilisation, pesticide application; Arcila-Pulgarin *et al.*, 2002; Proctor *et al.*, 2003); (b) the basis for the construction of crop growth simulation models and (c) a reference for assessing crop performance under variable inputs and conditions (e.g. Barlog & Grzebisz, 2004).

Based upon Zadoks' descriptions of cereals (Zadoks *et al.*, 1974), a general, uniform decimal code, known as the Biologische Bundesanstalt, Bundessortenamt, CHemische Industrie (BBCH) scale, was proposed by Bleiholder *et al.* (1991) and Lancashire *et al.* (1991). A more advanced scale, the extended BBCH scale, was proposed by Hack *et al.* (1992) and Hess *et al.* (1997). Later, the 'BBCH–Monograph' representing a group of 27 crops and weeds was published (Meier, 1997; Meier *et al.*, 2009*a*). Recently the Global Phenological Monitoring Network introduced and accepted the BBCH scale and its coding system to be used as the standard system to describe phenological stages of plants (van Vliet *et al.*, 2003). The BBCH scale is a universal two-digit coding system, flexible, which can be used worldwide (Hess *et al.*, 1997; Smith & Froment, 1998; Arcila-Pulgarin *et al.*, 2002; Garcia-Carbonell *et al.*, 2002). For some crops (e.g. rose, ginseng) a three-digit scale including the so called mesostages was used (Meier, 1997; Meier *et al.*, 2009*a,b*; Proctor *et al.*, 2003).

Cynara cardunculus L., commonly known as cynara, wild cardoon or thistle artichoke, is a perennial herbal (≈10 years), very deep-rooting C_3 plant of Mediterranean origin. It is well-adapted to the xerothermic conditions of southern Europe. Cynara has an annual growth cycle, in which the crop grows and develops during autumn, winter and spring and is ready for harvest during summer time. Cynara may achieve high biomass yields annually (Fernández *et al.*, 2006; Archontoulis *et al.*, 2008a; Angelini *et al.*, 2009) while requiring only modest inputs (Danalatos, 2008).

Cynara is a multipurpose crop that can be utilised as forage in winter and spring, as a raw material in the paper pulp industry, but most importantly as solid (pellets or chips) and/or liquid (biodiesel) biofuel in the bio-energy sector. Cynara may play a significant role in biofuel production in Mediterranean climates worldwide. In southern Europe the area cropped with cynara is at present exponentially expanding, from only some experimental hectares in 2005 to some thousand hectares in 2009. As this species of the genus *Cynara* is a new commercial crop, studies on phenology and ecophysiology are relevant in order to be able to design sustainable production systems.

The development stages of cynara have not yet been defined and described. This is the first attempt to develop a simple, illustrated description and coding

system, using the BBCH decimal coding system (Meier, 1997; Meier et al., 2009*a*), for the growth stages of *C. cardunculus* L. based on field observations in Greece.

Cynara species

Cynara cardunculus is a diploid (2*n* = 34) perennial species, belonging to the Asteraceae (Compositae) family. The small genus *Cynara* comprises about eight taxa (Duarte *et al*., 2006). The genus includes the cultivated *C.cardunculus* L. subsp. *scolymus* (L.) Hegi = *C. scolymus* L. (globe artichoke), *C. cardunculus* L. var. *altilis* D.C. (cultivated cardoon) and *C. cardunculus* L. var. s*ylvestris* Lam. (wild cardoon). The globe artichoke is a perennial rosette plant, grown throughout the world for its large fleshy heads. The cultivated cardoon is grown as a vegetable since ancient times for its succulent young leaves (Raccuia & Melilli, 2007a). The wild cardoon (or cynara or thistle artichoke) is a robust thistle with a characteristic rosette of large spiny leaves and branched flowering stems. It is cultivated for bio-energy production or industrial applications. The main differences between cultivated and wild cardoon are the larger production potential of the former and the distribution of the assimilates between shoot and root, with the wild type investing more carbohydrates in the roots providing more resistance to adverse climatic conditions (Raccuia & Melilli, 2004).

Cynara cultivation and yields

Cynara cardunculus is indigenous to many regions of the world (Europe, North Africa, Madeira and Canary Islands, and South America). It does well in harsh environments with high temperatures and water stress in summer, even on thin, unproductive and stony soils. Cynara is tolerant to water-limited conditions, thanks to its deep root system which may exceed 5 min depth. The life cycle may usually exceed 10 years. These two characteristics, large root system and perennial growth, together with the high annual biomass production (from 10 to 33 t dry matter ha^{-1}), give the crop a great advantage compared with many other, more common agricultural crops.

Field observations

The description below applies to Mediterranean climates (cool humid winters, hot and dry summers). Our measurements and observations on cynara were undertaken in several field experiments with crop stands of different ages and carried out at different sites across Greece (latitude of 39° ± 1.5°N; elevation range: 50–250 m asl; years 2006–2009).

Table 2.1: Phenological growth stages of *Cynara cardunculus* according to the BBCH scale

Code	Description	
Principal growth stage 0:[a] (assessed at crop level)		
	Germination	Sprouting, bud development
	(first growing cycle; only)	(second growth cycle; onwards)
00	Dry seed (achene)	—
01	Beginning of seed imbibition	Bud swelling
03	Seed imbibition complete	End of bud swelling
05	Radicle emerged from seed	—
06	Radicle elongated, root hairs developing	—
07	Hypocotyl with cotyledons emerged from seed	Beginning of sprouting or bud breaking
08	Hypocotyl with cotyledons growing towards soil surface	Shoot growing towards soil surface
09	Emergence: cotyledons emerge through soil surface	Buds showing green tips
Principal growth stage 1: Leaf development [b] (assessed at plant level)		
10	Cotyledons completely unfolded	First leaf spread/separated
11	First elliptic leaf visible	First leaf visible
12	Two elliptic leaves visible	Two leaves visible
13	Three elliptic leaves visible	Three leaves visible
14	Four elliptic leaves visible; leaf changing shape from elliptic to runcinate with lobed margins	Four leaves visible
15	Five leaves visible; two of them have different shapes	Five leaves visible
16	Six leaves visible (small rosette visible)	Six leaves visible
1.	Stages continue till…	Stages continue till…
19	Nine or more leaves visible (rosette developed)	Nine or more leaves visible
Principal growth stage 3: Rosette growth (crop cover; assessed at crop level)		
31	Leaves cover 10% of ground	
33	Leaves cover 30% of ground	
35	Leaves cover 50% of ground	
37	Leaves cover 70% of ground	
39	Crop cover complete: leaves cover 90% of ground	
Principal growth stage 4: Development of harvestable vegetative plant part [c] (crop level)		
41	10% of the maximum leaf mass reached	
43	30% of the maximum leaf mass reached	
45	50% of the maximum leaf mass reached	
47	70% of the maximum leaf mass reached	
49	90% of the maximum leaf mass reached	
Principal growth stage 5: Inflorescence emergence and development (whole plant) [c, d]		
51 501	Beginning of stem elongation; main inflorescence buds visible between the newly formed leaves (hardly detectable). No branching yet	
53 503	30% of the final stem height achieved; stem branching starts; buds swelling and become visible from above (green colour); caulicle leaves are formed	
55 505	Corymb formed; initial branch leaves visible; production of higher order branch; elongation of older branches	
57 507	Corymb reaches 70% of final volume; older buds enlarged and newly formed; buds have green colour	
59 509	Corymb reaches 90% of final volume; 90% of the buds formed; first flowers formed on primary branch; main stem fully elongated	
– 521	Second order stem (branch) inflorescence visible	
– 525	Second order stem (branch) elongated; bud enlarged	
– 529	First flower formed on secondary inflorescence	
– 5N1	n^{th} order stem (branch) inflorescence visible	
– 5N5	n^{th} order stem (branch) elongated; bud enlarged	
– 5N9	First flower formed on n^{th} inflorescence	
Principal growth stage 6: Flowering and capitulum formation (whole plant) [c]		
60 600	First flower petals visible on main stem inflorescence	
61 601	10% of heads in blossom	
63 603	30% of heads in blossom	
65 605	50% of heads in blossom	
67 607	70% of heads in blossom	

Table 2.1: Continued

Code		Description
69	609	End of flowering
–	620	First flower petal on secondary inflorescence
–	621	Beginning of flowering of secondary inflorescence: about 10% of flower petals visible
–	625	Full flowering of secondary inflorescence: at least 50% of flower petals visible
–	627	Majority of florets discolour (secondary inflorescence)
–	629	End of flowering of second order stem
–	6N1	Beginning of flowering of nth order inflorescence: about 10% of flower petals visible
–	6N.	Stages continuous till…
–	6N9	End of flowering of nth order stem inflorescence
Principal growth stage 7: Development of capitulum (or head) (whole plant)		
71	701	Heads have formed and are beginning to expand, seeds formed and expanded
75	705	50% of the heads have reached full size
79	709	Nearly all heads have reached full size; seeds full sized
–	721	Secondary head (on the second order stem) has formed and is expanding, seeds formed and expanded
–	725	Secondary head has reached 50% of final size
–	729	Secondary head has reached full size; seeds full sized
–	7N1	n^{th} head (on the nth order stem) has formed and is expanding; seeds formed and expanded
–	7N.	n^{th} head has reached 50% of final size
–	7N9	n^{th} head has reached has reached full size; seeds full sized
Principal growth stage 8: Capitulum and seed ripening (whole plant)		
80	800	Upper part of the primary head turning yellow. Mature lilac florets still present
81	801	10–20% of the heads turning yellow (upper part)
82	802	20–30% of the heads turning yellow (upper part)
83	803	<20% of the heads completely yellow
84	804	>20% of the heads completely yellow
85	805	Advance maturity: > 50% of the heads have completely brown-yellow colour. Only a few lilac florets visible
86	806	Pappus visible on the main head (upper part of the head opens, enlarged)
87	807	<20% of the heads have opened (pappus visible)
88	808	>20% of the head have opened (pappus visible)
89	809	Majority of heads are opened, brown-yellow, dry and senesced. Seeds fully ripped; dispersal evident
–	820	Upper part of the secondary head turning yellow. Mature lilac florets still present
–	821	10% of the secondary head turning yellow
–	823	30% of the head turning yellow
–	825	> 50% of the head has completely brown-yellow colour. Only a few lilac florets visible
–	826	Pappus visible on the secondary head (upper part of the head opens, enlarged)
–	829	Secondary head fully opened, brown-yellow, dry and senesced. Seeds fully ripped; dispersal evident
–	8N0	Upper part of the nth head turning yellow. Mature lilac florets still present
–	8N.	Stages continuous till…
–	8N9	n^{th} head fully opened, brown-yellow, dry and senesced. Seeds fully ripped; dispersal evident
Principal growth stage 9: Senescence [e] (whole plant)		
91		Shoot development completed
92		Basal leaves completely dead; caulicle and branch leaves discoloured and senesced
93		Stalk's moisture around 70%; head's moisture around 25%; Majority of leaves are dead
95		Stalk's moisture round 50% (green to yellow colour); head's moisture around 12%; beginning of head over ripening and seed dispersal; All leaves are dead
97		Stalk's moisture around 30%; seed dispersal enhanced
99		Plant dead and dry (moisture around 10%). New leaves from sprouting visible (= stage 110)

[a:] Germination of plants from true seeds as well as sprouting were classed in the same principal growth scale (stage 0) although they are completely different biological process.

[b:] Leaf development from seeds as well as from sprouting were also classed in the same growth scale (stage 1). Both ends in the development of a rosette plant.

[c:] Harvesting for forage.

[d:] Spring sowings may not produce inflorescences in the first year.

[e:] Harvesting seeds for biodiesel production or whole biomass for solid biofuel production.

Extended BBCH scale

The extended BBCH scale (Hack *et al*., 1992) considers 10 principal growth stages, numbered from 0 to 9 (Table 2.1). For cynara, growth begins with seed germination (first year) or sprouting/bud development (second and later years) (stage 0). Vegetative growth is represented by three principal growth stages corresponding to leaf development (stage 1), rosette growth (stage 3) and development of harvestable vegetative plant parts (stage 4). Inflorescence emergence and development is included in stage 5. Flowering (stage 6), development of capitulum and fruits (stage 7), inflorescence ripening (stage 8) and plant senescence (stage 9) complete the scale. In our case, some stages overlap or run concurrently, hence the code of the more advanced stage is used for phenology description or both stages are indicated separated by a diagonal stroke.

Secondary growth stages are referred to by a second digit in the code (numbered from 0 to 9; Table 2.1) and correspond to ordinal or percentage values of crop development. For instance, for leaf development (stage 1), the stage when the third leaf becomes visible is assigned a value of 13. In general easily detected criteria like number of leaves, size and colour were used for the codification of the secondary growth stages.

For some plants, a further subdivision may be necessary between principal and secondary stages, enlarging the code to a three-digit code. This intermediate stage is called mesostage and coded with a number from 0 to 9 (Hack *et al*., 1992). In our case, we adopted the three-digit scale to describe in more detail the principal stages 5–8 (Table 2.1). For example, stage 51 describes the formation of the main stem inflorescence, whereas stage 521 describes the formation of the secondary inflorescence (second order stem; branch). Additionally, stage 65 describes blossoming of the 50% of heads per plant; whereas stage 655 describes full flowering of the fifth inflorescence (fifth order stem).

Growth stages of cynara

Principal growth stage 0: germination/sprouting/bud development

The germination of the seed (first growth cycle or year of crop establishment) and the sprouting (second and later years during growth cycle) are both classified as the principal growth stage 0 (Table 2.1); even though they are the result of different biological processes they result in phenologically analogous structures (Lancashire *et al*., 1991).

The development of cynara from seeds (brown colour; moisture content of about 6–9%), starts in stage 0 and ends when cotyledons emerge through the soil

surface (stage 9; Fig. 2.1). Depending on temperature, soil moisture, sowing depth and sowing period the duration of this phase is 1–2 weeks approximately (for a spring sowing) to 1–2 months (for a late autumn sowing) or around 50–60◦C-days (using a minimum threshold temperature of 10°C). However, from the second year onwards the duration of this phase is much shorter compared with the first year (sprouting might occur before crop harvesting). After crop harvesting, regrowth starts from several vegetative buds that are positioned on the upper part of the root system (stage 01). This stage ends when buds show green tips (stage 09). Usually, two to four buds per plant are generated annually; they grow in parallel until competition for resources in advanced stages ceases growth of some of them (Fig. 2.2; see below).

Crop establishment is suggested to take place very early in autumn for the following reasons: (a) the crop will be ready for harvest from the first year, (b) the crop will emerge in a short period (1–2 weeks) because of high temperatures occurring in early autumn, (c) probably, a sooner establishment could help plants to better withstand winter cold and (d) autumn weeds are less competitive compared with spring weeds and usually cynara growth is not suppressed by them.
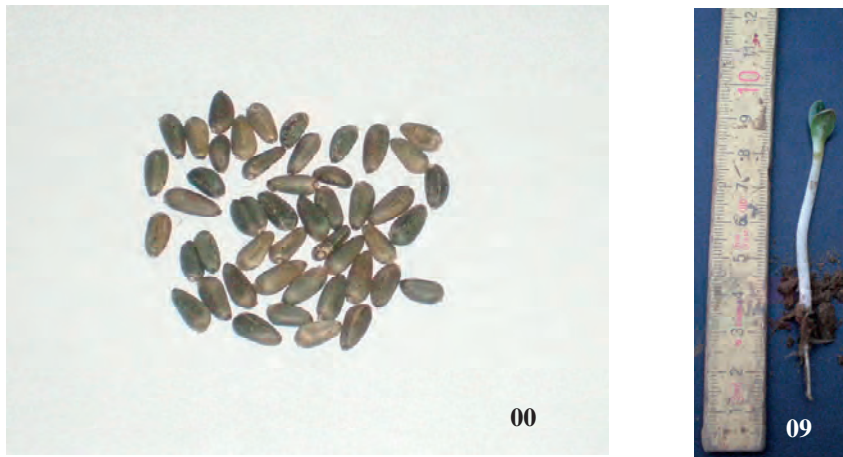
Figure 2.1: Dry seeds and cotyledons emerge through soil surface.

Principal growth stage 1: leaf development

This stage describes the aerial development of the young plant. The number of visible leaves including visible petioles) determines the code (Table 2.1). Very young, small leaves without petioles are not counted (Fig. 2.3). Leaf development from seeds begins after the cotyledons are fully unfolded (stage 10; Fig. 2.2). The first four rosulate leaves (stage 14; Fig. 2.2) are entire with an elliptic shape and

crenate margins; later on leaves are expanding in blade area and petiole elongates. After stage 14, the leaves change shape (from elliptic to runcinate with lobed margins) while one more lobed leaf is formed (stage 15; Fig. 2.2). Main stage 1 continues with the production of more leaves (stage 16, developing a small rosette; Fig. 2.2) and ends when at least nine leaves are visible (stage 19) in a rosette form.
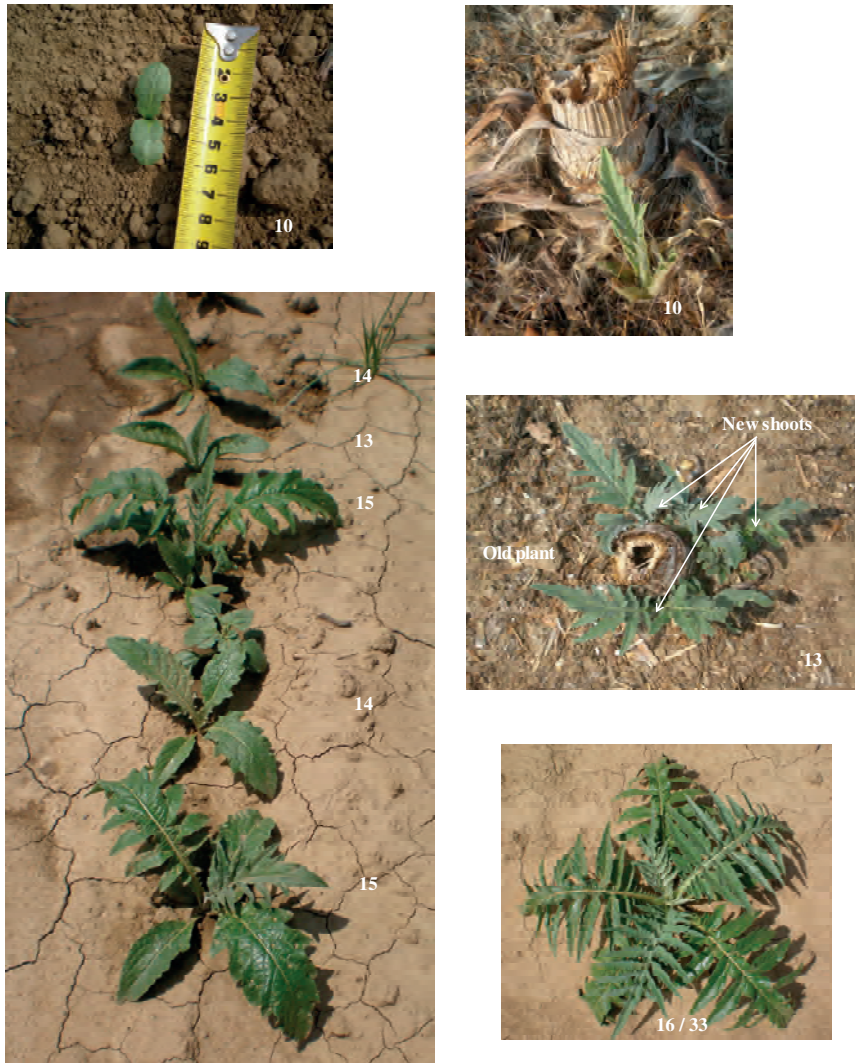
Figure 2.2: Leaf development from seeds and from sprouting (principal stage 1).

Leaf development from sprouting (second year onwards) begins after the first leaf is expanded (stage 10; Fig. 2.2). Very often two to four new leaves (and consequently shoots) per plant are formed and they grow in parallel (Fig. 2.2).

These leaves are divided having pinnatifid margins and they rapidly expand. The number of (the produced) leaves per plant determines the code. For instance, formation of three leaves is coded in stage 13, while formation of nine leaves in stage 19. The small rosette is obvious in stage 16 (Fig. 2.3).

Although leaf development within the first year and leaf development during the subsequent growth cycles follow different patterns, leaf development is classed into the principal growth stage 1 (Lancashire *et al.*, 1991), whilst both biological processes end with the development of a rosette plant (stage 19). Leaf development from sprouting is much faster than from seedlings, because the reserves in the roots are more abundant to support growth. This is also in agreement with studies on ginseng, another perennial herb (Proctor *et al.*, 2003). Stage 1 is usually overlapping with stage 3, hence the code of the more advanced stage is used for the description (Lancashire *et al.*, 1991). Usually after the development of the fifth and sixth leaves, the growth of the crop is assessed by the percentage of ground cover by the crop (see stage 3).

During stages 10–15 of first growing cycle farmers should pay particular attention to weed control, because the crop is not as competitive as in more advanced stages or in following cropping cycles (Danalatos, 2008).
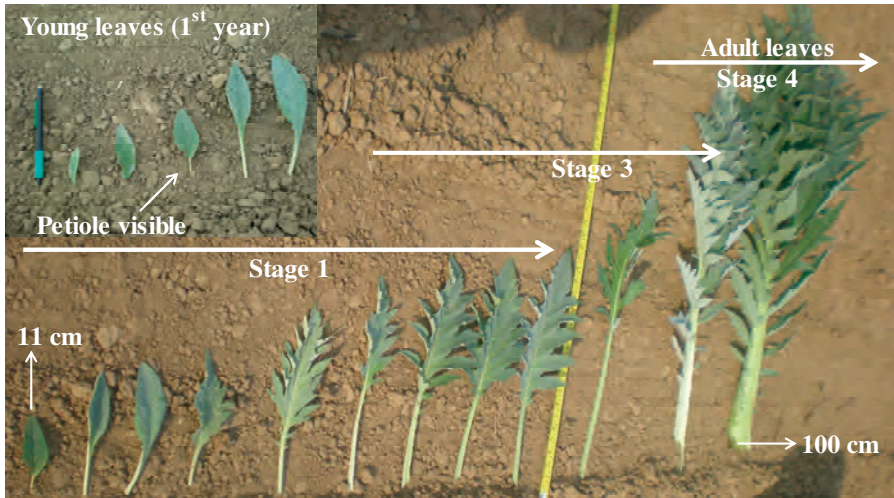
Figure 2.3: Leaf growth during stages 1–4. Leaves are counted when their petiole is visible. The illustration above depicts the leaf expansion during different stages. The leaves from seedlings are entire with an elliptic shape and crenate margins. Leaves are expanding in size and soon after the development of the fourth leaf, subsequent leaves start to change shape from elliptic to runcinate with lobed margins finally producing adult leaves with pinnatifid margins with an undetermined number of leaflets. Leaves from sprouting are usually divided, have pinnatifid margins and expand in size at a high rate. A full-grown leaf may reach 100 cm in length.

Figure 2.4: Rosette growth (crop cover, stage 3).

Principal growth stage 2: formation of side shoots/tillering

This is included as a stage within the BBCH scale, but is not applicable to the cynara crop.

Principal growth stage 3: rosette growth

This principal stage describes the proportion of ground cover by the plants. For instance stages 31 and 39 reflect 10% and 90% of the ground cover, respectively (Table 2.1; Fig. 2.4). The leaves are surrounded by small spines, which are mainly located on the petioles. During this stage leaves are further expanding (see Fig. 2.3). This stage is characteristic of the cynara growth cycle. It is crucial that the crop enters and/or passes this stage before winter time, when air temperatures fall below 10°C for long periods and when snow and frost are frequent under Mediterranean conditions, partially damaging the aerial part of the crop (Fig. 2.6).

In practice, particular attention should be given to the late autumn sowing time of the first year, because in that situation the crop requires more growing degree days to pass stage 3. In case of regrowth (second year onwards), the crop usually passes stage 3 before the winter period. Once the plant develops the rosette, it becomes rather tolerant to cold; it may stand severe frost (<−10°C; unpublished data). When the crop is planted at very low densities (<1 plant m^{-2}) stage 3 is overlapping with stage 4.

Figure 2.5: Development of harvestable vegetative plant part (stage 4).
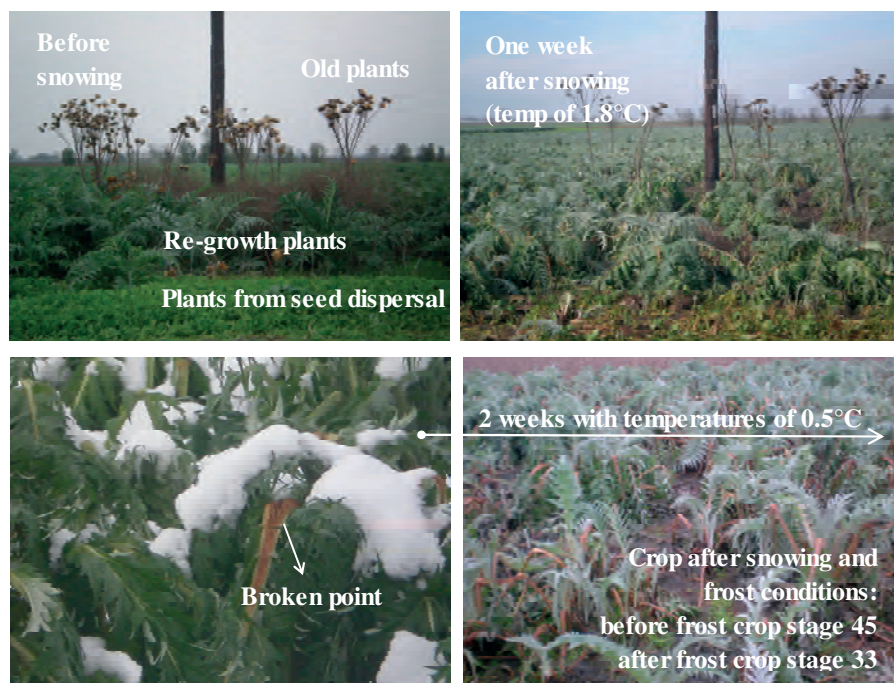
Figure 2.6: Aerial vegetative biomass damaged by snow and/or (excessive) frosts during winter time.

Principal growth stage 4: development of vegetative plant parts

This stage reflects the increase of leaf biomass as percentage of its maximum biomass (Table 2.1). After full ground cover (stage 40) the crop continues to increase in vegetative biomass until the crop reaches maximum biomass (stage 49; Fig. 2.5); the biomass is determined by genotype × management × environment interactions. The increase in biomass is attained by further leaf expansion and from the production of new leaves. The leaves of stage 4 (basal leaves) are often compound, very large in size, with leaflets arranged on both sides of the very fleshy petiole (Fig. 2.3). A fully developed basal leaf (1 m long) could have a leaf area of 0.45 m^2, and with 10 leaves per plant the leaf area of a single plant could be 4.5 m^2 (stage 49). During the principal stage 4, the older leaves senesce and litter (Fig. 2.5).

Under Mediterranean climate, the crop usually stays in this stage during the winter time until mid-spring. The biomass yield during this stage is very variable and depends on the variation in air temperature (Fig. 2.6). Although the crop is able to survive excessive snow and prolonged frosts, such conditions cause a reduction in biomass yield; however, the magnitude of yield reduction is strongly associated with the extent, the timing and the duration of the adverse conditions.

If the stress occurs in spring time the reduction in biomass yield will be very remarkable (even total yield loss in the season but with no consequences for crop survival). For example, excessive snow and frost conditions during the whole February in Greece reduced substantially cynara final dry biomass yield (Danalatos *et al*., 2007a). Under snow conditions (>10 cm of snow; Fig. 2.6), the petiole breaks because of the excessive weight it has to carry. The break usually occurs at the middle of the petiole. The crop recovers from an adverse event by producing new leaves, when air temperatures rise to satisfactory levels.

Within this principal stage 4, the crop can be harvested for forage purposes, however, farmers and advisors should be aware of the following consequences of harvesting: (a) the summer end biomass yield (biofuel purposes) will be much lower; (b) nutrient extraction will be significant (note that leaves are harvested fresh); (c) cynara in the absence of foliage biomass becomes sensitive to any adverse conditions that might occur after harvesting and (d) there is always the risk of soil compaction during the winter time. In general, winter harvests should be avoided, in order to preserve yield potential.

Principal growth stage 5: inflorescence emergence and development

These stages describe the inflorescence of the whole plant, with particular reference to the main stem inflorescence. If it is necessary to code the production of buds/inflorescences on the side branches, this may be performed by mesostages (Table 2.1). In general, the two digit code will be sufficient. At growth stage 51 (Fig. 2.7), the stem begins to elongate, the buds are present but initially surrounded by green leaves and are thus not easily detectable. These buds show swelling and become fully visible in stage 53 (Fig. 2.7).

During stage 53 the biomass partitioning changes a lot: the stem has reached 30% of its final height, (visible) branching starts and caulicle leaves (stem leaves) are being formed. Crop development continues with the production of higher order branches (new buds formed) and the elongation of the older branches (buds enlarged) giving finally rise to a corymb or a compound corymb (stage 55; Fig. 2.7). At the same time, new caulicle leaves and branch leaves are being formed and enlarge. The corymb increases in volume (stage 57) and this stage ends (stage 59; Fig. 2.7) when the corymb reaches 90% of its maximum volume (or alternatively when 90% of the buds have been formed). During stage 59, the stem and the older branches are fully elongated, the buds are soft (green colour) and surrounded by green soft erect spines. The primary inflorescence starts to discolour and the flowering petals starts to become visible (see Fig. 2.9).

Figure 2.7: Inflorescence emergence and development (stage 5).

The basic type of cynara inflorescence is the capitulum (head), in which the florets (flowers) are located on a flattened surface (receptacle), surrounded by bracts (erect spines; see Fig. 12). Inside the capitulum and subtending the florets, there are many bristles (interflower bracts) like stiff white hairs (Duarte *et al.*, 2006; Gominho *et al.*, 2009).

The final number of inflorescences per plant is strongly affected by genotype × management (viz. plant density) × environment interactions and it is usually ranging from some 1–4 to 8–12 inflorescences per plant for poor and fertile soils, respectively. During the establishment year the number of inflorescences per plant is considerably lower than that of the later years (approximately 50–70% lower considering an autumn sowing). In case of spring sowing the crop may not produce an inflorescence during the first growing cycle. Usually inflorescence emergence starts at the end of April and the development requires approximately 5 weeks (340°C–days).
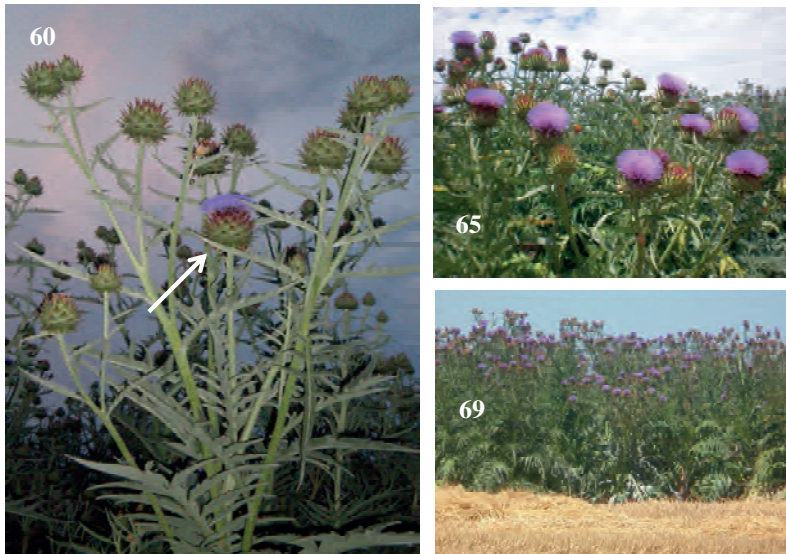
Figure 2.8: Flowering and capitulum (or head) formation (stage 6).

Principal growth stage 6: flowering and capitulum formation

Principal stage 6 assesses the flowering of the whole plant as a proportion of full flowering (blossoming). Stage 60 reflects the flowering of the main inflorescence (Fig. 2.8). Stages 61–69 represent the progressive blossoming of the heads, from 10% to 90%, respectively (Fig. 2.8). At flowering, florets have a lilac or bluish colour, while the upper part of the capitulum changes colour from green to dark

red (Fig. 2.9). After flowering this part is further discoloured to yellow (Fig. 2.9). During stages 59–69 the crop sustains its maximum fresh biomass yield, which can be harvested (whole plant) for forage production. Usually flowering is apparent during June. Stage 6 is overlapping with stage 7 and sometimes with stage 8, because cynara has an indeterminate growth pattern. A three-digit code should be used, when flowering is to be described on multiple branches (Table 2.1).
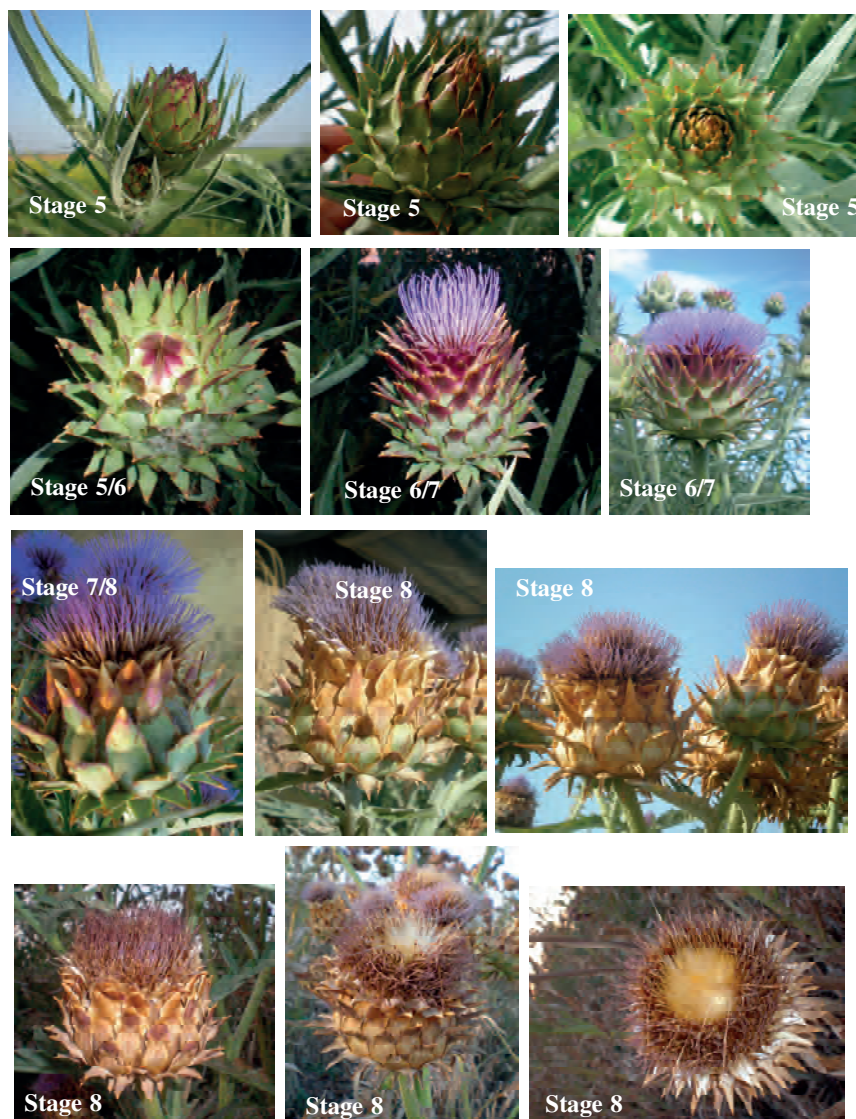
Figure 2.9: Inflorescence growth and development during stages 5–8.

Principal growth stage 7: development of capitulum and seeds

These stages refer to the development of the capitulum (heads) and fruits (seeds). A head is considered as fully developed when it has reached its maximum size (reflected by the basal head diameter), and it is fully surrounded by erect green spines (Figs 2.9 and 2.10). Principal stage 7 runs concurrently with principal stage 6 and sometimes is overlapping with the principal stage 8, because of the indeterminate growth pattern of the crop. Three secondary growth stages are defined: stage 71 when the capitulum is formed and starts to expand, seeds are formed and expanding as well; stage 75 (Fig. 2.10) when heads continue to enlarge while about the 50% of heads per plant have reached full size and stage 79 when >90% of the heads per plant have reached full size and seed have reached full size as well (Table 2.1). The seeds are attached to the receptacle (still soft; see also Fig. 2.12). With the development of the heads and seeds, the vegetative growth slows considerably down, whilst the senescence of the basal and lower positioned caulicle leaves is accelerated.

The final shape of the heads is ovate to globular and may vary in final size. The basal head diameter usually ranges from 3 to 10 cm, while the seed number per head ranges from 0 to 650 (Archontoulis *et al.*, 2008a). The chronological progression of the head formation/development determines the final size of each head, with the early formed heads (i.e. of the primary and secondary inflorescence) reaching the largest sizes. Heads with basal head diameters below 4 cm contain only a few seeds.

Figure 2.10: Development of inflorescence (head, stage 7). The principal stage 7 runs concurrently with principal stage 6, thus both stages are mentioned.

Figure 2.11: Capitulum and seed ripening (stage 8). The advanced secondary stages run concurrently with the early secondary stages of the principal stage 9, hence both stages are mentioned.

Principal growth stage 8: capitulum and seed ripening

Once the heads have reached physiological maturity, they start to change colour to yellow and to brownish-yellow (from the top to the bottom; Fig. 2.9). Initially, this is evident on the upper part of the primary head, the colour changing from dark red to yellow (stage 80). A head is regarded as discoloured, only when the

yellow colour covers at least one third of the head area. In case that 10–20% of the heads per plant has changed the colour of the upper part to yellow, the stage is coded 81, while if 20–30% then the stage is coded as stage 82 (Fig. 2.11).

When the colour intensifies and more heads become fully yellow, stages 83 (<20%) and 84 (>20%) are reached, respectively. Stage 85 refers to advanced maturity when at least 50% of the heads are brown-yellow (Fig. 2.11). Through stages 80–85, mature florets are still coloured, generally lilac, and the calyx changes into pappus (plumose crown of hairs), a structure that is required for seed dispersal (Duarte *et al.*, 2006; Gominho *et al.*, 2009). The pappus becomes visible in stage 86, usually on the primary head (Figs 2.11 and 2.12). Pappus appearance is accompanied by enlargement of the upper part of the head (head opens). The stage is continued with the opening of more heads of a plant (if <20% heads are opened then the plant is in stage 87; if >20% then stage 88 is reached). In stage 89 the majority of the heads are brown-yellow, dry, senesced and the pappus is clearly visible (Fig. 2.11). At the bottom of each pappus a seed (achene) is attached. The opposite part of the seed is connected to the receptacle (Fig. 2.12). At stage 89, the seeds are fully ripened and brown and have a moisture content of about 9–15%. Additionally, the receptacle is completely dry; hence seeds become free and dispersed through the pappus (Fig. 2.13). The dry weight of a mature head usually varies from 10 to 110 g, 30–40% of this is seed weight. The seeds are quite variable in colour (light to dark brown) and size, with the weight of 1000 seeds usually ranging from 15 to 55 g. For sowing, seeds with a weight above 30 g per 1000 seeds should be preferred (Archontoulis *et al.*, 2008a).
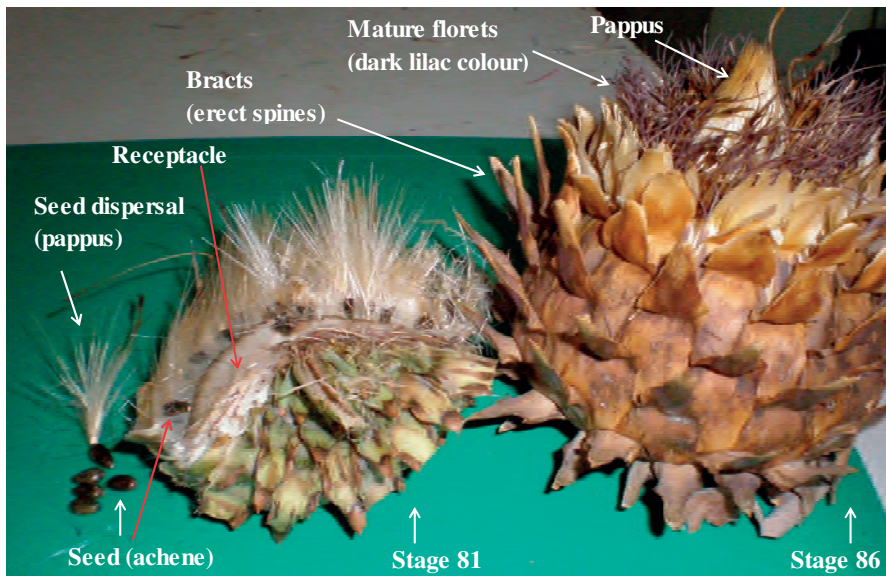
Figure 2.12: The capitulum (stage 8).
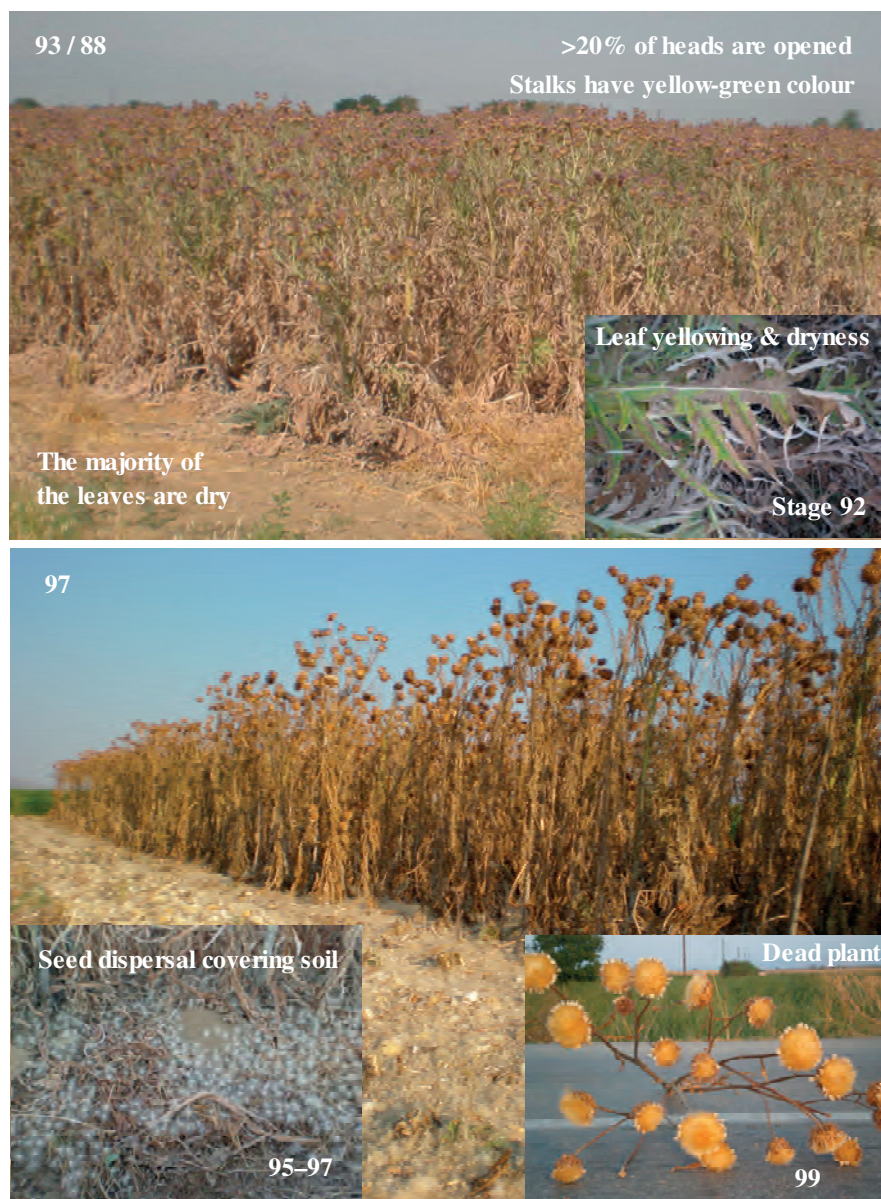
Figure 2.13: Plant senescence and harvesting (stage 9).

When cynara is cultivated for biodiesel production, it is wise to be harvested just before or during stage 89 in order to avoid seed dispersal (seed losses) which is also enhanced by the harvesting machinery. However, very often the stages 86–89 run concurrently with the stages 91–95; hence both stages are indicated by a diagonal stroke (Figs 2.11 and 2.13). Inflorescence ripening usually

occurs in July. Similarly to principal stage 5, 6 and 7, the three-digit code should be applied in case of more precise description of capitulum and seed ripening (Table 2.1).

Principal growth stage 9: senescence

This principal stage describes the gradual decrease of the plant moisture content (Table 2.1). It starts with stage 91, where the shoot development is completed and shifts to yellowing and dryness of the caulicle and branch leaves (stage 92; note that the basal leaves have already senesced; Fig. 2.13). Thereafter, principal stage 9 is assessed based on the decrease of the stalk (stem and branches) moisture content, from 70% (stage 93) to 50% (stage 95), then to 30% (stage 97) and finally to 10% (stage 99; Fig. 2.13). Stalks change colour during these stages (from green to yellow then to dry/brown). Stage 95 is identical to stage 89 (head moisture 12%), however, stage 95 describes the whole plant, while stage 89 only relates to the inflorescences. The number of open heads may be retained as a supplementary code. Plant senescence usually takes place from mid-July and continues during August.

It is remarkable that beyond stage 95/89, the seed dispersal is enhanced and soon the soil surface is covered with pappus (while depending on the wind velocity may travel to neighbouring fields; Fig. 2.13). This should be taken into consideration when scheduling harvesting treatments (either for seeds, biodiesel production or for the whole biomass including seeds, solid biofuel production). Actually, there is a trade off between advantageous end product moisture (viz. for seeds 9%, for whole biomass <15%) for industrial processing and seed/biomass yield. Seed harvesting should be at stage 95/89 and whole biomass harvesting should be at stage 97. Beyond stage 95, the regrowth processes for the next cropping cycle starts and this becomes apparent during stages 97–99 when the first leaves emerge from the soil surface (stage 09).

Discussion

Cynara is a rather complex crop in terms of morphology and growth. Two phases of growth of the crop can be distinguished: (a) the vegetative phase (principal stages 0–4, duration 220 days or 660°C-days, approximately from September to April) and (b) the reproductive phase (principal stages 5–9, duration 95 days or 1300°C-days, approximately from May to August). It is hard to specify the exact duration of each stage, because many growth stages are overlapping (e.g. 1/3 and 8/9; Figs 2.2 and 2.13) because of the indeterminate growth character of the crop. Moreover, studies concerning temperature and photoperiod effects on the development rate of cynara are lacking in literature. However, irrespective of the

rate of development that varies among regions and varieties, the presented phenological scale can be applied under all circumstances. Additionally, this study provides precise start and end points of each development stage, which are essential in studies on temperature versus development rate (Trudgill *et al*., 2005).

The BBCH scale proposed here can be used by anyone involved in cynara cropping. It is relevant to farmers, who must interpret information on input application and harvesting treatments, and for researchers who are working in the field of production and logistics. An essential aim of the corresponding BBCH coding system is that it facilitates scientific communication at an international level (Meier *et al*., 2009*b*).

The most important BBCH stages that require particular attention by the farmers and researchers are: (a) stages 00–15: presowing herbicide application and mechanical weed control during the first year; proper time for sowing according to climate of each production area; (b) principal stages 4–6: the crop can be harvested for forage feed; (c) principal stages 5–7: crop nutrients requirements maximised and (d) stages 93–97: harvesting the crop for seed and/or biomass production.

Chapter 3

Inflorescence characteristics, seed composition, and allometric relationships predicting seed yields in the biomass crop *Cynara cardunculus*

Abstract

Cynara (*Cynara cardunculus*) is a perennial C3 herb that has its potential as bioenergy crop. This paper aims (a) to derive empirical relationships to predict cynara seed yield per head and per unit area, avoiding laborious extraction of seeds from the complex structure of its inflorescences; (b) to determine the head-weight distribution per unit area, the seed composition and the oil profile of cynara seeds; and (c) to estimate the range of cynara biomass, seed and oil yield in representative parts of Greece. We analyzed 16 field experiments, varying in crop age and environmental conditions in Greece. Seed yield per head (SY_{head}) can be accurately predicted as a linear function of dry head weight (H_w): $SY_{head} = 0.429 \cdot H_w - 2.9$ (r^2=0.96; n=617). Based on this relationship, we developed a simple two-parameter equation to predict seed yield per unit area (SY): $SY = HN \cdot (0.429 \cdot \mu - 2.9)$, where μ is the mean head weight (g head^{-1}) and HN is the total number of heads per unit area, respectively. The models were tested against current and published data (n=180 for head-level; n=35 for unit area-level models), and proved to be valid under diverse management and environmental conditions. Attainable cynara seed yields ranged from 190 to 480 g m^{-2} y^{-1}, on dry soils and on aquic soils (shallow ground water level). This variation in seed yield was sufficiently explained by the analyses of head-weight distribution per unit area (small, medium and large heads) and variability of seed/head weight ratio at head level. Seed oil concentration (average: 23%) and crude protein concentration (average: 18.7%) were rather invariant across different seed sizes (range: 26 to 56 mg seed^{-1}) and growing environments.

Introduction

Cynara cardunculus (commonly known as cynara) is a perennial C_3 herb prioritized as a new energy crop for Mediterranean areas because of its multiple uses and good yields even under harsh conditions. The crop can be used for solid biofuel production (Danalatos, 2008), as well as for biodiesel production, fibre production and forage production (Fernández *et al.*, 2006). Cynara's perennial character, its large root system, and the winter–spring growth cycle (usually rainfed) are important advantages of the crop.

Four important variables determine whether it is feasible to include cynara into the current cropping systems: biomass yield, product quality, heating value and production cost. Studies in Mediterranean region showed that cynara cultivation has an energy output : input ratio in the range of 15–30 (Danalatos, 2008; Angelini *et al.*, 2009; Mantineo *et al.*, 2009). This ratio is lower compared with other perennials, viz. giant reed and miscanthus. However, particularly due to its lower resource input (e.g. propagated by seeds instead of rhizomes and growing without irrigation during winter–spring), compared with summer C_4 perennials researchers inferred that cynara could be introduced in southern Europe for biomass production.

Cynara's biomass yield under rainfed conditions is usually reported at 15 t ha^{-1} y^{-1} (Fernández *et al.*, 2005; Danalatos *et al.*, 2006a; Danalatos *et al.*, 2007a; Raccuia and Melilli, 2007a; Angelini *et al.*, 2009) while dry biomass yields in excess of 30 t ha^{-1}y^{-1} have been attained (Dalianis *et al.*, 1996; Archontoulis *et al.*, 2008). The average heating value of the cynara plant has been estimated at 15–17 MJ kg^{-1} (Piscioneri *et al.*, 2000; Fernández *et al.*, 2006; Grammelis *et al.*, 2008; Angelini *et al.*, 2009). This energy content depends on the fraction of each plant component and its chemical composition and especially on the proportion of the oil rich seeds. Normally, the heating value per individual plant component is rather invariant contrary to the partitioning fractions (e.g. oil/seed and seed/biomass weight ratio) which largely depend on the environment × management interactions. Obviously detailed quantification of these seed-related fractions is essential in view of using the crop in the bioenergy sector.

Cynara cardunculus seed oil concentration ranges from 18.6 to 32.4% across different environments (Piscioneri *et al.*, 2000; Curt *et al.*, 2002). Regarding seed yield and seed/biomass ratio current information is rather scarce. To the best of our knowledge, rainfed cynara's seed yields range from 80 to 250 g m^{-2} at planting densities of ≤ 2 plant m^{-2} (Foti *et al.*, 1999; Piscioneri *et al.*, 2000; Raccuia and Melilli, 2007a; Ierna & Mauromicale, 2010). However, seed yield under appropriate management (e.g. higher plant densities; Raccuia & Melilli, 2007b) and high yielding environments is unknown.

The relatively few reports on seed yield might be attributed to the complex structure of cynara inflorescences. The basic type of inflorescence is the capitulum (head), which is organized in a (compound) corymb form. Within a plant or a unit area the heads of *Cynara cardunculus* are variable in terms of size, number, maturity and position on the plant. Within a head, seeds (achenes) are positioned at the base of the head (receptacle) surrounded by hairs (pappus) and bracts (erect spines), making seed extraction extremely laborious and time-consuming (Archontoulis *et al*., 2010a). Moreover, the seed/head weight ratio varies considerably across different head weights, thus cannot be easily addressed by a default value (Archontoulis *et al*., 2009).

Quantitative (allometric) relations are commonly used to quantify the relation that exists between the growth rates of different plant components. Allometric relations have also been used to assess a crop's investment in reproductive growth, both in annual crop species (e.g. in soybean, sunflower, maize; Vega *et al*., 2000) and in perennial crop species (e.g. in *Lesquerella*; Ploschuk *et al*., 2005).

Taking into account aforementioned difficulties in measuring seed yield, the primary objectives of this paper is to derive simple quantitative relationships, which can be used in practice to estimate seed yield per head and per unit area based on easily measurable inflorescence traits of cynara. In view of the lack of adequate information on attainable seed yield under varying management × environmental conditions, we also investigate the head-weight distribution per unit area, the seed composition and the oil profile of cynara seeds as a function of seed size, and the range of *Cynara cardunculus* biomass, seed and oil yield in representative parts of Greece.

Materials and Methods

Experimental sites and treatments

The data used in this paper were taken from 16 diverse experiments conducted in eight sites representing a wide range of environments in Greece. Table 3.1 shows the geographic location and some soil characteristics of the eight sites. Table 3.2 provides details for each of the 16 experiments, including crop age, cycle length and sampling date. The experimental sites cover a wide range of soil types, fertility status, and ground water levels. The crop had been established in different years (2004–2008) providing plant samples from the 1st to the 6th growing cycle. Moreover, some crops were sown in spring (March 20th ± one week) and some in autumn (November 15th ± one week). Hence, the growing cycle length varied from 9 to 16 months (Table 3.2). Crops were kept free from

weeds during the period of crop establishment by applying a pre-sowing herbicide and by mechanical weeding during initial crop stages.

Table 3.1: Geographic location and some soil characteristics of the experimental fields

Location	Coordinates and altitude	Soil type and classification[a]	Ground water table[b] organic matter (OM) and pH
Palamas	39°25'49 N 22°05'09 E Alt. 107 masl	Loam Aquic Xerofluvent	Presence of shallow ground water OM=1.0–1.6% at 0–50 cm pH=8–8.2
Ermitsi	39°24'49 N 22°05'03 E Alt. 100 masl	Loam Aquic Xerofluvent	Presence of shallow groundwater OM=1.2–1.8% at 0–50 cm pH=7.9–8.1
Kalivakia	39°26'19 N 22°04'51 E Alt. 97 masl	Loam Aquic Xerofluvent	Presence of shallow groundwater OM=1.1% at 0–50 cm pH=8.2
Koskina	39°29'08 N 22°00'24 E Alt. 85 masl	Loam Aquic Xerofluvent	Presence of shallow groundwater OM=1.4% at 0–30 cm pH=8.1
Velestino	39°23'55 N 22°44'36 E Alt. 87 masl	Clay Calcixerollic Xerochrept	No groundwater table OM=1.5–2.3% at 0–30 cm pH=7.6–8.0
Elliniko	39°19'53 N 22°16'45 E Alt. 120 masl	Clay Vertic Xerochrept	Presence of shallow groundwater OM=2.5% at 0–30 cm pH=8.2
Fillo	39°24'52 N 22°11'84 E Alt. 107 masl	Clay Vertic Xerochrept	Presence of shallow groundwater OM=2.0% at 0–30 cm pH=8.2
Mataraga	39°24'47 N 22°03'52 E Alt. 102 masl	Silty clay Aquic Vertic Xerofluvent	Presence of shallow groundwater OM=1.6% at 0–30 cm pH=8.3
Kilkis	41°14'39 N 22°45'56 E Alt. 250 masl	Sandy loam Typic Xerochrept	No ground water table OM=1.0% at 0–30 cm pH=6.8 (Slope relief)

All fields located in Thessaly Plain (central Greece), except for Kilkis.
[a]: According to USDA, 1975.
[b]: Shallow means that ground water ranged from 250 to 600 cm below surface during May; for other cases (Velestino and Kilkis) groundwater was deeper than 20 m below surface.

At some sites (viz. Palamas, Velestino, Kilkis, Ermitsi) the levels of irrigation and nitrogen fertilization were varied. Briefly, at Palamas (Karditsa) site, a 2×3 factorial experiment was carried out in which cynara was grown under a) rainfed conditions (common farmer practice) with three N-application levels (0, 8 and 16 g N m^{-2}); and b) supplementary irrigation during BBCH 59–65 (2–3 irrigations; total 120–170 mm; Exp 5, 10 and 16) with the same N levels. The BBCH coding system (Archontoulis *et al.*, 2010a) is used here to assess specific growth stages. At the Velestino site (Magnesia), two experiments were carried out; one was sown during 2004 with a plant arrangement of 100×50 cm (Exp 11, 12; Table 3.2) and one was established during 2008 with a plant arrangement of 75×25 cm (Exp 1). During the subsequent year, Exp 1 was divided into two analogous experiments (Exp 8: irrigated with 138 mm during BBCH 53–63 and Exp 9: rainfed).

Within each experiment 5 N–rates were applied (0, 6, 12, 18 and 24 g N m^{-2}). At Kilkis, the crop was grown under rainfed conditions and three N rates were applied (0, 8 and 16 g N m^{-2}; Exp 7). At Ermitsi (Karditsa) site (second growth cycle) the field was fertilized with 0, 8, or 16 g N m^{-2} and irrigated once during BBCH 60 with 55 mm (Exp 6). In all fertilized fields, N application took place during BBCH 51–55. The other fields (Exp 2, 3, 4, 13 and 15) comprised commercial crops, grown without additional irrigation and fertilizer inputs. The size of the specific experiments varied from 0.1 to 0.4 ha (individual plot size: 48–90 m^2) and the commercial fields comprised an area of several hectares. Planting arrangement was 75×25 cm in all experiments except Exp 11 and 12. There were no pests or diseases in the experimental plots.

Table 3.2: Summary of the experimental details and final plant height

Exp. # (symbol)	Location	Growing season	Cycle[a] length (month)	Year	Sampling date	Number of Samples	Number of heads[b]	Plant height (cm)
Parameterization datasets								
1 (○)	Velestino	1st	9	2008	Aug 1	6	30	55
2 (○)	Kalivakia	1st	9	2009	Aug 20	6	18	131
3 (○)	Mataraga	1st	9	2009	Aug 20	5	16	76
4 (○)	Koskina	1st	9	2009	Aug 20	6	18	118
5c (□)	Palamas	2nd	16	2007	Aug 4	12	72	238
6 (□)	Ermitsi	2nd	16	2008	Aug 5	6	48	305
7 (□)	Kilkis	2nd	16	2008	Aug 8	9	48	114
8 (▣)	Velestino	2nd	10	2009	Aug 2	30	90	208
9 (□)	Velestino	2nd	10	2009	Aug 1	30	86	206
10 (Δ)	Palamas	3rd	11	2008	Aug 4	24	128	234
11 (+)	Velestino	5th	10	2008	Aug 2	6	33	144
12 (×)	Velestino	6th	10	2009	Aug 1	6	30	194
Total						146	617	
Validation datasets								
13 (●)	Fillo	1st	9	2009	Aug 19	10	31	99
14 (▲)	Elliniko	2nd	16	2009	Aug 4	10	31	191
15 (■)	Ermitsi	3rd	11	2009	Aug 4	11	36	263
16 (♦)	Palamas	4th	11	2009	Aug 3	24	82	245
Total						55	180	

[a]: from BBCH 10 to 95–97.

[b]: Refers to the heads that were used for seed separation and not to total heads per sample.

c: At six additional samples, the total head weight, the total head number and the total seed yield per sample were measured (see later, Table 3.5).

Sampling protocol and measurements

Plants were cut approximately 10 cm above ground level at BBCH 95–97 (total: n=201 samples from 16 fields, Table 3.2). The sampling area was always 1 m^2. Every harvested sample was separated into stalks (stem and branches) and

heads, and fractions were weighed fresh in the field. Plant height was measured as well (Table 3.2). Leaves were left out from our analysis since they were dry and usually fell off during sampling. The moisture content of the harvested plants was around 30%. The collected materials were put in a storage room to dry naturally. The moisture content in equilibrium with the storage environment was subtracted after assessing dryness of random sub-samples by weighing in an oven at 70°C until constant weight.

After drying, stalks were weighed again to determine the total stalk dry weight m^{-2}. Per sample the heads were counted and weighed individually using an electronic balance (2-digits); the sum of the individual weights provided the total dry head weight m^{-2}. Total aerial dry biomass weight m^{-2} was calculated as the sum of the weights of stalks and heads. Then, 3–8 heads per sample (small: <20 g, medium: 20–40 g and large: >40 g; for abbreviations see Table 3.3) were randomly selected to manually separate the seed (n=797 heads, Table 3.2). The diameters of the selected heads were accurately measured too. The extracted seeds per head were counted and weighed. The quotient between seed weight and seed number expresses the individual seed weight (*SW*, Table 3.3).

Table 3.3: List of terms and abbreviations

Symbol	Definition	Unit
Small	Head weight size class: < 20 g head^{-1}	–
Medium	Head weight size class: 20–40 g head^{-1}	–
Large	Head weight size class: > 40 g head^{-1}	–
HN	Total number of seed-bearing heads per unit area	heads m^{-2}
HW	Total weight of seed-bearing heads per unit area	g m^{-2}
H_w	Single head weight	g head^{-1}
H_{base}	Threshold H_w required for seed set	g head^{-1}
HI_{head}	Seed / head weight ratio	g g^{-1}
SY_{head}	Seed weight per head	g seed head^{-1}
SY	Seed yield per unit area	g m^{-2}
SN_{head}	Seed number per head	seeds head^{-1}
SN	Seed number per unit area	seeds m^{-2}
SW	Individual seed weight (*SY / SN × 1000*)	mg seed^{-1}
µ	Mean head weight (*HW / HN*)	g head^{-1}

Seed composition and oil profile

Cynara cardunculus fruit (called seed for simplicity) is an achene, formed by the embryo (also called true seed or kernel) and the pericarp (hull). Seed materials were forwarded to chemical laboratories soon after processing, to avoid any hydration of the stored grain as observed by Maccarone *et al.* (1999). Two sets of experiments were performed. In 2008, medium sized seeds (30–40 mg seed^{-1})

were analyzed per location (Palamas, Ermitsi, Velestino and Kilkis). In 2009, seeds were graded into five weight classes (very small: <20 mg, small: 20–30, medium: 30–40, large: 40–50 and very large: >50 mg per seed) and analyzed for seed composition (oil, protein, cellulose, free fatty acids and ash). The concentrations (%) were expressed on dry weight basis, while total oil and protein content per seed (mg seed^{-1}) were calculated as *SW* multiplied by the concentration of each component. Seed protein concentration was approximated by the product of nitrogen concentration times (the default value of) 6.25, referred to as crude protein hereafter. Fatty acid composition of the extracted oil per group was also determined by gas chromatography. All data reported are expressed on dry-weight basis.

Data analysis

Seed parameters (weight and number) were first determined per head and subsequently converted into values per unit area. Two explanatory variables were initially assessed: (i) the weight of a single head and (ii) the diameter of a single head. Both variables are easily measurable inflorescence traits. Head weight is considered as an accurate measure while diameter as a fast and non-destructive measure. Among several methods/models in literature (e.g. Vega *et al.*, 2000), we selected the following two types of "allometric" models (simple and biologically meaningful) to fit our data:

Linear: $Y = a + bX$

Non-linear: $Y = Y_{max} \times \{2 / (1+\exp(-c \times (X - X_{base})))-1\}$

where *Y* denotes the dependent variable; *X*, is the independent variable; *a* is a constant parameter; *b*, is the slope of the regression (allometric coefficient); Y_{max} is the asymptote of the dependent variable; *c* is the parameter determining the steepness of the curve for the non-linear model; X_{base} is the intercept of the *X*-axis denoting a threshold value. In order to fit our models we used 12 datasets (parameterization sets: Exp 1–12, n=617; Table 3.2). Model validations were conducted using four independent datasets (Exp 13–16, n=180; Table 3.2).

Head-weight distribution

Per sample the heads were graded into three classes (small, medium and large; see Table 3.3) and frequency distribution histograms were produced per experiment. Statistical descriptors such as kurtosis (*k*), a measure of the "peakedness" of the frequency distribution, skewness (*s*), a measure of the asymmetry of the probability distribution, mean head weight μ, and standard

deviation σ, a measure of the variability in head weight, were calculated. The uniformity or the relative variability of the head-weight distribution per unit area was assessed by the coefficient of variation (CV, %), calculated as $\sigma/\mu \times 100$.

Thereafter, the 16 experiments were separated into three major groups. Group 1 comprises the first growth cycle experiments (Exp 1, 2, 3, 4, and 13; Table 3.2). Groups 2 and 3 refer to subsequent growth cycles experiments. Group 2 represents the experiments carried out on soils with no ground water (Exp 7, 8, 9, 11 and 12; Table 3.1 and 3.2) and Group 3 refers to the experiments carried out on soils with shallow ground water levels (Exp 5, 6, 10, 14, 15 and 16; Table 3.2).

Statistics

Analyses of variance were performed using GenStat software (12th Edition). At head-level, linear regression with groups (given the accumulated analysis of variance table) was performed to examine whether regression slopes and intercepts differed significantly among different experiments. Non-linear model parameters were derived from non-linear least-square regression in GenStat. The model's goodness of fit was assessed graphically (measured vs. predicted, residual plots) and by calculating r^2, *bias*, and rRMSE (relative root mean square error), as follows:

$$Bias = \frac{1}{n}\sum_{i=1}^{n}(O_i - P_i)$$

$$rRMSE = \frac{1}{\overline{O}}\sqrt{\frac{1}{n}\sum_{i=1}^{n}(O_i - P_i)^2}$$

where P_i and O_i are the predicted and observed values, respectively, $\overline{O}$ is the observed mean value and n is the number of observations. The *bias* measures the average difference between observed and predicted data. The rRMSE measures the relative difference between observed and predicted data, while a model's fit improves as rRMSE approaches zero. Seed and oil composition parameters across five seed sizes were assessed following one-way analysis of variance. Similarly, the parameters of the head-weight distribution per group were also subjected to one-way ANOVA.

Weather conditions

Thessaly Plain (central Greece) is characterized by a typical Mediterranean climate with hot, dry summers and cool, humid winters. A 30-year Thessaly

climatic average (1974–2006; data from Hellenic National Meteorological Service) reports mean annual precipitation of 568 mm (172, 113, 70 and 211 mm during winter, spring, summer and autumn periods, respectively) and a mean daily air temperature of 16.0 °C (7.5, 20.1, 25.3 and 11.1 °C during winter, spring, summer and autumn periods, respectively). The major part of cynara's growth cycle takes place in winter and spring, during which usually no irrigation is applied. The total amounts of effective precipitation at the experimental fields of Thessaly (period: October–July) were 449, 378 and 709 mm for the 2007, 2008 and 2009 seasons, respectively. For Kilkis (2008) the precipitation was 401 mm. Temperature did not fluctuate much from its climatic mean values.
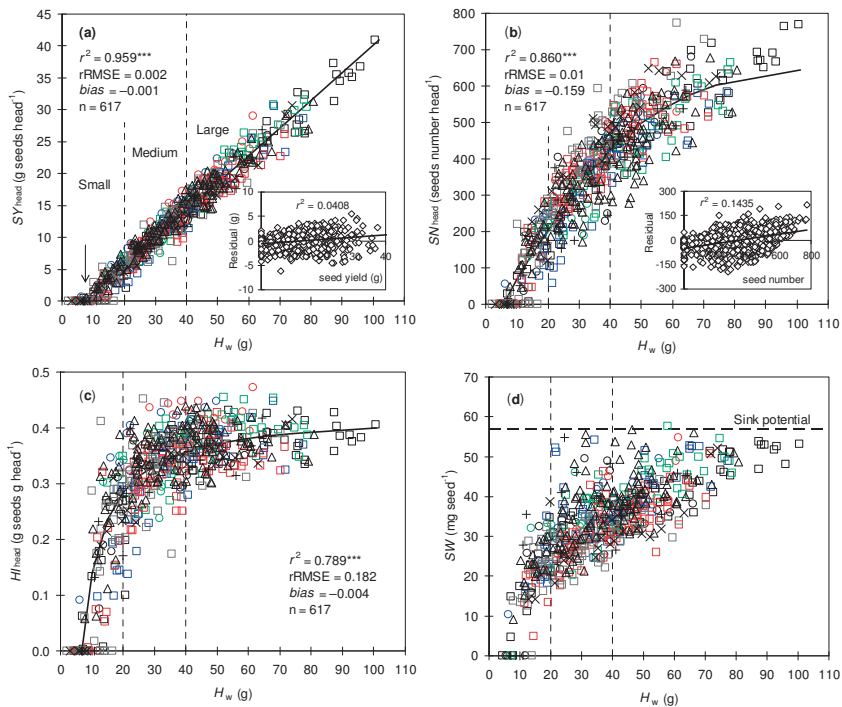
Figure 3.1: (a) Seed weight per head (SY_{head}), (b) seed number per head (SN_{head}), (c) seed/head weight ratio (HI_{head}) and (d) individual seed weight (SW) as a function of head weight (H_w). Different symbols indicate material collected from different environments (Exp 1–12; Table 3.2). Fitted equations (solid bold lines) and parameters are provided in the text. *Y*-variable residuals are shown in the insets. Vertical broken lines indicate three classes of different head weights (small, medium, large; Table 3.3). Horizontal broken line (panel d) indicates seed sink potential. Arrow (panel a) indicates the threshold head weight required for seed set (H_{base}). *** indicates significant at *P*<0.001; *bias* and rRMSE definitions are provided in the text.

Results

Seed yield

Figure 3.1 illustrates the relationships between seed yield per head (SY_{head}), seed number per head (SN_{head}), seed/head weight ratio (HI_{head}) and individual seed weight (SW) as a function of head weight (H_w, Table 3.3).

SY_{head} ranged from 0 to 41 g head^{-1} and H_w ranged from 2.5 to 100 g (Fig. 3.1a). SY_{head} showed a linear relationship with H_w for each treatment × experiment combination included in the study (n=146 sets; Table 3.2). Regression analyses showed that lines ran almost parallel, and the intercepts were very similar. Thus, treatments within each experiment were grouped and 12 regression lines were constructed (Table 3.4).

Table 3.4: Parameters (standard error in parenthesis) of the linear regression ($Y=a+bX$) between seed yield per head and two explanatory variables for 12 independent sets

	Variable 1: head weight (g)			Variable 2: head diameter (cm)			
Exp.	b	a	r^2	b	a	r^2	n
1	0.432 (0.01)	–3.091 (0.54)	0.97	3.90 (0.30)	–11.44 (1.75)	0.86	30
2	0.408 (0.03)	–1.952 (0.87)	0.93	3.02 (0.36)	–7.27 (2.11)	0.81	18
3	0.469 (0.02)	–2.384 (0.57)	0.98	5.33 (0.59)	–17.66 (3.31)	0.85	16
4	0.446 (0.03)	–1.314 (1.33)	0.93	3.50 (0.58)	– 6.34 (3.96)	0.70	18
5	0.425 (0.01)	–3.003 (0.38)	0.98	5.09 (0.19)	–17.46 (1.30)	0.92	72
6	0.448 (0.01)	–3.165 (0.73)	0.95	4.70 (0.36)	–15.06 (2.52)	0.79	48
7	0.448 (0.02)	–4.161 (0.63)	0.95	6.49 (0.50)	–29.29 (3.26)	0.79	48
8	0.412 (0.01)	–3.007 (0.32)	0.96	4.64 (0.20)	–15.74 (1.18)	0.86	90
9	0.443 (0.01)	–3.453 (0.38)	0.94	4.78 (0.32)	–16.06 (1.69)	0.72	86
10	0.410 (0.01)	–1.933 (0.34)	0.95	4.85 (0.21)	–17.45 (1.35)	0.81	128
11	0.431 (0.01)	–3.185 (0.54)	0.97	3.63 (0.36)	– 9.24 (2.18)	0.77	33
12	0.424 (0.01)	–2.777 (0.44)	0.98	4.28 (0.39)	–13.12 (2.30)	0.82	30

All regressions were significant at P <0.0001.
Details per experiment are provided in Table 3.2.
n, number of individuals per set.

This analysis showed that slopes did not differ significantly across environments (P=0.123). Accordingly, data from all experiments were pooled (n=617). Within this complete dataset, we further examined possible differences in slope between head weight classes (small, medium and large). Three regression lines were constructed and stepwise regression analysis revealed that SY_{head} vs. H_w relationship remained unchanged for the different head weight classes (P=0.075; Fig. 3.1a). Hence, SY_{head} could be described adequately by a single, simple linear regression model (r^2=0.96; Fig. 3.1a):

$$SY_{head} = 0.4293 \, (\pm 0.003) \cdot H_w - 2.9048 \, (\pm 0.144) \tag{1}$$

where SY_{head} is the seed yield per head and H_w is the single head weight. Values in parenthesis represent ± standard error of the regression estimates. SY_{head} becomes zero when $H_w = 6.76$ g. The value of 6.76 g thus indicates the threshold head weight, required for seed set (hereafter H_{base}). Thus, Eq. (1) is applicable to $H_w \geq 6.76$ g. The slope of the regression (viz. 0.4293) is an allometric coefficient that expresses the fraction of head growth above the threshold allocated to seeds.

Eq. (1) was validated by using four independent data sets (Exp 13–16, Table 3.2). Graphical visualization of its performance is depicted in Fig. 3.2. Statistical criteria revealed that the model performed well ($r^2 = 0.89$–0.97; rRMSE = 0.12–0.19; *bias* = –0.35 to 0.68 g; Fig. 3.3) and was therefore accurate enough for further use. Consequently, Eq (1) was applied to every head present in a sample, thus upscaling individual head weights to seed yield per unit area level (SY, g m^{-2}) as indicated below:

$$SY = \frac{\sum_{i=1}^{n}(0.4293 \cdot H_{wi} - 2.9048)}{A_s} \tag{2}$$

where A_s refers to the size of the sample area (m^2). Eq. (2) was used in our study to derive seed yields per treatment. This procedure implies separate weighing of all heads (n parameters) included in a sample. To obtain a more convenient procedure for determining seed yield, Eq (2) can be simply re-written also as:

$$SY = HN \cdot (0.4293 \cdot \mu - 2.9048) \tag{2a}$$

or

$$SY = 0.4293 \cdot HW - 2.9048 \cdot HN \tag{2b}$$

where μ is the mean head weight, HN and HW ($= \mu \times HN$) are the total number and weight of all seed-bearing heads per unit area respectively (Table 3.3). Eq. (2a or 2b) simply shows that SY increases with an increase of HW, whereas the term $2.9048 \cdot HN$ accounts for the cumulative threshold head weights required for seed set. Eq. (2a and b) illustrates a two-parameter model, comprising a much faster and easier way to calculate total seed yield per unit area. For such a purpose, barren heads (≤ 6.76 g head^{-1}) should be excluded in the calculation.
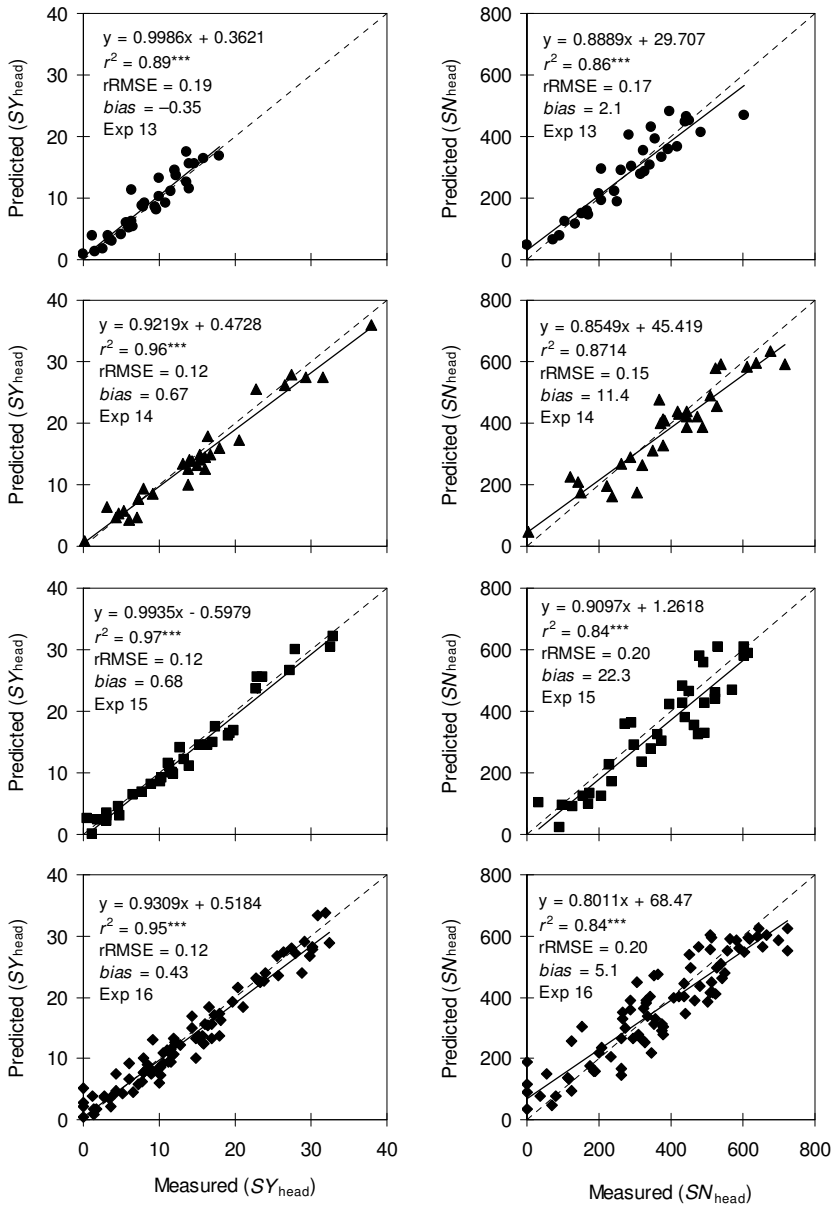
Figure 3.2: Predicted versus measured seed yield per head (SY_{head}, left panels) using Eq. (1) and seed number per head (SN_{head}, right panels) using Eq. (3). Four independent datasets (Exp 13–16; 1st, 2nd, 3rd and 4th growing cycle; Table 3.2) were used to evaluate Eq. (1) and (3) goodness of fit at head-level. Diagonal broken lines are 1:1. Statistics as in Fig. 3.1.

Five independent data sets (Table 3.5) were used to evaluate the ability of Eq. (2b) to predict total seed yields (Fig. 3.3). Eq. (2b) performed very well for data from Exp 5 (μ=33 g m^{-2}; rRMSE=0.07; Fig. 3.3) and for the published data from Piscioneri *et al*. (2000), Raccuia & Melilli (2007a) and Ierna & Mauromicale (2010) (μ = 18 g m^{-2}; rRMSE=0.24; Fig. 3.3). Data from Foti *et al*. (1999) were not predicted well (Fig. 3.3), most probably due to a low μ (= 12 g head^{-1}), which led us to suspect that non seed-bearing heads ($\leq$ 6.76 g) were included in the sample. However, the general trend across all datasets (n=35) indicated a good agreement between predicted and measured seed yield (r^2=93%; *bias*=14 g m^{-2}; rRMSE=0.23; n=35; Fig. 3.3). Predictions using Eq. (2b) would be further improved, if information on number of barren heads ($\leq$ 6.76 g) per sample was known for the published data sets.

Table 3.5: Validation datasets used to test the performance of Eq. (2b) at unit area level

Set	Year[a]	Genotype(s)[b]	Density	μ	n	Source[c]
1	1994 1995	Bianco avorio Gigante di Lucca	1.2 pl m^{-2}	13.0	4	Foti *et al*. (1999)
2	1995 1996	9 genotypes (see reference)	1 pl m^{-2}	19.2	18	Piscioneri *et al*. (2000)
3	1999 2000	Bianco avorio Cardo di Nizza	2 pl m^{-2}	17.7	4	Raccuia & Melilli (2007a)
4	1999 2000 2001	Cardo gigante di Romagna	1.3 pl m^{-2}	15.0	3	Ierna & Mauromicale (2010)
5	2007	Bianco avorio	5 pl m^{-2}	32.1	6	This study (Exp 5)[d]

[a]: Observation year.

[b]: All genotypes belong to the botanical variety *C. cardunculus* L. var. *altilis* DC.

[c]: Literature data on total head weight, number and seed yield were recorded from tables or read from figures and refer to mean values. Presence or absence of non seed-bearing heads (<6.76 g) in the sample is unknown. Experiments were carried on clay soils (without groundwater).

[d]: Barren heads were excluded.

n, number of data per set; μ, mean head weight per set.
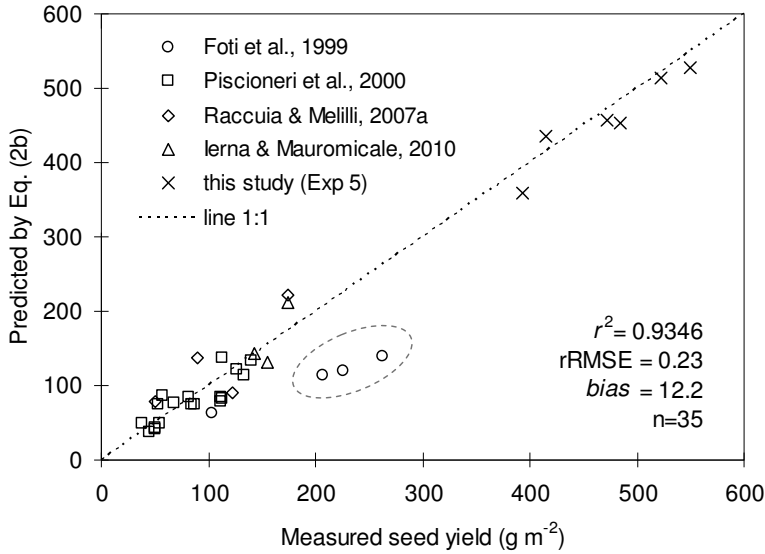
Figure 3.3: Seed yield of *Cynara cardunculus* predicted by Eq. (2b) versus measured seed yield. Details on the validation datasets are provided in Table 3.5. Statistical indices refer to all data (n=35). The three encircled points are outliers, resulting from the low mean head weight (μ=13 g head^{-1}).

Seed number

Across the 12 experiments, seed number per head (SN_{head}) showed a non-linear relationship with H_w (Fig. 3.1b). We described this relationship using the following non-linear model (r^2=0.86; n=617):

$$SN_{head} = 665.2(\pm 16.9) \cdot \left(\frac{2}{1 + \exp(-0.0436(\pm 0.002) \cdot (H_w - 5.422(\pm 0.526)))} - 1 \right) \tag{3}$$

Values in parenthesis represent ± standard error of the estimates. Eq. (3) estimated the threshold head weight for seed set at 5.4±0.53 g head^{-1}, which is (not surprisingly) close to the threshold estimated based on seed yield by Eq. (1). To avoid any misunderstandings, we propose that Eq. (3) should be applied to heads ≥ 6.76 g, similar to the seed yield model. The maximum seed number per head was most often 650–680 (Fig. 3.1b).

The non-linear model can also be parameterized separately for specific experiments. To test whether Eq. (3) was valid for material collected from different experiments (Exp 1–12; Table 3.2), Eq. (3) (with three parameters) was compared with the experiment-specific model (12 experiments × 3 parameters =

36 estimates). Predictions were assessed using the adjusted r^2 in order to account also for the degrees of freedom (slightly higher prediction is counterbalanced by a loss of degrees of freedom). The experiment-specific model improved predictions only slightly, from $r_{adj}^2 = 0.860$ to $r_{adj}^2 = 0.884$, meaning that the combined three-parameter model was adequate enough for further use.

Eq. (3) fitted the data well if H_w ranged from 6 to 75 g, and slightly underestimated seed number at very large head weights (>75 g; Fig. 3.1b inset). However this is of low importance, since such large heads are rare, even under optimum conditions. We also tested other non-linear models such as negative exponential and rectangular hyperbola, to see whether this underestimation would disappear. The r^2 values, residual plots, and biases were similar for all model types. Therefore, we continued our analysis using Eq. (3) because its parameters have a clear biological meaning.

The higher scattering of the seed number data compared with seed weight data, caused slightly lower prediction ability of Eq. (3). Similar to Eq. (1), Eq. (3) was also evaluated with four independent datasets (Exp 13–16; Table 3.2) and statistics showed that predictions were good ($r^2 \approx 0.85$; rRMSE ≈ 0.18; *bias* ≈ 10; Fig. 3.2). Consequently, model (3) was applied to every seed-bearing head present in a sample, thus upscaling individual head weight to seed number per unit area level (*SN*, seeds m^{-2}) as indicated below:

$$SN = \frac{\sum_{i=1}^{n}\left(665.2 \cdot \left(\frac{2}{1+\exp(-0.0436 \cdot (H_{wi}-5.422))}-1\right)\right)}{A_s}$$

(4)

The calculated seed number m^{-2} ranged from a minimum of 1764 to a maximum of 20566 seeds m^{-2}.

Seed harvest index and individual seed weight

Fig. 3.1c depicts the relationship between the seed/head weight ratio HI_{head} (g g^{-1}) and H_w. This relationship was described from Eq. (1) by dividing both parts with H_w, as follows:

$$HI_{head} = 0.4293 - \frac{2.9048}{H_w}$$

(5)

Eq. (5) implies that HI_{head} increases with increasing H_w. The mean HI_{head} per head class was: 0.18, 0.33 and 0.39 g g^{-1} for small, medium and large heads respectively. The low determination coefficient of Eq. (5) ($r^2 = 0.79$; Fig. 3.1c) is

due to the large data scatter caused by the combined random error of SY_{head} and H_w.

Fig. 3.1d shows that the individual seed weight, (SW, calculated as SY_{head}/SN_{head}) varied considerably across different H_w. It ranged from about 10 to a maximum value of 57 mg seed^{-1} (data mean: 33.4 mg seed^{-1}). This upper threshold value gives an indication of the potential sink capacity of *Cynara cardunculus* seed under Greek conditions (Fig. 3.1d).

Head diameter and head surface area as predictors

Head samples collected from different environments, although having similar weights, showed differences in shape (ovate to globular). Small, medium and large heads had diameters of 2–5, 3–7 and 4–10 cm, respectively (Fig. 3.4a). Contrary to H_w, the head diameter (non-destructive method) did not strongly correlate with SY_{head} (see r^2 in Table 3.4) and SN_{head} (data not shown). Fig. 3.4a illustrates the relationship between SY_{head} and head diameter, while Table 3.4 presents the regression slopes and the constant values for the 12 experiments (parameterization datasets). Slopes of the regressions were significantly different ($P<0.01$) among the 12 sets, thus our hypothesis on using head diameter as an appropriate means to estimate seed yield was rejected. We also examined the head surface area as the predictor (Fig. 3.4b) but regression slopes were still significantly different among environments. Our analysis indicated that neither head diameter nor surface area should be used as predictors for SY and SN.
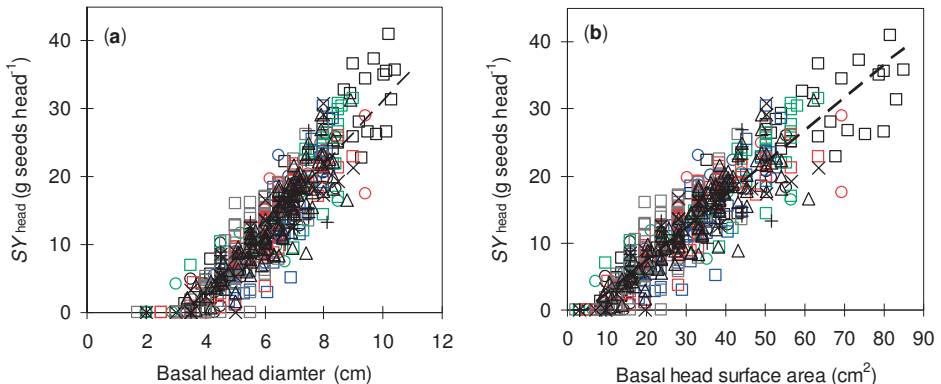
Figure 3.4: (a) Seed weight per head (SY_{head}) as a function of head diameter and (b) of head surface area. Different symbols indicate material collected from different environments (Exp 1–12; Table 3.2). Broken bold lines indicate linear regressions.

Head-weight distribution

Cynara cardunculus is an indeterminate crop species and forms many heads of various weights. Small, medium and large head-weight frequency distributions as well as statistical descriptors per experiment are illustrated in Fig. 3.5. The analyses indicated that the head distributions, the total number of heads, and the mean head weight varied significantly across 16 experiments, in contrast to coefficient of variation, kurtosis and skewness that varied only slightly.
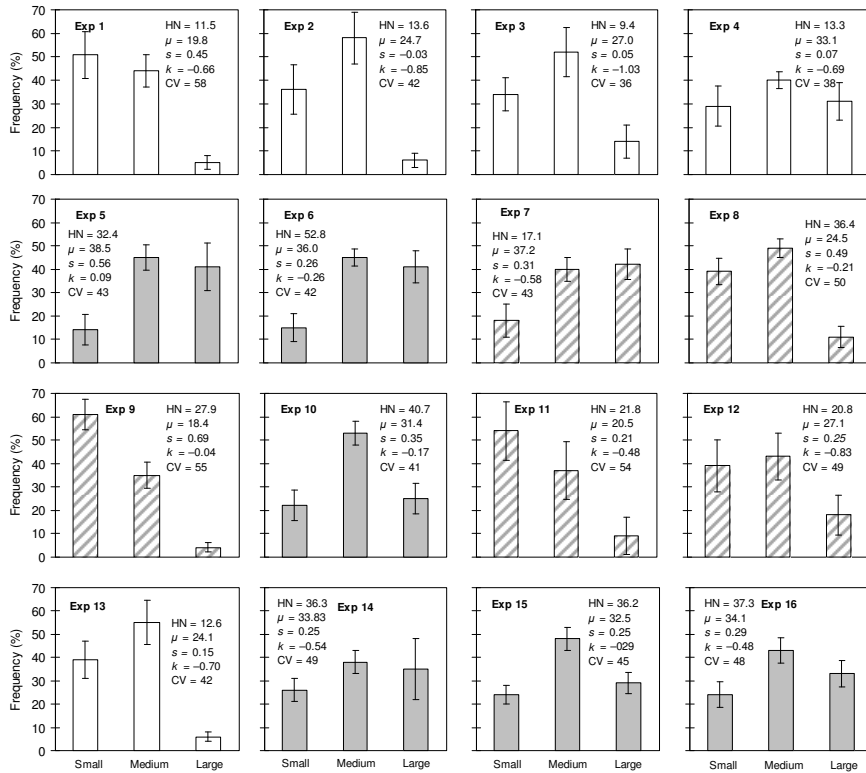
Figure 3.5: Frequency distributions (± standard deviation) of *Cynara cardunculus* heads per m² (small, medium and large; Table 3.3) for 16 experiments carried out in Greece in 2007–2009. Open columns represent the 1st cropping cycle experiments. Partially and fully gray columns refer to experiments from 2nd to 6th growing cycle, for dry and aquic soils, respectively. Details on the experiments are provided in Tables 3.1 and 3.2. *HN* = total number of head per m², *μ* = mean head weight (g head⁻¹), *s* = skewness, *k* = kurtosis, CV = coefficient of variation, for other symbols see Table 3.3.

In the present analysis, we classified the experiment-to-experiment variability into three major groups (Group 1: 1st cycle; Group 2 and Group 3 refer to subsequent cycles on dry and aquic soil types, respectively; Table 3.6 and Fig. 3.5). Under the prevailing management conditions in Greece (note planting arrangement 75×25 cm), cynara produced about 12 heads m^{-2} during the establishment year. During subsequent years, the crop formed 25 and 40 heads m^{-2} on dry and on aquic soils types, respectively ($P<0.001$; Table 3.6).

Table 3.6: Inflorescence characteristics of *Cynara cardunculus* during crop establishment cycle (Exp. 1, 2, 3, 4 and 13: group 1) and during subsequence growing cycles on dry (Exp. 7, 8, 9, 11 and 12: group 2) and on aquic soils (Exp. 5, 6, 10, 14, 15 and 16: group 3) in Greece in 2007–2009

Exp.	Number of heads per m^2							μ	CV	k	s
	Total	Small		Medium		Large					
Group	#	#	%	#	%	#	%	g head^{-1}	%	–	–
Group 1	12.1a	4.8a	38b	5.8a	50a	1.4a	12a	25.8a	43a	–0.8c	0.14a
Group 2	24.8b	11.1a	42b	10.1ab	41a	3.6ab	17a	25.6a	50a	–0.4ab	0.39b
Group 3	39.8c	8.1a	20a	18.5c	46a	13.2c	34b	34.5b	44a	–0.2a	0.34b
Mean	25.6	8.0	33	11.5	46	6.1	21	28.6	46.0	–0.5	0.29

Different letter within a column indicates significant difference at $P < 0.05$.

CV, coefficient of variation; k, kurtosis; s, skewness, for other symbols see Table 3.3.

Fig. 3.5 depicts that the frequency distributions, and particularly the distributions of small and large heads were significantly affected across different sets of experiments ($P<0.05$; Table 3.6). Nevertheless, the CV was unchanged for these sets of experiments (CV = 46%; $P=0.22$; Table 3.6). This is because on dry sites the distribution was: small 42%, medium 41% and large 17%, whereas on aquic sites the distribution was: small 20%, medium 46% and large 34%. Hence, it can be inferred that beyond the 1st cycle, under conditions of high soil moisture availability (shallow ground water) an increased *HN* by some 35% (large heads by 72%) may be expected compared to conditions of moderate water stress (dry soils). This is expected since cynara – as all crops – performs much better on aquic soils where high seed yields are expected (see later Fig. 3.6). Across different experiments the mean head weight, μ, was ≤ 40 g head^{-1} (Fig. 3.5), indicating an upper threshold value.

Analysis of skewness and kurtosis showed that on average *Cynara cardunculus* head-weight distribution was platykurtic (k = –0.48) and positively skewed (s = 0.29; Table 3.6). On aquic soil types this distribution tended to reach the normal distribution, since k and s shifted from –0.39 to –0.22 and from 0.41 to 0.34, respectively (Table 3.6; Fig. 3.5).

Seed composition

Seed composition parameters for different *SW* classes are presented in Table 3.7. Oil concentration significantly increased with an increase in seed size from 17 to 26 mg seed^{-1} (*P*=0.016), while in the range from 26 to 52 mg seed^{-1}, the oil concentration was rather constant at 22.9%. Calculating oil content per seed (mg oil seed^{-1}), a significant effect of seed size was detected (*P*<0.001), throughout the range of seed weights studied (Table 3.7). Crude protein concentration (%) was not significantly affected by seed size (average 18.7%; *P*=0.252), but for protein content (mg protein seed^{-1}), the effect proved significant (*P*<0.001). Seed ash concentration significantly decreased with increasing seed size (*P*=0.01), whereas cellulose (mean: 22.1%), free fatty acids (mean: 1.18%) and seed moisture (mean: 5.9%) contents were not affected by seed size (*P*>0.05; Table 3.7). Seed samples collected from different environments (2008), showed similar oil (*P*=0.132) and protein (*P*=0.992) concentrations (data not shown). Across four different sites, *Cynara cardunculus* seed oil concentration ranged from 20.9 to 25.9%, while crude protein ranged from 14.1 to 20.9% (average: 18%).

Table 3.7: *Cynara cardunculus* seed composition (*n*=3) as affected by seed size

Seed size (mg)		Oil		Crude protein		Cellulose	Ash	FFA	Moisture
Range	Aver.	%	mg	%	mg	%	%	%	%
< 20	17a	17.01a	2.73a	19.76a	3.06a	24.31a	4.41a	2.40a	6.39a
20–30	26b	21.38b	5.57b	19.46a	5.05b	21.95a	3.97b	1.61a	6.38a
30–40	35c	23.20b	8.06c	18.21a	6.26c	21.48a	3.44c	0.93a	5.69a
40–50	46d	23.09b	10.62d	16.98a	7.81d	21.74a	3.44c	0.61a	5.53a
>50	52e	22.53b	11.94d	19.32a	10.23e	21.96a	3.28c	0.51a	5.24a
Mean	35.07	21.81	7.81	18.68	6.44	22.09	3.61	1.18	5.85

Different letter within a column indicates significant difference at *P* < 0.05.
FFA, free fatty acids.

Oil composition

The oil composition for different *SW* is provided in Table 3.8. Gas chromatography allowed to separate methyl esters of fatty acids from C12:0 (lauric) to C24:0 (lignoceric). No significant differences were observed for any of the studied gas chorography parameters (*P*>0.05), indicating that chemical composition of cynara seed oil was conservative. The average fractions of the major fatty acids were: 12.2% palimitic (C16:0), 3.7% strearic (C18:0), 27.9% oleic (C18:1) and 54.0% linoleic (C18:2). These four acids amounted to 97.8% of the total, while the remaining 2.2% was divided over several minor acids (C14:0 =

0.14%, C16:1 = 0.23%, C17:0 = 0.05%, C18:3 = 0.06%, C20:0 = 0.40%, C22:0 = 0.13%, C24:0 = 0.23%, etc.). The effect of location on oil profile was not significant (data not shown).

Table 3.8: Major fatty acid composition (*n*=2) of the seed oil obtained from different seed sizes

Seed mg (range)	C16:0 (palmitic)	C18:0 (stearic)	C18:1 (oleic)	C18:2 (linoleic)
< 20	15.47a	4.84a	28.83a	47.66a
20–30	11.96a	3.70a	27.64a	54.58a
30–40	11.10a	3.20a	24.89a	59.12a
40–50	11.10a	3.42a	28.18a	55.25a
>50	11.19a	3.53a	29.98a	53.44a
Mean	12.16	3.74	27.90	54.01

Different letter within a column indicates significant difference at $P < 0.05$.
Values expressed in %.

Cynara yields in Greece

Figure 3.6 presents average biomass, seed and oil yields per experiment. During the year of establishment, *Cynara cardunculus* biomass productivity was about 550 g m^{-2}, while during subsequent cycles, the biomass productivity increased to 1300 g m^{-2} on dry and to 2700 g m^{-2} on aquic soils, respectively (Fig. 3.6a). Harvest index ranged from 0.104 to 0.196 g g^{-1} (Fig. 3.6b), and the lower values were obtained on dry soils. Seed yields ranged from 100 g m^{-2} during the first cycle to 190 (dry soils) and to 480 g m^{-2} (aquic soils) during subsequent crop cycles (Fig. 3.6b). The range of *Cynara cardunculus* oil yield potential in Greece was 23 to 110 g m^{-2} (Fig. 3.6c). Seed number ranged from about 3200 (1st cycle) to 6000 on dry soils and finally to 14000 seeds m^{-2} on aquic soil types, respectively (data not shown).

By combining Eq. (2a) and Eq. (4) the average *SW* per m^{-2} was calculated for each experiment (32 ± 4 mg seed^{-1}; Fig. 3.6d). Despite the great variation in biomass, seed yield and seed number across experiments (e.g. Fig. 3.6a and b), the average seed weight (mg seed^{-1}) was rather invariant and varied only by 10%.
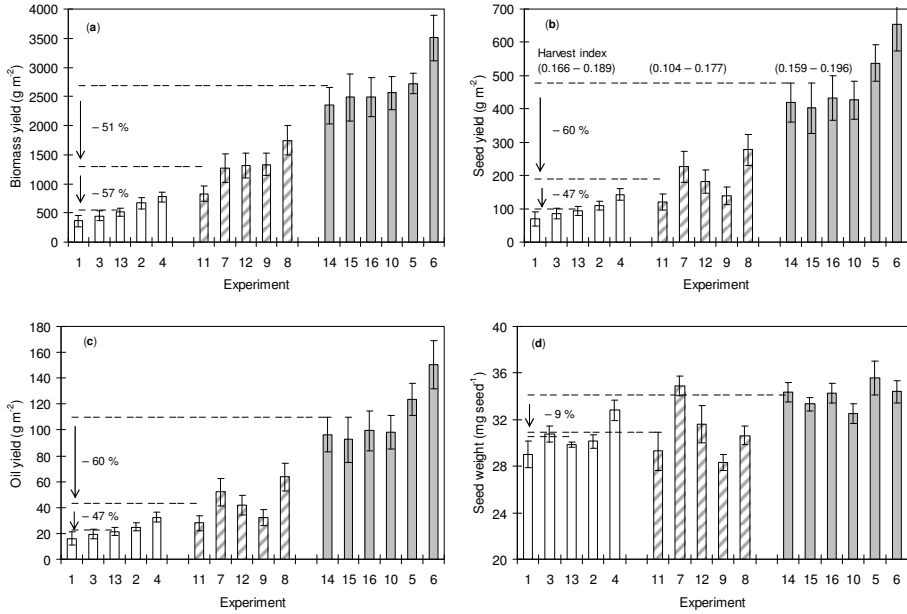
Figure 3.6: (a) *Cynara cardunculus* average (± standard deviation) biomass yield, (b) seed yield (calculated from Eq. 2a), (c) oil yield (estimated at 23% of *SY*) and (d) individual seed weight (calculated as *SY/SN*) for 16 experiments carried out in Greece in 2007–2009. Open columns represent the 1st cropping cycle experiments (group 1). Partially and fully gray columns refer to experiments from 2nd to 6th growing cycle, for dry (group 2) and aquic (group 3) soils, respectively. Details on the experiments are provided in Tables 3.1 and 3.2. Broken lines refer to average values per group (as in Table 3.8) while arrows accompanied by a percentage value indicate yield reduction from group 3 to group 2 and from group 2 to group 1. The range of seed harvest index (g g^{-1}; leaves were excluded in calculations) per group is also provided in panel b.

Discussion

This paper provides information on head weight, head number, seed quantity and seed quality of *Cynara cardunculus*. We provide an easy and robust methodology for estimating seed yield under varying management × environmental conditions, thus improving our understanding of the reproductive allometry of this perennial species.

Seed yield in relation to inflorescence traits

This study documented that in *Cynara cardunculus* the threshold head weight required to support seed set is 6.8 g per head and that of all additional biomass investments in the head a fraction of 0.43 is allocated to the seeds (Fig. 3.1a). These allometric coefficients were the same for different growing situations in Greece (e.g. crop age, location, soil types etc; Table 3.4). Environmental as well as management variables affect seed yield through their effects on μ and HN (Fig. 3.5 and 3.6). Based on these parameters (H_w, μ, and HN) we presented a variety of allometric models, which can be used from organ- to land-level studies, depending on the research interest.

At head-level, using H_w as independent variable, the seed yield can be estimated very accurately (r^2=0.96; Eq. 1; Fig. 3.1a) while seed number can also be estimated but with somewhat lower accuracy (r^2=0.86; Eq. 3; Fig. 3.1b). This is attributed to the observed variability in seed number per head (Fig. 3.1b). Harper *et al.* (1970) stated that seed number and seed size represent alternative strategies in the allocation of reproductive resources, while Sadras (2007) mentioned that seed number is plastic and highly sensitive to resource availability. Due to this sensitivity, the SN_{head} model (Eq. 3) could not be as precise as the SY_{head} model (Eq. 1). Lastly, at organ level, a strong association between HI_{head} over varying H_w was presented (Fig. 3.1c). With larger heads (>40 g) the initial investment (6.8 g) is supported by more seeds, resulting in a higher HI_{head} (average: 0.39) compared to smaller heads (<20 g; average HI_{head}: 0.18; Fig. 3.1c), meaning that growers and researchers should aim for practices resulting in a higher number of large heads. In literature, Foti *et al.* (1999), Piscioneri *et al.* (2000), Fernández *et al.* 2005; Fernández *et al.* (2007a) and Gominho *et al.* (2009) reported HI_{head} from 0.18 to 0.40 g g^{-1}, which fits within our range.

At unit area-level, the parameters of Eq. 2a or 2b are two easily measurable inflorescence traits (HW and HN), which are commonly determined in cynara ecophysiological studies (e.g. Piscioneri *et al.*, 2000). The fact that SY model performed well (r^2=0.93; Fig. 3.3) across a wide range of published data (Foti *et al.*, 1999; Piscioneri *et al.*, 2000; Raccuia & Melilli, 2007a; Ierna & Mauromicale, 2010) and the current data (Table 3.5) including different management techniques, environmental conditions as well as different genotypes, implies the potential applicability of the present empirical model.

This model could also assist yield component analysis. Eq. (2a) indicates that seed yield is determined by mean head weight (μ) and total head number per unit area (HN). Simply increasing the number of heads will be beneficial for seed yield as long as this doesn't put a too strong burden on μ. According to Fig. 3.5 and Table 3.5, the μ is largely dependent on management × environment interactions.

Our analysis implies advantage can be gained from developing a crop with larger heads (higher μ) and secondly from increasing the number of heads, particularly in high yielding environments, in order to minimize the loss caused by the initial investment in heads before seed set. This view is confirmed by Raccuia & Melilli (2007b), who – while increasing planting density from 1 to 4–8 plants m^{-2} (1st cycle) – noticed that branching and head number plant^{-1} reduced, resulting in a higher μ, and consequently higher seed yield per unit area (more than double). Moreover, the same authors' (Raccuia & Melilli, 2007a), found a great variability in seed yield among several (cultivated and wild cardoon) genotypes; indicating therefore that breeding programs can also assist in developing cultivars suitable for varying cropping systems.

This study also depicted the range of attainable yields of *Cynara cardunculus* (biomass, seed and oil) in representative parts of Greece. Maximum observed biomass production was 3500 g m^{-2} – in line with Dalianis *et al*. (1996) – and it was obtained on aquic soils after a growth period of 16 months. Actually, at one of the sites with this soil type, the depth of cynara's main roots was measured up to 180 cm whereas the fine roots were found at a depth up to 330 cm (in May), providing evidence that the crop can make use of deep ground water. Across three growing seasons on aquic soils the average biomass production was 2700 g m^{-2} y^{-1}, which was 51% higher than obtained in dry environments (see Fig. 3.6 and also Piscioneri *et al*., 2000; Fernández *et al*., 2005; Danalatos *et al*., 2007a). Similarly, the seed yield on aquic soils (480 g m^{-2} y^{-1}) was 60% higher compared with yield on dry soils. Cynara seed yields are even close to sunflower grain yields obtained in Greece.

Great differences were also found for *SN* among 16 experiments. Nevertheless, the individual seed weight, *SW*, varied less than 10% among the 16 experiments (32 ± 4 mg seed^{-1}; Fig. 3.6d) and this might give an indication for the attainable sink capacity of *Cynara cardunculus* seeds under Greece conditions. Experimental average *SW* values are in accordance with literature data (Foti *et al*., 1999; Raccuia & Melilli, 2007a; Ierna & Mauromicale, 2010). However, despite the great head-to-head variability in *SW*, it seems that the average *SW* at unit area level was rather conservative, similarly to most common grain crops (Sadras, 2007).

Seed quality

Four parameters define the potential of cynara as an oil crop: seed yield, seed oil content, fatty acid profile and heating value (Fernández *et al*., 2006). This paper addresses three of those. The higher oil heating value has been measured at 33 MJ kg^{-1} (Fernández & Curt, 2004). The current results on seed oil concentration are in close agreement (±5%, Table 3.9) with data obtained in previous works from

Spain (Curt *et al.*, 2002), Portugal (Carvalho *et al.*, 2006) and from Italy (Piscioneri *et al.*, 1999; Raccuia & Melilli, 2007a). Usually high temperatures during grain filling result in lower oil concentrations (Fernández-Moya *et al.*, 2005). Under Greek conditions, cynara seed contains approximately 23% oil, which is lower than common annual oil seed crops growing in the Mediterranean region for biodiesel production (viz. sunflower, rapeseed: 40–46%; S.V. Archontoulis, unpublished results).

The observed stabilization/constancy of the seed-oil concentration at medium–large sized seeds (Table 3.7) might be attributed to the oil distribution within the seed. Curt *et al.* (2002) reported that the seed fraction to hull (44.5%) and to kernel (55.5%) was similar between different seed sizes. Stabilization of oil concentration across different kernel weights has also been observed for maize (Borrás *et al.*, 2002).

The fatty acid composition of the oil determines its suitability for either food or industrial uses. The current findings have shown 10.9% higher palmitic, 4.5% lower stearic and 3.6% lower oleic acid and 3.5% higher linoleic acid compared to data on cynara oil profile from other countries (Table 3.9).

Table 3.9: Oil concentration and fatty acids composition of cynara, sunflower and maize seeds

Crop	Location	Oil (%)		Fatty acid composition (%)			
		Aver.	Range	C16:0	C18:0	C18:1	C18:2
Cynara[a]	Italy (40.9°N)[b]	20.7	18.6–23.6	7.7	3.6	26.1	61.5
Cynara[a]	Italy (37.2°N)[c]	24.1	22.8–25.1	10.3	2.8	21.8	62.7
Cynara	Spain (37.2–41.3°N)[d]	25.0	20.0–32.4	10.6	3.7	24.9	59.7
Cynara	Portugal[e]	24.3	–	10.9	3.3	23.1	61.2
Cynara[a]	Greece (39.2°N)[f]	23.2	20.9–25.9	11.1	3.2	24.9	59.1
Sunflower	Greece (39.2°N)[g]	43.3	37.5–48.8	6.6	3.9	34.6	51.9
Maize	Greece (39.2°N)[g]	4.7	3.62–5.80	10.9	2.5	31.2	51.9

[a]: cv. Bianco avorio.
[b]: Piscioneri *et al.* (2000).
[c]: Maccarone *et al.* (1999), Raccuia & Melilli (2007a).
[d]: Curt *et al.* (2002).
[e]: Carvalho *et al.* (2006).
[f]: This study; based on medium–sized seeds (30–40 mg seed[-1]; see Table 3.7 and 3.8)
[g]: Unpublished results (S.V. Archontoulis)

When comparing the cynara oil profile with sunflower and maize oil profiles (Table 3.9), it can be inferred that cynara has a profile similar to sunflower oil and rather close to maize (Maccarone *et al.*, 1999). Moreover, Carvalho *et al.* (2006) found that cynara's fatty acid composition did not differ significantly also from canola, cannabis, and safflower, and that cynara oil is suitable for production of human nutrients after a refining process. Regarding

crude protein, results from Greece confirms the high nutritive value of cynara seeds in line with reports from Spain and Italy (Curt *et al.*, 2002; Raccuia & Melilli, 2007a). Cynara seeds scored high crude protein (viz. 18 %), which is 10% lower than in sunflower seed and 47% higher than in maize kernels growing in the same environment in central Greece (S.V. Archontoulis, unpublished results).

Conclusions

The present work provides a robust and easily applicable methodology to estimate seed yield of *Cynara cardunculus*. Our approach overcomes problems arising from the compound crop structure of inflorescences, and head (capitulum) structure as well. By measuring two simple inflorescence traits (total weight and number of all seed-bearing heads per unit area), the accuracy of seed yield prediction was > 93%. In representative parts of Greece (16 experiments), attainable *Cynara cardunculus* seed yields (beyond 1st cycle) ranged from 190 to 480 g m^{-2} y^{-1}, on dry soils and on aquic soils (shallow ground water level). During the 1st cropping cycle, seed yields were 57 to 80% lower than in subsequent cycles. This variation in seed yield was sufficiently explained by the analyses of head-weight distribution (small, medium and large heads) and variability of seed/head weight ratio at head level. Our proposed methodology can be easily applied in any environment as well as under variable management practices.

Seed quality characteristics such as oil (23%) and protein (18.7%) concentration was rather invariant through different seed sizes (range: 26 to 56 mg seed^{-1}) as well as growing environments meaning that under Greek conditions, these fixed values can be used to estimate seed oil and protein yields.

Seed/biomass as well as oil/seed fractions are now quantified precisely and this can assist (a) researchers to more efficiently estimate crop heating value for solid and/or liquid biofuel production; and (b) policy makers to better plan land uses.

Chapter 4

Temporal dynamics of light and nitrogen vertical distributions in canopies of sunflower, kenaf and cynara

Abstract

To enhance eco-physiological and modelling studies, we quantified vertical distributions of light and nitrogen in canopies of three Mediterranean bio-energy crops: sunflower (*Helianthus annuus*), kenaf (*Hibiscus cannabinus*) and cynara (*Cynara cardunculus*). Field crops were grown with and without water stress in 2008 and 2009. Canopy vertical distributions of leaf area index (LAI), photosynthetically active radiation (PAR), specific leaf area (SLA), nitrogen concentration (N_{conc}) and specific leaf nitrogen (SLN) were assessed over time for each crop × year × water input combination. Light and nitrogen distributions were quantified by the Beer's law (exponential model) and extinction coefficients for light (K_L) and nitrogen (K_N) were calculated. Within a year, K_L did not change significantly over the studied period in all irrigated crops, but differences in K_L were significant between years (sunflower: 0.74 vs. 0.89; kenaf: 0.62 vs. 0.71; cynara: 0.77). K_L estimates were always lower (–48 to –65%) in water-stressed sunflower and kenaf crops because of the reduction in leaf angle. These results should be taken into account, when simulating water-limited biomass production. Vertical SLN distributions were found in canopies when LAI was > 1.5 (40 from 51 cases). These distributions were significantly correlated with the cumulative LAI from the top (r^2=0.75–0.81; P<0.05), providing parameters to upscale photosynthesis from leaf to canopy levels. Vertical SLN distributions followed species-specific patterns over the crop cycle and varied less compared to PAR distributions between years. Lastly, we observed strong associations between SLN and PAR distributions in irrigated sunflower and kenaf canopies (r^2>0.66; P<0.001). However, observed SLN distributions were less steep than the distributions that would maximize canopy photosynthesis.

Introduction

A sharp increase in energy production from biomass in the coming years (Tuck *et al*., 2006), requires that new energy crops (e.g. cynara) will be included in the cropping systems while the production area of other crops (e.g. sunflower) would need to be expanded. The global Scientific Committee on Problems of the Environment (SCOPE) announced that expansion of biofuel production on area basis must be achieved in the context of a 50% increase in food production by 2030 (Connor & Hernandez, 2009). This means that a sustainable increase in bioenergy production must come from greater productivity of existing arable land. Crop modelling is an appropriate way to explore such objectives by conducting scenario studies.

A prerequisite to model crop growth and productivity is an appropriate quantification of crop canopy dynamics (light penetration and nitrogen allocation) in response to management and environmental conditions. Vertical distributions of light and nitrogen in a crop canopy have been quantified by so-called extinction coefficients for light (K_L) and for nitrogen (K_N). In simple crop models such as LINTUL (van Ittersum *et al*., 2003), K_L is widely used to calculate light interception by the canopy and to predict biomass yields based on the light use efficiency concept. More detailed approaches, in which both K_L and K_N are used to scale up photosynthetic CO_2 fluxes from leaf to canopy levels (Leuning *et al*., 1995; de Pury & Farquhar, 1997), have been incorporated into crop growth simulation models such as GECROS (Yin & van Laar, 2005). However, research is needed to parameterize these models for new energy crops.

Even for well-known food crops such as wheat, little is known about the dynamic changes in K_L and K_N (Bertheloot *et al*., 2008), nor about the effects of drought on these changes (O'Connell *et al*., 2004). Without water stress, vertical distributions of light and nitrogen in a canopy were sufficiently described by assuming an exponential decline over canopy depth - the Beer's law (Hirose & Werger, 1987; Monsi & Saeki, 2005). In most studies, K_N was shown to be closely related to K_L, indicating that nitrogen allocation is driven to some extent, either directly or indirectly, by light distribution (e.g. Evans, 1993, Anten *et al*., 1995; Milroy *et al*., 2001; Pons *et al*., 2001; Bertheloot *et al*., 2008). Under water stress, the light and nitrogen distributions over canopy depth are more complicated because water stress affects not only appearance and elongation of leaves and uptake and partitioning of nitrogen, but also morphological aspects of leaf positioning, angle and azimuth angle.

In this work, we aim to quantify extinction coefficients for light (K_L) and for nitrogen (K_N) for potential energy crops sunflower (*Helianthus annuus*), kenaf (*Hibiscus cannabinus)* and cynara (*Cynara cardunculus*), crops with contrasting leaf area distributions along the stem. Sunflower, kenaf and cynara were chosen for

this study because (i) they have a great potential in terms of seed and biomass production in Mediterranean type climates (Geronikolou *et al*., 2005; Archontoulis *et al*., 2010b; Danalatos & Archontoulis, 2010; and references therein), including regions like southern Australia, South Africa, Southern California, and Chile (Estienne & Godard, 1970); and (ii) they cover a large range of bio-industrial applications (biodiesel for transport, pellets for heating, biomass for electricity production, bio-products for buildings, fibres; Karp & Shield, 2008).

Our specific research questions were (i) Can light and nitrogen distributions in canopies of sunflower, kenaf and cynara be accurately described by Beer's (exponential) formula? (ii) How do K_L and K_N depend on species, canopy development, water limitation, time of season and year? (iii) Which generalizations about values of K_L and/or K_N can be made that are suitable for implementation in models? and (iv) Can conservative associations between K_L and K_N be derived from this study? To investigate these questions, we studied three energy crops in the field under two irrigation regimes for two consecutive years in Greece.

Materials and methods

Growing conditions, species, management and climate

All experiments were carried out on a loamy fertile soil (Aquic xerofluvent; high ground water levels; Archontoulis *et al*., 2010b) in central Greece (Thessaly Plain, Karditsa, 39°25'N, 22°05'E, 107 m asl.) in 2008 and 2009. The crops, sunflower, kenaf and cynara, were grown in different sections of the same field in east-west rows (plot size: 184 m^2). No attempt was made to include species into a common layout for practical reasons (irrigation application and inter-plot interference). Per crop, pests were controlled chemically and manually, while there were no obvious diseases. Sunflower and kenaf are fast growing summer crops (Figs. 4.1 and 4.2), while cynara is a perennial crop with annual cycles of 11 months each (for growth stages see Archontoulis *et al*., 2010a).

Table 4.1 provides an overview for the studied species and summarizes details such as growing conditions, management practices and water treatments. Per crop, the combination of two years × two irrigation rates resulted in four water treatments: T_1= 2009, irrigated; T_2 = 2009, water stressed; T_3 = 2008, irrigated; T_4 = 2008, water stressed (Table 4.1). Irrigation was applied via a drip irrigation system. For the summer crops T_1 and T_3, the irrigation rate was based on class A-pan evaporation measurements (for site-specific calculations see Danalatos & Archontoulis, 2010) at weekly intervals (Fig. 4.2a and b). Water-stressed summer crops (T_2 and T_4) received one irrigation application during early growth. For cynara the water treatments were: 3–4 irrigation applications

(T_1 and T_3) during the period of rapid increase in biomass (BBCH 55–65; May–June) and no irrigation application (T_2 and T_4) as is common for cynara.

Full weather data were recorded hourly by an automatic meteorological station (DL2, Delta–T, UK) which was installed at the experimental site. The mean air temperature during summer was 25.9 °C for 2008 and. 24.6 °C for 2009 (Fig. 4.1), close to the long-term average for this site of 25 °C. Precipitation during winter–spring season varied considerably between years: 103 and 295 mm for 2008 and 2009, respectively (Fig. 4.2c). Radiation is not a limiting factor in this region (summer period: 25 MJ m^{-2} d^{-1}).
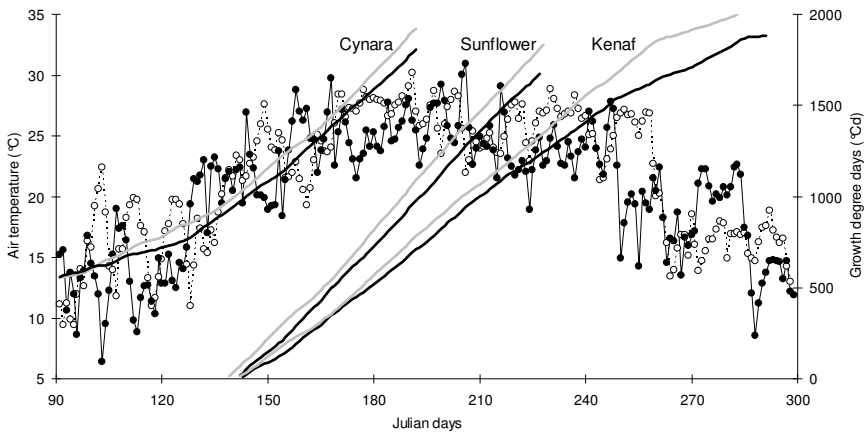
Figure 4.1: Mean daily air temperature (······o······: 2008 and —•—: 2009 year) and accumulated degree days per crop (sunflower, kenaf and cynara) and per year (——: 2008 and ——: 2009 year). X-axis intercepts depict the day of 50% crop emergence for sunflower and kenaf. Cynara re-emerged around September 22nd in both years (not visible).

Sampling protocol

In sunflower and kenaf, first the fraction of intercepted photosynthetically active radiation (PAR) was measured, followed by sampling, and assessments of leaf area, dry weight and nitrogen (N) concentration. Measurements began when the canopy height was at least 25 cm; at the first sampling the canopy was not divided into layers. Later on, when plant height increased (Fig. 4.2d and e), the number of layers was increased progressively to three for sunflower and to five for the kenaf crop. These successive canopy layers had equal vertical thickness per crop (calculated based on plant height). PAR extinction was measured during vegetative stages for kenaf and during vegetative and flowering stages for

sunflower. However, vertical N distribution in the canopy was measured throughout the crop cycle for both crops (Table 4.1).

In cynara PAR and N profiles were assessed separately at different periods (Table 4.1) for practical reasons. PAR penetration was measured at vegetative stages (BBCH 10–37; no layer defined) because later during reproductive growth, the canopy was too voluminous to allow us to perform accurate measurements (note LAI>7). Vertical N distributions were undertaken during reproductive growth (BBCH 59–82; 4 layers of equal vertical thickness were defined) because at vegetative stages leaves formed a rosette. Periods of PAR and N measurements per species are provided in Table 4.1. Sampling frequency can be seen in Fig. 4.2.

Measurements

Fraction of PAR intercepted by the successive canopy layers was measured using a 1-m light sensor (Delta–T Devices, Cambridge, UK). We measured under clear skies to avoid poor quality of incident PAR (O'Connell *et al*., 2004) and around maximum sun height (11:30–13:30 h summer time; diffuse/total≈0.2; radiation≈1000 MJ m^{-2} s^{-1}) when differences in leaf angle due to solar tracking – evident in sunflower and kenaf– would be minimal (Sassenrath-Cole, 1995). In each measurement, a reference light sensor was placed above the canopy to provide simultaneous readings of incident PAR. At the bottom height of the canopy layers defined beforehand, the 1-m light sensor was placed diagonally across two rows (in an X pattern) and 10 readings were taken at each depth in the canopy. Few measurements above the canopy were also taken to check the reference light sensor. Per sampling event (combination of crop species × year × water level × date), measurements were taken from two to four independent samples.

Early during the following morning, plant samples were taken (2 rows of 0.66 m long each = 1 m^2) and green leaf lamina area (henceforth leaf area index, LAI) was determined per layer using a LI-COR area meter (LI-3000A, Nebraska, USA). Leaf samples (excluding petioles) were dried at 70 °C to constant weights and weighed. Then materials were analyzed for total nitrogen concentration on a mass basis (N$_{conc}$, g N kg^{-1} dry weight) using the Kjeldahl method. When measuring light extinction and sampling for N profiles, the senesced leaves (>50% green surface area) were removed; this is in line with many reports (e.g. Connor *et al*., 1995; Hall *et al*., 1995). When the proportion of a partially senesced leaf (<50% of green area) appeared desiccated and brittle; this part was separated from green laminae and excluded from analysis in order to avoid leaf area measurement inaccuracy. This was evident a few times in sunflower and cynara.

Table 4.1: Species description (all dicots) and summary of experimental details for the two study years

Crop species	Sunflower	Kenaf	Cynara
General description			
Latin name	*Helianthus annuus*	*Hibiscus cannabinus*	*Cynara cardunculus*
Family	Asteraceae	Malvaceae	Asteraceae
Photosynthesis	C_3	C_3	C_3
Growth cycle	annual	annual	perennial (10 cycles)
Cycle length (days) [a]	110	180	330
Growth habit	Determinate	Indeterminate	Indeterminate
Leaf or leaflet shape [b]	Cordate	Cordate	Elliptic or runcinate
Commercial product	Seeds (oil)	Stalks (fibre)	Seeds and stalks
Experimental details			
Genotype	Panter (high oleic)	Everglades 41	Biango avorio
Sowing time [c]	13/5/08 and 15/5/09	13/5/08 and 15/5/09	13/4/06 and 30/11/08
Observed shoots m^{-2}	6.6 ± 0.8	13 ± 3.8	4.3 ± 1.1
Row-to-row distance (cm)	75	75	75
N–P–K input ($g\ m^{-2}$) [d]	8–5–5	8–5–5	8–5–5
Water treatments (mm) [e]			
T_1	378	628	755
T_2	143	227	617
T_3	370	611	513
T_4	82	83	377
Base temperature (°Cd)	5	10	7.5
Cycle length (°Cd) & growth stages (BBCH) [f]	2100 (BBCH 10–97)	1900 (emergence–flowering)	650 + 1600 = 2250 (BBCH 10–49; 50–97)
Periods of profile assessment [g]			
Light	BBCH 35–73	Vegetative	BBCH 10–37
Nitrogen	BBCH 35–85	Vegetative to flowering	BBCH 59–82

[a]: under Greek conditions (39.2°N).

[b]: adult cynara leaves have an undetermined number of leaflets (details in Archontoulis et al., 2010a).

[c]: for perennial cynara crop, 1st sowing (April 2006) refers to 2nd and 3rd growth cycle during the   studied years (2008 and 2009) when N profiles were measured while 2nd sowing (November 2008) refers to 1st growth cycle when PAR profiles were measured.

[d]: P, K applied before sowing; N applied during crop growth.

[e]: T_1= 2009, irrigated; T_2 = 2009, water stressed; T_3 = 2008, irrigated; T_4 = 2008, water stressed. Values (mm) are sums of precipitation plus irrigation from emergence until last sampling (Fig. 4.2a, b and c).

[f]: For sunflower (Lancashire *et al*., 1991) and cynara (Archontoulis *et al*., 2010a) the BBCH coding system was used to assess specific growth stages. Degree days (°Cd) refer to the corresponding BBCH period. For cynara degree days were further separated for vegetative (autumn to spring) and reproductive growth (spring to summer). For kenaf °Cd counted from 50% emergence to 90% flowering. Values are means across two years (Fig. 4.1).

[g]: PAR measurements ceased after a certain period to avoid confounding from biomass partitioning and excessive leaf senescence.

Calculations of morphological and phenological indexes

We distinguish LAI (surface area of green laminae per unit ground area, $m^2\ m^{-2}$) from the green area index (GAI, surface area of green tissues per unit ground area, $m^2\ m^{-2}$). To calculate GAI, the projected surface area of the petioles was added to LAI. Stem and inflorescence surface areas were not included. Specific leaf area (SLA, m^2 laminae kg^{-1} dry laminae mass) was calculated by dividing green laminae area by the dry laminae mass. The quotient between N_{conc} and SLA expresses the leaf laminae nitrogen per unit leaf area (specific leaf nitrogen, SLN, g N m^{-2} leaf laminae).

Growth degree days (GDD, °Cd) were calculated based on daily maximum and minimum air temperatures using threshold values of 5 °C for sunflower, 7.5 °C for cynara and 10 °C for kenaf. GDD was counted from 50% crop (re)emergence in all species. The threshold temperatures for the studied genotypes were derived from plots of seed germination rates versus temperature (S.V. Archontoulis & E. Skoufogianni unpublished) and agree well with published data for sunflower (e.g. Villalobos *et al.*, 1996), kenaf (Carberry & Abrecht 1990) and cynara (Virdis *et al.*, 2009).

Estimation of light and nitrogen extinction coefficients

PAR was assumed to be attenuated through the canopy following Beer's law (Monsi & Saeki, 2005), based on GAI or LAI:

$$I_i = I_o \cdot e^{-K_L \cdot GAI_i} \ \ \text{or} \ \ I_i = I_o \cdot e^{-K_L \cdot LAI_i} \tag{1}$$

where GAI_i or LAI_i is the cumulative GAI or LAI from the top of the canopy downwards; K_L (m^2 ground m^{-2} green tissue or laminae) is the direct light extinction coefficient at noon; I_o and I_i (µmol $m^{-2}\ s^{-1}$) are the PAR (photosynthetically active radiation) values in a horizontal plane above the canopy and at depth i, respectively. Unless specified otherwise, our analysis for K_L is mainly based on GAI to account for the capture of PAR by non-laminar green tissues.

Light interception and photosynthesis are intrinsically area-based processes; therefore, analysis of the vertical nitrogen distribution is most meaningful when expressed per unit leaf area (SLN). The vertical gradient of SLN was described as a function of the absolute LAI (Del Pozo & Dennett, 1999; Lötscher *et al.*, 2003; Yin *et al.*, 2003a; van Oosterom *et al.*, 2010):

$$SLN_i = SLN_o \cdot e^{-K_N \cdot LAI_i} \tag{2}$$

where K_N (m^2 ground m^{-2} green lamina) is the nitrogen extinction coefficient; SLN_o and SLN_i are the SLN at the top of the canopy (i.e. $LAI_i = 0$) and at depth i, respectively. A common alternative in literature to describe the exponential SLN distribution is to use the relative LAI, i.e. LAI_i/LAI (e.g. Hirose & Werger, 1987). We used eq. (2) in order to account for the dynamic change of LAI and to obtain a K_N with the same unit as K_L. It is worthy to note that the nitrogen extinction coefficient obtained by Eq. (2) and the relative one, are mathematically related as: $K_{relative} = K_N \cdot LAI$.

By eliminating LAI_i from equations 1 and 2, SLN_i and I_i/I_o are related as:

$$\frac{SLN_i}{SLN_o} = \left(\frac{I_i}{I_o} \right)^{\frac{K_N}{K_L}}$$

(3)

Eq. (3) was used to examine associations between light and nitrogen distributions. Eq. (3) allows the use of the combined data of SLN_i and I_i/I_o to estimate SLN_0 and the power term (K_N / K_L). This approach bypasses the use of LAI_i data, but requires that light and nitrogen vertical distributions are measured on the same dates and at the same positions of the canopy. We also investigated associations between light and nitrogen distributions indirectly (based on LAI data) by calculating the quotient of K_N (Eq. 3) to K_L (Eq. 1).

Statistics

Values of parameters in equations 1, 2 and 3 were estimated from iterative nonlinear least-square regression using the Gauss method, as implemented in PROC NLIN procedure in SAS software (version 9.1). The goodness of fit was assessed by calculating r^2.

To examine whether estimates varied among dates of sampling, water levels and species, equations were log-transformed to the linear form and then subjected to analysis of variance by applying linear regression with groups (given the accumulated analysis of variance table) in Genstat software (12th edition). Slopes and intercepts were further evaluated separately (multiple *t*-tests) to identify (i) whether lines differed due to differences in intercepts and/or due to differences in slopes, (ii) significant differences within a group of lines. Significance of differences among and between estimates were assessed based on *F* and *t* tests (*P*=0.05). To examine differences among canopy layers in N_{conc}, SLA and SLN, one-way ANOVA was performed for each treatment separately. Similar analysis was done to examine differences in N_{conc}, etc., over time of season per layer for each treatment.
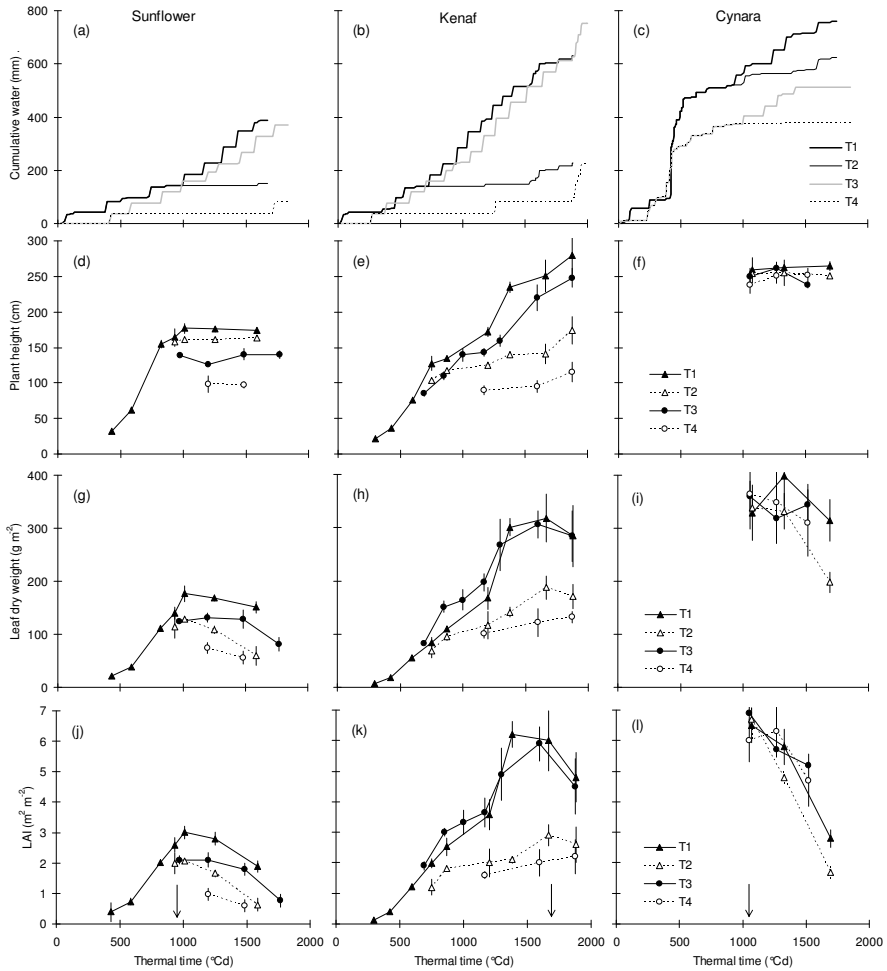
Figure 4.2: Per crop (sunflower: left; kenaf: middle and cynara: right panels), cumulative precipitation plus irrigation application (panels: a, b and c), plant height (panels: d, e and f), leaf laminae dry weight (panels: g, h and i) and leaf area index (panels: j, k and l). Data are means (± standard error bars) of two to four independent replicates. Vertical arrows in the lower panels indicate flowering. T_1 = 2009, irrigated; T_2 = 2009, water stressed; T_3 = 2008, irrigated; T_4 = 2008, water stressed. Note: From 600 to 1000°Cd, cynara had LAI > 7, while the plant height increased from 160 to 250 cm.

Results

Canopy dynamics in relation to species and to irrigation application

Species showed different dynamics in height, leaf weight and LAI, maximum values being obtained around flowering (Fig. 4.2). Irrigated kenaf attained much higher LAI values and realized longer periods with LAI > 3 than irrigated sunflower (Fig. 4.2j and k). Cynara had LAI > 3 from 350 to 1600 °Cd, with maximum values of 11 m^2 m^{-2} around 650 °Cd (inflorescence emergence; BBCH 50; not shown). Species had also contrasting canopy structures in terms of leaf area distribution along the stem (Fig. 4.3). The largest fractions of leaf mass and area in well developed crops were allocated at the middle, top and bottom of the canopy for sunflower, kenaf and cynara, respectively (Fig. 4.3). Additionally, species have different leaf shapes (all broad-type, Table 4.1) with different maximum leaf or leaflet surface areas (sunflower: 500, kenaf: 120 and cynara 280 cm^2). Differences in height, leaf weight and area between irrigated and water-stressed summer crops were significant in both years beyond 900 °Cd ($P<0.05$; Fig. 4.2). Canopy traits for cynara were not affected by supplementary irrigation in either years ($P>0.05$; Fig. 4.2f, i and l), because crops had received ample water (≥ 400 mm; Fig. 4.2c).

Light extinction in relation to growing degree days, water stress, year and species

We present our results, all using GAI as independent variable (Fig. 4.4). K_L estimates based on LAI (not shown) were approximately 2.2%, 5.6% and 12.1% higher –compared to the estimates based on GAI– for the sunflower, kenaf and cynara crop, respectively. Eq. (1) adequately described all PAR sets (n=24; $P=0.04$–0.0001). Best fits were found to data obtained under irrigated conditions or at initial stages of water stress ($r^2=0.69$–0.98; Fig. 4.4). Under prolonged drought periods, Eq. (1) described PAR distribution rather poorly ($r^2=0.42$; Fig. 4.4b), because the leaf angle tended to shift from a horizontal orientation (0–30° from horizontal) to a vertical one (60–90° from horizontal). In kenaf leaf rolling was also evident.

   K_L did not change significantly during the studied period in sunflower (T_1, $P=0.188$–0.916 among lines; T_2, $P=0.451$; T_3, $P=0.133$; Fig. 4.4a, inset) or in cynara ($P=0.376$–0.889; Fig. 4.4c, insert). For irrigated kenaf, although no significant effect of time of season on K_L (T_1, $P=0.057$–0.982; T_3, $P=0.306$–0.905) was observed, there was an increasing trend from 600 to 1200°Cd (Fig. 4.4b, inset). For water-stressed kenaf crops, K_L significantly declined over time (T_2, $P=0.01$; Fig. 4.4b, insert),

indicating that under drought we cannot use a common K_L value over the entire crop cycle to assess light interception/distribution. In sunflower and kenaf, K_L estimates were always lower in water-stressed crops than in irrigated crops (Fig. 4.4a and b insets). As drought prolonged, the differences between irrigated and water-stressed plants became larger and statistically significant ($P<0.05$).

Per summer crop, data from irrigated treatments were pooled per year (T_1 and T_3) and the effect of year on K_L was investigated. Year effects on K_L were significant for both sunflower (0.89 vs. 0.74, $P=0.001$) and kenaf (0.71 vs. 0.62, $P=0.008$) as revealed by t-tests. Consequently, in order to compare light extinctions among species we used only the 2009 data. Statistics revealed a significantly ($P=0.016$) greater K_L value for sunflower compared to other two species (Fig. 4.4) and no significant difference between kenaf and cynara ($P=0.66$).

Vertical SLN distributions in relation to GDD, water stress, year and species

From 51 datasets (51 crop × water treatment × date combinations), we found obvious vertical SLN distributions in canopies when LAI was larger than 1.5 (40 sets; Figs. 4.5 and 4.6). When LAI was ≤ 1.5, i.e. at early or late growth stages or in water-stressed canopies (Fig. 4.2), there were no obvious SLN gradients (e.g. Fig. 4.5). Eq. 2 described distributions adequately, when they existed. However, in some SLN/LAI plots linear models also gave proper predictions, while in a very few sets, polynomials gave the best fits. We continue our analysis based on Eq. (2) because coefficients have clear biological meaning and can be compared with literature reports.
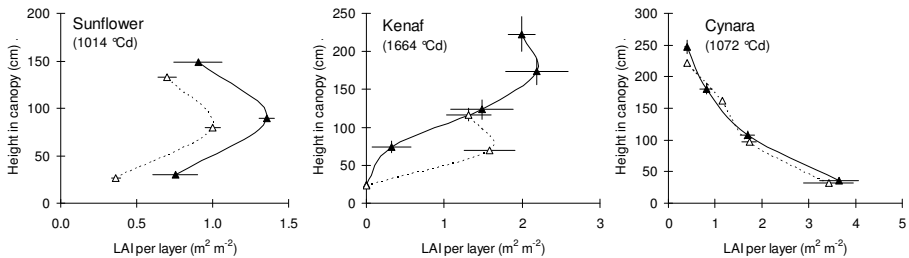
Figure 4.3: Distribution of leaf area (expressed by LAI) within sunflower, kenaf and cynara canopies at flowering (fully developed plants). Canopy height calculated from the ground level. Data are means (± standard error bars) of two to four independent replicates. Symbols refer to water treatments: — ▲ —: T_1 (2009, irrigated crops); ·····Δ·····: T_2 (2009, water stressed crops). Y-axis intercept in kenaf indicates absence of leaves at bottom canopy layer during that period.
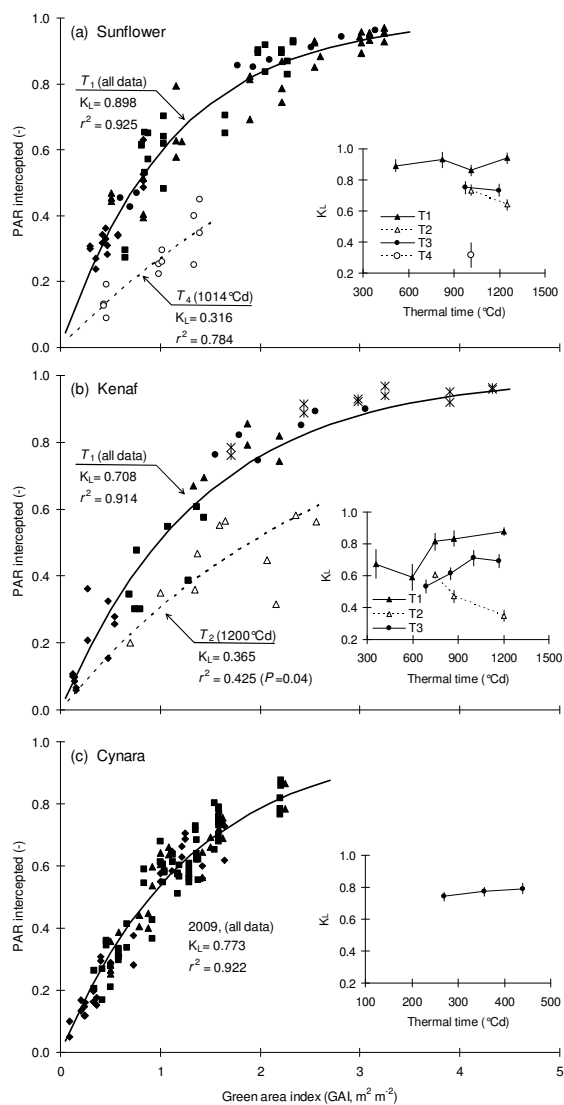
Figure 4.4: Main panels: fraction PAR interception as a function of green area index (GAI) for irrigated (full symbols; different shapes refer to different dates) and water stress crops (open symbols). Inset panels: Light extinction coefficients (K_L ± standard error bars) per water treatment (T_1 =2009, irrigated; T_2 = 2009, water stressed; T_3 = 2008, irrigated; T_4 = 2008, water stressed) as a function of thermal time. Fitted lines in the main panels (a, b) indicate fits of the model $Y=1–exp(–K_L X)$ to data with the largest and the smallest K_L values. In panel (c) an average fit is given. All fits were significant at $P<0.001$, unless indicated in the panel (viz. kenaf T_2).
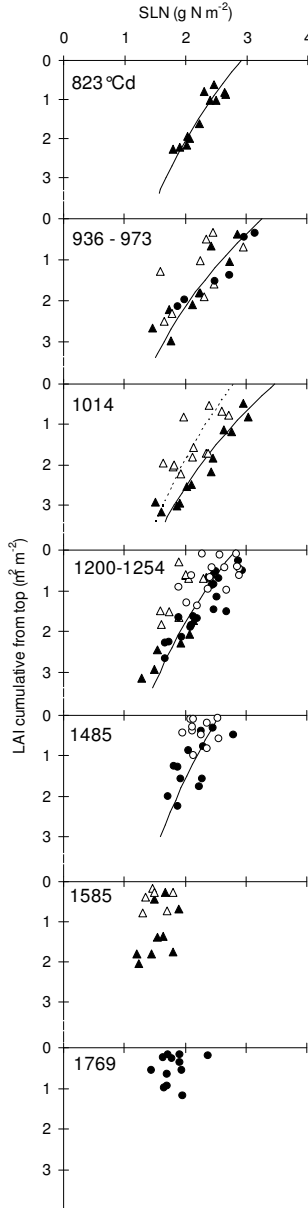
Figure 4.5: Cumulative LAI counted from the top of the canopy versus sunflower leaf laminae nitrogen content per unit area (SLN) at different times (expressed as thermal time). ▲: T_1 = 2009, irrigated; △: T_2 = 2009, water stressed; ●: T_3 = 2008, irrigated; ○: T_4 = 2008, water stressed. Lines (—: irrigated; ⋯⋯: water stressed), when given indicate significant ($P<0.05$) fits from Eq. (2) to datasets. Parameters and statistics are presented in Table 4.2.

Sunflower vertical SLN distributions

At early growth stages (GDD<600 °Cd; LAI<1.5), there were no vertical SLN distributions. Later, with increasing LAI (823–1014 °Cd; Fig. 4.2j), yellowing of lower leaves was reflected in more steeply declining vertical distributions (Fig. 4.5). At that period, SLN non-uniformities were maximal. After anthesis and towards maturity (1200–1769 °Cd; Fig. 4.5) lamina N_{conc} at the top of the canopy declined sharply (Fig. 4.7a) while at the same time senescence of the bottom leaves accelerated (reflected by the decrease in LAI, Fig. 4.2j). The combination of these two processes resulted in progressively declining SLN profiles (1485 °Cd; Fig. 4.5). Above 1500 °Cd there were no vertical SLN distributions (Fig. 4.5). Eq. (2) gave significant fits in eight out of the fifteen sunflower canopies (Table 4.2). Within these eight canopies, SLN_o significantly decreased from flowering towards maturity (T_1, P=0.017–0.596; T_3, P=0.01–0.14 among lines; Table 4.2). For K_N, while t-tests among dates showed no significant decrease over time (T_1, T_3, P>0.106), there was an obvious decreasing trend from 973 to 1485°Cd (Table 4.2; Fig. 4.5). Similarly, water stress (1014 °Cd) reduced both SLN_o (P=0.002) and K_N (P=0.372; Fig. 4.5). In general, drought stress accelerated senescence of bottom leaves, minimizing or even overruling any SLN gradients.

Table 4.2: Probability (P), determination coefficient (r^2), and parameters of Eq. (2) used to assess sunflower vertical SLN distributions in Fig. 4.5. Estimates, SLN_o and K_N, are presented per thermal time (GDD) for each water treatment (▲,●,Δ,○)

GDD	Symbol[a]	P	r^2	SLN_o	K_N
Irrigated sunflower canopies					
823	▲	0.000	0.85	2.91 (0.10)	0.183 (0.02)
936	▲	0.000	0.86	3.10 (0.20)	0.213 (0.04)
973	●	0.004	0.90	3.44 (0.19)	0.243 (0.04)
1014	▲	0.000	0.92	3.48 (0.15)	0.217 (0.02)
1200	●	0.000	0.79	3.06 (0.12)	0.215 (0.03)
1254	▲	0.004	0.72	2.60 (0.19)	0.172 (0.04)
1485	●	0.012	0.48	2.57 (0.17)	0.159 (0.05)
1585	▲	0.123	0.31	1.82	0.131
1769	●	0.479	0.05	1.89	0.080
Water stressed sunflower canopies					
936	Δ	0.079	0.38	2.73	0.157
1014	Δ	0.009	0.51	2.78 (0.23)	0.178 (0.05)
1200	○	0.056	0.25	2.74	0.164
1254	Δ	0.052	0.49	2.23	0.158
1485	○	0.960	0.00	2.24	0.004
1585	Δ	0.674	0.05	1.60	0.122

Standard error of estimates in parenthesis is given when P<0.05; otherwise estimates are shown to depict the course of SLN vertical distribution throughout the cycle.
[a]: symbols refer to Fig. 4.5.

Kenaf vertical SLN distributions

Significant fits of Eq. (2) were observed in 20 out of 24 kenaf canopies or from 596 to 1879 °Cd (*P*<0.05; r^2=0.61–0.95; Fig. 4.6a). Vertical SLN distributions maximized during mid-season for the irrigated crops (1000–1201 °Cd; height≈170 cm; Fig. 4.2e) because differences in leaf age between top–bottom canopy layers (reflected by the SLA or N_{conc}; Figs. 4.7b and e) were maximal at that period, imposing strong SLN gradients (Fig. 4.7h). Beyond flowering (usually October), crop growth is constrained by temperature (Fig. 4.1), resulting in fast leaf senescence.

Multiple *t*-tests comparing dates in irrigated crops indicated no significant (*P*>0.057) change in SLN_o. For K_N, marginally significant differences (*P*=0.015–0.042) were observed only between mid- and late-season. When SLN_o or K_N were regressed separately with thermal time (see Fig. 4.6a-inset) or with LAI by using combined irrigated data over two years (n=14), we still did not find changes in SLN_o (*P*>0.256) but a significantly reduction of K_N with time (*P*=0.001) or LAI (*P*=0.003). This is because SLN declined over time particularly in the bottom shade leaves (through the decrease in N_{conc}) while the SLN in the top layer almost remained unchanged due to continuous production of new leaves (Fig. 4.7h). In water-stressed canopies, when SLN distributions existed (T_2, T_4: 1378–1875 °Cd) these remained unchanged over time (SLN_o: *P*>0.168; K_N: *P*>0.310) most probably due to minor growth (see also LAI; Fig. 4.2k). Irrigation application significantly affected SLN_o in only a few cases but did not significantly affect the K_N parameter (*P*>0.098; Fig. 4.6a).

Cynara vertical SLN distributions

Beer's law described significantly all sets (*P*<0.05; r^2=0.56–0.91; n=12; Fig. 4.6b). Within the experimental period (1052–1693 °Cd), vertical SLN distributions varied little with time (SLN_o: *P*=0.055; K_N: *P*=0.904; Fig. 4.6b-inset) or water stress (SLN_o: *P*=0.025; K_N: *P*=0.742). This is because the decrease of N_{conc} was counterbalanced by the decrease in SLA and thus SLN distributions remained almost constant over the studied period (Fig. 4.7c, f and i). Only the last T_2 profile at 1693 °Cd differed significantly from the other 11 profiles. Beyond 1693 °Cd, there were practically no vertical distributions in cynara (see fast decrease in LAI; Fig. 4.2l). In cynara, the top canopy layer (1/4 of the plant's height; LAI<1; Fig. 4.3) consisted of branch type leaves. These leaves are very thick with dense vein structures and small leaflet areas resulting in very low SLA values (Fig. 4.7f), and consequently in high SLN values (Fig. 4.7i). These values have been visualized in the upper part of Fig. 4.6b (LAI<1; above dotted horizontal line). We investigated whether exclusion of these top leaves (little contribution to total LAI; Fig. 4.3)

would improve Eq. (2) fits, but this proved unsuccessful because of the loss of degrees of freedom in the regression analysis.
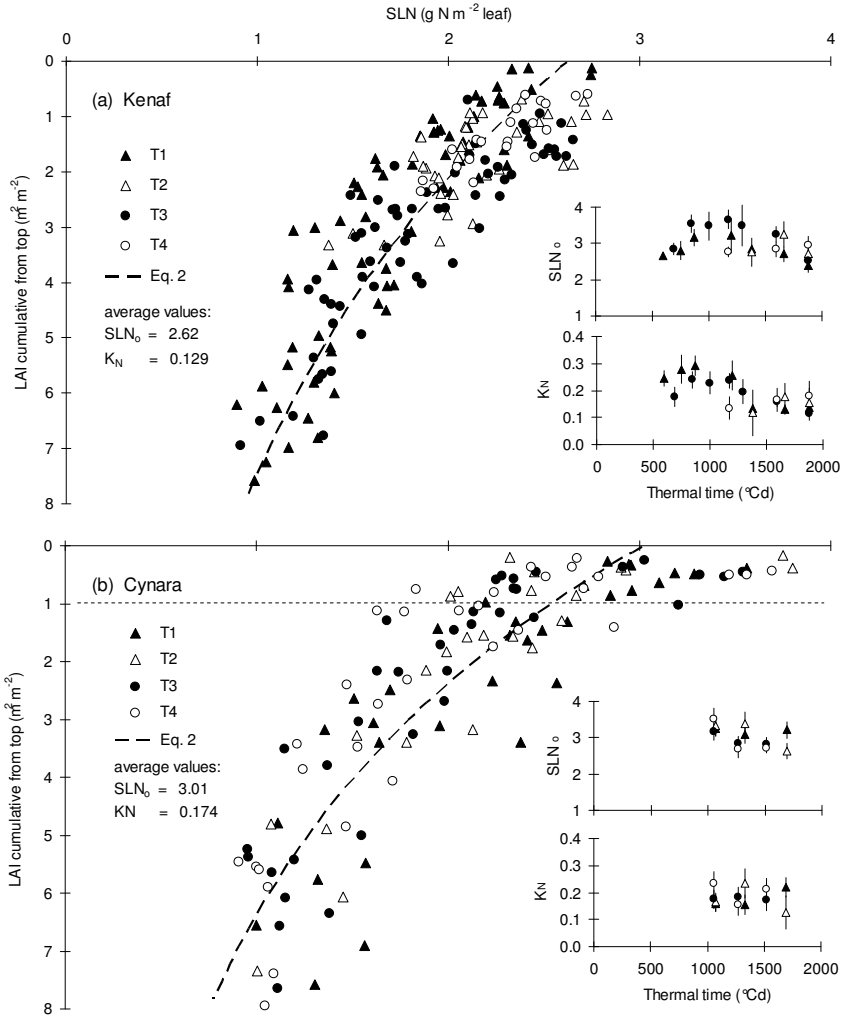
Figure 4.6: Main panels: Cumulative LAI counted from the top of the canopy versus leaf lamina nitrogen per unit area (SLN), for kenaf (a) and cynara (b) canopies. Symbols are measurements and dashed lines are average fits from Eq. 2, to facilitate comparison between species. The horizontal dotted line in panel (b) indicates the height of the branch leaves. Inset panels: Estimates (± standard error bars) of Eq. (2) versus thermal time for each set of data with a significant fit. SLN_o: SLN at the top; K_N: nitrogen extinction coefficient. T_1 = 2009, irrigated; T_2 = 2009, water stressed; T_3 = 2008, irrigated; T_4 = 2008, water stressed.

Year and species effects on vertical SLN distributions

Vertical SLN distributions varied little between years for each crop (Figs. 4.5 and 4.6). To assess differences in SLN distributions among species we used sets that satisfied two criteria: (i) irrigated canopies in both years and (ii) flowering periods (±10 days), in order to avoid any confounding effects from GDD and water levels. Results are presented in Table 4.3, indicating steeper vertical SLN distributions in sunflower ($P<0.05$) than in kenaf and cynara. It was shown earlier (3.3.2) that within a species K_N decreased with increasing LAI. It follows that the difference in K_N among species might be an artefact because of the higher LAI of the latter two crops at flowering periods (Fig. 4.2).

Table 4.3: Parameters of Eq. (2) used to describe vertical SLN distribution in three irrigated crops during flowering periods (±10 days). All fits were significant at $P<0.001$

Species	Period (°Cd)	SLN_0	K_N	r^2	n
Sunflower	936–1254	3.12b	0.214b	0.731	54
Kenaf	1378–1879	2.59a	0.124a	0.780	55
Cynara	1052–1327	2.88ab	0.142a	0.745	48

Different letters within a column indicates significant differences at $P<0.05$.

Spatiotemporal variations in N_{conc} and SLA determine vertical SLN distributions

In irrigated crops, top–down SLN distributions were due to the combined effects of higher N_{conc} (Fig 4.7a, b and c; $P<0.01$) and lower SLA values (Fig 4.7d, e and f; $P=0.005–0.581$) for top leaves. This was also evident in water-stressed crops albeit less so (not shown). In sunflower and kenaf, variation in N_{conc} within layers (top–bottom) was much larger than variation in SLA within layers; the opposite was observed for cynara (Fig. 4.7).
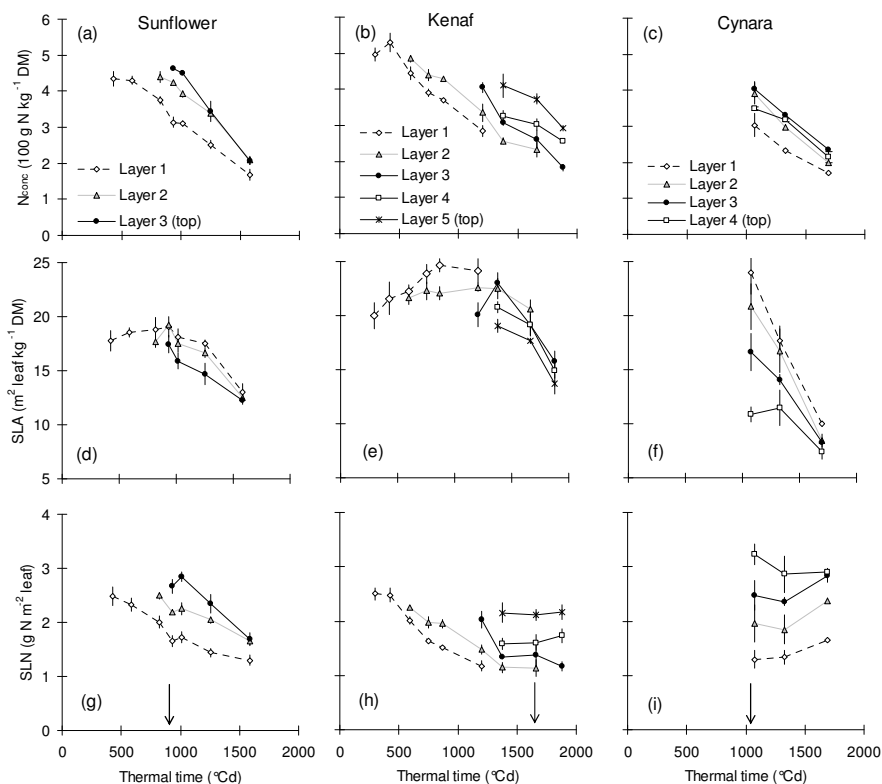
Figure 4.7: Dynamics of leaf nitrogen concentration (N_{conc}; panels a–c), specific leaf area (SLA; panels: d–f) and laminae nitrogen per unit leaf area (SLN; panels: g–i) at different canopy layers (layer 1 being the bottom layer) in sunflower, kenaf and cynara canopies. Data are means (± standard error bars) of two to four independent replicates for the water treatment T_1 (2009, irrigated). Vertical arrows in the lower panels indicate flowering.

Relationships between SLN and PAR distributions

To examine whether the difference in vertical distribution of SLN can be explained by different light climates within the crop canopies, SLN (expressed on a relative scale) was plotted against relative PAR (I/I_o). For eight sunflower and 11 kenaf canopies –PAR and SLN data obtained on same dates–, the relationship was convex (Fig. 4.8). The power function, Eq. 3, gave significant fits for each crop when the data were pooled across sampling dates (irrigated, *P*<0.001, r^2=0.66–0.81; water stressed canopies, *P*<0.017, r^2=0.38–0.60; Fig. 4.8 main panels). Individual sets were significant at *P*<0.09 (Fig. 4.8 inset panels).

Cynara was excluded from this analysis because SLN and PAR data were collected at different periods (Table 4.1). In both crops, GDD and water stress significantly affected the shape of the PAR–SLN relation through the significant ($P<0.05$) change in the SLN_o parameter (Eq. 3). The power term changed only slightly ($P>0.048$), implying that the ratio K_N/K_L was rather conservative over the measuring period. The term K_N/K_L was higher in water stressed than in irrigated crops, because under drought K_L decreased (Fig. 4.4a and b) and hence the K_N/K_L increased. Similar results were obtained when the K_N/K_L ratio was calculated using estimates derived from LAI equations (see Figs. 4.4 and 4.6; Table 4.2).
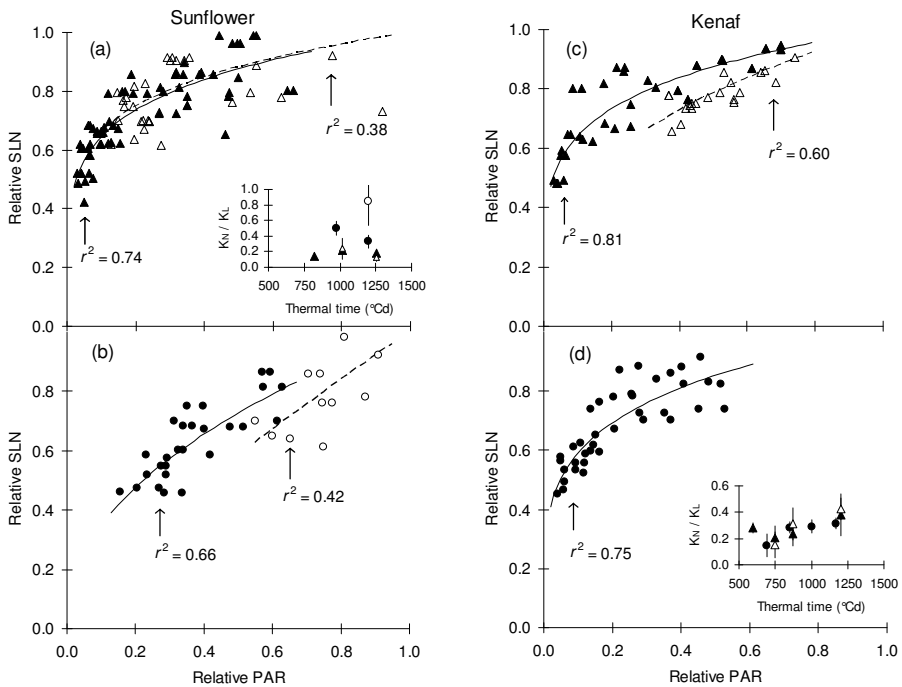
Figure 4.8: Main panels: Relationships between relative SLN (SLN_i/SLN_o) and relative PAR (I_i/I_o) in sunflower (leaf panels: a, b) and kenaf (right panels: c, d) canopies for different water treatments (▲: T_1 = 2009, irrigated; △: T_2 = 2009, water stressed; ●: T_3 = 2008, irrigated; ○: T_4 = 2008, water stressed). Per crop and per water treatment (pooled data across dates) an average fit from Eq. (3) is given (——: irrigated; - - - -: water stressed). Inset panels indicate individual estimates (± standard error bars) of the power term (K_N / K_L, Eq. [3]) over thermal time for each crop. Estimates of the second parameter of the Eq. (3), the SLN_o, are not presented here because values were very close to that presented in Table 4.2 and Fig. 4.6a for sunflower and kenaf respectively.

Discussion

Light extinction coefficient and implications for crop modelling

K_L might be affected by many factors influencing canopy structure, and factors associated with solar position. In our study we focussed on (i) the effect of water stress, because water stress is the major concern in the Mediterranean area, and on (ii) the effect of time (season and year) in order to examine the widely used assumption in crop models that K_L remains constant over time (Evers *et al.*, 2009). Regarding the effect of time of day (not assessed in this study), in literature there are at least two generic approaches to convert noon to daily K_L values (Charles-Edwards & Lawn, 1984; Sinclair, 2006); see Pereyra-Irujo & Aguirrezábal (2007) for an application.

Beer's law

As was expected, our data were significantly described by Eq. (1). However, under prolonged drought periods, the assumption that light attenuates exponentially with canopy depth was poorly confirmed (*P*=0.04; Fig. 4.4b) because of the irregular reduction in leaf angle and due to leaf rolling. In cynara, application of Beer' law beyond growth stage BBCH 37 implies measurement inaccuracy due to complex crop structure (Archontoulis *et al.*, 2010a). Thus, indirect approaches (cf. leaf angle or plant geometry or even 3D modelling; Vos *et al.*, 2010) should be applied in order to further explore K_L.

Crop age and year effects on K_L

Without water stress, use of an average K_L value per crop cycle in sunflower, kenaf and cynara probably does not result in excessively large errors in modelling. Between years, we observed some variations (12–17%; *P*<0.05) in K_L values in sunflower and kenaf (Fig. 4.4). This is a common phenomenon in literature (Kiniry *et al.*, 1999; Lindquist *et al.*, 2005; Dercas & Liakatas, 2007) and it is most likely attributed to differences in cloudiness (ratio of direct to diffuse light), while some variation in water condition, plant density, time of day at which measurement occurred etc., always exists between years.

Our findings for irrigated sunflower agree well with Gimenez *et al.* (1994) who found a constant K_L value with time of season and Sadras *et al.* (1991) who reported significant changes in K_L only beyond BBCH 80. Moreover, for sunflower Rawson *et al.* (1984) and Zaffaroni & Schneiter (1989) related K_L to LAI by using the equation: $K_L \approx 1.4 \cdot LAI^{-0.5}$ (r^2=0.69). This equation shows a severe K_L reduction with increasing LAI at low LAI values (<1.0) and near constant K_L

values of 0.9 at LAI values from 1 to 4 (similar to our findings; Fig. 4.4a). Such a relation between K_L and LAI would be advantageous because sunflower canopies can maintain high light-utilization efficiency over the entire cycle. For irrigated kenaf earlier studies from Muchow (1992), Manzanares *et al.* (1993) and Losavio *et al.* (1999) including different genotypes and management practices indicated constant K_L values per experimental season (K_L of 0.56, 0.72 and 0.35 respectively). In our study we found K_L values of 0.62 to 0.71 from year to year and an increasing trend of K_L with the time of season (P=0.057; Fig. 4.4b). For cynara there are no relevant data to compare our findings with.

Water stress effects on K_L

Under water limited conditions K_L values were always smaller (Fig. 4.4 insets) than under irrigated conditions, as a result of irregular adjustment of leaf orientation to incident radiation particularly during midday. Sadras *et al.* (1991) working with short and tall sunflower hybrids under different water regimes (255–446 mm) found K_L values of 0.54 to 0.67, while Ferreira & Abreu (2001) studying rainfed (128 mm) sunflower crops found K_L values of 0.44–0.65. These K_L estimates –in line with our data under water limited conditions– were substantially lower than the estimates obtained for irrigated sunflower crops (K_L=0.74–0.89; Fig. 4.4a and Bange *et al.*, 1997; Flénet *et al.*, 1996; Gimenez *et al.*, 1994). The same statements also hold for kenaf (Fig. 4.4b), although there are no relevant literature data to benchmark our data. Therefore, crop modellers should include a water supply or transpiration-based reduction factor to account for a lower K_L when simulating water-limited productivities. Our view is supported by O'Connell *et al.* (2004) who also stated that use of K_L and radiation use efficiency parameters in models should be limited to environments where these values were measured.

However, to mechanistically quantify K_L in response to water stress, it is necessary to first understand what causes the decline of K_L under the stress. A possible reason is that the stomatal closure induced by water stress leads to high leaf temperature that will consequently alter leaf angle. This is a common plant strategy, which is also called structural photoprotection (Valladares *et al.*, 1999 and references therein) to avoid excessive light capture inducing high rates of transpiration. An alternative model approach is to establish an empirical function for use in crop models. For that, an experiment is needed in which various severities of water stress would be imposed to plants.

Leaf shape, position and orientation effects on K_L

Despite the large differences in vertical leaf area distribution among the studied species (C_3, dicot, Fig. 4.3) we found only 30% differences in K_L values (0.62 to 0.89; no water stress; Fig. 4.4). Estimates are close to the range reported for species with broad-leaf type (0.7–1.0; Monsi & Saeki, 2005). According to leaf shape, it seems that species with larger individual leaf or leaflet surface area showed the higher K_L values (sunflower > cynara > kenaf). Given the rapid reduction in K_L (–48 to –65%; Fig. 4.4) under water stress due to a decrease in leaf angle, we can infer that foliage position in the canopy (also leaf shape) is less important than foliage inclination (Goudriaan, 1988; Yin & van Laar 2005) in determining K_L. For a review on the effects of foliage inclination and position on light penetration see Niinemets (2010).

Canopy vertical SLN distributions

All species showed non-uniform SLN distributions, particularly in periods when LAI was ≥1.5 (e.g. Fig. 4.5). Non-uniformity has been reported for many crops (cf. Shiraiwa & Sinclair, 1993; Wright & Hammer, 1994; Anten *et al*., 1995; Bange *et al*., 1997; Del Pozo & Dennett, 1999; Lötscher *et al*., 2003; van Oosterom *et al*., 2010) but few studies treated the canopy as a dynamic system. In all irrigated canopies, observed high SLN values at the top leaves (2.2–3.8 g N m^{-2}; Fig. 4.7g, h and i) are comparable with observations of leaf photosynthesis in sunflower (Connor *et al*., 1993; Bange *et al*., 1997), kenaf (Muchow, 1990) and cynara (Archontoulis *et al*., 2008b), where maximum net assimilation rates were saturated at SLN > 2.0. SLN values at the canopy bottom, were around 1.0 g N m^{-2} when LAI was ≥ 3 in all species (Figs. 4.5 and 4.6). Apparently canopy vertical SLN distribution approached values required for photosynthetic saturation at the top and SLN decreased to values equivalent to minimum photosynthetic activity roughly at high LAI values where much of the radiation had already been intercepted (Fig. 4.4).

Quantification of vertical SLN distributions

Beer's law (Eq. 2) approximated well SLN distributions in 40 canopies with average r^2 values of 0.75, 0.81 and 0.79 for sunflower, kenaf and cynara, respectively (Figs. 4.5, 4.6; Tables 4.2, 4.3). Bange et al. (1997) found a linear SLN/LAI relation for sunflower approximately a week after flowering (SLN = 2.5 – 0.26·LAI; r^2 = 0.76), whereas the slope of the line (K_N) and the initial SLN value (SLN_o) were close to our results. In contrast, Hall et al. (1995) observed curvilinear SLN/LAI plots between anthesis and physiological maturity for sunflower. In our study we showed that in sunflower vertical SLN distributions practically existed only for about 20–25 days during BBCH: 59–75 (Fig. 4.5; Table 4.2). For kenaf and cynara there are no literature data to compare our findings.

Anten *et al*. (1995) and Sands (1995) modified Eq. (2) to reflect the distribution of the effective SLN (=SLN – SLN_{base}; where SLN_{base} is the minimum SLN required for photosynthesis) that is associated with photosynthesis. This modified version uses three input parameters, SLN_o, SLN_{base} and the effective K_N ($K_{Neffective}$). We used –derived from leaf photosynthesis/SLN plots– SLN_{base} values of 0.3 for sunflower (Connor *et al*., 1993), 0.43 for kenaf (Muchow, 1990) and 0.42 for cynara (authors' unpublished data; see Chapter 5) and then applied this modified "effective" equation to our datasets (not shown). Analysis indicated that nitrogen extinction coefficients calculated from different equations provided much different estimates for the same dataset ($K_{Neffective}$ = 1.28 · K_N – 0.0003, n=40, r^2=0.91). This result agrees well with previous observations by Yin *et al*. (2003a) and therefore explains fairly well the large discrepancy among nitrogen extinction values reported in literature, even within the same species.

Year, time of season and water stress effects on vertical SLN distributions

Between years, SLN distributions were rather conservative per crop species, meaning that common estimates (SLN_o and K_N) can be used in modelling (Figs. 4.5 and 4.6). Within a season, each crop showed a species-specific vertical SLN distribution (Table 4.3). However, in all species, higher SLN_o were associated with higher K_N estimates (r^2=0.55; *P*=0.002; n=40 canopies), which is not too surprising considering that those canopies with greater SLN_o have a steeper decline in SLN in the canopy (e.g. Fig. 4.5).

In sunflower, the remarkable non-uniformity at flowering disappeared in the course of the grain filling period (Fig. 4.5; Table 4.2) in line with Sadras *et al*. (1993) and Connor *et al*. (1995). In kenaf, despite the coexistence of leaves of varying age in the same canopy layer –due to a continuous increase in height (Fig. 4.2e)– a vertical SLN distribution was apparent for the most of the growing cycle (Fig. 4.6a). Overall the data from 20 kenaf and 12 cynara canopies suggest

fairly common SLN profiles over the studied periods with little variation across water treatments (Fig. 4.6). It seems that during crop growth with and without water stress, N_{conc} and SLA, the two components of the SLN (Fig. 4.7), changed in such a way that changes in SLN are small over thermal time and between water regimes.

For common agricultural crops, lack of change in vertical SLN distributions over a large part of the growing cycle has also been reported for wheat (Bertheloot *et al*., 2008), soybean (Shiraiwa & Sinclair, 1993) and peanut canopies (Wright & Hammer, 1994). Lastly, it should be added that crops responded to irrigation by increasing their LAI (Fig. 4.2j and k) or maintaining high LAI values for a longer period (Fig. 4.2l) rather than changing the pattern of SLN distribution (Figs. 4.5 and 4.6).

Associations between PAR and SLN distributions

This study has shown that SLN distributions in irrigated sunflower and kenaf canopies appeared to be largely associated with the light environment ($r^2 > 0.66$; $P < 0.001$; Fig. 4.8). Such associations between light and nitrogen gradients have been found in many crops (Sadras *et al*., 1993; Anten *et al*, 1995; Del Pozo & Dennett 1999; Milroy *et al*., 2001; Lötscher *et al*., 2003), and are explained either from an adaptive response to irradiance gradient in order to maximise canopy photosynthesis (Hirose & Werger, 1987) or as a consequence of the mediation by cytokinins in the transpiration stream on the response to light (Pons *et al*., 2001).

By calculating the ratio of $K_{Neffective}/K_L$ as the optimization theory requires (Sands, 1995), we found values much below unity. This means that observed (actual) vertical distributions in sunflower and kenaf canopies were less steep than the optimal one that would maximize canopy photosynthesis. Gimenez *et al*. (1994) and Connor *et al*. (1995) showed that the advantage in canopy photosynthesis between actual and optimal distributions was small in sunflower (3 to 14%) while Hirose & Werger (1987) showed theoretical gains up to 20% in daytime canopy photosynthesis.

Conclusions

Light and nitrogen extinction coefficients were quantified for the C_3 dicots sunflower, kenaf and cynara. Per crop species, K_L was rather conservative in the course of the study (no water stress), but values differed between years (12–17%). Water-stressed summer crops had significantly lower K_L values (–48 to –65%) than irrigated crops. We found non-uniform SLN distributions in all crops when LAI was $\geq$ 1.5. These vertical distributions were significantly correlated with cumulative LAI from the top ($r^2 > 0.75$ all crops), providing new equations to

upscale photosynthesis from leaf to canopy levels. Vertical SLN distributions generally were showed a strong association with light distributions (r^2>0.66; sunflower and kenaf), but not always intimately so since observed SLN distributions were less steep than those that would maximize canopy photosynthesis. Our results can be used to estimate light interception and canopy photosynthesis, thereby enhancing our ability to assess potential and water-limited yields of these energy crops.

Chapter 5

Leaf photosynthesis and respiration of three bioenergy crops in relation to temperature and leaf nitrogen: How conservative are biochemical model parameters among crop species?

Abstract

Given the need for parallel increases in food and energy production from crops in the context of global change, crop simulation models and data sets to feed these models with photosynthesis and respiration parameters are increasingly important. This study provides information on photosynthesis and respiration for three energy crops (sunflower, kenaf, cynara), reviews relevant information for five other crops (wheat, barley, cotton, tobacco, grape), and assesses how conservative photosynthesis parameters are among crops. Using large datasets and optimization techniques we parameterized the C_3 leaf photosynthesis model of Farquhar et al. (FvCB) and an empirical night respiration model for tested energy crops accounting for effects of temperature and leaf nitrogen. Instead of the common approach of using information on net photosynthesis response to CO_2 at stomatal cavity (A_n–C_i), we parameterized the model by analysing the photosynthesis response to incident light intensity (A_n–I_{inc}). We first provided convincing evidence that maximum Rubisco-carboxylation rate or maximum electron transport rate was very similar whether derived from A_n–C_i or from A_n–I_{inc} datasets. We then determined parameters characterizing Rubisco limitation, electron transport limitation, the degree to which light inhibits leaf respiration, night respiration, and the minimum leaf nitrogen required for photosynthesis. Model predictions were validated against independent sets. Only few FvCB parameters were conservative among crop species, thus species-specific FvCB model parameters are needed for crop modelling. Therefore, information from readily available but under-explored A_n–I_{inc} data should be re-analyzed, thereby expanding the potential of combining classical photosynthetic data and the biochemical model.

Introduction

In conventional crop modelling leaf photosynthesis is calculated from net photosynthesis light response curves (A_n–I_{inc}) at ambient atmospheric CO_2 level using empirical functions (e.g. SUCROS; Goudriaan & van Laar, 1994). In the context of better understanding biological processes and exploring the impact of climate change, recent crop models (e.g. GECROS; Yin & van Laar, 2005), 3D models (e.g. Evers *et al.*, 2010) or terrestrial ecosystem models (e.g. LPJmL; Beringer *et al.*, 2011), calculate photosynthesis based on the mechanistic model of Farquhar, von Caemmerer & Berry (1980; the FvCB model hereafter).

The FvCB model describes photosynthesis as the minimum of the Rubisco-limited rate and the electron transport limited rate. The key parameters of the model are the maximum Rubisco-carboxylation rate (V_{cmax}; see symbols explanation in Table 5.1), the maximum electron transport rate (J_{max}), and the mitochondrial day respiration (R_d). These biochemical parameters are influenced both by the physiological status of a leaf such as the amount of leaf nitrogen per unit area (N_a) (e.g. Harley *et al.*, 1992) and by short- and long-term changes of environmental variables such as temperature, light (e.g. Hikosaka, 2005), CO_2 (e.g. Makino *et al.*, 1994) and drought (e.g. Galmes *et al.*, 2007).

Usually, the FvCB parameters are obtained by analysis of net photosynthesis response to CO_2 at stomatal cavity (A_n–C_i) (e.g. Sharkey *et al.*, 2007) or by combining A_n–C_i and A_n–I_{inc} curves (e.g. Braune *et al.*, 2009) or by combining these curves with chlorophyll fluorescence measurements (Yin *et al.*, 2009). Obviously, to parameterize the FvCB model, information on A_n–C_i is predominantly considered to be essential, and an ongoing discussion is mainly focused on improving the methods of analyzing these A–C_i curves (Ethier *et al*. 2004; Sharkey *et al.*, 2007; Gu *et al.*, 2010).

In the context of forward crop modelling typically for predictions at ambient CO_2 level, the FvCB model is used to project leaf photosynthetic rates in response to both temporal (diurnal and seasonal) and spatial (within a crop canopy) variation in incoming light intensity. This implies that in the context of inverse modelling important FvCB-model parameters J_{max} and V_{cmax} should and can be estimated from A_n responses to I_{inc}. This would reflect better the tradition that crop modellers describe leaf photosynthesis from its response to light intensity (e.g. Goudriaan, 1979), in contrast to the tradition that photosynthesis physiologists study gas exchange measurements mainly across various levels of CO_2 (e.g. von Caemmerer & Farquhar 1981). In fact, the FvCB model can be parameterized from analysis of A_n–I_{inc} data alone (Niinemets & Tenhunen, 1997; Kosugi *et al.*, 2003), but so far there is no information about the accuracy of J_{max} and V_{cmax} parameters derived from such an analysis. If J_{max} and V_{cmax} estimates

derived from analysis of A_n–I_{inc} are similar to those obtained from the common A–C_i analysis or combined analysis of A_n–C_i and A_n–I_{inc} curves, it may generate an opportunity to reduce empiricism in crop models by using readily available A_n–I_{inc} data. Therefore the first objective of this paper is to explore this opportunity by parameterising the FvCB model using A_n–I_{inc} data.

In the light of current trends for parallel increase in food and energy production from crop species in the context of climate change, the use of the FvCB-based simulation models together with an urgent need to feed these models with appropriate photosynthetic and respiration parameters has been increased (e.g. see Beringer *et al.*, 2011). In literature, reports on J_{max}, V_{cmax}, R_d and night respiration (R_n) parameters in relation to environmental and management factors are few for economically important crop species and especially for new bioenergy species, compared to the rich information found for trees. This is highly noticeable in recent studies (Medlyn *et al.*, 2002a; Müller *et al.*, 2005; Braune *et al.*, 2009). Therefore, the second objective of this paper is three-fold: (i) to provide new information on photosynthesis and respiration for three Mediterranean energy crops (*Helianthus annuus,* sunflower; *Hibiscus cannabinus*, kenaf; and *Cynara cardunculus,* cynara); (ii) to summarize existing information for five major cash crops (wheat, barley, cotton, tobacco and grape); and (iii) to assess how conservative FvCB parameters are among crop species to better assist modellers in this exploitation.

Our analysis is based on the FvCB model and focuses on the effects of temperature and N_a. This is because earlier studies on V_{cmax} and J_{max} temperature dependencies showed great species-to-species variability (Leuning, 2002; Medlyn *et al.*, 2002a) and because use of an "average leaf" (neglecting N_a) to represent whole leaf life-span resulted in large errors in modelling (Wilson *et al.*, 2001). N_a is linearly related to Rubisco content that drives CO_2 fixation (Makino *et al.*, 1994), reflects well leaf dynamics (leaf age, rank; Archontoulis *et al.*, 2011a), and comprises a reference index for scaling photosynthetic CO_2 assimilation from leaf to canopy levels (de Pury & Farquhar, 1997).

Sunflower, kenaf and cynara crops were chosen because of their diverse bio-energy uses. Recently, relevant information for modelling like light and nitrogen distribution within crop canopies was derived for these crops (Archontoulis *et al.*, 2011a). Among these crops, the perennial cynara has long annual growth cycles (~ 10 months each; Archontoulis et al., 2010a). Given the numerous reports together with their diverse findings on photosynthetic and respiratory acclimation to growth environment (Atkin *et al.*, 2005; Ow *et al.*, 2008; Yamori *et al.*, 2005, 2010; Silim *et al.*, 2010), we also investigate seasonal acclimation effects on photosynthesis and respiration for the cynara crop.

Table 5.1: List of main symbols used in this study with their definition and unit

Symbol	Definition	Unit
A_c	Rubisco limited net photosynthetic rate	$\mu mol\ CO_2\ m^{-2}\ s^{-1}$
A_n	Net assimilation rate	$\mu mol\ CO_2\ m^{-2}\ s^{-1}$
A_j	Electron transport limited net photosynthetic rate	$\mu mol\ CO_2\ m^{-2}\ s^{-1}$
$A_{n,max}$	Light saturated A_n	$\mu mol\ CO_2\ m^{-2}\ s^{-1}$
a_R	Constant parameter in Eq. 12	$\mu mol\ CO_2\ m^{-2}\ s^{-1}$
b_R	Slope parameter in Eq. 12	–
C_c	CO_2 chloroplast partial pressure	μbar
C_i	Intercellular CO_2 partial pressure	μbar
D_j, D_v	Deactivation energy of J_{max} and V_{cmax} (Eq. 6)	$J\ mol^{-1}$
E_{Kmc}, E_{Kmo}	Activation energy for K_{mc} and for K_{mo}	$J\ mol^{-1}$
E_j, E_{Rn}, E_v	Activation energy of J_{max}, Rn and V_{cmax} (Eqs. 5–6)	$J\ mol^{-1}$
$E_{Rn(a)}$	Constant parameter (Eq. 11)	$J\ mol^{-1}$
$E_{Rn(b)}$	Slope parameter in (Eq. 11)	$J\ m^{-2}\ mol^{-1}\ g^{-1}\ N$
g_m	Mesophyll conductance for CO_2 diffusion	$mol\ m^{-2}\ s^{-1}$
g_s	Stomatal conductance for H_2O	$mol\ m^{-2}\ s^{-1}$
I_{inc}	Incident light on leaf surface	$\mu mol\ photons\ m^{-2}\ s^{-1}$
J	Photosystem II electron transport rate	$\mu mol\ e^-\ m^{-2}\ s^{-1}$
J_{max}	Maximum electron transport rate	$\mu mol\ e^-\ m^{-2}\ s^{-1}$
J_{max25}	Value of J_{max} at 25°C	$\mu mol\ e^-\ m^{-2}\ s^{-1}$
K_{mc}	Michaelis-Menten constant for CO_2	μbar
K_{mo}	Michaelis-Menten constant for O_2	$mbar$
N_a	Leaf nitrogen per unit area	$g\ N\ m^{-2}\ leaf$
N_b	Minimum N_a required for photosynthesis	$g\ N\ m^{-2}\ leaf$
O	Oxygen partial pressure of the air (=210)	$mbar$
R	Universal gas constant (=8.314)	$J\ K^{-1}\ mol^{-1}$
R_d	Day respiration rate	$\mu mol\ CO_2\ m^{-2}\ s^{-1}$
R_n	Night respiration rate	$\mu mol\ CO_2\ m^{-2}\ s^{-1}$
R_{n25}	Value of R_n at 25°C	$\mu mol\ CO_2\ m^{-2}\ s^{-1}$
S_j, S_v	Entropy term for J_{max} and V_{cmax} (Eq. 6)	$J\ K^{-1}\ mol^{-1}$
V_{cmax}	Maximum carboxylation rate	$\mu mol\ CO_2\ m^{-2}\ s^{-1}$
V_{cmax25}	Value of V_{cmax} at 25°C	$\mu mol\ CO_2\ m^{-2}\ s^{-1}$
Γ_*	C_i based CO_2 compensation point in the absence of R_d	μbar
θ	Convexity factor for the response of J to I_{inc}	–
κ_{2LL}	Conversion efficiency of I_{inc} into J at low light	$mol\ e^-\ mol^{-1}\ photons$
Φ_{CO2LL}	Apparent quantum yield of A_n at low I_{inc}	$mol\ CO_2\ mol^{-1}\ photons$
χ_j	Slope of the J_{max25} and N_a relationship (Eq. 10)	$\mu mol\ e^-\ g^{-1}\ N\ s^{-1}$
χ_R	Slope of the R_{n25} and N_a relationship (Eq. 8)	$\mu mol\ CO_2\ g^{-1}\ N\ s^{-1}$
χ_v	Slope of the V_{cmax25} and N_a relationship (Eq. 9)	$\mu mol\ CO_2\ g^{-1}\ N\ s^{-1}$

Materials and Methods

Literature data (A_n–C_i versus A_n–I_{inc})

As stated in Introduction, the first objective of this study was to compare V_{cmax} and J_{max} estimates derived either from A_n–C_i or from A_n–I_{inc} curves with those from the combination of the two types of curves. For this we used published data from Yin *et al*. (2009) for *Triticum aestivum* (cv. Minaret). This set contains the dependences of A_n to both C_i and I_{inc}, while all relevant parameter values required to fit the FvCB model to dataset were available, therefore avoiding any statistical artifact in V_{cmax} and J_{max} estimation (see below). In addition, wheat measurements (4 replicates; all at 25°C) were conducted at leaves with different N_a status (15 sets of A_n–C_i and 15 of A_n–I_{inc} curves), allowing the comparison of J_{max} and V_{cmax} estimates to be made over a wide range of their values. For more information about the measurements see Yin *et al*. (2009).

Energy crop species and study site

Sunflower (cv. Panter), kenaf (cv. Everglades 41) and cynara (cv. Biango avorio) crops were grown in different sections of the same field (for details see Archontoulis *et al*., 2011a) in central Greece (39º25′43.4′′ N, 22º05′09.7′′ E, 105 m asl) for three years (2007–2009). The site has a Mediterranean climate with cold/wet winters and warm/dry summers (Fig. S-5.1 in supplementary files). The soil was loamy, classified as Aquic Xerofluvent, with shallow groundwater table (1.8–2.8 m below surface during May). In general, crops grown at that site produce much higher biomass yields than crops grown on dry soils (e.g. Archontoulis et al., 2010b). During summer, sunflower and kenaf crops were frequently irrigated at intervals of 4–6 days according to potential evapotranspiration (for site-specific calculations, see Danalatos & Archontoulis, 2010) while cynara was irrigated only a few times, when necessary during May–June but not during November–April (see precipitation in Fig. S-5.1).

Gas exchange measurements and experimental protocol

Leaf gas exchange (GE) measurements were implemented *in situ* in fully expanded leaves using a portable open gas exchange system with a 6.25 cm² clamp-on leaf chamber (ADC, LCi/LCpro+, Bioscientific Ltd., Hoddesdon, UK). CO_2/H_2O exchanged by the leaf was measured using an infrared gas analyzer in a differential mode. The system allowed for an automated micro-climate control in the leaf chamber. Before each measurement, attached leaves were adapted 10–45 min to chamber conditions, depending on leaf age, time of the day and season.

Day-time GE measurements were taken within one to two days after irrigation application and during morning hours to ensure no water stress and to avoid photosynthesis midday depression. Night-time GE measurements were initiated 30–45 min after sunset and lasted for 4–5 hours each time.

To parameterize the model, a common experimental protocol was applied per species, including four different sets of GE measurements. In all sets, CO_2 concentration was kept at 380±5 µmol mol^{-1}. The first set aimed to determine the response of net photosynthesis (A_n) to incident light (I_{inc}). Accordingly, at fixed leaf temperature and measured N_a, A_n was determined in eleven I_{inc} steps (2000, 1500, 1000, 500, 250, 200, 150, 100, 50, 20 and 0 µmol photons m^{-2}s^{-1}); in total 76 curves were constructed. Adaptation time to each I_{inc} level was approximately 5 min, except for I_{inc}=0 where it was >10 min; three to five replicated A_n measurements were taken at each I_{inc} step to ensure stability and precision of measurements. Given that the examination of steady-state photosynthesis takes considerable time and that GE measurements should be done within a limited time frame in order to avoid stress conditions (see above), we determined the response of A_n to leaf temperature (set II) at three I_{inc} levels, 450, 900 and 1800 µmol photons m^{-2}s^{-1}. N_a was also determined. At each I_{inc}, leaf temperature was increased or decreased up to 10°C from the ambient temperature in steps of 2–4°C and replicated A_n measurements were recorded every 5 min.

To establish the relationship between net photosynthesis and N_a (set III), it was necessary to evaluate leaves with as wide a N_a range as possible. So, in addition to earlier sets, A_n measurements were done at saturated I_{inc} (1600–1800 µmol photons m^{-2} s^{-1}) on leaves from different insertion height in the canopy, from different growth stages and from plots with different N-status. Per leaf (approx. 180 leaves assessed), 5–10 measurements were taken at leaf temperature close to the ambient temperature. To obtain direct measurements of the mitochondrial respiration occurring in the night (R_n), the response of R_n to temperature was investigated (set IV). Leaf temperature increased or decreased up to 10°C from the ambient temperature at small steps of 1–2°C and replicated R_n measurements were recorded every 4 min. Measurements were done on leaves with (as much as possible) variable N_a.

To validate the models we used GE measurements obtained at the same genotypes growing in the same site during summer 2005 and 2006 (set V). Sunflower and kenaf GE measurements were collected using similar techniques and time frames as described for sets I to IV. In cynara, a different protocol was followed. The external unit that controls chamber microclimate was removed and measurements refer to real ambient conditions. Measurements were recorded every 4–8 minutes while climatic variables were continuously changing following 24 diurnal trends.

The wide range of measuring temperature used (15–40°C) unavoidably resulted in variation in vapour pressure difference (VPD). An effort was made to reduce that variation by keeping humidity high at high temperature. In most cases, VPD was maintained below 3 kPa to prevent stomata closure (Bernacchi *et al.*, 2001). Although VPD was sometimes above 3 kPa at the highest temperatures, the stomatal conductance for H_2O vapour was not less than 0.30 mol m^{-2} s^{-1} (as in Yamori *et al.*, 2005).

To minimize artifacts associated with commercial photosynthesis systems (for a review, see Pons *et al.*, 2009), we took the following actions: a) we corrected for the CO_2 respired under the gasket surface (total 4 mm width; R. Newman, pers. comm.) following the common approach of Pons & Welschen (2002) and b) we increased the number of replications and observations to reduce the measurement noise, especially when low CO_2 exchange rates were measured (e.g. respiration). All gas exchange characteristics were re-calculated according to von Caemmerer & Farquhar (1981).

The portion of the leaf used for measurements was cut and its area was measured with a Li-Cor area meter. The leaf material was then weighed after drying at 70°C to constant weight and its total nitrogen concentration was measured using the Kjeldahl method. From these measurements, the leaf nitrogen content N_a (g N m^{-2}) was calculated.
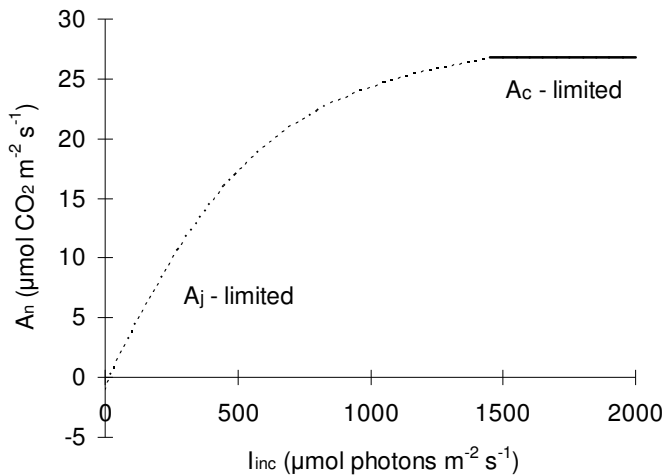
Figure 5.1: Typical net photosynthesis light response curve (A_n–I_{inc}) at ambient CO_2 concentration. Curve regions for the Rubisco-carboxylation limited rate (A_c-limited, Eq. 2; ──) and electron transport limited rate (A_j-limited, Eq. 3; - - -) are indicated. Usually, A_c-limitation occurs above 1500 μmol photons m^{-2} s^{-1}; however, it is also possible that the entire A_n–I_{inc} curve is described as A_j-limited.

Model and its parameterization

The FvCB model predicts net assimilation rate (A_n μmol CO_2 m^{-2} s^{-1}) as the minimum of two processes (see Fig. 5.1), Rubisco-carboxylation limited rate (A_c) and RuBP-regeneration or electron transport limited rate (A_j):

$$A_n = \min\{A_c, A_j\}$$

(1)

Rubisco limited photosynthesis is calculated as a function of maximum carboxylation capacity (V_{cmax}, μmol CO_2 m^{-2}s^{-1}):

$$A_c = \frac{V_{c\max}(C_i - \Gamma_*)}{C_i + K_{mc}\left(1 + O/K_{mo}\right)} - R_d$$

(2)

where C_i (μbar) and O (mbar) are the intercellular partial pressures of CO_2 and O_2 respectively, K_{mc} (μbar) and K_{mo} (mbar) are the Michaelis-Menten coefficients of Rubisco for CO_2 and O_2, respectively, Γ_* (μbar) is the CO_2 compensation point in the absence of R_d (day respiration in μmol CO_2 m^{-2} s^{-1}, which comprises mitochondrial CO_2 release occurring in the light other than photorespiration; von Caemmerer *et al.*, 2009).

There are various equations to describe the rate of photosynthesis when RuBP regeneration is limiting (Farquhar & von Caemmerer 1982; Yin *et al.*, 2004). The most widely used form is given by:

$$A_j = \frac{J(C_i - \Gamma_*)}{4C_i + 8\Gamma_*} - R_d$$

(3)

where J (μmol e$^-$ m^{-2} s^{-1}) is photosystem II electron transport rate that is used for CO_2 fixation and photorespiration. J is related to the amount of incident photosynthetically active irradiance (I_{inc}; μmol photons m^{-2} s^{-1}) by:

$$J = \frac{\left(\kappa_{2LL}I_{inc} + J_{\max} - \sqrt{(\kappa_{2LL}I_{inc} + J_{\max})^2 - 4\theta J_{\max}\kappa_{2LL}I_{inc}}\right)}{2\theta}$$

(4)

where J_{max} (μmol e$^-$ m^{-2} s^{-1}) is the maximum electron transport rate at saturating light levels, θ is a dimensionless convexity factor for the response of J to I_{inc}, and κ_{2LL} (mol e$^-$ mol^{-1} photons) is the conversion efficiency of I_{inc} into J at limiting light levels (Yin *et al.*, 2009; Yin & Struik, 2009a). The formulation of Eqs (2) and (3) assumes infinitive mesophyll conductance (g_m) for CO_2 transfer to chloroplast, so that C_i is used as the proxy to chloroplast CO_2 level (C_c). There is increasing

evidence that g_m might be low enough to allow a significant drawdown of C_c from C_i in most species (Warren, 2004; Flexas *et al.*, 2008). However based on our available gas exchange data it was risky to evaluate g_m (Pons *et al.*, 2009; von Caemmerer *et al.*, 2009; Yin & Struik, 2009b), hence we were obliged to use the forms of Eqs (2) and (3) as in most earlier studies (e.g. Medlyn *et al.*, 2002a; Kosugi *et al.*, 2003). Omitting g_m in our analysis means that an appropriate consideration is needed in choosing values of the Rubisco kinetic constants (see below).

The temperature responses of respiration and of Rubisco kinetic properties (K_{mc} and K_{mo}) are described using an Arrhenius function (Eq. 5) while the temperature responses of V_{cmax} and J_{max} were explored using a peaked Arrhenius function (Eq. 6); both functions were normalized with respect to their values at 25°C:

$$X = X_{25} \exp\left[\frac{E_x(T-25)}{298R(T+273)}\right]$$
(5)

$$X = X_{25} \exp\left[\frac{E_x(T-25)}{298R(T+273)}\right] \cdot \left[\frac{1+\exp\left(\dfrac{298S_x - D_x}{298R}\right)}{1+\exp\left(\dfrac{(T+273)S_x - D_x}{R(T+273)}\right)}\right]$$
(6)

where T is the leaf temperature (°C); X_{25} is the value of each parameter at 25°C (R_{n25}, K_{mc25}, K_{mo25}, V_{cmax25}, J_{max25}); E_x is the activation energy of each parameter (E_{Rn}, E_{Kmc}, E_{Kmo}, E_v and E_j; in J mol^{-1}); D_x is the deactivation energy for J_{max} and V_{cmax} (D_j and D_v in J mol^{-1}); S_x is the entropy term for J_{max} and V_{cmax} (S_j, S_v in J K^{-1} mol^{-1}) and R is the universal gas constant (= 8.314 J K^{-1} mol^{-1}). Given that Eq. (5) is a special case of Eq. (6), *F*-tests were performed to determine whether Eq. (6) described temperature responses of V_{cmax} and J_{max} significantly better than Eq. (5) did. When Eq. (6) was over-parameterized, as often observed in literature (Medlyn *et al.*, 2002a; Dreyer *et al.*, 2001), then we fixed S_x at 650 J K^{-1} mol^{-1} (Harley *et al.*, 1992).

Rubisco kinetic properties are generally assumed constant among C$_3$ species (von Caemmerer *et al.*, 2009). However, values of these constants and their temperature dependency reported in the literature vary appreciably, so the choice of Rubisco parameters is a matter of considerable uncertainty (Dreyer *et al.*, 2001). In this work, similar to many other reports (e.g. Medlyn *et al.*, 2002a; Müller *et al.*, 2005) we selected Rubisco parameters reported by Bernacchi *et al.* (2001) because (i) these values were estimated from *in vivo* measurements without disturbance of the leaf, and (ii) they were derived using the C$_i$–based FvCB model and hence compatible with our analysis assuming an infinite g_m (see

above). The parameter values are: K_{mc25}=404.9 µbar; K_{mo25}=278.4 mbar; E_{Kmc}=79430 J mol^{-1}; and E_{Kmo}=36380 J mol^{-1} (Table 5.1). Furthermore, using these values the temperature dependence of Γ^* was calculated as (Yin *et al.*, 2004):

$$\Gamma^* = 0.5 O \frac{K_{mc}}{K_{mo}} \left[\exp\left(-3.3801 + \frac{5220}{298R(T+273)} \right) \right]$$

(7)

where the factor 0.5 is mol CO_2 released when Rubisco catalyses the reaction with 1 mol O_2 in photorespiration. The term in the brackets was derived using Bernacchi *et al.* (2001) parameters for temperature dependence of maximum carboxylation and oxgenation rates of Rubisco.

The basal capacity of R_{n25}, V_{cmax25} and J_{max25} is linearly related to N_a (Harley *et al.*, 1992; Hirose *et al.*, 1997; Müller *et al.*, 2005; Braune *et al.*, 2009):

$$R_{n25} = \chi_R (N_a - N_b)$$ (8)
$$V_{c\max 25} = \chi_v (N_a - N_b)$$ (9)
$$J_{\max 25} = \chi_J (N_a - N_b)$$ (10)

where χ_R (µmol CO_2 g^{-1} N s^{-1}), χ_v (µmol CO_2 g^{-1} N s^{-1}) and χ_j (µmol e[-] g[-1] N s^{-1}) are the slopes for R_{n25}, V_{cmax25} and J_{max25} respectively, and N_b (g N m^{-2}) is the minimum value of N_a at or below which A_n is zero. In principle, this N_b is practically impossible to be measured and its estimation depends on the statistical methods used and on the available datasets. For instance, different N_b estimates were found when different datasets were examined (A_n or V_{cmax} or J_{max}; e.g. Harley *et al.*, 1992; Müller *et al.*, 2005; Table S-5.1 in the supplementary file) or when N_b was estimated simultaneously with other parameters in optimization procedures or when different equations (linear or non-linear) were applied to the same dataset (Niinemets & Tenhunen, 1997). Given the simplicity required in modelling and the lack of biological interpretation of different N_b values for the same species, we determined a unique N_b value (per species) beforehand from direct assessments of A_n–N_a plots. Then this estimate was used as input parameter.

Besides the basal capacities, there is some evidence that the activation energy for respiration (E_{Rn}) depends on the position of the leaf in the canopy (Bolstad *et al.*, 1999; Griffin *et al.*, 2002) and perhaps E_{Rn} is also associated with N_a since a close relation between leaf canopy position and N_a usually exists (Archontoulis *et al.*, 2011a). We tested this by assuming a linear relation between E_{Rn} and N_a:

$$E_{Rn} = E_{Rn(a)} + E_{Rn(b)} N_a$$

(11)

and checked whether the slope parameter $E_{Rn(b)}$ differed significantly from zero.

So far, we have described temperature and nitrogen relations for R_n, as we had extensive GE measurements during the night period. However, the FvCB requires estimates for R_d, which is much more difficult to measure. To estimate R_d we applied regression analysis to the linear sections of the A_n–I_{inc} curves for each species (Kok method; see Sharp *et al*., 1984). From this analysis, R_d was calculated as the y-axis intercept of the linear regression (I_{inc} range: 20–150 µmol photons m^{-2} s^{-1}) and the corresponding R_n was estimated as the mean of the A_n values at 0 µmol photons m^{-2} s^{-1}. Additionally, the apparent quantum efficiency at limiting light (Φ_{CO2LL}, mol CO_2 mol^{-1} photons) on the incident light basis was calculated from the slope of the regression. We then related the estimated R_d to R_n as:

$$R_d = b_R \cdot R_n + a_R \tag{12}$$

where b_R and a_R are the slope and the constant parameter of the linear model, respectively. By assuming that activation energies for R_d and R_n are similar and taking into account the precise quantification of R_n based on a large dataset, the temperature and nitrogen dependencies of R_d can be calculated from combining Eqs. 5, 8, 11 and 12. This approach allows us to estimate R_d values for sets II and III (see above) where I_{inc} exceeds 350 µmol m^{-2} s^{-1}, for which we were unable to use the Kok method for estimating R_d.

Summary of parameters and statistics

The basic equations of the FvCB model, Eqs. (1–4), capture the response of A_n to C_i and to I_{inc}. Coupled with auxiliary temperature (Eqs. 5–6) and nitrogen (Eqs. 7–12) equations, the model also quantifies leaf photosynthesis and respiration (R_d and R_n) in response to these environmental variables. Data from sets I to IV were analyzed using step-wise optimization procedures. Per crop, 16 parameters were estimated following the order: step 1: N_b; step 2: χ_R, $E_{Rn(a)}$, $E_{Rn(b)}$; step 3: b_R, a_R; step 4: χ_v, E_v, D_v, S_v; step 5: κ_{2LL}; step 6: χ_j, E_j, D_j, S_j, and θ (see results). Inputs to the model are: C_i, I_{inc}, leaf temperature and N_a.

For each step, regression fitting was carried out using the GAUSS method in PROC NLIN of SAS (SAS institute Inc,). To investigate for seasonal effects of acclimation on photosynthesis and respiration rates of cynara, datasets were split into two periods: a cold period with low light from November to April and a warm period with high light from May to June (Fig. S-5.1). Then, we introduced dummy variables (Z1=1 and Z2=0 for warm and Z1=0 and Z2=1 for cold periods, respectively) into regression analysis to separate for the effects. Dummy variable was also used to best estimate the N_b parameter (see Results).

The goodness of model fit was assessed by calculating r^2 and the relative mean root square error (*r*RMSE). A sensitivity analysis was also performed. Model predictions were validated against independent datasets (set V).

Re-analysis of the wheat datasets (A_n–C_i vs. A_n–I_{inc})

V_{cmax} and J_{max} estimates per set of data for the wheat (Yin *et al.*, 2009) were calculated by applying the same curve-fitting techniques in SAS. The following parameters were set as inputs to the model (see Eqs. 1–4 and 7): K_{mc25} and K_{mo25} from Bernacchi *et al.* (2001); and R_{d25}, R_{n25}, κ_{2LL} and θ per set of data from Yin *et al.* (2009). V_{cmax} and J_{max} were successfully estimated simultaneously in 40 out of the 45 cases (15 sets × 3 methodologies). In five cases, we failed to estimate V_{cmax} from A_n–I_{inc} curves analysis because in these cases the entire curve was A_j-limited (Fig. 5.1). Then we calculated V_{cmax} directly from Eq. 2 with simple substitution using data points where $I_{inc} >1500$ μmol photons m^{-2} s^{-1}, and by setting V_{max} as an input to the model we estimated again the J_{max} parameter. To be consistent, results for all A_n–I_{inc} curves were presented following the two-step approach, because estimates from both approaches were very close.
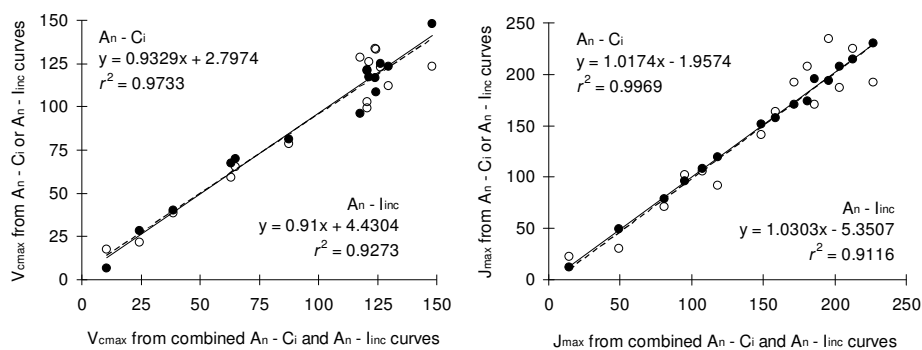
Figure 5.2: Relationships between V_{cmax} (μmol CO_2 m^{-2} s^{-1}) and J_{max} (μmol e$^-$m^{-2} s^{-1}) estimated from photosynthetic light response curves at ambient CO_2 concentration (○; A_n–I_{inc}) or from photosynthetic CO_2 response curves at saturated light (●; A_n–C_i) versus estimates obtained from an analysis of combined A_n–I_{inc} and A_n-C_i curves. Data for A_n–C_i and A_n–I_{inc} measurements are from Yin *et al.* (2009) for *Triticum aestivum* (n=15).

Results

V_{cmax} *and* J_{max} *estimates from* A_n–C_i *and/or* A_n–I_{inc} *curves*

Fig. 5.2 illustrates V_{cmax} and J_{max} from A_n–C_i and from A_n–I_{inc} curves versus the combination of those curves. As expected, V_{cmax} and J_{max} estimates obtained from A_n–C_i curves were almost identical to the estimates based on the combined data (r^2 = 0.97–0.99). However, we found that A_n–I_{inc} curves alone provided also sufficient estimates (r^2=0.91–0.93) and thus can be considered as alternative to predominant A_n–C_i curves to parameterize the FvCB model. In fact, regression lines in Fig. 5.2 were matching across a very wide range of V_{cmax} and J_{max} values. Even in cases where photosynthetic responses to light was entirely A_j–limited (Fig. 5.1), V_{cmax} estimates obtained either from A_n–I_{inc} or A_n–C_i data were close (Fig. 5.2). The slight discrepancy of the estimates at high V_{cmax} and J_{max} values (Fig. 5.2) caused a lower r^2 for the A_n–I_{inc} compared to A_n–C_i estimates.

Table 5.2: Estimates (standard error in parenthesis) of the non-linear equation used to describe data illustrated in Fig. 5.3. A_{max} is the maximum net assimilation rate (μmol CO_2 m^{-2} s^{-1}) at saturated light, maximal leaf nitrogen content, ambient CO_2 concentration and at optimum (filled symbols) and non-optimum (open symbols) temperature ranges; c is a dimensionless factor determining the steepness of the non-linear model; and N_b is the minimum leaf nitrogen content (g N m^{-2}) required for photosynthesis

Species	Symbol[1]	A_{max}	c	N_b[2]
Sunflower	filled (26–34°C)	36.6 (2.48)	1.19 (0.195)	0.387 (0.078)
	open	26.4 (1.45)	1.65 (0.313)	
Kenaf	filled (27–35°C)	35.8 (2.18)	1.29 (0.269)	0.390 (0.126)
	open	29.2 (2.12)	1.45 (0.334)	
Cynara	filled (22–31°C)	36.4 (2.41)	1.08 (0.191)	0.416 (0.097)
	open	23.9 (2.16)	1.22 (0.725)	

[1]: symbols used in Fig. 5.3.
[2]: the confidence limits for N_b are: 0.231 to 0.541, 0.139 to 0.640 and 0.225 to 0.608 for sunflower, kenaf and cynara, respectively.

Step-wise estimation of model parameters

Step 1: N_b *estimation*

Measured light saturated A_n ($A_{n,max}$) responded non-linearly to increasing N_a in all tested crops (Fig. 5.3; r^2>0.81; P<0.001). An effect of temperature was detected in this relationship only at high N_a (Fig. 5.3). To properly estimate the N_b value from these plots we used a dummy variables approach, in order to obtain a unique N_b estimate per crop, while allowing the equation to vary with different temperatures (optimum vs. non-optimum temperature ranges; Fig. 5.3). Derived

parameters are listed in Table 5.2. N_b values for all crops were close to 0.4 g N m^{-2}, while the lack of N_a data below 0.7 g m^{-2} caused a high standard error of the estimate for N_b (Table 5.2).
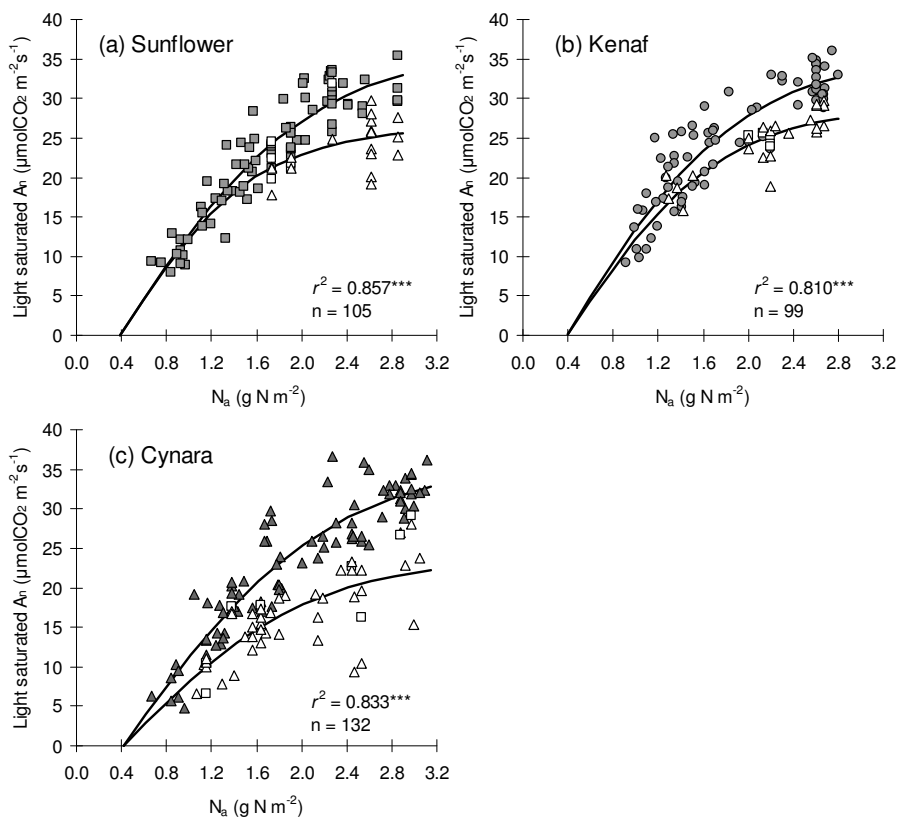
Figure 5.3: Relationships between light saturated net photosynthesis, A_n (I_{inc} >1500 µmol m^{-2}s^{-1}; CO_2=380 µmol mol^{-1}) and leaf nitrogen content, N_a. Filled symbols refer to data obtained at temperatures near the optimum temperature for photosynthesis per species (sunflower: 26–34°C; kenaf: 27–35°C; cynara: 23–31°C) and open symbols refer to data obtained at sub- (□) or supra- (Δ) optimum temperature ranges. Each point is an average of 4 to 10 measurements. Lines are fits from a three-parameter non-linear equation: A_n=A_{max}\{2/(1+exp(−c(N_a–N_b)))−1\}, (see Sinclair & Horie 1989); where A_{max} is the asymptote (maximum value) of the dependent variable; c is the parameter determining the steepness of the curve; N_b is the intercept of the X-axis denoting a threshold leaf nitrogen value at or below A_n equals zero. Estimates of parameters are given in Table 5.2. Cynara's data points were mostly collected during May–June.

Step 2: R_n in relation to temperature and N_a

By combining equations 5, 8 and 11, R_n parameters were estimated (Table 5.3). In the case of cynara, an additional seasonal effect was found with significantly higher R_n rates for the winter/cold compared to summer/warm growing leaves (Fig. 5.4). Incorporation of this effect into the model improved r^2 from 0.68 to 0.72. Of the two R_n parameters, temperature sensitivity (E_{Rn}) was significantly ($P<0.01$) affected by season; but the slope of the R_n–N_a relation (χ_R) was not ($P=0.263$), thus a common χ_R value was calculated (Table 5.3). R_n models' goodness of fit was satisfactory ($r^2> 0.72$; rRMSE <0.28 across species).
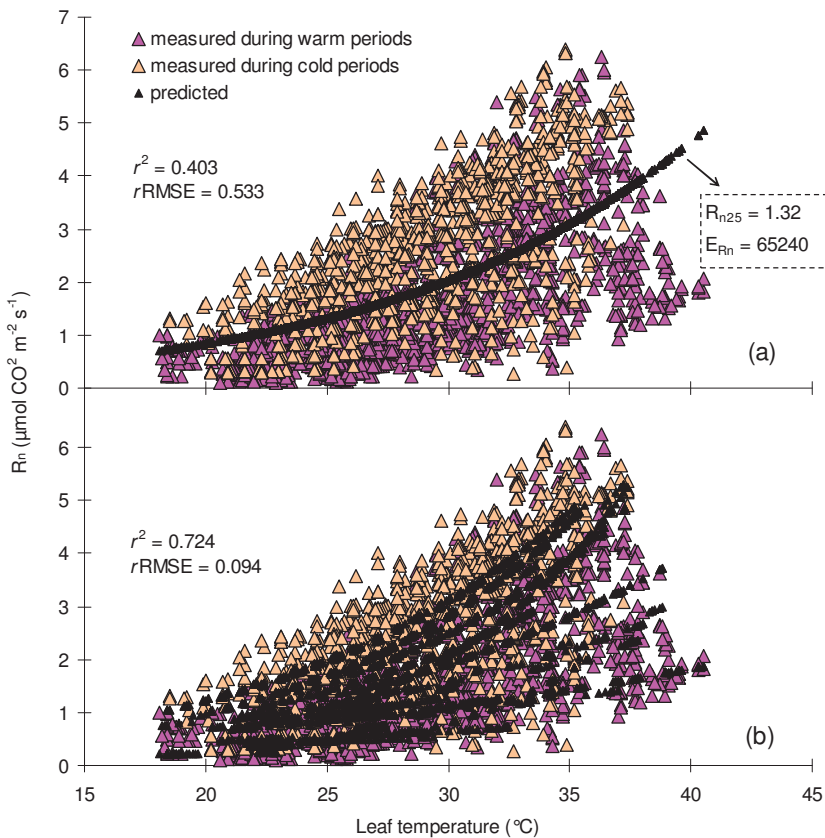
Figure 5.4: Cynara's night respiration rates (R_n) in relation to leaf temperature. Data is presented per growth season and includes leaves with various N_a. Panel (a) shows the predicted R_n from a simple temperature sensitive model (Eq. 5; used parameter values shown in panel a), while panel (b) shows the predicted R_n from a combined nitrogen, temperature and acclimation sensitive model (see parameter values in Table 5.3).

Table 5.3: Estimates (standard error in parenthesis) of parameters used to describe temperature and nitrogen sensitivities of photosynthesis and respiration rates in three bioenergy crops. For cynara, when significant differences between warm and cold season were found, two estimates are given

	Parameter	Sunflower	Kenaf	Cynara-warm[a]	Cynara-cold[a]
R_n	χ_R	0.609 (0.006)	0.954 (0.015)	0.775 (0.009)	
	$E_{Rn(a)}$	117912 (1814)	100740 (3250)	−10900 (5617)	146956 (4281)
	$E_{Rn(b)}$	−23346 (770)	−15743 (1455)	33040 (2490)	−26640 (1858)
	n (night)[b]	2492	1403	3212	
	r^2	0.799	0.793	0.724	
R_d/R_n	b_R			0.843 (0.040)	
	α_R			0.390 (0.107)	
V_{cmax}	χ_v	73.8 (0.94)	66.7 (0.92)	65.2 (0.62)	
	E_v	53688 (1631)	61812 (1402)	190831 (33853)	
	D_v	205638 (355)	0	158486 (30907)	
	S_v	650[c]	0	550 (108.2)	
J	χ_j	144.2 (3.4)	122.1 (1.88)	100 (0.91)	92.2 (0.88)
	E_j	43295 (5122)	28584[d] (1131)	23111 (971)	
	D_j	125324 (12653)	0[d]	204489 (218)	
	S_j	405 (38.47)	0[d]	650[c]	
	κ_{2LL}	0.255 (0.018)	0.278 (0.013)	0.314 (0.014)	0.419 (0.011)
	θ	0.607 (0.027)	0.627 (0.023)	0.847 (0.011)	
	n (day)[b]	1366	2042	2334	
	r^2	0.928	0.909	0.916	
Ratio	J_{max}/V_{cmax} [e]	1.95	1.83	1.53	1.41
	R_d/V_{cmax} [e]	0.0057	0.0103	0.0085	

For units see Table 5.1.

[a]: warm period, from early May to end of June; cold period, from November to mid-April; see Fig. S-5.1

[b]: number of data used in analysis

[c]: fixed value (see Materials and methods).

[d]: alternatively the following parameters: E_j = 28149, D_j = 474614 and S_j = 1482 (with a temperature optimum of 41.7°C) gave equal temperature sensitivities but values were rejected due to high standard error of estimate.

[e]: normalized to 25°C.

Step 3: Relation between R_d and R_n

Plotting R_d vs. R_n gave a robust linear relation with no significant differences among species (P=0.225; Fig. 5.5; Table 5.3). Analysis showed that mitochondrial respiration was inhibited by about 28% in the light for the species studied. The observed x-axis intercept (a_R=0.39) differed significantly from zero (P=0.0039), indicating that R_n and R_d were not entirely proportional (Fig. 5.5). Additionally,

no effect of N_a ($r^2=0.01$; $P=0.67$) but a significant effect of temperature ($r^2=0.18$; $P=0.008$) was found on the R_d/R_n ratio, showing that the ratio approached unity at high temperatures. Similarly, the ratio of $R_n/A_{n,max}$, which ranged from 7–11% across species, was insensitive to changes in N_a ($P>0.05$), but increased significantly with increasing temperature ($r^2=0.62$; $P<0.01$; data not shown).

Step 4: V_{cmax} in relation to temperature and N_a

The relationships of V_{cmax} with temperature and N_a were quantified by fitting Eqs 2 and 5–12 to data obtained at very high light levels ($I_{inc}\geq1500$ µmol photons m^{-2}s^{-1}) to ensure that A_n is limited only by Rubisco. All required parameters (χ_v, E_v, D_v and S_v) were well estimated. Across species, there were small differences (<12%; Table 5.3) in χ_v, and large differences in temperature sensitivities above 30°C (Fig. 5.6a; including other crops).

Sunflower temperature sensitivity was best described by the peaked Arrhenius equation ($r^2=0.736$; $P<0.001$; Table 5.3), showing an optimum temperature for V_{cmax} at 38.7°C (calculated from Eq. A1 in the Appendix). For kenaf and cynara no optimum temperature was observed within our measurement range (18–41°C; Fig. 5.6a). To explore any acclimation of V_{cmax} to growth environments in cynara, we allowed the model to estimate different parameters for two contrasting seasons. We did not find any significant effect of the growing season on χ_v (65.8 vs. 64.3; $P=0.094$) neither on E_v, D_v and S_v parameters ($P=0.247$), meaning little seasonal V_{cmax} acclimation.

Step 5: κ_{2LL} in relation to temperature and N_a

In a next analysis we used the entire dataset and earlier estimates for V_{cmax} to calculate electron transport parameters using the full model. The optimization procedure failed to simultaneously estimate six parameters (over-fitting). Therefore, we first estimated κ_{2LL} indirectly from Φ_{CO2LL} information (see equation A2), and then set κ_{2LL} as an input to the model. To that end, correlations of κ_{2LL} with temperature, light and nitrogen were investigated. Results indicated poor correlations with N_a ($r^2=0.26$, $P=0.025$), leaf temperature ($r^2=0.19$, $P=0.104$), and the combination of the above ($r^2=0.44$, $P<0.01$; data not shown). However, better relationships were obtained when κ_{2LL} was regressed against seasonal temperature ($r^2=0.40$, $P=0.004$) and radiation data ($r^2=0.34$, $P=0.003$), showing a long-term κ_{2LL} acclimation. This became clearer when average κ_{2LL} values per crop and per growth environments were considered (Fig. 5.7). Our findings were supported fairly well by literature data (Fig. 5.7). Based on this analysis, we considered average κ_{2LL} values per species in further analyses (including acclimation effect for cynara, Table 5.3).
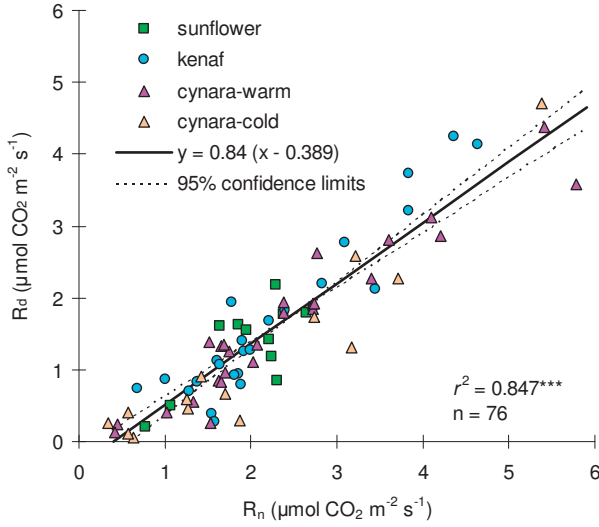
Figure 5.5: Relationship between day (R_d) and night (R_n) respiration rates (see Table 5.3).
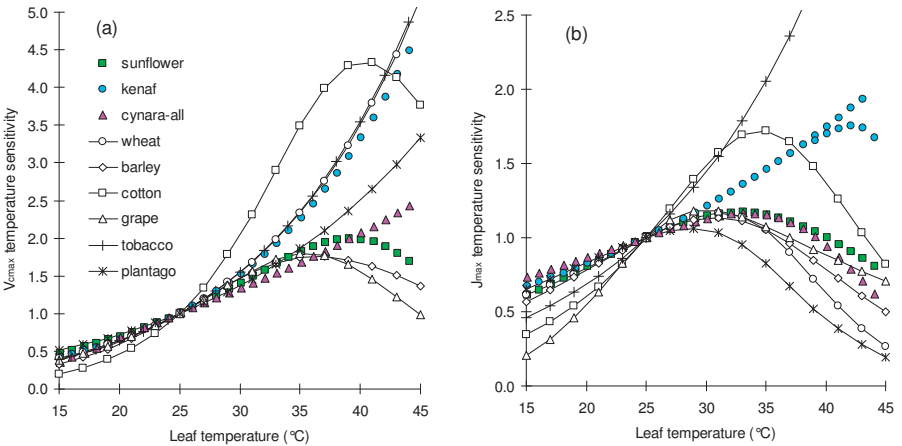
Figure 5.6: Temperature sensitivities for V_{cmax} (a) and J_{max} (b). Values normalized to 1 at 25°C. Filled symbols refer to bioenergy crops while open symbols refer to wheat (de Pury & Farquhar, 1997), barley (Braune *et al.*, 2009), cotton (Harley *et al.*, 1992), grapevine (Schultz, 2003), tobacco (Bernacchi *et al.*, 2001; 2003) and to perennial *Plantago asiatica* (Ishikawa *et al.*, 2007). For kenaf both observed J_{max} temperature sensitivities are plotted (see Table 5.3; note that for kenaf the measurement range was up to 41°C).
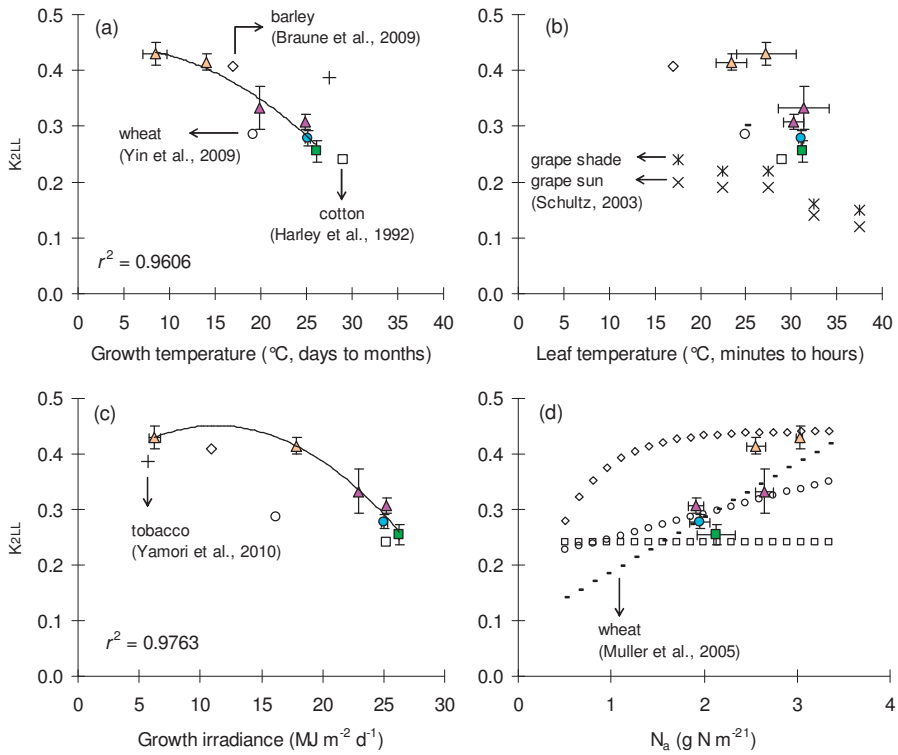
Figure 5.7: Conversion efficiency of incident light into electron (κ_{2LL}) in relation to (a) seasonal growth temperature, (b) short-term changes in leaf temperature, (c) seasonal irradiance and (d) N_a, for three bioenergy crops (filled symbols; ■: sunflower, ●: kenaf, ▲: cynara warm, ▲: cynara cold) and four major field crops (open symbols; see panels for details). Growth temperatures and irradiances calculated from Fig. S-5.1. For sunflower and kenaf one average κ_{2LL} value (± vertical standard error) was calculated because measurements (set I) were conducted during the July–August period when temperature and radiation do no change much (Fig. 5.1). In contrast, for cynara (cold and warm) four average κ_{2LL} values were calculated, reflecting the months: November, April, May and June, respectively. Horizontal bars (when larger than symbols) indicate the mean standard error of the explanatory variable. We could not retrieve information on growth temperature and irradiance from Müller *et al.* (2005) and Schultz (2003) studies.

***Step 6: J*max *in relation to temperature and N*a**

All J_{max} temperature sensitivities (except kenaf; Table 5.3) were best described using Eq. (6). Across species, J_{max} temperature sensitivity was highly variable (Fig. 5.6b including other crops), while the maximum J_{max} was obtained at lower temperature than the maximum V_{cmax} (temperature optimum of 32, 42 and 33°C for sunflower, kenaf and cynara, respectively; Fig. 5.6). As a result, there was a decreasing trend of J_{max}/V_{cmax} ratio with increasing temperature (Fig. 5.8). For cynara, a significant ($P<0.05$) temporal change was found for the χ_j parameter (Table 5.3). The χ_j parameter showed a larger variability (36% change) than χ_v (12% change) among species and growth environments studied (Table 5.3). The parameter θ was lower for sunflower (0.60) and higher for cynara (0.84), but close to the commonly used value of 0.75 in all cases. All these differences (including temperature and nitrogen sensitivities) among species and growth environments became smaller when the J_{max}/V_{cmax} ratio was plotted against leaf temperature (Fig. 5.8).
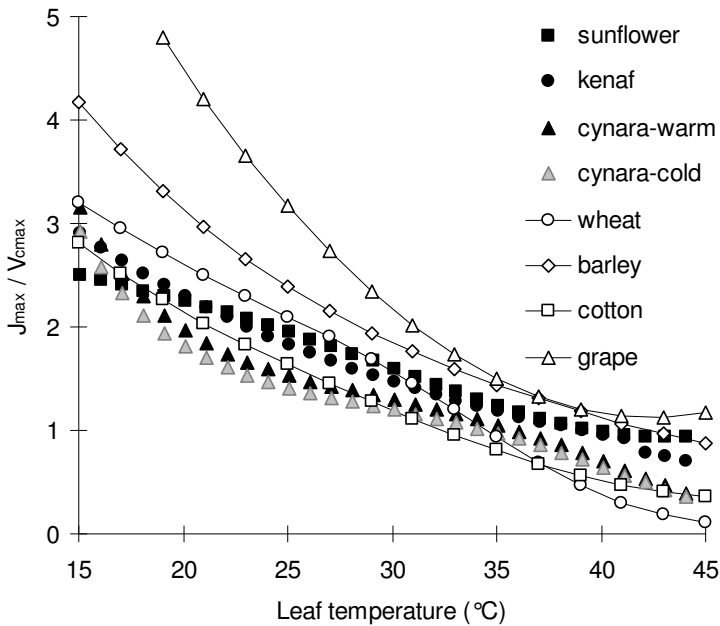
Figure 5.8: J_{max}/V_{cmax} ratio versus leaf temperature. Coloured symbols refer to bioenergy crops, the remaining symbols to major field crops (symbols and references as in Fig. 5.6). Note for cynara two lines were plotted because the parameter J_{max25} differs between seasons (see Eq. 10 and Table 5.3).

Sensitivity and validation analysis

To investigate the uncertainty introduced in our estimates by the chosen Rubisco kinetic parameters, the initial values of Bernacchi *et al*. (2001) were increased or decreased by 20% and optimization procedures were repeated. Not surprisingly a maximum change was obtained in the estimated V_{cmax25}, whereas the remaining parameters were less affected (<5%; data not shown). Given that even the maximum change in V_{cmax} was ca 11% in response to a 20% change, our parameter estimates were quite stable despite the uncertainties in values of Rubisco kinetic constants. A further analysis showed that the predicted A_n was sensitive to a 20% decrease in χ_v and χ_j whereas its sensitivity to other changes was weak (Fig. 5.9).
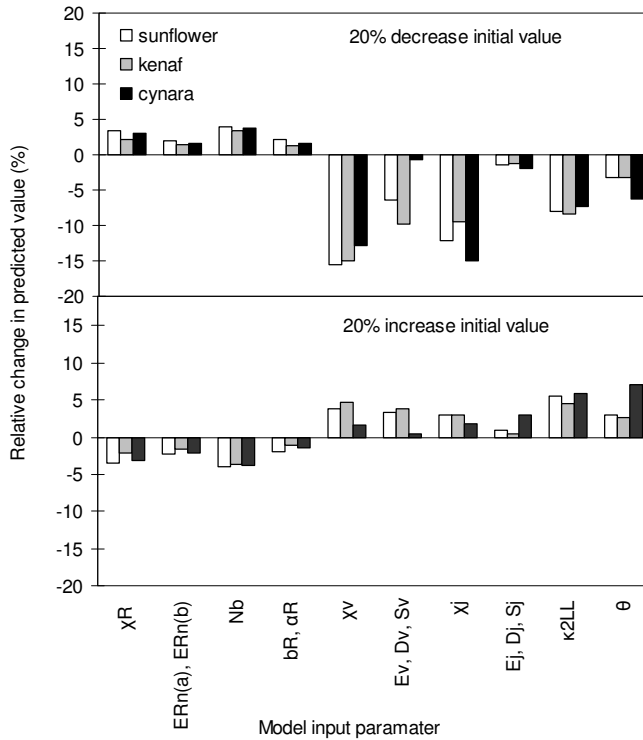
Figure 5.9: Sensitivity analysis of the predicted A_n in response to ± 20% change in input parameter values for the photosynthesis model. Relative change in predicted value was calculated as: $100\times(A_n$, predicted $- A_n$, predicted, original)$/A_n$, predicted, original. When input parameters were part of a linear or polynomial equation (e.g. E_j, D_j, S_j; Eq. 6) and strongly intercorrelated, a combined change was implemented.

Lastly we intended to validate the models against independent datasets (Fig. 5.10). Predictions vs. observations for sunflower and kenaf were satisfactory (*r*RMSE<0.15; Fig. 5.10a and b). For cynara we tested the FvCB model using measurements from a series of 24 h diurnal cycles (Fig. 5.10c), where stress conditions were unavoidably present (datasets outside our calibration range). In general, predictions were close to actual measurements, except for those data obtained from 14:00h to 18:00h, where a systematic overestimation was detected (Fig. 5.10c). The FvCB model responded to lowering temperature in late afternoon by increasing A_n, however, actual measurements indicated that the photosynthetic apparatus could not recover so quickly from the 'photosynthesis midday depression'. The failure in predicting the depression and its after-effect during the recovery hours (Fig. 5.10c) might be attributed to the "steady state" character of the FvCB model. These results suggest that prediction of diurnal photosynthesis for species grown in the Mediterranean region requires more detailed approaches in which g_m, recovery functions for A_n (midday depression), and the effects of leaf water potential should be included.
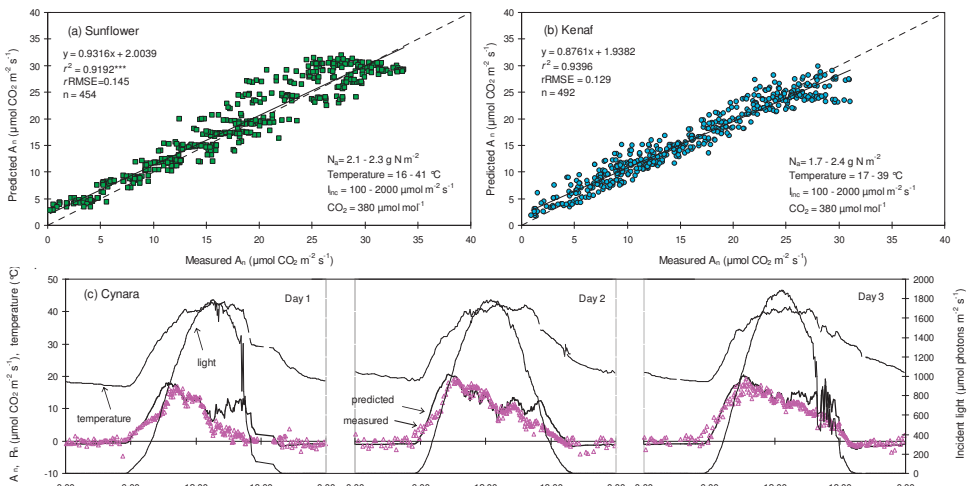
Figure 5.10: Measured versus predicted photosynthesis (all panels) and measured versus predicted night respiration (only at the lower panel c). In panel c, canopy CO_2 varied from 350–380 during day time to 450–600 µmol mol^{-1} during night time; VPD followed temperature variations, and stomata conductance ranged from 0.05 mol m^{-2} s^{-1} during night up to 0.48 mol m^{-2} s^{-1} during day time. The model predicted diurnal trends moderately (r^2=0.814, *r*RMSE=0.553, n=720). When midday measurements were excluded (14:00–16:00h), the model fit was improved (r^2=0.930, *r*RMSE=0.335, n=543).

Discussion

Use of A_n–I_{inc} curves to parameterise the FvCB model

The parameters of the FvCB model, J_{max} and V_{cmax} in particular, have been predominantly estimated from data of A_n–C_i curves (Harley *et al*., 1992; Medlyn *et al*., 2002a). The value of A_n–C_i curves for parameterising the FvCB model is confirmed in our analysis (Fig. 5.2). We also showed that V_{cmax} and J_{max} can be estimated sufficiently well by an appropriate analysis of A_n–I_{inc} data alone (r^2=0.91–0.93; Fig. 5.2). Our analysis indicated that unlike J_{max}, V_{cmax} cannot be always estimated from A_n–I_{inc} curves, i.e. when the entirely curve is A_j-limited (Fig. 5.1). This is often observed in field crops (e.g. cotton; Wise *et al*., 2004). Actually, Boote & Pickering (1994) used only the A_j-equation of the FvCB model to calculate leaf photosynthesis in their canopy photosynthesis model. For the purpose of using the complete FvCB model, we propose the two-step approach to estimate both V_{cmax} and J_{max} from A_n–I_{inc} data (see M&M), in line with Niinemets & Tenhunen (1997). In contrast, Kosugi *et al*. (2003) and Müller *et al*. (2005) who also parameterized the FvCB model using A_n–I_{inc} data, assumed a fixed J_{max} / V_{cmax} ratio of 2.1 at 25°C (based on Wullschleger, 1993). However, this approach does not allow for the flexibility of the ratio as observed for different species or for the same species when grown under different environments, thereby introducing many uncertainties in parameter value (see Fig. 5.8 and discussion below).

Our results indicated that the information of A_n–I_{inc} curves has been under-explored. Use of A-I_{inc} curves has an additional advantage in that data of A_n-C_i curves may be uncertain due to CO_2 leakage during gas exchange measurements when CO_2 set point values are either below or above ambient-air CO_2 level (Flexas *et al*. 2007). Crop modellers used to measure photosynthetic light response curves under an ambient CO_2 condition, upon which an empirical model for light-response curves is parameterised. Provided that values of C_i across I_{inc} levels are properly monitored, re-analysing readily available A_n–I_{inc} data to parameterise the FvCB model will strengthen photosynthesis calculation in crop models. This would expand the potential of combining classical photosynthetic data and the biochemical FvCB model to assess the impact of climate change on crop production and to examine options of bioenergy production under a changing climate.

Below we discuss temperature, N_a and seasonal effects on the parameters of the FvCB–photosynthesis model and respiration equations, i.e. J_{max}, V_{cmax}, R_d, R_n, κ_{2LL} and θ, all derived from A_n–I_{inc} data for three bioenergy crops sunflower, kenaf and cynara. We will compare our findings with those obtained for wheat, barley, cotton, tobacco and grapevine based on A_n–C_i or combined A_n–C_i and A_n–I_{inc} datasets.

Night and day respiration parameters: χ_R, $E_{Rn(a)}$, $E_{Rn(b)}$, b_R, a_R

This study is among few in literature providing direct R_n measurements, underlining the high importance of respiration in carbon budgets (Valentini *et al.*, 2000). Our estimates for χ_R (range: 0.61–0.95 μmol CO_2 g^{-1} N s^{-1}; Table 5.3), agree well with previous reports for crops (Hirose *et al.*, 1997; Reich *et al.*, 1998; Müller *et al.*, 2005; Braune *et al.*, 2009), but current values are almost double compared to those for trees (Griffin *et al.*, 2002; Bolstad *et al.*, 1999). The temperature sensitivity for respiration (E_{Rn}) was significantly correlated with N_a in all species (Eq. 11; Table 5.3), indicating that respiration in leaves with high N_a values (young/sun leaves) was less sensitive to changes in temperature, while leaves with lower N_a values were more sensitive (senescence/shade leaves). Griffin *et al.* (2002) and Bolstad *et al.* (1999) working with tree leaves that were positioned in different canopy layers – having also different N_a values – found temperature sensitivities similar to those in our study, while Turnbull *et al.* (2003) reported the opposite. However, in none of these studies E_{Rn} was significantly correlated with N_a.

For cotton, Harley *et al.* (1992) reported a simple temperature sensitive R_n model for leaves with variable N_a. Our analysis indicated that it is useful to calculate both R_n components as a function of N_a (e.g. Fig. 5.4; across all species, r^2 scaled from 0.53 to 0.77). The component R_{n25} accounted for the 27% and E_{Rn} for the other 5% of this improvement in r^2. However, the high remaining unexplained variability in night datasets (see r^2 in Table 5.3; Fig. 5.4) means that apart from N_a, other factors should be explored.

Unlike R_n, R_d is hard to measure directly. Its value is empirically estimated indirectly using various methods (for a comparison see Yin *et al.*, 2011), or is commonly fixed as 1% of V_{cmax} or as 50% of R_n (de Purry & Farquhar, 1997; Wohlfahrt *et al.*, 1998; Medlyn *et al.*, 2002a; Kosugi *et al.*, 2003; Braune *et al.*, 2009). Here, application of the Kok method (Sharp *et al.*, 1984) indicated a 28% reduction in R_d compared to R_n (light inhibition of respiration), which estimate is positioned at the lowest reported range (inhibition range: 24–90%; Buckley & Adams, 2011 and references therein).

Rubisco and electron transport parameters: N_b, χ_v, χ_j, κ_{2LL}, θ, E_v, E_j, D_v, D_j

The parameter N_b has a vital role in all nitrogen equations. Our findings (Fig. 5.3) along with published data support the idea that this threshold value for photosynthesis (N_b) is not affected by temperature (Sage & Pearcy, 1987; Makino *et al.*, 1994; Niinemets & Tenhunen, 1997), CO_2 (Harley *et al.*, 1992; Hirose *et al.*, 1997) or irradiance levels (Makino *et al.*, 1997). Excluding the statistical bias that usually exists in N_b estimations (see Materials and Methods) it is believed that a

common N_b is 0.3–0.4 g N m^{-2} for C$_3$ crop species (excluding legume crops; Table S-5.1). For the use in modelling, we showed that ±20% change in N_b value resulted in less than 5% change in the predicted A_n (Fig. 5.9).

The relationships between light saturated A_n and N_a at near-optimum temperature ranges for sunflower, kenaf and cynara (Fig. 5.3) agreed well with several non-legume C$_3$ species (Fig. S5.2). The observed decline of A_n at high temperature (Fig. 5.3; $N_a > 2$ g N m^{-2}) is associated with g_m (Bernacchi *et al*., 2002) and/or V_{cmax} and J_{max} limitations of photosynthesis (Fig. 5.6). Nevertheless, the observed constancy among A_n–N_a plots (Fig. S-5.2) along with the similar χ_v estimates for sunflower, kenaf, cynara, cotton, wheat and barley (range: 60–82 μmol CO$_2$ g^{-1} N s^{-1}; Table 5.3; Harley *et al*., 1992; de Pury & Farquhar, 1997; Müller *et al*., 2005, 2008; Braune *et al*., 2009) suggests that χ_v is very conservative for this plant group ($A_{n,max}$=30–35 μmol CO$_2$ m^{-2} s^{-1}; Fig. S-5.2).

Unlike χ_v, χ_j for the same group was highly variable (90–165 μmol e$^-$ g^{-1} N s^{-1}). However, parameter χ_j (which determines J_{max25}; Eq. 10) is not independent of, but interrelated with, the values of κ_{2LL} and θ (see Eq. 4). The increase of one parameter is somewhat counterbalanced by the decrease in the value of the other parameter in Eq. (4). This means that use of a constant κ_{2LL} and θ values across species and environments will bias J_{max} estimates and therefore the J_{max}/V_{cmax} ratio. Among sunflower, kenaf and cynara, χ_j varied by 36%, κ_{2LL} by 39% and θ by 28%, but in different directions (Table 5.3). When we fixed κ_{2LL} to 0.3 and θ to 0.7 (commonly assumed values; de Pury & Farquhar, 1997; Medlyn *et al*., 2002a), χ_j variation among crops and growing environments became smaller (15%), and the J_{max}/V_{cmax} ratio less variable.

Our analysis showed that variation in electron transport rate among bioenergy crops followed changes in environmental conditions during growth (Fig. S-5.1), with higher J rates for cynara in low light (<700 μmol m^{-2} s^{-1}; winter period) and higher J rates for sunflower and kenaf in high light conditions (>700 μmol m^{-2} s^{-1}; summer period; Table 5.3, Eq. 4). This is consistent with recent findings for tobacco (Yamori *et al*., 2010) where plants grown under low light enhanced the efficiency of light acquisition while those grown under high light enhanced the capacity of light utilization, through changes in Chl contents, Chl *a/b* ratio, cyt *f* and Rubisco contents.

In earlier studies (Wullschleger 1993; Dreyer *et al*., 2001; Medlyn *et al*., 2002a) the parameter κ_{2LL} was fixed as a constant (0.18, 0.24 and 0.30, respectively) across species, crop stages and environments. However, Yin *et al*. (2009) demonstrated directly a positive relation between κ_{2LL} and N_a, which was confirmed by the results of model curve-fitting procedure (Müller *et al*., 2005; Braune *et al*., 2009; Yamori *et al*., 2010). In Fig. 5.7, we summarized κ_{2LL} information for eight crops and interpreted this large variation in the light of long or short-term response to temperature or irradiance. Across species, higher κ_{2LL} values were found for

crops grown under low irradiance and temperature conditions (Fig. 5.7a and c). To understand this, it is necessary to underline the components of the κ_{2LL} parameter (see Eq. A3 derived by Yin *et al.*, 2004; 2009; Yin & Struik, 2009a; also see Eq. 6 in Niinemets & Tenhunen, 1997).

The fraction of I_{inc} absorbed by the leaf photosynthetic pigments (parameter β in Eq. A3) is affected by long-term changes in light and temperature through its chances in leaf morphology. Leaves grown at high temperature are generally thinner, with a lower ability to absorb light (Poorter & Evans, 1998; Yamori *et al.*, 2005) providing therefore a reasonable explanation for the observed κ_{2LL} reduction with increasing temperature. On the other hand, leaves grown at high irradiance are thicker (Niinemets & Tenhunen, 1997) indicating that κ_{2LL} variation is much more complex and still not fully understood. Nonetheless, caution should be exercised when modelling canopy photosynthesis based on the sun/shade approach (de Pury & Farquhar, 1997; Yin & van Laar, 2005) because κ_{2LL} increases with increasing N_a (Fig. 5.7d), while κ_{2LL} also increases with decreasing light (Schultz, 2003; shade leaves which generally have low N_a values; Fig. 5.7b).

The normalized temperature functions of V_{cmax} and J_{max} were highly variable across crops (Fig. 5.6), particularly above 30°C in line with Leuning (2002). This mean that the assumption used in crop modelling, unique A_n response to temperature across crop species, is inappropriate when photosynthesis is calculated by the FvCB model. In case of no available data, we suggest researchers as a first approximation to use V_{cmax} and J_{max} temperature parameters from species that belong to the same family (see Fig. 5.6; cotton and kenaf belong to *Malvaceae*; sunflower and cynara to *Asteraceae*).

The J_{max}/V_{cmax} ratio provides an estimate of the relative activities of RuBP regeneration and Rubisco carboxylation and incorporates both temperature and N_a effects. This study confirms (Table 5.3) the general reported J_{max}/V_{cmax} value of 2.0±0.5 (Wullschleger, 1993; Poorter & Evans, 1998; Bunce, 2000; Leuning, 2002; Medlyn *et al.*, 2002a). However, this ratio should not be considered constant in an absolute term. V_{cmax} is dependent on Rubisco parameters used (up to 11% change; see also Medlyn *et al.*, 2002a) and J_{max} is affected by the assumed κ_{2LL} and θ values used (see earlier discussion). For instance, grape showed much higher J_{max}/V_{cmax} ratio compared to other crops (Fig. 5.8). Apart from the effect of species, there are two possible artifacts for that; the different Rubisco parameters used in that study (Schultz, 2003) and the lower grape κ_{2LL} values compared to the other crops (Fig. 5.7b). Also use of C_i instead of C_c affects this ratio. Thus approaches (e.g. Kosugi *et al.*, 2003; Müller *et al.*, 2005) that fix J_{max}/V_{cmax} ratio at a constant value to parameterize the FvCB model are not supported from this study.

Seasonal effects on photosynthesis and respiration in cynara

Direct interpretation of the seasonal effects on A_n and R_n for cynara is difficult because both the climate (Fig. S-5.1) and the plant stage are different, with new and old leaves being present (Archontoulis *et al*., 2010a; Searle *et al*., 2011). In general, R_n acclimated to cold and warm environment to a larger extent than A_n did (Table 5.3; Fig. 5.4). This is consistent with previous studies in growth chambers (Yamori *et al*., 2005; Ow *et al*., 2008; Silim *et al*., 2010).

The nature of R_n acclimation is highly variable within and among plant species and it is usually related either to changes in E_{Rn} and/or to changes in R_{n25} (Atkin *et al*., 2005; Searle *et al*., 2011). Nevertheless, since the χ_R estimate did not change between seasons (*P*=0.269; Table 5.3) and given that the measured winter leaves had higher N_a values than the summer leaves (on average 2.48 vs. 1.53 g N m^{-2}; see also Fig. 5.7d), this indicates that basal capacity, R_{n25}, plays an important role in this acclimation. Secondly, E_{Rn} was also higher during winter periods. Apparently, cynara follows an "acclimation type II" (Atkin *et al*., 2005) where the overall elevation of the R_n–temperature response was affected by season and growth stage (Fig. 5.4).

Among several photosynthetic parameters analyzed, we found seasonal effects on two electron transport parameters, χ_j and κ_{2LL} (Table 5.3 and earlier discussion) and none related to V_{cmax}. Literature information on photosynthetic acclimation is diverse among studies (Hikosaka, 2005; Wilson *et al*., 2000; Medlyn *et al*., 2002a; Bernacchi *et al*., 2003; Yamori *et al*., 2005; Braune *et al*., 2009; Silim *et al*., 2010). To our knowledge, only Wilson *et al*. (2000) reported both χ_j and χ_v seasonal changes in trees, while Braune *et al*. (2009) for barley found only χ_j variation as in this study. For cynara, the normalized V_{cmax} and J_{max} temperature functions were slightly changed between seasons, in contrast to growth chamber studies where tobacco (Bernacchi *et al*., 2003), spinach (Yamori *et al*., 2005), *Plantago* spp. (Ishikawa *et al*., 2007), and barley (Braune *et al*., 2009) grown only at different temperatures. The fact that we assessed leaves with different N_a status may be a reason. Other field studies (Schultz, 2003; Medlyn *et al*., 2002b) reported also no seasonal effect of season on the normalized V_{cmax} and J_{max} temperature functions. This shows an inconsistency between actual field and controlled chambers studies.

The J_{max}/V_{cmax} ratio has been reported to be either sensitive or insensitive to growth temperature (see discussion by Hikosaka *et al*., 2005), growth irradiance (Poorter & Evans, 1998; Yamori *et al*., 2010) and seasonal changes (Bunce, 2000; Medlyn *et al*., 2002b). Our results suggest that cynara regulates the balance between RuBP regeneration and Rubisco carboxylation to maintain the J_{max}/V_{cmax} ratio almost constant (change <8%; Table 5.3) across seasons and growth stages.

Model requirements for further development

Present coupled FvCB–photosynthesis and empirical-respiration model can predict A_n under varying levels of C_i, I_{inc}, temperature and N_a and R_n under varying levels of temperature and N_a for three bioenergy crops (Table 5.3; Fig. 5.10). To increase further present model prediction and application ability, future research should focus on developing: (i) g_s and g_m sub-models for CO_2 transfer resistances from atmosphere to stomatal cavity and to chloroplast (Yin & Struik, 2009a); (ii) functions to relate biochemical parameters to leaf water potential (Vico & Porporato, 2008); and (iii) algorithms to quantify diurnal midday depression (Tuzet *et al.*, 2003) and recovery period of photosynthesis, which are very important for Mediterranean species (Fig. 5.10c). It should be mentioned that a later modification of the FvCB model to account for the TPU limited rate (Sharkey, 1985) was not considered here because this was not possible to be estimated from A_n–I_{inc} datasets as in Niinemets & Tenhunen (1997).

Conclusions

This study brings new information on photosynthesis and respiration rates for three bioenergy crops, sunflower, kenaf and cynara. It provides an alternative way to parameterize the FvCB model from A_n–I_{inc} data, instead of using A_n–C_i data that are more expensive to obtain. We showed that major FvCB model parameters, V_{cmax} and J_{max}, derived either from A_n–C_i or A_n–I_{inc} analysis are very close (r^2=0.92). Present models can predict photosynthesis under varying levels of C_i, I_{inc}, temperature and leaf nitrogen, and can estimate night respiration under varying levels of temperature and leaf nitrogen, for three bioenergy crops. Comparisons of FvCB model parameters among sunflower, kenaf, cynara, cotton, wheat, barley, tobacco and grapevine indicated that only few parameters were conservative. This means that in order to feed properly crop models, species-specific FvCB model parameters are needed. In this context, readily available A_n–I_{inc} data – that has been under-explored – can assist in that respect. By combining classical photosynthetic data and the biochemical model, the potential of crop growth models to assess the impact of climate change on crop production and to examine options of bioenergy production under a changing climate is enlarged. Further research is needed to reliably quantify the effects of photosynthetic acclimation and diurnal midday depression identified in this study.

Appendix

1. Estimating the optimum temperature from the peaked Arrhenius equation

The optimum temperature for V_{cmax} or J_{max} in Eq. (6) is given by the following equation (Medlyn *et al.*, 2002a):

$$T_{opt} = \frac{D_x}{S_x - R \cdot \ln\left(\dfrac{E_x}{D_x - E_x}\right)}$$

(A1)

2. The relation between κ_{2LL} and Φ_{CO2LL}

By dividing both parts of Eq. (3) by I_{inc} and re-arranging, the efficiency of incident light conversion into e$^-$, κ_{2LL}, can mathematically be calculated from Φ_{CO2LL}:

$$\Phi_{CO_2LL} = \left.\frac{A_n + R_d}{I_{inc}}\right|_{I_{inc}\to 0} = \kappa_{2LL}\frac{C_i - \Gamma_*}{4C_i + 8\Gamma_*} \Leftrightarrow \kappa_{2LL} = \Phi_{CO_2LL}\frac{4C_i + 8\Gamma_*}{C_i - \Gamma_*}$$

(A2)

This approach was also used by Niinemets *et al.* (2001), but lacks any further interpretation.

3. Components of parameter κ_{2LL}

Yin *et al.* (2004) described a generalized stoichiometric equation for A_j, where the linear photosystem II (PSII) electron transport rate (J) was replaced by the total electron transport rate passing PSII (J_2) and fractions of the total e$^-$ flux passing PSI that follow cyclic (f_{cyc}) and pseudocyclic (f_{pseudo}) pathways. Again, at low light conditions, dividing J by I_{inc} yields κ_{2LL} as follows (Yin *et al.*, 2009; Yin & Struik, 2009a):

$$\kappa_{2LL} = \left.\frac{J}{I_{inc}}\right|_{I_{inc}\to 0} = \frac{J_2}{I_{inc}}\left(1 - \frac{f_{pseudo}}{1 - f_{cyc}}\right) = \rho_2 \beta \Phi_{2LL}\left(1 - \frac{f_{pseudo}}{1 - f_{cyc}}\right)$$

(A3)

By definition, the variable J_2 can be replaced by the term $\varrho_2 \cdot \beta \cdot \Phi_{2LL} \cdot I_{inc}$, where ϱ_2 is the fraction of absorbed irradiance partitioned to PSII (usually assumed 0.5), β is the fraction of I_{inc} absorbed by the leaf photosynthetic pigments, and Φ_{2LL} is the PSII e$^-$ transport efficiency under limiting light.

Supplementary materials (Chapter 5)

Table S-5.1: Reported N_b values (minimum leaf nitrogen for photosynthesis, in g N m^{-2}) for various species. Data grouped into four categories: C_3 crops and weeds, C_3 legume crops, C_3 trees and C_4 crops. The dataset used and the model applied (L=linear and NL=non-linear) by the authors to derive the N_b value is given. A_n = light saturated net assimilation rate at ambient CO_2 concentration and at near-optimum temperature (μmol CO_2 m^{-2} s^{-1}); A_g = A_n plus day respiration (μmol CO_2 m^{-2} s^{-1}); R_n = night respiration rate (μmol CO_2 m^{-2} s^{-1}); V_{cmax25} = maximum carboxylation rate at 25°C (μmol CO_2 m^{-2} s^{-1}); J_{max25} = maximum electron transport rate at 25°C (μmol e$^-$ m^{-2} s^{-1}); and N_a = leaf nitrogen content (g N m^{-2})

Source	Species	Common name (cultivar)	N_b (±SE)	Dataset	Model
C_3 Crops and weeds (Average value = 0.305 ± 0.027)					
[1]	*Triticum aestivum* L.	Wheat (Yecora 70)	0.30[a]	A_n–N_a	NL
[2]	*Triticum aestivum* L.	Winter wheat (Orestis)	0.36	A_n–N_a	NL
[2]	*Triticum aestivum* L.	Winter wheat (Orestis)	0.09	V_{cmax25}–N_a	L
[3]	*Triticum aestivum* L.	Spring wheat	0.29	A_n–N_a	NL
[4]	*Triticum aestivum* L.	Spring wheat (Minaret)	0.38	A_n–N_a	L
[5]	*Triticum aestivum* L.	Spring wheat (Minaret)	0.318	A_g–N_a	L
[6]	*Hordeum vulgare* L.	Spring barley (Barke)	0.085	A_n–N_a	L
[6]	*Hordeum vulgare* L.	Spring barley (Barke)	0.198[b]	V_{cmax25}–N_a	L
[6]	*Hordeum vulgare* L.	Spring barley (Barke)	0.229[b]	J_{max25}–N_a	L
[7]	*Gossypium hirsutum* L.	Cotton (Coker 315)	0.16	V_{cmax25}–N_a	L
[7]	*Gossypium hirsutum* L.	Cotton (Coker 315)	0.05	J_{max25}–N_a	L
[8]	*Gossypium hirsutum* L.	Cotton (Sicala V-2*i*)	0.65	A_n–N_a	NL
[9]	*Helianthus annuus* L.	Sunflower (Prosol 35)	0.30 (0.05)	A_n–N_a	NL
[9]	*Helianthus annuus* L.	Sunflower (Prosol 35)	0.24	R_n–N_a	NL
[10]	*Helianthus annuus* L.	Sunflower (Suncross 41)	0.48 (0.01)	A_n–N_a	NL
–	*Helianthus annuus* L.	Sunflower (Panter)	0.386 (0.08)[c]	A_n–N_a	NL
[11]	*Brassica napus* L.	Oilseed rape (Lirajet)	0.40	A_n–N_a	L
[5]	*Brassica napus* L.	Oilseed rape (Aries)	0.106	A_g–N_a	L
[12]	*Brassica napus* L.	Oilseed rape (Ceres)	0.318	A_n–N_a	NL
[13]	*Brassica oleracea* L.	Cauliflower (Fremont)	0.395	A_g–N_a	L
[14]	*Oryza sativa* L.	Rice (Notohikari)	0.35[a]	A_n–N_a	NL
[15]	*Oryza sativa* L.	Rice	0.30	A_n–N_a	NL
[35]	*Oryza sativa* L.	Rice (Araure 4)	0.359	A_n–N_a	L
[16]	*Beta vulgaris* L.	Sugar beet (MSBI×NB4)	0.08	A_n–N_a	NL
[17]	*Solanum tuberosum* L.	Potato (Vebeca)	0.50[d]	A_n–N_a	NL
[18]	*Hibiscus cannabinus* L.	Kenaf (Guatemala)	0.43 (0.06)	A_n–N_a	NL
–	*Hibiscus cannabinus* L.	Kenaf (Everglades 41)	0.39 (0.12)[c]	A_n–N_a	NL
–	*Cynara cardunculus* L.	Cynara (Bianco avorio)	0.416 (0.09)[c]	A_n–N_a	NL
[19]	*Chenopodium album* L.	–	0.111–0.421	A_n–N_a	L
[20]	*Chenopodium album* L.	–	0.23	A_n–N_a	L
[21]	*Chenopodium album* L.	–	0.64–0.78	A_n–N_a	L
[22]	*Abutilon theophrasti* L.	–	0.35	A_g–N_a	NL
[22]	*Ambrosia artemisiifolia* L.	–	0.39	A_g–N_a	NL
[23]	*Alocasia macrorrhiza* L.	–	0.10	A_n–N_a	L
[23]	*Alocasia macrorrhiza* L.	–	0.116	V_{cmax25}–N_a	L
[23]	*Alocasia macrorrhiza* L.	–	0.146	J_{max25}–N_a	L
[23]	*Colocasia esculenta* L.	–	0.261	V_{cmax25}–N_a	L
[23]	*Colocasia esculenta* L.	–	0.10	J_{max25}–N_a	L

Table S-5.1: Continued

Source	Species	Common name (cultivar)	N_b (±SE)	Dataset	Model
C₃ Legumes crops (Average value = 0.531 ± 0.059)					
[15]	*Glycine max* L.	Soybean	1.00	A_n–N_a	NL
[35]	*Glycine max* L.	Soybean (Merr)	0.406	A_n–N_a	L
[24]	*Arachis hypogaea* L.	Peanut	0.46	A_n–N_a	L
[24]	*Arachis hypogaea* L.	Peanut	0.60	A_n–N_a	NL
[25]	*Vicia faba* L.	Bean (Tina)	0.66	A_n–N_a	NL
C₄ Crops (Average value = 0.211 ± 0.010)					
[26]	*Sorghum bicolor* L.	Sorghum (Dekalb DK55)	0.20 [d]	A_n–N_a	NL
[26]	*Sorghum bicolor* L.	Sorghum (Savannah)	0.20 [d]	A_n–N_a	NL
[35]	*Sorghum bicolor* L.	Sorghum (Pioneer)	0.175	A_n–N_a	L
[26]	*Zea mays* L.	Maize (Dekalb XL82)	0.20 [d]	A_n–N_a	NL
[27]	*Zea mays* L.	Maize (Lincoln)	0.25	A_n–N_a	NL
[15]	*Zea mays* L.	Maize (Skyliner)	0.20	A_n–N_a	NL
[36]	*Zea mays* L.	Maize (2–02R10074)	0.242 [b]	A_n–N_a	L
[28]	*Saccharum spp.*	Sugarcane, 8 clones	0.222	A_n–N_a	NL
C₃ Trees (Average 0.30 ± 0.05)					
[29]	*Acer saccharum* L.	Red maple	0.277	A_n–N_a	L
[29]	*Acer saccharum* L.	Sugar maple	0.216	A_n–N_a	L
[30]	*Acer saccharum* L.	Sugar maple	0.105	A_n–N_a	L
[31]	*Acer saccharum* L.	–	0.12	A_n–N_a	L
[31]	*Acer saccharum* L.	–	0.40	A_n–N_a	NL
[32]	*Acer rubrum* L.	Red maple	0.333–0.431	V_{cmax25}–N_a	L
[33]	*Prinus persica* L.	Nectarine (Fantasia)	0.609	A_n–N_a	NL
[34]	*Pinus radiate* L.	–	0.150 [a]	A_n–N_a	L
[34]	*Pinus radiate* L.	–	0.100 [a]	V_{cmax20}–N_a	L
[20]	*Quercus myrsinaefolia* L.	Oak	0.052	A_n–N_a	L
[29]	*Quercus myrsinaefolia* L.	Oak	0.655	A_n–N_a	L
[32]	*Quercus alba* L.	White oak	0.299–0.576	V_{cmax25}–N_a	L
[32]	*Quercus prinus* L.	Chestnut oak	0.222	V_{cmax25}–N_a	L

[a]: read from their figure.

[b]: estimated through optimization runs and not from simple regression analysis.

[c]: this study.

[d]: fixed by the authors.

References according to the number given in Table S-5.1

[1] **Evans JR. 1983**. Nitrogen and photosynthesis in the flag leaf of wheat (*Triticum aestivum* L.). *Plant Physiology* 72: 297–302.

[2] **Müller J, Wernecke P, Diepenbrock W. 2005**. LEAFC3–N: a nitrogen sensitive extension of the CO_2 and H_2O gas exchange model LEAFC3 parameterized and tested for winter wheat (*Triticum aestivum* L.). *Ecological Modelling* 183: 183–210.

[3] **Bindraban PS. 1999.** Impact of canopy nitrogen profile in wheat on growth. *Field Crops Research* 63: 63–77.

[4] **Dreccer MF, van Oijen M, Schapendonk AHCM, Pot CS, Rabbinge R. 2000.** Dynamics of vertical leaf nitrogen distribution in a vegetative wheat canopy. Impacts on canopy photosynthesis. *Annals of Botany* 86: 821–831.

[5] **Dreccer MF, Schapendonk AHCM, van Oijen M, Pot CS, Rabbinge R. 2000.** Radiation and nitrogen use at the leaf and canopy level by wheat and oilseed rape during the critical period for grain number definition. *Australian Journal of Plant Physiology* 27: 899–910.

[6] **Braune H, Müller J, Diepenbrock W. 2009.** Integrating effects of leaf nitrogen, age, and growth temperature into the photosynthesis-stomatal conductance model LEAFC3-N parameterized for barley (*Hordeum vulgare* L.). *Ecological Modelling* 220: 1599–1612.

[7] **Harley PC, Thomas RB, Reynolds JF, Strain BR. 1992.** Modelling photosynthesis of cotton grown in elevated CO_2. *Plant, Cell and Environment* 15: 271–282.

[8] **Milroy SP, Bange MP. 2003.** Nitrogen and light response of cotton photosynthesis and implication for crop growth. *Crop Science* 43: 904–913.

[9] **Connor DJ, Hall AJ, Sadras VO. 1993.** Effects on nitrogen content on the photosynthetic characteristics of sunflower leaves. *Australian Journal of Plant Physiology* 20: 251–263.

[10] **Bange MP, Hammer GL, Rickert KG. 1997.** Effect of specific leaf nitrogen on radiation use efficiency and growth of sunflower. *Crop Science* 37: 1201–1207.

[11] **Müller J, Diepenbrock W. 2006.** Measurements and modelling of gas exchange of leaves and pods of oilseed rape. *Agricultural and Forest Meteorology* 139: 307–322.

[12] **Gammelvind LH, Schjoerring JK, Mogensen VO, Jensen CR, Bock JGH. 1996.** Photosynthesis in leaves and siliques of winter oilseed rape (*Brassica napus* L.). *Plant Soil* 186: 227–236.

[13] **Alt C, Stützel H, Kage H. 2000.** Optimal nitrogen content and photosynthesis in cauliflower (*Brassica oleracea* L. botrytis). Scaling up from a leaf to the whole plant. *Annals of Botany* 85: 779–787.

[14] **Makino A, Sato T, Nakamo H, Mae T. 1997.** Leaf photosynthesis, plant growth and nitrogen allocation in rice under different irradiances. *Planta* 203: 390–398.

[15] **Sinclair TR, Horie T. 1989.** Leaf nitrogen, photosynthesis, and crop radiation use efficiency: a review. *Crop Science* 29: 90–98.

[16] **Nevis DJ, Loomis RS. 1970.** Nitrogen nutrition and photosynthesis in sugar beet (*Beta vulgaris* L.). *Crop Science* 10: 21–25.

[17] **Vos J, van der Putten PEL. 1998.** Effect of nitrogen supply on leaf growth, leaf nitrogen economy and photosynthetic capacity in potato. *Field Crops Research* 59: 63–72.

[18] **Muchow RC. 1990.** Effects of leaf nitrogen and water regime on the photosynthetic capacity of kenaf (*Hibiscus cannabinus* L.) under field conditions. *Australian Journal of Agricultural Research* 41: 845–852.

[19] **Sage RF, Sharkey TD, Pearcy RW. 1990.** The effect of leaf nitrogen and temperature on the CO_2 response of photosynthesis in the C_3 dicot *Chenopodium album* L. *Australian Journal of Plant Physiology* 17: 135–48.

[20] **Hikosaka K, Hanba YT, Hirose T, Terashima I. 1998.** Photosynthesis nitrogen–use efficiency in leaves of woody and herbaceous species. *Functional Ecology* 12: 896–905.

[21] **Sage RF, Rearcy RW. 1987.** The nitrogen use efficiency of C_3 and C_4 plants. II. Leaf nitrogen effects on the gas exchange characteristics of *Chenopodium album* L. and *Amarathus retroflexus* L. *Plant Physiology* 84: 959–963.

[22] **Hirose T, Ackerly DD, Traw MB, Ramseirer D, Bazz FA. 1997.** CO_2 elevation, canopy photosynthesis and optimal leaf area index. *Ecology* 78: 2339–2350.

[23] **Sims DA, Pearcy RW. 1989.** Photosynthetic characteristic of a tropical forest

understory herb, *Alocasia macrorrhiza*, and a related crop species, *Colocasia esculenta* grown in contrasting light environments. *Oecologia* 79: 53–59.

[24] **Sinclair TR, Bennett JM, Boote KL. 1993.** Leaf nitrogen content, photosynthesis and radiation use efficiency in peanut. *Peanut Science* 20: 40–43.

[25] **del Pozo A, Dennett MD. 1990.** Analysis of the distribution of light, leaf nitrogen, and photosynthesis within the canopy of *Vicia faba* L. at two contrasting plant densities. *Australian Journal of Agricultural Research* 50: 183–189.

[26] **Muchow RC, Sinclair TR. 1994.** Nitrogen response of leaf photosynthesis and canopy radiation use efficiency in field grown maize and sorghum. *Crop Science* 34: 721–727.

[27] **Vos J, van der Putten PEL, Birch CJ. 2005.** Effect of nitrogen supply on leaf appearance, leaf growth, leaf nitrogen economy and photosynthetic capacity in maize (Zea mays L.). *Field Crops Research* 93: 64–73.

[28] **Meinzer FC, Zhu J. 1998.** Nitrogen stress reduces the efficiency of the C_4 CO_2 concentrating system, and therefore quantum yields, in *Saccharum* (sugarcane) species. *Journal of Experimental Botany* 49: 1227–1234.

[29] **Reich PB, Walters MB, Ellsworth DS. 1991.** Leaf age and season influence the relationships between leaf nitrogen, leaf mass per area and photosynthesis in maple and oak trees. *Plant, Cell and Environment* 14: 251–259.

[30] **Ellsworth DS, Reich PB. 1993.** Canopy structure and vertical patterns of photosynthesis and related leaf traits in a deciduous forest. *Oecologia* 96: 169–178.

[31] **Niinemets U, Tenhunen JD. 1997.** A model separating leaf structural and physiological effects on carbon gain along light gradients for the shade-tolerant species *Acer saccharum*. *Plant, Cell and Environment* 20: 845–866.

[32] **Wilson KB, Baldocchi DD, Hanson PJ. 2000.** Spatial and seasonal variability of photosynthetic parameters and their relationship to leaf nitrogen in a deciduous forest. *Tree Physiology* 20: 565–578.

[33] **Rosati A, Esparza G, DeJong TM, Pearcy RW. 1999.** Influence of canopy light environment and nitrogen availability on leaf photosynthetic characteristics and photosynthetic nitrogen-use efficiency of field-grown nectarine trees. *Tree Physiology* 19: 173–180.

[34] **Walcroft AS, Whitehead D, Silvester WB, Kelliher FM. 1997.** The response of photosynthetic model parameters to temperature and nitrogen concentration in *Pinus radiate*. *Plant, Cell and Environment* 20: 1338–1348.

[35] **Anten NPR, Schieving F, Werger MJA. 1995.** Patterns of light and nitrogen distribution in relation to whole canopy carbon gain in C_3 and in C_4 mono- and dicotyledonous species. *Oecologia* 101: 504–513.

[36] **Yin X, Sun Z, Struik PC, van der Putten PE, van Ieperen W, Harbinson J. 2011.** Using a biochemical C_4–photosynthesis model and combined gas exchange and chlorophyl fluorescence measurements to estimate bundle-sheath conductance of maize leaves differing in age and nitrogen content. *Plant, Cell and Environment* (*in press*).
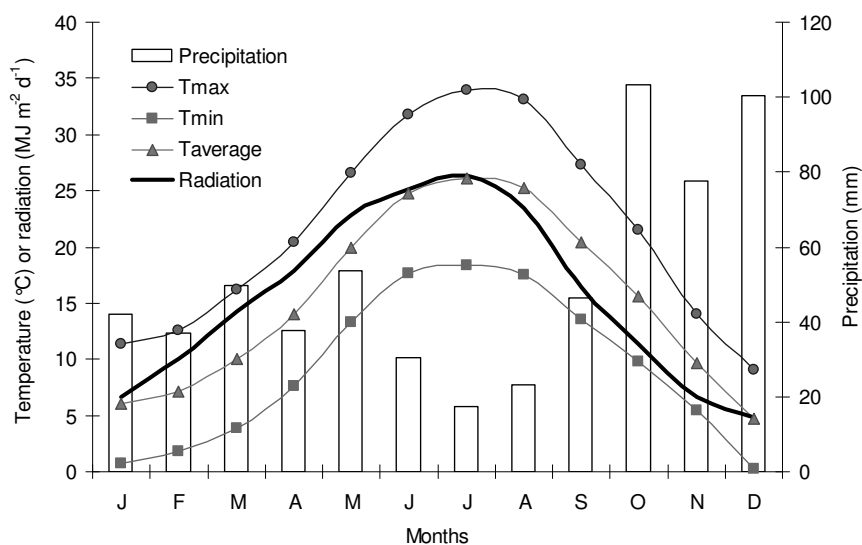
Figure S-5.1: Average monthly temperatures, radiation and precipitation at the experimental site (period: 2007–2009). Sunflower measurements were taken from July to August; kenaf measurements from July to September and cynara measurements from November to June.
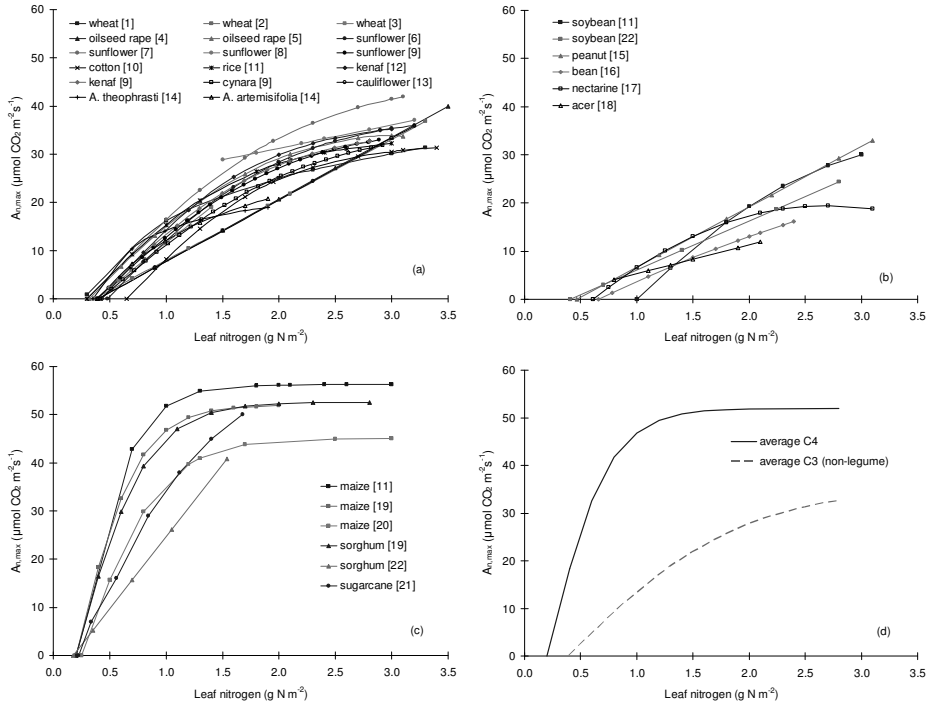
Figure S-5.2: Reported relationships between saturated net assimilation rate at ambient CO_2 concentration and at near-optimum temperature ($A_{n,max}$ in μmol $CO_2\,m^{-2}\,s^{-1}$) and leaf nitrogen content (g N m^{-2}) for C_3 crops (panel a), C_3 legume crops and trees (panel b) and C_4 crops (panel c). Panel (d) shows an average relationship for C_3 and C_4 crops.

References according to the number given in Fig. S-5.2

[1] **Bindraban PS. 1999.** Impact of canopy nitrogen profile in wheat on growth. *Field Crops Research* 63: 63–77.

[2] **Müller J, Wernecke P, Diepenbrock W. 2005.** LEAFC3–N: a nitrogen sensitive extension of the CO_2 and H_2O gas exchange model LEAFC3 parameterized and tested for winter wheat (*Triticum aestivum* L.). *Ecological Modelling* 183: 183–210.

[3] **Dreccer MF, van Oijen M, Schapendonk AHCM, Pot CS, Rabbinge R. 2000.** Dynamics of vertical leaf nitrogen distribution in a vegetative wheat canopy. Impacts on canopy photosynthesis. *Annals of Botany* 86: 821–831.

[4] **Müller J, Diepenbrock W. 2006.** Measurements and modelling of gas exchange of leaves and pods of oilseed rape. *Agricultural and Forest Meteorology* 139: 307–322.

[5] **Gammelvind LH, Schjoerring JK, Mogensen VO, Jensen CR, Bock JGH. 1996.** Photosynthesis in leaves and siliques of winter oilseed rape (*Brassica napus* L.). *Plant Soil* 186: 227–236.

[6] **Bange MP, Hammer GL, Rickert KG. 1997.** Effect of specific leaf nitrogen on radiation use efficiency and growth of sunflower. *Crop Science* 37: 1201–1207.

[7] **Connor DJ, Hall AJ, Sadras VO. 1993.** Effects on nitrogen content on the photosynthetic characteristics of sunflower leaves. *Australian Journal of Plant Physiology* 20: 251–263.

[8] **Fredeen AL, Gamon JA, Field CB. 1991.** Responses of photosynthesis and carbohydrate partitioning to limitations in nitrogen and water availability in field grown sunflower. *Plant, Cell and Environment* 14: 963–970.

[9] Relationships for sunflower, kenaf and cynara reported in this study (Fig. 5.3).

[10] **Milroy SP, Bange MP. 2003.** Nitrogen and light response of cotton photosynthesis and implication for crop growth. *Crop Science* 43: 904–913.

[11] **Sinclair TR, Horie T. 1989.** Leaf nitrogen, photosynthesis, and crop radiation use efficiency: a review. *Crop Science* 29: 90–98.

[12] **Muchow RC. 1990.** Effects of leaf nitrogen and water regime on the photosynthetic capacity of kenaf (*Hibiscus cannabinus* L.) under field conditions. *Australian Journal of Agricultural Research* 41: 845–852.

[13] **Alt C, Stützel H, Kage H. 2000.** Optimal nitrogen content and photosynthesis in cauliflower (*Brassica oleracea* L. botrytis). Scaling up from a leaf to the whole plant. Annals of Botany 85: 779–787.

[14] **Hirose T, Ackerly DD, Traw MB, Ramseirer D, Bazz FA. 1997.** CO_2 elevation, canopy photosynthesis and optimal leaf area index. *Ecology* 78: 2339–2350.

[15] **Sinclair TR, Bennett JM, Boote KL. 1993.** Leaf nitrogen content, photosynthesis and radiation use efficiency in peanut. *Peanut Science* 20: 40–43.

[16] **del Pozo A, Dennett MD. 1990.** Analysis of the distribution of light, leaf nitrogen, and photosynthesis within the canopy of *Vicia faba* L. at two contrasting plant densities. *Australian Journal of Agricultural Research* 50: 183–189.

[17] **Rosati A, Esparza G, DeJong TM, Pearcy RW. 1999.** Influence of canopy light environment and nitrogen availability on leaf photosynthetic characteristics and photosynthetic nitrogen-use efficiency of field-grown nectarine trees. *Tree Physiology* 19: 173–180.

[18] **Ellsworth DS, Reich PB. 1993.** Canopy structure and vertical patterns of photosynthesis and related leaf traits in a deciduous forest. *Oecologia* 96: 169–178.

[19] **Muchow RC, Sinclair TR. 1994.** Nitrogen response of leaf photosynthesis and canopy radiation use efficiency in field grown maize and sorghum. *Crop Science* 34: 721–727.

[20] **Vos J, van der Putten PEL, Birch CJ. 2005.** Effect of nitrogen supply on leaf appearance, leaf growth, leaf nitrogen economy and photosynthetic capacity in maize (*Zea mays* L.). *Field Crops Research* 93: 64–73.

[21] **Meinzer FC, Zhu J. 1998.** Nitrogen stress reduces the efficiency of the C_4 CO_2 concentrating system, and therefore quantum yields, in *Saccharum* (sugarcane) species. *Journal of Experimental Botany* 49: 1227–1234.

[22] **Anten NPR, Schieving F, Werger MJA. 1995.** Patterns of light and nitrogen distribution in relation to whole canopy carbon gain in C_3 and in C_4 mono- and dicotyledonous species. *Oecologia* 101: 504–513.

Chapter 6

The agronomy of bioenergy crops in central Greece

6.1 Agronomy of *Cynara cardunculus* growing on an aquic soil in central Greece

6.2 The effect of nitrogen fertilization and irrigation on seed and biomass productivity of *Cynara cardunculus* growing in a semi-arid environment in central Greece

6.3 Irrigation and N-fertilization effects on the growth and productivity of sunflower growing in an aquic soil in central Greece

6.4 Irrigation effects on the growth and biomass productivity of two kenaf genotypes growing in an aquic soil in central Greece

Chapter 6.1

The agronomy of *Cynara cardunculus* growing on an aquic soil in central Greece

Abstract

The aim of the present work is to provide more insight into the factors that determine biomass and seed productivity in *Cynara cardunculus* (cynara) in central Greece. For this, a two-year (2006–2007) field experiment was conducted on an aquic soil and the effects of irrigation and N-fertilization were investigated. Crop growth and biomass productivity were monitored over time by means of periodical sampling together with measurements of leaf photosynthesis and N concentrations per plant component. We found that cynara maintained very high leaf area indices (above 3) for the most of the 16 month growing period. During May, when air temperature was at near optimum level (viz. 22°C) for photosynthesis (28 μmol CO_2 m^{-2} s^{-1}), the crop performed maximum rates of increase in biomass (range: 215–250 kg ha^{-1} d^{-1}). N-fertilization and irrigation had a significant effect on seed productivity but not on stalk biomass yield. On average the crop performed well, producing a total aerial dry biomass of 27 t ha^{-1} and a seed yield of 5 t ha^{-1} on average values. Such yields are among the highest that have ever been reported in literature. At the end of the cropping cycle, total nitrogen uptake ranged from 170 to 300 kg N ha^{-1} in response to N-fertilization and irrigation, while the nitrogen-use efficiency (NUE) varied from 97 to 132 kg kg^{-1}.

Introduction

Cynara cardunculus L., commonly known as cynara or cardoon or Spanish thistle artichoke, is a perennial herbal, very deep-rooting C_3 plant of Mediterranean origin, well-adapted to the xerothermic conditions of southern Europe. Cynara has annual growth cycles, with the crop to be developed during autumn, winter and spring and to be ready for harvest during summer time, achieving yields of 9–30 t dm ha^{-1} depending on water availability (Dalianis *et al.*, 1996; Foti *et al.*, 1999; Piscioneri *et al.*, 2000; Gherbin *et al.*, 2001; Curt *et al.*, 2002; Gonzáles *et al.*, 2004; Fernández *et al.*, 2005, 2006; Danalatos *et al.*, 2007a; Panoutsou, 2007; Raccuia & Melilli, 2007a).

Apart from the obvious low production costs that this crop has, due to its perennial growth cycle (10–15 year), cynara has also a large range of industrial and other applications, providing many reasons for inclusion in near future land use schemes. Indeed, cynara can be cultivated for fibre production in the pulp industry (25% fibres in volume), for forage production, but most importantly for solid and/or liquid biofuel (Quilhó *et al.*, 2004; Fernández *et al.*, 2006; Danalatos, 2008). Additionally, it can be used in pharmacology, since active compounds like cynarin, silymarin (from leaves; Curt et al., 2002) and inulin (from roots; Sonnante *et al.*, 2007) can be extracted, and lastly from the florets a kind of cheese for human consumption can be produced (Duarte *et al.*, 2006).

Regarding environmental issues, cynara is a very competitive plant (White & Holt, 2005), thus it can be cultivated without the use of agro-chemicals after the 2nd growing cycle. Cultivation of cynara keeps the soil covered throughout most of the year, thus minimizing the risk of soil erosion and desertification that threatens more than 35% of the Mediterranean areas (Danalatos *et al.*, 2008). Its deep and effective rooting system takes perfect advantage of the soil's inherent fertility, avoiding risks of N-leaching, and prevents soil and groundwater pollution. It can also be grown in areas with salinity problems, which are frequently observed under Mediterranean conditions (Raccuia *et al.*, 2004; Benlloch-Gonzales *et al.*, 2005).

Although cynara's adaptability and market potential have been studied around the Mediterranean region, there are still many important agronomic aspects that need to be addressed in order to design sustainable cynara cultivation systems. Thus, in this work we aim to provide more insight into the factors that determine cynara's biomass production. Potential and water/nitrogen limited crop growth will be studied, including light- and temperature-response curves of leaf photosynthesis. These quantitative datasets will be used later to parameterize the dynamic simulation model GECROS (Yin & van Laar, 2005).

Materials and methods

Field management

A two-year field experiment was carried out on the Western Thessaly Plain (Palamas, coordinates: 39°25′N, 22°05′E, alt. 105 m) in 2006–2007. The soil at the site was a deep, fertile loamy soil classified as Aquic Xerofluvent according to USDA (1975), having a shallow groundwater table. A 2×3 factorial spit–plot design was used in four blocks with the main plots comprising two irrigation treatments (I_1=rainfed, I_2=irrigated), and subplots comprising three nitrogen dressings (N_1=control, N_2=80, and N_3=160 kg N ha^{-1}).

Seeds of cynara (cv. Bianco avorio) were sown on April 13 (50% emergence 11 days later) with a plant density of 5.3 pl. m^{-2} (75 cm × 25 cm). Before sowing, all plots received a basal fertilization with 50 kg P-K, while N-fertilization of 80 and 160 kg N ha^{-1} (fertilizer: 26% N – 0% P – 0% K plus 13% S, with 18.5% NH_4 and 7.5% NO_3) was applied in the second year just before inflorescence emergence on April 28th 2007. The crop received irrigation via an automatic drip irrigation system. In the first year, the crop was irrigated with a total of 200 mm in the period July–August (5 applications); in the second year (2007), the crop received a total of 120 mm in two applications, on May 7 and 16, respectively. Weather data, such as incident solar radiation, air temperature, rainfall, relative humidity, wind speed and class-A pan evaporation rate, were recorded hourly using an automatic meteorological station, which was installed in the experimental field. All measured and derived data were subjected to analysis of variance using GenStat (7th edition).

Measurements

Growth parameters (plant height, specific leaf area and leaf area index) and above-ground dry biomass productivity per plant component (stem, branches, leaves and storage organs) were measured in subsequent destructive harvests throughout the growing period, at the following dates: 20/6, 3/7, 28/7, 14/8, 9/9 and 15/11 in 2006, and 14/1, 29/1, 21/3, 27/4, 6/5, 15/5, 1/6, 19/6, 18/7 and 6/8 in 2007. In each manual harvest, the sample was divided into the various plant organs and weighed fresh in the field. Then the samples were oven-dried at 90°C until constant weight (2–4 days) and weighed again in order to determine the dry weights per plant component. Leaf area (green leaves) was measured using an automatic LI–COR area meter (LI–3000A). Samples of the last harvest were dried at 70°C and then analyzed for their nitrogen concentrations (Kjeldahl method).

Given the complex structure of cynara's inflorescence, in order to determine seed yield we developed an allometric equation to upscale seed weight from head to crop level. For that a sample of 72 randomly chosen heads were analysed (see methodology in

Chapter 3). The allometric equation that was used in this study was: seed weight per head = 0.4403 × head weight – 3.1215 (r^2=0.981, n=72). For more details see Chapter 3.

Photosynthesis was measured in the field, using an open exchange system (ADC, LCpro+, UK) equipped with an adjustable light source and ventilation for temperature control. Measurements were undertaken during November (fully expanded leaflet). Response curves of net assimilation (A, µmol CO_2 m^{-2} s^{-1}) to light (Q, µmol m^{-2} s^{-1}), and to temperature were constructed (see methodology in Chapter 5). All gas exchange parameters were re-calculated according to equations described by von Caemmerer & Farquhar (1981).

Results

Weather conditions

Figure 6.1.1 illustrates maximum, minimum air temperatures and sunshine duration at the experimental site in 2006–2007. The winter of 2007 was the hottest and the driest of the last 5 years at this specific site (viz. 7.5 °C in 2007 vs. 4.5 °C in the 5-year average). During spring and August 2007, the mean average daily temperatures were 14.8 and 25.9 °C, respectively, while the A-pan mean evaporation rates for the same periods were 4.3 and 7.6 mm d^{-1}. Regarding the effective precipitation (from sowing to harvest), 420 and 290 mm were recorded, for the 2006 and 2007, respectively.
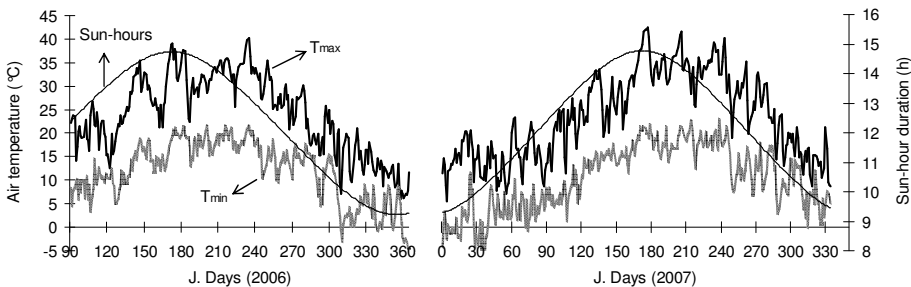
Figure 6.1.1: Maximum and minimum daily air temperatures and maximum sunshine duration at the experimental site (central Greece) during 2006–2007.

Leaf photosynthesis

Determination of photosynthesis light and temperature response curves is very important for crop growth modelling, since many parameters can be estimated from them (e.g. see Chapter 5). Here we report only the basic information. Fig. 6.1.2 illustrates that cynara's photosynthesis was light saturated above 750 µmol m^{-2} s^{-1}, while the maximum net assimilation rate depended on leaf temperature (viz. 28.1 and 20.7 µmol

CO_2 m^{-2} s^{-1} at 20 °C and 36 °C, respectively). The temperature response curves illustrate that the optimum range for photosynthesis (during winter time) increased with an increased light level; under saturated light (clear days) and limited light (overcast days) the optimum temperature range was 19–23 °C and 18–22 °C, respectively. Below and beyond this optimum the photosynthetic rate was lower. In the sub-optimum part, the photosynthetic apparatus was limited by the enzymatic reaction rates (kinetic properties of Rubisco are temperature-dependent), while in the supra-optimum part, the oxygenation reaction of Rubisco increased more than the carboxylation, so that photorespiration became more important (cf. Atwell *et al.*, 1999). Lastly, it seemed that below 7.5 °C photosynthesis became zero, and this might be a good indication for the base temperature of plant growth.
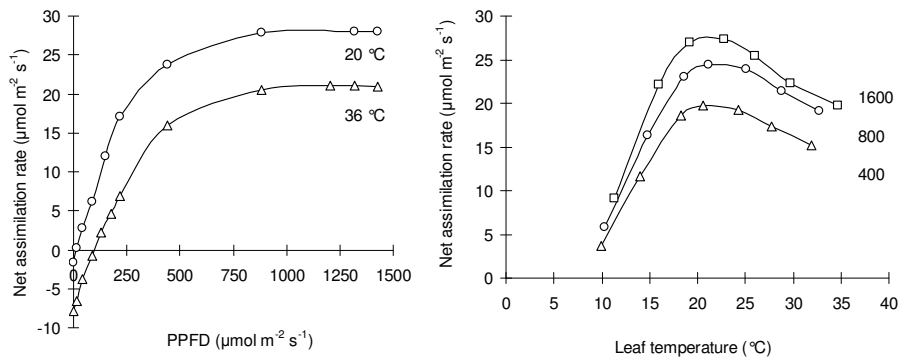
Figure 6.1.2: Leaf net photosynthesis (a) light- and (b) temperature-response curves of *Cynara cardunculus* growing in central Greece. Data points are mean values of 5 measurements. Light curves presented for two temperature regimes (a; 20 and 36°C) and temperature curves for three light levels (b; 400, 800 and 1600 μmol m^{-2}s^{-1}). Measurements were taken during November.

Crop growth

No significant interactions between irrigation and nitrogen fertilization levels ($P>0.05$) were observed in any of the measured parameters during the growing cycle. Figures 6.1.3 and 6.1.4 depict the time course of plant height, specific leaf area, leaf area index, fresh and dry biomass as affected by the various treatments. Both irrigation and fertilization applications had a positive impact on fresh and dry matter production and leaf area index ($P<0.05$; Figs. 6.1.3 and 6.1.4), while no significant differences were found in cases of specific leaf area and plant height ($P>0.05$; Figs. 6.1.3 and 6.1.4).

After an initial lag phase of crop establishment (root development; May 2006), the crop passed to the rosette stage (complete soil cover; June 2006) and thereafter developed a fully closed canopy (July 2006). At this stage the crop had a height of 50 cm, a leaf area index (LAI) of about 4.3 and a dry weight of 4.2 t ha^{-1}.
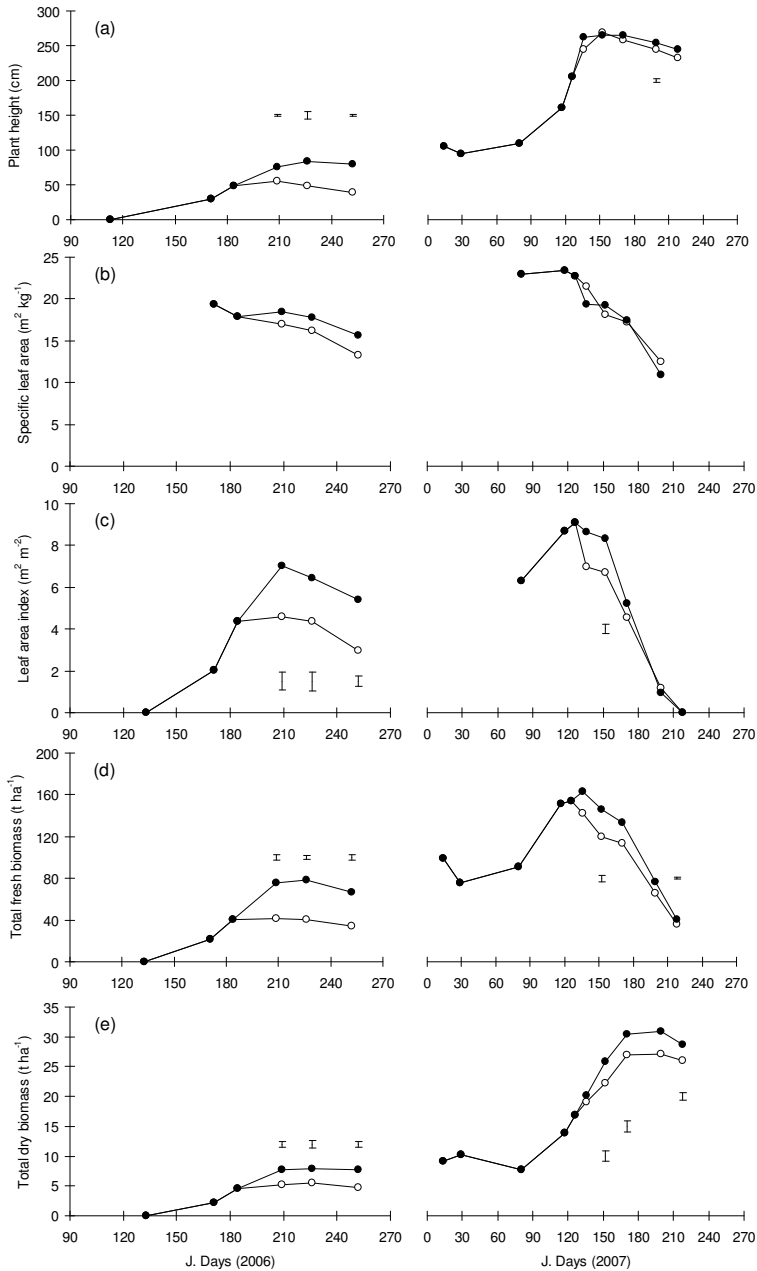
Figure 6.1.3: Time course of (a) plant height; (b) specific leaf area; (c) leaf area index; (d) fresh and (e) dry biomass of *Cynara cardunculus*, grown under irrigated (●) and rainfed (○) condition in central Greece in 2006–2007. Vertical bars (LSD at *P*< 0.05) when visible indicate significant differences between two irrigation levels. Each point represents the mean of the three N levels.
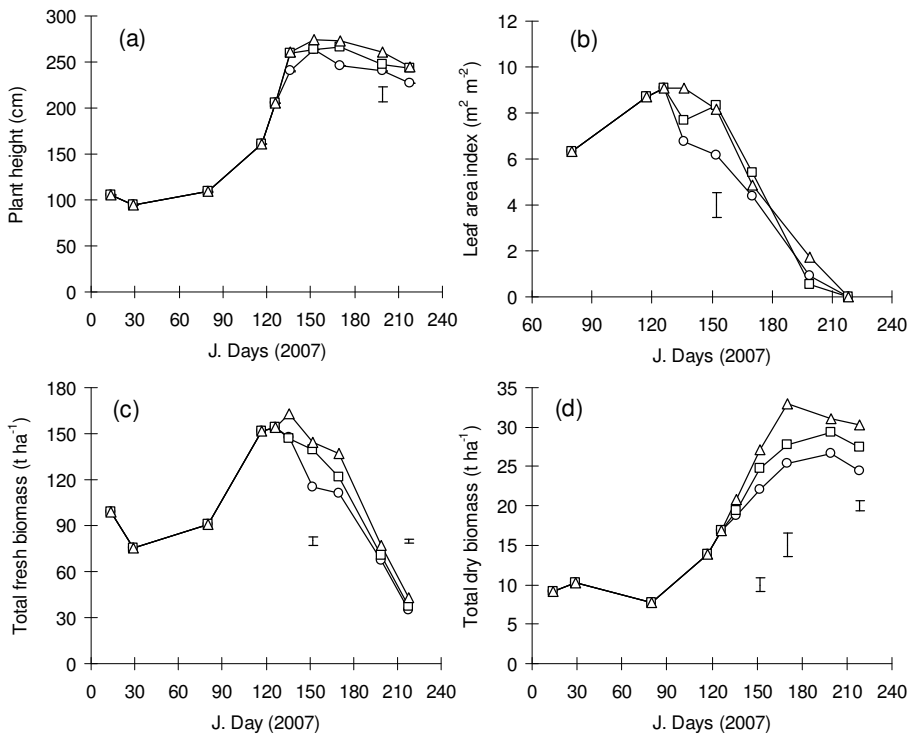
Figure 6.1.4: Time course of (a) plant height; (b) leaf area index; (c) total fresh and (d) total dry biomass of *Cynara cardunculus*, grown under three N levels (○: control; □: 80 and △: 160 kg N ha^{-1}) in Palamas in 2007. Vertical bars (LSD at *P*<0.05) when visible indicate significant differences among N-levels. Each point represents the mean value of the two water-supply levels.

Thereafter and until mid-September 2006 the crop further increased in height, biomass, and LAI. Irrigation application significantly increased crop growth rates (*P*<0.05; Fig. 6.1.3). During autumn and winter, cynara remained in the vegetative growth stage with some fluctuation in the aerial biomass. The fluctuation in biomass was due to the variability of weather; in frost periods the foliage was damaged and biomass decreased, while the crop recovered after an increase in temperature and so on.

During spring 2007, when temperature and radiation increased (Figs. 6.1.1 and 6.1.2), the crop showed maximum growth rates (250 and 215 kg ha^{-1} d^{-1} for the irrigated and rainfed crop, respectively) reaching maximum biomass yields of 30.4 and 27.1 t ha^{-1} for the irrigated and rainfed treatments, respectively (*P*<0.05; Fig. 6.1.3). This period coincided with a rapid stem elongation (viz. 2.7 cm d^{-1}), inflorescence emergence, and flowering initiation. Within this period, LAI reached maximum values of 6.9 and 8.5 (for I_1 and I_2, respectively, *P*<0.05; Fig. 6.1.3), while specific leaf area (average canopy measure) decreased without considerable differences among treatments. Significant

differences between nitrogen inputs were detected for fresh and dry weight and LAI during mid–May to mid–June, as well ($P<0.05$; Fig. 6.1.4).

During June and July 2007, the crop passed through fruit development, ripening and senescence stages, by dropping the leaf mass, increasing dry/fresh ratio and finally it was ready for harvest during mid-August 2007. Within this period the nitrogen concentration in stems and heads were 0.47 and 1.37%, respectively. The maximum nitrogen uptake of 312 kg N ha^{-1} was found in the high input treatments, while the NUE ranged among treatments from 132 to 97 kg kg^{-1} (Table 6.1.1).

Table 6.1.1: Nitrogen concentration, total aerial nitrogen uptake and nitrogen use efficiency (NUE) of *Cynara cardunculus* growing in central Greece in 2007. Data refer to the last sampling (August) and are average values

N supply (kg ha^{-1})	N concentration (%)		Total N uptake (kg ha^{-1})	NUE (kg aerial dm) (kg Nup)$^{-1}$
	Stalks	Heads		
Irrigated crops				
0	0.40	1.13	203.3	128.0
80	0.50	1.27	254.0	112.5
160	0.48	1.47	312.8	100.4
Rainfed crops				
0	0.43	1.10	171.5	132.8
80	0.50	1.25	235.6	110.9
160	0.50	1.43	298.9	97.7

Biomass production

At final harvest, total fresh (average: 38.5 t ha^{-1}) and total dry biomass (average: 27.4 t ha^{-1}) were significantly affected by irrigation and nitrogen inputs (Table 6.1.2; $P<0.05$), while dry heads and dry seed yield (average: 5.16 t ha^{-1}) were affected statistically only by nitrogen applications (Table 6.1.2; $P<0.05$). Stem yields and fractions of the various plant components over the total biomass were not affected significantly (Table 6.1.2; $P>0.05$). At harvest, the plant components had different moisture contents (viz. seeds: 6–9%, heads: 12–14%, stems: 35–45%), resulting in different seed harvest index: 13% expressed on fresh basis and 19% expressed on dry basis (Table 6.1.2).

Table 6.1.2: Cynara's yield components during the final harvest (6 August 2007) in central Greece. No significant irrigation × fertilization interactions were observed

Parameter	I_1	I_2	P	N_1	N_2	N_3	P
Total FW (t ha^{-1})	36.31	40.79	*0.008*	34.87	37.4	43.37	*0.001*
Total DW (t ha^{-1})	26.05	28.68	*0.001*	24.41	27.37	30.32	*<0.001*
Stalk DW (t ha^{-1})	12.24	13.84	*0.086*	12.11	13.13	13.88	*0.231*
Head DW (t ha^{-1})	13.81	14.84	*0.268*	12.30	14.24	16.44	*0.005*
Seed DW (t ha^{-1})	04.90	05.36	*0.154*	04.24	05.20	05.97	*0.004*
Fraction (fresh basis)							
Stalk / total	0.563	0.58	*0.561*	0.592	0.560	0.563	*0.347*
Head / total	0.436	0.419	*0.561*	0.407	0.440	0.436	*0.347*
Seed / total	0.135	0.132	*0.701*	0.123	0.139	0.138	*0.104*
Fraction (dry basis)							
Stalk / total	0.473	0.481	*0.752*	0.498	0.477	0.456	*0.322*
Head/ total	0.527	0.519	*0.752*	0.502	0.523	0.544	*0.322*
Seed / total	0.187	0.187	*0.986*	0.174	0.19	0.197	*0.090*

For symbols explanation see Materials and methods.

FW, fresh weight; DW, dry weight.

Discussion

This work highlights the high potential of *Cynara cardunculus* for biomass and seed production in central Greece. The observed total dry biomass yields (24–30 t ha^{-1}) are among the highest that have ever been reported (Dalianis *et al*., 1996; Foti *et al*., 1999; Gonzáles *et al*., 2004; Raccuia & Melilli, 2007a; Danalatos *et al*., 2007). Due to spring sowing (see April 2006), the crop remained in the vegetative phase from summer 2006 to spring 2007 (in total 16 months) and this provided an advantage to the crop (longer growing period), compared to the annual growth cycles (~10 months) that this crop commonly experiences after the 2nd year.

According to Fernández *et al*. (2006), a minimum of 400 mm as rainfall is required during autumn-spring in order for cynara to achieve good yields. In our case (dry plots), during that period some 440 mm of precipitation were recorded. Commonly the water-use efficiency (WUE) is examined to provide more insight into the process efficiency of turning water and CO_2 into biomass. Various ways of calculating WUE have been reported (Jorgensen & Schelde, 2001). Here we estimate the WUE according to Passioura (2002), by plotting above-ground biomass against the amount of water supplied. The results show a WUE (estimated as the slope of the plot) of 2.7 and 3.6 g dm (kg water)$^{-1}$, for the irrigated and non-irrigated crop, respectively, while the evaporation from the soil (estimated as the *x*-axis intercept) was found at similar level for both the irrigated and rainfed crops (50 mm; data not shown). Our estimated WUE is in line with reports from

Spain (AIR2-CT92-1089) for cynara, and is much higher than that for other common agricultural C_3 crops (viz. 1.6 ± 0.4 g kg^{-1}; Jorgensen & Schelde, 2001).

The observed fluctuation in dry biomass accumulation rate from October 2006 until March 2007 was due to fluctuation in temperature (from 1.3 to 21.4 °C; average 9.7 °C) and due to fluctuation in daily total radiation (from 0.4 to 19 MJ m^{-2} d^{-1}). Figure 6.1.2 relates these variables to photosynthesis, explaining the observed variation in dry biomass. From April to mid-June, the mean day-time air temperature was 21.4 °C, which is within the optimum range for maximum photosynthesis of cynara (Fig. 6.1.2b). This, in combination with the saturated light (above 750 µmol m^{-2} s^{-1}), the low night-time temperatures (14.8 °C, very low respiration losses) and the fully closed canopy (see LAI > 3, in all cases), explains the high growth rates that were observed within this period (215–250 kg ha^{-1} d^{-1}).

The observed high nitrogen uptake rates (Table 6.1.1) are most probably attributed both to the high growth rates observed in 2007 (N demand approach) and also to soil availability (N supply approach; Gastal & Lemaire, 2002). It was estimated that the study soil can provide some 90–120 kg N ha^{-1} by mineralization while the additional 50–80 kg N ha^{-1} comprise the residual nitrogen from previous years extracted by the extensive cynara rooting in deeper soil layers (root zone depth measured at 300 cm in June 2007), and also partly by the nitrogen in the previous crop litter. Reports from Spain mentioned nitrogen uptake rates of about 125–145 kg N ha^{-1}, under water and nitrogen limited conditions (Fernández *et al.*, 2006). Considering such high uptake rates, restoration seems to be essential for maximize yield. Nitrogen balance approaches deserve additional caution, since cynara produces some 7–12 t ha^{-1} leaf and petiole litter (see LAI; Figs. 6.1.3 and 6.1.4) with a minimum nitrogen concentration of 1.3% and 0.6%, respectively. In our case, some 95–110 kg N ha^{-1} had been added to the soil in total.

The NUE of cynara ranged from 97 to 132 kg kg^{-1}, which is rather high compared to common agricultural crops (maize-grains and biomass: 66 and 111, wheat-grains: 83 to 87 and potato: 73 kg kg^{-1}; Beale & Long, 1997; Jorgensen & Mortensen, 2000) and somewhat lower compared to "woody" energy crops (miscanthus: 135–700, hemp: 169–179 and kenaf: 117–144 kg kg^{-1}; Beale and Long, 1997; Flengmark, 2000; and authors' unpublished data). The lower NUE of cynara compared to C_3 hemp is because of the production of seeds that have a high nitrogen concentration (~3%). Cardoon seeds are economically valuable products that can be used directly for bio-diesel production or can be added to the whole biomass, increasing the heating value of the product.

Conclusions

This study provides for the first time an overall assessment of growth and biomass productivity of *Cynara cardunculus* in an aquic soil. Light and temperature response curves were also reported for the first time in literature for this crop. We found

maximum net assimilation rate of 28 μmol CO_2 m^{-2} s^{-1}, a value that is close to the maximum photosynthesis for C_3 species. We recorded very high total dry biomass yields from 24 to 30 t ha^{-1} (in response to irrigation and N-fertilization application) in this particular experiment. These large biomass yields even under zero inputs make cynara by far the most interesting energy crop for solid biofuel production in Greece.

Chapter 6.2

The effect of nitrogen fertilization and irrigation on seed and biomass productivity of *Cynara cardunculus* growing in a semi-arid environment in central Greece

Abstract

The effects of nitrogen fertilization and irrigation on growth, biomass and seed yield of *Cynara cardunculus* were investigated in a dry environment of central Greece (Velestino, 2008/2009) during the crop's second growth cycle. The growth was monitored by periodical destructive sampling. Nitrogen input–yield relations were analysed using a three-quadrant diagram. We found that nitrogen fertilization and irrigation significantly ($P<0.001$) increased total dry biomass yield (24% increase), head weight (43% increase) and seed yield (50% increase). Final productivities in the studied area ranged from 12.8 to 17.5 t ha^{-1} (biomass) and from 1.4 to 2.8 t ha^{-1} (seed) for dry and irrigated crops, respectively. Irrigation contributed most to this yield increase, because it prolonged the growing period by two weeks and increased crop growth rates from 170 (rainfed) to 246 (irrigated) kg ha^{-1} d^{-1}. Nitrogen effect was more evident at advanced growth stages when head (and seed) growth created a strong sink for nitrogen. Cynara's nitrogen use efficiency was estimated at 125 kg dm kg^{-1} N. The studied soil provided to the crop 64 to 95 kg N ha^{-1} (basic uptake). The efficiency of fertilizer application (recovery fraction) was 28 and 49% under rainfed and irrigated conditions, respectively. These estimates can serve as reference in nitrogen restoration approaches.

Introduction

Cynara cardunculus L. (cynara) is a perennial herb with a C_3 photosynthetic pathway. Cynara's perennial character, its large root system, and its winter–spring growth cycle are important advantages of the crop. In Greece, biomass production of rainfed cynara crops ranges from 15 t ha^{-1} on dry sites (Danalatos *et al.*, 2006a, 2007a) to some 25–35 t ha^{-1} on aquic sites (Archontoulis *et al.*, 2008a, 2009). Differences in crop growth and development between dry and aquic areas become evident after inflorescence emergence (coinciding with stem elongation; principal growth stage 5 based on BBCH system; Archontoulis *et al.*, 2010a). In Greece, this period occurs in May. Usually, during May, crop transpiration increases as temperature increases, when the prevailing water deficit is no longer satisfied by precipitation and/or the available soil moisture in the dry soils.

The larger water deficit on dry soils has the following chronological consequences for the cynara crop (compared with a crop on aquic soils): i. formation of fewer heads per plant (end of May), ii. acceleration of the senescence of the basal leaves, reduction of leaf area index, lower light interception as well as lower growth rates (end of June), iii. incomplete head growth and a relatively smaller proportion of seeds in the total head, iv. lower biomass (and seed) yields. Given these consequences, we hypothesised that supplemental irrigation accompanied with nitrogen application during the principal growth stage 5 might increase biomass and seed yield in a semi-arid (dry) environment of central Greece.

Thus the objective of this work was to investigate the growth and the biomass productivity of cynara under supplemental irrigated and under rainfed conditions (control) in central Greece. Within each plot, the effect of five nitrogen application rates (range: 0–240 kg N ha^{-1}) was also investigated. Emphasis was given on nitrogen extraction during the final harvest in order to determine parameters what will serve as reference in nitrogen restoration approaches. Nitrogen input–yield responses were analyzed with the so-called 'three quadrant diagrams' (van Keulen, 1982; de Wit, 1992; Vos, 1997, 2009). With such a diagram the 'agronomic response', i.e. yield versus N supply (quadrant I), is split up into its components: the relation between yield and N uptake (quadrant II) and the relation between N supply and N uptake (quadrant III). Yield–N uptake relation is primarily determined by the physiology of the plant, while N supply–N uptake relationship is governed by processes in the soil.

Materials and Methods

Experimental site and design

The field experiment was carried out on a clay soil with no ground water level (moderate fertility) in the Experimental Farm of the University of Thessaly (Velestino, Magnesia, coordinates: 39°23′ N, 22°44′ E, altitude 87 m asl). The soil is classified as Calxixerollic

Xerochrept according to USDA (1975). The crop was established on November 27th, 2007 at a sowing density of 5.3 pl. m^{-2} (plant arrangement: 75 × 25 cm) and grew without any additional water and nutrient application inputs during the first cycle (2007/2008).

   After crop harvesting (August 2008) and before new sprouts became visible (BBCH stage 10) the plantation was modified to a 2×5 split-plot experiment in six blocks (60 experimental units). Main factor comprised the two irrigation treatments (I_1 = rainfed and I_2 = with supplementary irrigation) and the sub-factor comprised the five N fertilization dressings (F_1=0, F_2=60, F_3=120, F_4=180 and F_5=240 kg N/ha). N-fertilization (fertilizer: 34.5–0–0) was applied on April 28th 2009 (inflorescence emergence; BBCH stage 50). Irrigation was applied using a drip irrigation system from 20/5 to 10/6, with a total amount of 138 mm in three applications. The present study reflects the 2nd growth cycle of the crop (2008/2009).

Measurements

Growth and biomass productivity data were collected during five different crop stages: April 28th (stage 50), May 19th (stage 57), June 5th (stage 63), July 2nd (stage 82) and August 3rd 2009 (stage 97). In each destructive harvest (area: 1 m^2), the sample was weighed fresh in the field, and then a sub-sample (usually one or two representative off-shoots/sample) was taken for further analyses. The sub-sample was divided into various biomass fractions (green leaves, dead leaves, petioles, stem, branches and heads). Materials were oven-dried at 70°C until constant weights and weighed again to determine the respective dry weights. Before drying, green lamina leaf area was measured using an automatic LI–COR area meter (LI–3000A). During the final harvest, different plant components were also analyzed for nitrogen concentration (% dry weight) using the Kjeldahl method.

Calculations

The leaf area index (LAI, m^2 green leaf m^{-2} ground) was determined as the product of green leaf dry weight (kg m^{-2} ground) times the specific leaf area (SLA in m^2 leaf kg^{-1}). Green petiole area was excluded in LAI estimations.

   The course of dry biomass over time for each treatment ($I \times F$) was described using the beta growth function (Yin *et al*., 2003b):

$$W = W_{max}\left(1 + \frac{t_e - t}{t_e - t_m}\right)\left(\frac{t}{t_e}\right)^{\frac{t_e}{t_e - t_m}} \tag{1}$$

where W_{max} is the maximum biomass weight (W), t is the days after emergence, t_m is the day when the increment of biomass is maximal, and t_e is the day where $W = W_{max}$. From

Eq. (1) the maximum crop growth rate (*CGR*, kg ha^{-1} d^{-1}), which is achieved at time t_m, was calculated as (Yin *et al.*, 2003b):

$$CGR = \frac{2t_e - t_m}{t_e(t_e - t_m)} \left(\frac{t_m}{t_e}\right)^{\frac{t_m}{t_e - t_m}} W_{\max} \tag{2}$$

Seed yield (*SY*) was estimated using the following allometric equation (Archontoulis *et al.*, 2010b; see Chapter 3):

$$SY = HN \cdot (0.4293 \cdot \mu - 2.9048) \tag{3}$$

where μ is the mean head weight per unit area (g head^{-1}) and *HN* is the total number of all seed-bearing heads per unit area.

Nitrogen input–biomass yield responses were analyzed using the three quadrant diagram and by calculating the common nitrogen use efficiency index:

$$NUE = yield / N_{upt} \tag{4}$$

where NUE is the nitrogen use efficiency (kg dry matter per kg nitrogen taken up), yield refer to total biomass or to seed yield (t ha^{-1}) and N_{upt} is the nitrogen that has been taken up by the crop or by the seeds (kg N ha^{-1}). NUE approximates the physiological efficiency (quadrant II). The slope of the (linear regression) line in quadrant III indicates the average nitrogen recovery fraction (kg N taken up per kg N supplied), while the intercept indicates the basic N uptake. Similarly the slope of the (linear regression) line in quadrant I indicates the average agronomic efficiency (kg dm produced per kg N supplied).

Statistics

All measured and derived datasets were subjected to analysis of variance using GenStat (12th edition) following a split-plot design. Statistically significant differences were assessed at $P<0.05$, while the LSD$_{0.05}$ criterion was used to examine differences among means. Curve fittings were implemented in SAS software from iterative non-linear least-square regression.

Results and Discussion

Weather conditions and crop phenology

During growth, the crop received 590 mm as effective precipitation (autumn: 173; winter: 254, spring: 111 and summer: 52 mm; Fig. 6.2.1). This precipitation was 25% and 50% higher compared with an average and with a dry year for this area, respectively (Danalatos & Archontoulis, 2009). Thus the growing season of 2008/2009 is characterized as a moist season, exceeding the empirical value of 400 mm required for realization of good cynara yields (Fernández *et al.*, 2006). Irrigation (138 mm; Fig. 6.2.1) during growth stages 53–63 partially fulfilled the transpiration deficit generated by the increased temperature (+8°C) and the relatively low precipitation (59 mm) during May–June (Fig. 6.2.1).

During September–October the crop experienced good temperatures (17.5 °C) and precipitation amounts (131 mm). This resulted in a prompt re-sprouting and a fast soil cover (stage 39), avoiding any competition from weeds. Thereafter the crop passed to (principal) stage 4 (November) and it remained in that stage until mid-April. During the winter period, vegetative (foliage) biomass yield fluctuated following the temperature variation (average minimum: –4.5 °C; average maximum: 17.4 °C; average mean: 6.5 °C; Fig. 6.2.1). Note that cynara's leaf photosynthesis practically ceases below a temperature of 7.5 °C (Archontoulis *et al.*, 2008a). The crop entered into the reproductive stage (BBCH 51) at the end of April–early May and it was ready for harvest (BBCH 97) during the first week of August.
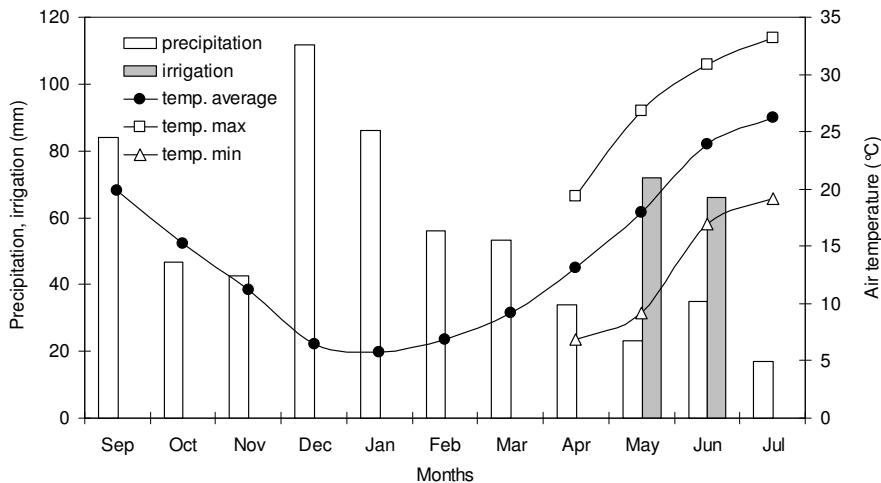

Figure 6.2.1: Monthly precipitation, supplemental irrigation during May–June and monthly temperature records in the study area of Velestino (central Greece) in 2008/2009.

Crop growth and maximum biomass yields

Stalk height (stem + branches) was 156 cm on April 28th (BBCH 50) and increased with a rate of 1.5 cm d^{-1} to reach a final height of 210 cm on June 5th (BBCH 61; *P*>0.05 among treatments). During April 28th LAI was 6.7 m^{2}m^{-2} and thereafter decreased progressively until the first week of July. The decrease of LAI was more evident in the control plots compared with high-input plots, although this was not statistically significant (*P*>0.05; data not shown). Basal leaves were the first to senesce and litter, causing a strong LAI reduction (note that basal leaves comprised 55–70% of the total LAI during May–June). A relevant study on an aquic soil (Archontoulis *et al*., 2008a) confirms that in central Greece cynara's maximal LAI is observed during the end of April until May (stage 5) and thereafter LAI decreases because assimilates are distributed to reproductive organs to support head and seed growth. However, the level of the maximum LAI in this site was 32% lower compared to what was observed in a site with aquic soil (6.7 vs. 9.8 m^{2}m^{-2}).

Fig. 6.2.2 presents the dynamic course of the total dry matter (aerial part) in response to five nitrogen treatments (range: 0–240 kg N ha^{-1}) under both rainfed and irrigated conditions. Results indicated that N-dressing had a minor effect on biomass productivity in the dry plots (see also Table 6.2.1). Some significant differences were detected at advanced growth stages (July 2nd and August 2nd; Fig. 6.2.2). On July 2nd, differences were evident between the control plot and the highly fertilized plots (180–240 kg N ha^{-1}; *P*=0.005). However, differences between 60 and 120–240 kg N ha^{-1} were not significant. Crops with supplemental irrigation showed a stronger response to nitrogen application (Fig. 6.2.2). Soil nitrogen mineralization and crop N uptake were favoured by water supply and thus the wet control plot (I_2–F_1) reached 35% higher maximum productivity than the dry control plot (I_1–F_1; Fig. 6.2.2). Significant differences (*P*<0.05) in biomass production were observed between the 0–60 and the 180–240 kg N ha^{-1} application input levels (Fig. 6.2.2). In an adverse year (frost during February) at this particular site, Danalatos *et al*. (2007a) reported no effect of nitrogen fertilization (range: 0–100 kg N ha^{-1}) on biomass production.

The effect of nitrogen on biomass productivity became evident after mid–June (Fig. 6.2.2). This is attributed to the fact that this period coincides with the head growth and seed development, thus the crop develops a strong sink for nitrogen after mid–June. On average across five N-dressings, maximum dry weight (W_{max}) was 20.8 and 28.7 t ha^{-1} for the dry and wet crops, respectively (Table 6.2.1). This maximum yield was attained on June 16th (t_e) for the dry plots and two weeks later for the wet plots (June 30th, Fig. 6.2.2 and Table 6.2.1). This delay is due to the higher resource availability of the I_2–plots compared with the I_1–plots (higher soil moisture enhanced soil nitrogen mineralization and crop N uptake). This increase in N availability is reflected by the higher growth rates (I_2 = 246 vs. I_1 = 170 kg ha^{-1} d^{-1}; Table 6.2.1), which finally resulted in a higher W_{max} (28% increase).

Within *I*–plots, N-supply also delayed t_e by 1–3 weeks, increasing therefore the W_{max} by 14–22% (Table 6.2.1). However, supplemental irrigation had the largest effect in delaying t_e, while increasing *CGR* and W_{max} as well. By comparing the control plots (I_1F_1 vs. I_2F_1), t_e was delayed by about four weeks and *CGR* almost doubled (126 vs. 212 kg ha^{-1}d^{-1}; Table 6.2.1). Thus it can be inferred that on dry sites, farmers should first aim to irrigate the plantations during May and secondly to apply fertilizers. The latter also depends on the specific soil properties of each site. During July (principal BBCH stages 8 and 9), the crop dries out and a substantial amount of foliage biomass is lost, decreasing thereafter W_{max}. Additionally, mitochondrial biomass respiration caused further decrease in the final biomass yield (Fig. 6.2.2).
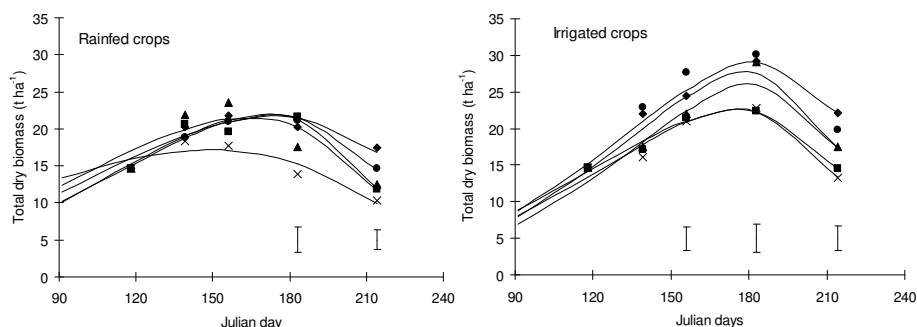
Figure 6.2.2: Time course of total dry biomass as affected by five nitrogen application levels (F_1–F_5) on a dry (left) and on a wet plot (right) in Velestino in 2008/2009. Symbols (F_1:×; F_2:▲; F_3:■; F_4:●; and F_5:♦) refer to observations while lines represent fits from Eq. (1); parameters are given in Table 6.2.1. Vertical bars (LSD at $P<0.05$) when visible indicate significant differences among N-leaves. F_1–F_5 represents five nitrogen application rates: 0, 60, 120, 180 and 240 kg N ha^{-1}.

Table 6.2.1: Parameters of Eq. (1) used to describe biomass time course in Fig. 6.2.2

Parameter		I_1: Rainfed crops					I_2: Irrigated crops				
		F_1	F_2	F_3	F_4	F_5	F_1	F_2	F_3	F_4	F_5
W_{max}	(t ha^{-1})	17.1	21.9	21.4	21.8	21.7	22.5	22.5	26.3	27.6	28.7
t_e	(days)	150	171	164	174	175	177	177	183	181	185
t_m	(days)	55	110	94	110	100	123	119	135	132	132
P		0.007	0.005	0.019	0.000	0.004	0.004	0.004	0.009	0.017	0.001
CGR (kg ha^{-1}d^{-1})		126	193	176	185	168	212	204	263	275	276

For symbol explanation see Materials and methods.
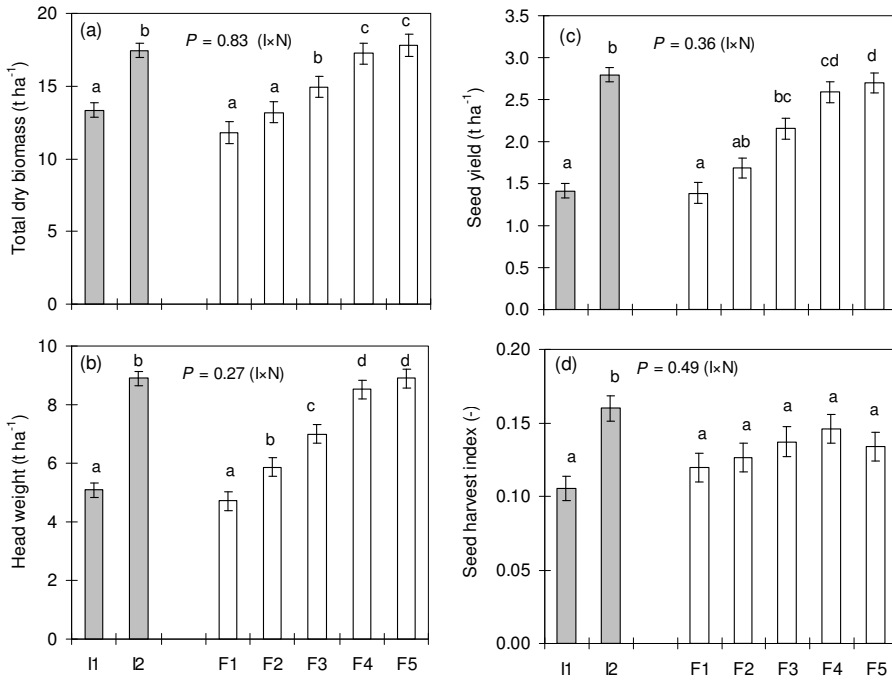
Figure 6.2.3: Total dry biomass weight (a), head dry weight (b), seed yield (c) and seed harvest index (d) during the final harvest of the crop. I_1 = dry and I_2 = irrigated plots, F_1–F_5 represent five nitrogen application rates: 0, 60, 120, 180 and 240 kg N ha^{-1}. Vertical bars indicate standard error of difference of means. Different letters within a factor indicate significant differences between/among means at $P<0.05$, as detected by the LSD test.
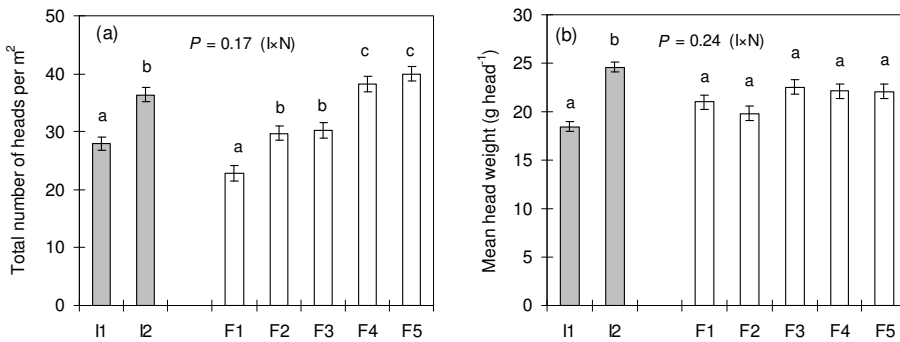
Figure 6.2.4: Total number of heads per unit area (a) and mean head weight (b) during the final harvest of the crop. Symbols and statistics as in Fig. 6.2.3.

Final biomass and seed yield

Final harvest took place on August 2nd (stage 95–97), when the plant materials had an average moisture content of 23%. Stalks had higher moisture contents (31%) than heads (9%). Basal leaves were lying on the ground (dry), whereas stem- and branch-leaves remained on the plant stand (dry). In our analysis, all leaves were left out since they were dry and usually fell off during sampling. Hence, total dry biomass yield was estimated as the sum of stalk and head weights. Data of the final harvest are presented in Figs. 6.2.3 and 6.2.4 as average values per factor studied since no significant interactions were found between factors (*P*>0.05).

Irrigation had a significant effect on total dry biomass yield (*P*=0.009; 24% increase; Fig. 6.2.3a), and a paramount effect on the head weight (*P*<0.001; 43% increase, Fig. 6.2.3b), seed yield (*P*<0.001; 50% increase; Fig. 6.2.3c) and on seed harvest index (*P*<0.001; 34% increase; Fig. 6.2.3d). Similarly, N-supply significantly affected the above-mentioned parameters (15 to 46% increase) except for harvest index (Fig. 6.2.3). Not surprisingly, stalk biomass yield (stems plus branches) was unaffected by water (*P*=0.639) and nitrogen supply (*P*=0.183). This is because stalk formation and development ceased after growth stage 59 (approximately end of May). Thus the effects of water and nitrogen application were more pronounced in the reproductive biomass (Fig. 6.2.3b and c, 46% increase) rather than in the total biomass yield (Fig. 6.2.3a, 25% increase). Given that water application doubled seed yield (from I_1 = 1.4 to I_2 = 2.8 t ha^{-1}) and the overall seed/biomass ratio increased by 25% (Fig. 6.2.3d), it can be stated that the overall heating value of the crop was increased. Note that the heating value of the seeds is 26% higher than that of stalks (22.6 vs. 16.7 MJ kg^{-1}; Fernández *et al*., 2006; Grammelis *et al*., 2008).

Cynara's final productivities in the dry area of Velestino (2nd growth cycle) ranged from 12.8 to 17.5 t ha^{-1} (biomass) and from 1.4 to 2.8 t ha^{-1} (seed) for dry and wet plots, respectively. The lower final yields were obtained in the control plots (10.3 and 0.9 t ha^{-1}; for biomass and seed yield, respectively), and the higher final yields in the I_2-F_4 plots (20.1 and 3.4 t ha^{-1}; for biomass and seed yield, respectively). Such findings are in accordance with previous studies in this dry area (Danalatos *et al*., 2006a; 2007a), with many literature findings for dry sites (Fernández *et al*., 2005; Angelini *et al*., 2009; Raccuia & Melilli, 2007a; Ierna & Mauromicale, 2010) and values are 50% lower compared with yields obtained on aquic soils (see Chapters 3 and 6.1). This indicates that cynara's biomass yields obtained on aquic soils cannot be realized on dry soils, even when crops are appropriately managed (water and nitrogen supply).

Since water and nitrogen effects were more pronounced in the reproductive biomass (heads) and especially in seed yield, this study also provides a seed yield component analysis according to Eq. (3). Results indicated that supplemental irrigation increased the number of the seed-bearing heads by 20% (Fig. 6.2.4a) and the mean head weight by 26%

(Fig. 6.2.4b), while the effect of nitrogen was significant only on head number and not on mean head weight (Fig. 6.2.4). This is because μ is the ratio of weight (Fig. 6.2.3b) over the number (Fig. 6.2.4a) and since both increased with N-supply, μ remained constant and about 21.3 g head^{-1}. Usually μ varies from 13 to 40 g head^{-1} (see Chapter 3).

Nitrogen input – yield relations

Nitrogen–yield relations are presented in the form of a three-quadrant diagram (van Keulen, 1982). Fig. 6.2.5 consists of three graphs. Quadrant I depicts the N supply–yield relations. It shows that irrigation application increased the yield of the control crops by 22% ($I_1 = 10.3$ vs. $I_2 = 13.2$ t ha^{-1}), and thereafter for every additional kg nitrogen supplied, the yield increased by 21 and 31 kg ha^{-1} for the dry and wet crops, respectively (agronomic efficiency).

Quadrant II (N uptake – yield) shows that a strong proportional relation existed between biomass yield and N uptake, irrespective of water application (Fig. 6.2.5). A second order polynomial curve was fitted through the pooled data ($r^2 = 0.98$). At low N-uptake rates, the relation was linear; while as N-uptake increased, dry matter production per unit nitrogen uptake declined but a 'point of saturation' was not reached in the experimental data (Fig. 6.2.5). This is also observed in many crop species (van Keulen, 1982; Vos, 1997; 2009).

NUE for total biomass was somewhat higher for the dry compared to the wet crop (135 vs. 117 kg dm produced per kg N taken up) because dry crops are associated with lower N uptake rates (Fig. 6.2.5). The lower uptake rates were caused by the lower proportion of the nitrogen-rich seeds in the biomass. NUE progressively declined with an increase in N-supply (13–22% reduction at high N-levels compared to controls, Fig. 6.2.5). Our estimates (dry soil) are very close to what was found on an aquic soil (NUE = 100–128 kg kg^{-1} Archontoulis *et al.*, 2008a), lower compared with miscanthus (160–190 kg kg^{-1}) and sorghum (130–190 kg kg^{-1}), and similar compared with kenaf (117–144 kg kg^{-1}) and maize (97–111 kg kg^{-1}; Beale & Long, 1997; Danalatos *et al.*, 2007b; 2009; Cosentino *et al.*, 2007). The NUE for the seeds was relatively low (viz. 35 kg kg^{-1}) compared with total biomass because of the higher N concentration of the seeds (~3%) compared with the average biomass N concentration (~1%). This estimate for the cynara crop is close to the NUE for sunflower grains (33 kg kg^{-1}), higher compared with rapeseed (16–23 kg kg^{-1}) and considerably lower compared with maize kernels (66–76 kg kg^{-1}) and with wheat grains (53 kg kg^{-1}; Beale & Long, 1997; Danalatos *et al.*, 2009; Danalatos & Archontoulis, 2009).
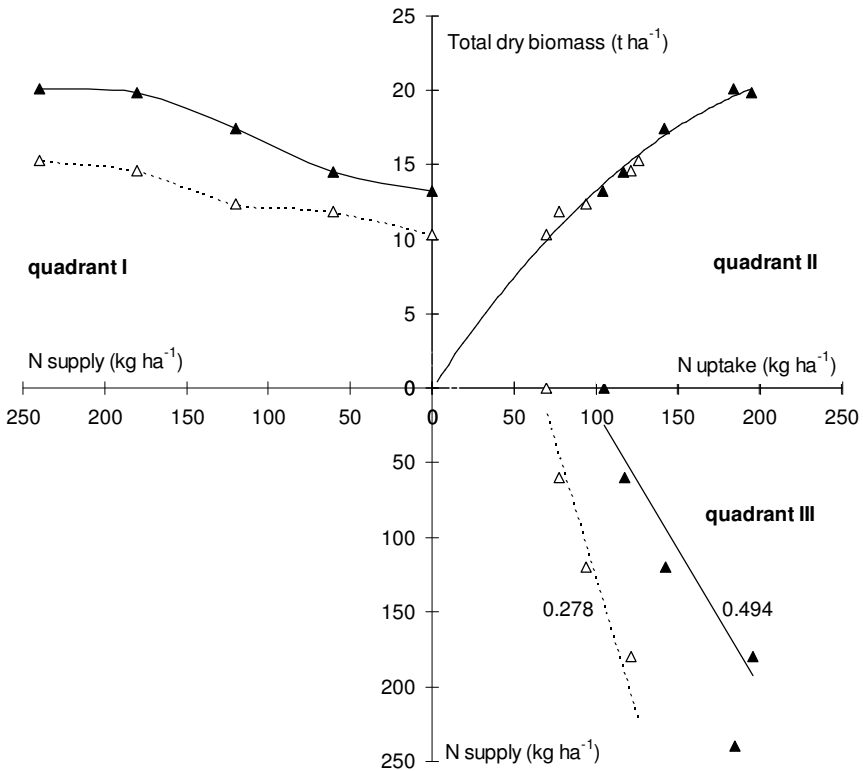
Figure 6.2.5: Three-quadrant diagram of *Cynara cardunculus* biomass production response to nitrogen application on a dry soil in central Greece (▲: irrigated and △: rainfed crops). In quadrant III, the slopes of the regression lines (recovery fraction of the applied fertilizers) are illustrated.

The relation between fertilizer application and total uptake by the crop is illustrated in quadrant III (Fig. 6.2.5). Linear regression analysis was performed to characterize this relation (up to maximum N uptake). The basic N uptake rate (intercept) was 65.4 and 95.2 kg N ha^{-1} for the dry and the wet plots, respectively. This parameter represents the inherent fertility of the studied soil, governed (a) by the quantity and quality of the organic matter present in the soil and (b) by the environmental conditions, notably soil temperature and soil moisture, which govern the rate of decomposition of the organic matter and the ultimate fate of the nitrogen mineralized or immobilized during this process (van Keulen, 1982). The efficiencies of the fertilizer (recovery fraction, Fig. 6.2.5) were estimated at 27.8% and 49.4% for the dry and wet plots, respectively ($r^2 > 0.92$), indicating clearly the important role of soil moisture on N-uptake. These estimates are very useful for proper calculations of nitrogen budgets in this environment.

However, the fertilizer efficiency is also dependent on the timing of N-application. In this study, N-supply took place during BBCH 50 (end of April), when the canopy was fully closed (LAI > 5). The efficiency of fertilization application at different growth stages (e.g. stage 1; considering practical matters) is still unknown. Thus, future studies should address this.

Conclusions

Irrigation and nitrogen application during inflorescence emergence stage (May), significantly increased final biomass (24%) and seed (46%) yields in a dry soil of central Greece. Irrigation played the most dominant role in this yield increase, because it expanded the growing period by two weeks and doubled crop growth rates in that site. Nitrogen effect was more evident at advanced growth stages, when seed growth created a strong sink for nitrogen. Cynara's nitrogen use efficiency was estimated at 125 kg dm kg^{-1} N, while the basic nitrogen uptake was ranged from 65 to 95 kg N ha^{-1} in that site. We concluded that even under appropriate management techniques, i.e. irrigation and nitrogen application at critical crop stages, cynara's biomass yields in Eastern Thessaly Plain (dry soils) can never reach the high biomass yields that obtained in aquic soils of Western Thessaly Plain, central Greece.

Chapter 6.3

Irrigation and N–fertilization effects on the growth and biomass productivity of sunflower growing in an aquic soil in central Greece

Abstract

Biomass and seed productivity of the new released sunflower hybrid "70–G–3920" in relation to irrigation and nitrogen fertilization were assessed in central Greece during 2006. Farm budgets and profitability of the sunflower cultivation were also estimated. A 3 (irrigation levels) × 3 (nitrogen levels) split-plot experiment (36 plots) was carried out on an aquic soil. The results demonstrated no significant effect ($P > 0.05$) of irrigation and nitrogen input on the growth and seed yield of sunflower, due to both shallow groundwater table and high fertility status of the soil. Sunflower biomass yields in fully irrigated/fertilized and control plots were 13.9 and 12.8 t ha^{-1}, respectively, while the harvest index was rather constant (0.34), resulting in final seed yields of 4.7 and 4.4 t ha^{-1}, respectively. Present findings (2006) suggest that cultivation of sunflower in this area is economically feasible and therefore a very good option for increasing county's biodiesel production, in line with the EU targets.

Introduction

Sunflower (*Helianthus annuus* L.) is one of the most important oilseed crops worldwide. In Greece sunflower is traditionally grown in the northern parts of Greece as rainfed crop with a seed yield of 1.5 t ha^{-1} (Kallivroussis *et al*., 2002). In central Greece sunflower was not cultivated over the last two decades because the cotton cultivations had a dominant role in this region (Thessaly Plain). However, after the adoption of Directive 2003/30/EC on the promotion of biofuels for transport, research on sunflower increased in order to identify the best genotypes and the best cultivation techniques for central Greek conditions. In literature, agronomic information on sunflower is generally rich (Connor *et al*., 1993; Villabolos *et al*., 1996; Rinaldi, 2001; Ruffo *et al*., 2002; Rinaldi *et al*., 2003; Albrizio & Steduto, 2005), but adaptability and productivity data for the specific soil-climatic conditions of central Greece are very few (Danalatos *et al*., 2005; Geronikolou *et al*., 2005). Such data are of high importance in order to design profitable sunflower cultivations in this region.

Cultivation of sunflower in central Greece and under new CAP conditions will be possible if farmers get similar or higher profits than the profits made now by the cotton, maize and alfalfa (traditional for the area) cultivations. Sunflower seeds are rich in nitrogen (~3.3% concentration), while irrigation application is very important for realizing adequate seed yields in Mediterranean environments (Zuibillaga *et al*., 2002; Goskoy *et al*., 2004). We hypothesized that sunflower cultivations on aquic fertile soils of central Greece could reach high seed yields under minimum input applications, and therefore it can provide a stimulus to Greek farmers to shift from cotton to sunflower cultivation in order to increase country's biodiesel production.

In this context, we assessed biomass and seed productivity of a recently released sunflower hybrid "70–G–3920" on an aquic soil in central Greece under different irrigation and nitrogen application inputs. Farm budgets were also constructed to investigate whether sunflower cultivation can be profitable in this region.

Materials and Methods

A field experiment was carried out in the Western Thessaly Plain (Palamas, central Greece; 39°25'N and 22°05'E, 107 m asl.) in 2006. The soil at the site was a deep, fertile, loamy soil, classified as Aquic Xerofluvent, due to the occurrence of shallow groundwater table (Table 6.3.1). The soil is a calcareous (pH=8.0–8.2) loam (sand 40–42%, silt 40–41%, clay 18–19%), and has an organic matter content of more than 1% at a depth of 50 cm. A 3×3 split-plot field experiment in four replicates (36 plots) was carried out, where the main factor comprised the three irrigation regimes (I_1= 0, I_2= 50 and I_3= 100% of ETm) and the sub-factor comprised the three nitrogen regimes (N_1= 0, N_2= 60 and N_3= 120 kg N ha^{-1}).

The crop was sown on May 18th, while herbicide- and basal fertilization application with 50 kg P ha^{-1} and 50 kg K ha^{-1} took place one day prior to sowing. N-fertilization was applied at the phenological stage V6 (three pairs of fully expanded leaves) according to the Schneiter & Miller (1981) phenological scale for sunflower. Irrigation was applied using an automatic drip irrigation system approximately every week, starting one month after crop emergence (Table 6.3.1, Fig. 6.3.1). The irrigation regimes were calculated based on maximum evapotranspiration (ETm), using sunflower crop specific coefficients and class-A pan evaporation rate. The amount of irrigation water applied and some other relevant phenological, agronomic and weather data are summarized in Table 6.3.1.

During the cropping cycle, six destructive harvests were conducted every 2–3 weeks on: 20th June, 3rd July, 16th July, 28th July, 17th August and 9th September 2006. Each time, the growth (plant height, number of leaves per plant, leaf area index, specific leaf area), and biomass production of leaves, stems, and storage organs were measured. At each manual harvest, the crop samples were divided into the various plant organs and weighed in the field. Leaf area (green leaves) was measured using an automatic LI−COR area meter (LI−3000A). Then the samples were oven-dried at 90°C until constant weights (2–3 days) and weighed again in order to determine the dry weights per plant component. Weather data such as radiation, air temperature, precipitation, air humidity, wind speed and class A-pan evaporation were recorded hourly by a fully automatic meteorological station which was installed at the borders of the experimental site. All datasets were subjected to analysis of variance (ANOVA) using GenStat (7th edition).

Table 6.3.1: Basic information regarding the sunflower cultivation in 2006

Date of 50% crop emergence	22 May 2006
Final harvest date	9 Sept 2006
Density of surviving plants (plants m[-2])	7.6 ± 0.1
Eo (A-class evaporation pan) (mm)	726
Estimated ETm (mm)	581
Effective rainfall (mm)	46
Maximum irrigation applied from 22/6 to 1/9/06 (mm)	394
Groundwater level at sowing (cm)[a]	190
Cumulative heat-units (°C days)[b]	2350

[a]: measured from a tube

[b]: Base temperature 4°C (Villalobos *et al.*, 1996)

Results

Weather parameters

Fig. 6.3.1 illustrates maximum and minimum air temperature and incident global radiation. The average daily temperature during the growing season was around 25 °C. June 2006 was somewhat cooler (–2.2 °C) compared to the long term climatic average (data not shown), due to the occurrence of some rainfalls that accompanied by days with heavy cloud cover. Mean incident global radiation during the cropping cycle was 24.7 MJ m^{-2} s^{-1}.
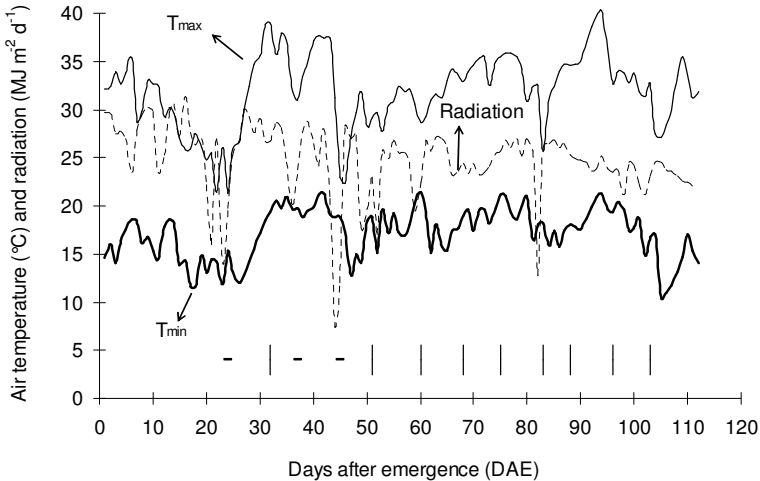
Figure 6.3.1: Daily air temperature and radiation during the experimental period. Vertical bars refer to time of irrigation, while dashes refer to time of precipitation (for amounts see Table 6.3.1).

Growth parameters

No significant interactions (irrigation × nitrogen) were observed for any of the measured or calculated variables (P>0.05). Sunflower plant height increased from crop emergence onwards with rates of 3.5 cm d^{-1}, reaching a final height of 210 cm during flowering irrespective of irrigation or nitrogen input (P> 0.05; data not shown). No significant effect of irrigation and N-fertilization on specific leaf area (SLA) was observed (P> 0.05). SLA was around 20 m^2 kg^{-1} until the beginning of flowering (53 DAE) and then it decreased gradually during seed feeling period to 15 m^2 kg^{-1} (data not shown).

The LAI increased rapidly from crop emergence upon flowering initiation to reach a maximum value of 3.5–4.1 m^2 m^{-2} (Fig. 6.3.2). Irrigation application affected significantly LAI (*P*< 0.05) after the flowering phase. The crop had a closed canopy (LAI >3) for 58 growing days (Fig. 6.3.2).
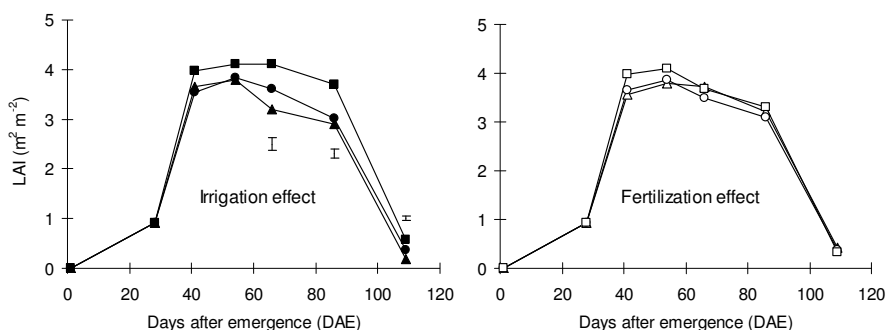
Figure 6.3.2: Time course of leaf area index (LAI) as affected by three irrigation (■: 100%, ●: 50% and ▲: 0% of ETm) and three N fertilization inputs (□: 120, ○: 60, and Δ: 0 kg N ha^{-1}) in central Greece in 2006. Vertical bars (LSD at *P*<0.05) when visible indicate significant differences among irrigation or N-fertilization treatments.

Biomass production

Irrigation and nitrogen fertilization application did not affect significantly (*P*>0.05) sunflower biomass production during the growing, despite the somewhat higher values found for the high-input treatments (viz. I_3 and N_3; Fig. 6.3.3). The crop showed high growth rates from V6 stage (3 pairs of leaves) until the end of anthesis (265 and 239 kg ha^{-1} d^{-1}; for full- and non-irrigated plants, respectively). During the seed filling period until maturity the crop increased with lower growth rates (~ 60 kg ha^{-1} d^{-1}), reaching a final biomass of 13.9, 12.9, 12.8 t ha^{-1} for I_3, I_2 and I_1 plants, respectively (Fig. 6.3.3). At the end of the growth cycle (crop ready for harvest: 9th September), the storage organs comprised on average the 48% of the total dry biomass, while the seed/head ratio on a dry basis was averaged 0.7 resulting in a seed harvest index of 0.34 (kg seeds kg total dry weight^{-1}) and seed yields of 4.69 and 4.41 t ha^{-1} for the irrigated and water/nitrogen stressed plants.
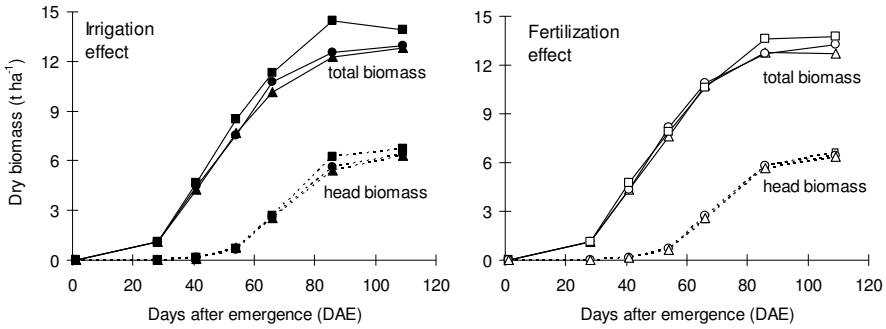
Figure 6.3.3: Time course of total dry and storage organ biomass as affected by irrigation (■: 100%, ●: 50% and ▲: 0% of ETm) and N-fertilization (□: 120, ○: 60, and Δ: 0 kg N ha^{-1}) in central Greece in 2006.

Biomass allocation

Since no differences were observed among treatments, the data were pooled to assess the biomass allocation to various plant components. This is illustrated in Fig. 6.3.4. At maturity (109 DAE; 2350 °Cd) storage organs (heads), stems and leaves (green and yellow) comprised 48, 36 and 16% of the total biomass respectively.
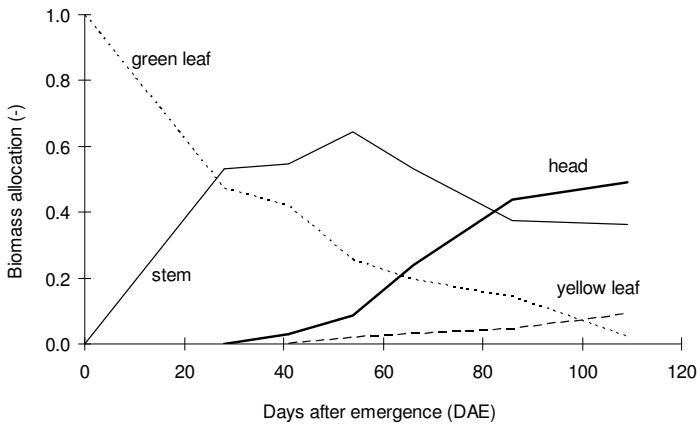
Figure 6.3.4: Biomass allocation to different plant components for the sunflower crop.

Production cost

Table 6.3.2 summarizes the production cost, gross margin and net farmer's income from a sunflower cultivation on an aquic soil under fully and water/nitrogen stress conditions. The total cultivation cost ranged from 400 until 600 € ha^{-1} depending on the management (full or no irrigation/nitrogen). Taking into account a selling price of 200 € t^{-1} for the sunflower seeds (2006), the net farmer's income was estimated at 345 and 470 € ha^{-1} under high and low input management practices.

Table 6.3.2: Farm budget of a sunflower cultivation in the experimental site of central Greece

Category	Unit	Potential	Limited
Field preparation including plowing, disc-harrowing, & sowing	€ ha^{-1}	190	190
Material supply including seeds, herbicide, and nutrients	€ ha^{-1}	110	50
Field management including weeding, irrigation, and harvest	€ ha^{-1}	300	160
Total cost	€ ha^{-1}	600	400
Total biomass yield	t ha^{-1}	13.9	12.8
Seed harvest index	kg kg^{-1}	0.34	0.34
Selling price	€ t^{-1}	200	200
Gross margin	€ ha^{-1}	945	870
Net income	€ ha^{-1}	345	470

Potential refers to I_3N_3 and limited to I_1N_1 treatment (see Materials and methods).
Subsidies are not taken into account.

Discussion

Growth

This study shows that a sunflower seed yield of 4.5 t ha^{-1} can be obtained on aquic soils of central Greece under minimum inputs of water and N-fertilization. The observed seed yield (hybrid: 70–G–3920) is comparable to yields found for other hybrids in that site (cf. Sanbro, Sanluka, Favorit, Peredovick, Panter, Turbo, and Golden Word; Danalatos *et al.*, 2005), and thus is recommended for biodiesel production. The observed yield is three times higher compared to sunflower yields obtained in northern Greece and is similar to those reported in literature under non-limiting growing conditions: 3.5–5 t ha^{-1} in Argentina (Zuibillaga *et al.*, 2002; Ruffo *et al.*, 2003), 4.1 t ha^{-1} in Turkey (Goskoy *et al.*, 2004) and 4.3–4.5 t ha^{-1} in Italy (Rinaldi *et al.*, 2001; Albrizio & Steduto, 2005). The observed harvest index was 0.34 irrespective of irrigation and nitrogen application, in line with other studies (Zuibillaga *et al.*, 2002; Ruffo *et al.*, 2003; Goskoy *et al.*, 2004).

Sunflower has an optimum temperature for growth of 28 °C (Villalobos *et al.*, 1996) and an optimum temperature for photosynthesis of 18–31 °C (Connor *et al.*, 1993). Thus

the high growth rates and yields obtained in central Greece can be explained by the favourable weather conditions (Fig. 6.3.1) and by the associated very high net assimilation rates of this genotype (35 μmol CO_2 m^{-2} s^{-1}; data not shown). The decrease of the crop growth rate from 250 to 60 kg ha^{-1} d^{-1} and of the crop light-use efficiency from 1.62 to 0.55 g MJ^{-1} intercepted light (data not shown) during the post-anthesis period is the consequence of higher carbon cost of lipids synthesis during seed-filling (Albrizio & Steduto, 2005).

The experimental site has shallow ground water table (Table 6.3.1), and this is the main reason for the small effects of irrigation on sunflower growth and yield in this area. In addition during that year rainfalls from March 1st to May 18th (sowing time) amounted 160 mm. We observed a slight LAI reduction in response to water availability (Fig. 6.3.2), but in all cases LAI was above the critical value of 2.89 m^2 m^{-2} that is required by sunflower in order to achieve maximum seed yields (Ruiz & Maddonni, 2006). Irrigation and N-fertilization application did not affect seed and biomass yields. This is probably explained by the high fertility status of the soil given also that during the previous 4 years this field was cultivated with cotton that had received excessive amounts of N fertilization. This study lacks analysis of N in various plant components, but it is believed that N fertilization rate of 60 kg ha^{-1} would suffice for adequate sunflower seed yields at this site. In literature there are several recommendations for N-fertilization in sunflower (from 40 to 190 kg N ha^{-1}; Zuibillaga *et al*., 2002; Lopez-Bellido *et al*., 2003).

Economic appraisal

Earlier studies at this site indicated that sunflower has an energy output : input ratio of 7.36:1 (Geronikolou *et al*., 2005), which is almost double compared to the 4.5:1 reported for northern Greece (Kallivrousis *et al*., 2002; using the same methodology). In terms of net return, sunflower cultivation for biodiesel production today (2006/2007) could provide to the farmer a net income of 345 to 470 € ha^{-1} (excluding subsidies). This profit is lower compared to profits made from the cotton cultivations in this area. Assuming a higher selling price of 250 € t^{-1}, the net farmer profit would be 580–688 € ha^{-1}, approaching the profits made by cultivating cotton. Presently, there is an uncertainty regarding oil, materials and end-product selling prices. This means that sunflower cultivation can be considered as a good alternative to traditional cotton, maize and alfalfa cultivations for this region. Supplementary, sunflower stems (viz. 38% of the total dry biomass; Fig. 6.3.4) can be used for solid biofuel production, in view of increasing farmer profitability.

Since sunflower seed yields had been stabilized in that area at about 4.5 t ha^{-1} for a number of hybrids (Danalatos *et al*., 2005), different cropping strategies should be designed to increase farmer profitability. For example, sowing sunflower during March to mid-April (very early sowing), the crop can make better use of the spring rainfalls, thus it can further reduce production costs. In Italy, Rinaldi (2001) investigated this scenario using a simulation model and found that early sowing is more profitable than a

late one in terms of yielding potential and net returns (1300 vs. 400 € ha^{-1}). A second strategy could be a very late sunflower planting just after wheat harvesting in the same field for a supplementary income. These hypotheses should be tested in further studies in central Greece.

Concluding remarks

The newly released sunflower hybrid gave very high seed yield (4.5 t ha^{-1}), even under minimum nitrogen input and little supplemental irrigation. Given the obligation to use biodiesel at rates of 2% (in 2006) – 6% (in 2010) of the annual diesel consumption at national level, sunflower cultivation in Western Thessaly Plain (central Greece) is highly recommended.

Chapter 6.4

Irrigation effects on the growth and biomass productivity of two kenaf genotypes growing in an aquic soil in central Greece

Abstract

The effects of varying irrigation supply on growth and biomass productivity of two kenaf genotypes (Tainung 2 and Everglades 41) were investigated in an aquic soil of central Greece in 2006. On May 18th, the crops were planted at 75 cm row-to-row distances (plant density of 13.5 pl. m^{-2}). During the growing period, plant height, leaf area index (LAI), specific leaf area (SLA) and biomass productivity per plant component were measured or calculated. We found a significant effect ($P<0.05$) of irrigation on total dry biomass and plant height, although the absolute differences among treatments were relatively small (10–20%). Cv. Tainung 2 showed slightly higher values for the assessed parameters, compared to Everglades 41. On average, the crop reached a height of 3.9 m, a maximum LAI of 7.5 m^2 m^{-2}, while SLA fluctuated around 18.5 m^2 kg^{-1} for a large part of the growing period. The crop reached maximum biomass yields of 19.6, 22.8 and 24.5 t ha^{-1} under no-, moderate- and full irrigation regimes, respectively. These yields are among the highest that have ever been recorded under Mediterranean conditions.

Introduction

Kenaf (*Hibiscus cannabinus* L.,) is a warm-season annual C_3 fibre crop that can be cultivated for various purposes, including textile, paper pulp, building materials, substrates and bioenergy. In 2003, a European Network was established, BioKenaf, aiming to study kenaf adaptability, productivity and market potential in south Europe (Alexopoulou *et al*., 2005). In this project, kenaf's biomass productivity was investigated in different experimental sites (cf. Greece, Italy, Spain, Portugal, France) following the same experimental protocols. Results over the period 2003 to 2005 demonstrated high biomass yields up to 22 t ha^{-1} in Greece (Danalatos *et al*., 2006b).

Among cultivars tested, Tainung 2 and Everglades 41 (late-mature) showed the highest yields in the Mediterranean region (Alexopoulou *et al*., 2005). Between these two cultivars there are noticeable differences in leaf morphology, but no differences in photosynthesis and respiration (Archontoulis *et al*., 2006a, b). Both cultivars are short-day plants; flowering did not occur above a critical photoperiod of 12.9 h (Carberry *et al*., 1992).

According to BioKenaf experimental protocol, all kenaf varieties were planted at a row-to-row distance of 50 cm. In central Greece, this sowing distance implies mechanical constraints (e.g. sowing, weeding and/or harvesting machines) because the traditional maize and cotton crops are sown at 75 and 95 cm row-to-row distance, respectively. Therefore our first objective was to investigate the growth and biomass productivity of the cv. Tainung 2 and Everglades 41 at row-to-row distance of 75 cm, similar to that of maize to assist crop mechanization. The second objective was to investigate water deficit effects on Everglades 41, as the response of this cultivar to irrigation had not been studied so far in BioKenaf project.

Material and Methods

A field experiment was carried out in central Greece (Palamas, 39°25′ N and 22°05′E, 107 m asl) in 2006. The soil at the site was a deep, fertile, loamy soil, classified as Aquic Xerofluvent, due to the occurrence of shallow groundwater table (Table 6.4.1). The soil is calcareous (pH=8.0−8.2) loam (sand 40−42%, silt 40−41%, clay 18−19%), and has an organic matter content of more than 1% at a depth of 50 cm. A 3×2 split–plot design was used in five replications (30 plots) with the main plots comprising the three irrigation treatments (I_1=0, I_2=50, and I_3=100% of the ETm), and the subplots comprising the two cultivars (E41 = Everglades 41 and T2 = Tainung 2).

The crop was sown on May 18th at distances of 0.75 m between the rows and 0.083 m within the rows (or 16 plants m^{-2}). Herbicides and basal fertilizer (50 kg P

ha^{-1} and 50 kg K ha^{-1}) were applied one day prior to sowing; N–fertilizer (60 kg N ha^{-1}) was applied at the onset of the basic vegetative phase (plant height ≈ 0.5 m). Irrigation applied by a drip irrigation system to ensure high accuracy of water inputs. The quantity of water applications was determined by the maximum evapotranspiration (ETm). The plants were irrigated every 6–7 days (about 50–60 mm per application in I_3 treatment). The total amount of irrigation water and some other relevant agronomic and weather data are summarized in Table 6.4.1.

Table 6.4.1: Basic information regarding the kenaf cultivation in 2006

Date of 50% emergence	22 May 2006
Date of 50% flowering	17 October 2006
Density of survived plants (plants m^{-2})	13.5 ± 0.2
Mean air temperature (°C)	23.29
Mean relative humidity (%)	65.01
Mean wind speed (m s^{-1})	1.38
Maximum irrigation applied from 22/6 to 12/9/06 (mm)	482
Estimated ETm (mm)	408
Eo (A-class evaporation pan) (mm)	470
Effective rainfall (mm)	
Emergence to September	49
September to flowering	210
Ground water level (cm) [a]	
Upon sowing	190
At flowering	405

[a]: measured in a tube denoting that the real ground water level was much higher in the soil.

Plant height, number of nodes per plant, specific leaf area (SLA), leaf area index (LAI) and dry biomass productivity per plant component were measured in throughout the growing period, i.e. on the dates 20–Jun; 3–Jul; 28–Jul; 14–Aug; 1–Sept; 2–Oct and 28–Oct–2006. In each manual harvest, the sample was divided into the various plant organs and weighed in the field. Then the samples were oven-dried at 90 °C until equal weights (2–4 days) and weighed again in order to determinate the dry weights per plant component. Leaf area (green leaves) was measured using an automatic LI–COR area meter (LI–3000A). All measured and derived data were subjected to analysis of variance (ANOVA), using GenStat (7th edition). Weather data were recorded hourly by an automatic meteorological station, which had been installed at the borders of the experimental site at 2 m height.

Results and Discussion

Weather conditions

In general the study area is characterized by a typical Mediterranean climate with hot, dry summers and cool, humid winters. During the summer period (June–August), the air temperature fluctuated between 18 °C (night) and 32 °C (day-time), whereas only 50 mm of precipitation was recorded (see also Fig. 6.3.1). Contrary to previous experimental years (cf. Danalatos & Archontoulis, 2004; 2005), the autumn in 2006 was surprisingly wet (Table 6.4.1), reflecting well year-to-year variability. The sharp decrease in the air temperature during September (by 5.8 °C; data not shown) and the high precipitation (Table 6.4.1) greatly influenced kenaf phenology, growth and biomass production (see below).

Table 6.4.2: Kenaf plant height (cm) over time as affected by treatments in 2006. No significant interaction between irrigation and cultivar on plant height was found ($P>0.05$)

	3 July	28 July	14 August	1 September	2 October	28 October
Irrigation effect						
I_1	102a	176a	215a	234a	314a	330a
I_2	102a	186b	230b	247a	352b	371b
I_3	102a	189b	237b	272b	382c	393b
Cultivar effect						
E41	97a	178a	217a	242a	342a	350a
T2	106b	189b	237b	260b	356b	379b

For symbol explanation see Materials and methods.
Different letters within a factor and within a day indicate significant differences at $P<0.05$

Growth characteristics

No irrigation × cultivar interactions were observed for any of the measured or estimated growth characteristics ($P>0.05$). The results demonstrated a significant effect of irrigation ($P<0.05$) on plant height, with the I_3-irrigated plants to reach higher rates of increase (3.5 cm d^{-1}; Table 6.4.2) than the water stressed plants. Also, T2 reached at higher plant height that E41 did (Table 6.4.2). Kenaf reached on average a plant height of 250 cm at the end of the basic vegetative phase and at the onset of the photoperiod induced phase (see sun-duration ≈ 11.8 h; 1st decade of September). From then on, and due to intensive rain (Table 6.4.1) that occurred at the site, the crop postponed the transition to the next phenological stage (viz. reproductive growth) and continued growing at high rates (3.4 cm d^{-1}; Table 6.4.2). The crops reached final plant heights during flowering of 395 and 330 cm, for full– and non– irrigated treatments, respectively (Table 6.4.2).

Plotting the total number of nodes per plant and the nodes per plant without leaves (hereafter "dead") against plant height, a good fit was observed with high determination coefficients, viz. r^2= 0.946 and 0.931, respectively (Fig. 6.4.1). Note that one node can produce more than one leaf and that the node production ends at flowering time. The final number of nodes per plant was higher compared to other experiments at higher plant densities (Danalatos & Archontoulis, 2004; 2005). This is also in line with earlier findings (Carberry *et al.*, 1992).
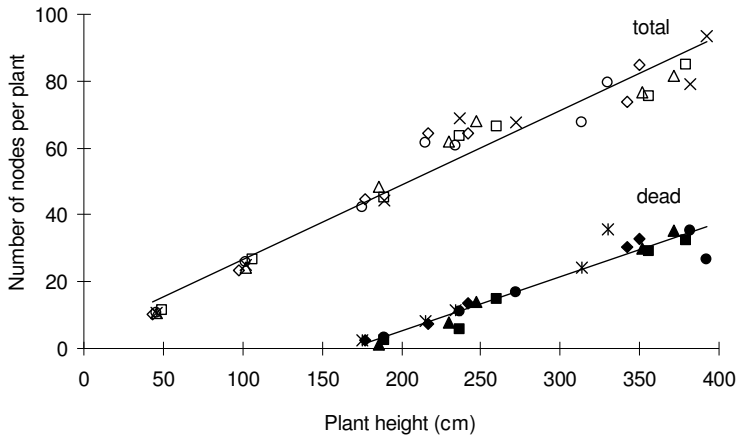
Figure 6.4.1: Total number of nodes per plant (open symbols) and number of nodes without petioles and leaves (full symbols; "dead") as a function of plant height. The regression lines are: total: y=0.23.9·x, r^2=0.946; dead: y=0.162·x − 27.27, r^2=0.932. Different symbols refer to different treatments (irrigation × cultivar).

Fig. 6.4.1 depicts clearly that the littering of the shaded leaves started when the plant reached a height of ~170 cm (usually 1st decade of August). The total node production rate is 1 node per 5 cm. Beyond 170 cm in height, the rate of increase of the number of dead nodes is 1 node per 6.25 cm, meaning that the net gain in node production rate after the critical plant height is 1 new node per 12.5 cm (Fig. 6.4.1). This analysis is useful when simulating kenaf leaf area developments (e.g. see approach developed by Carberry & Muchow, 1992). Furthermore, the littering of the shaded leaves had no impact on LAI (Fig. 6.4.2) as LAI remained high (above 4).

After a temporary initial lag period of about one month (root development), LAI increased rapidly over time (Fig. 6.4.2). Slight differences among *I*–inputs did exist but were not statistically significant. T2 produced somewhat higher LAI values than E41 but this difference was not consistently significant (Fig. 6.4.2). LAI reached values of 4.9, 5.3, and 6.1 for I_1, I_2, I_3 plants, respectively, at the end of August (Fig. 6.4.2).
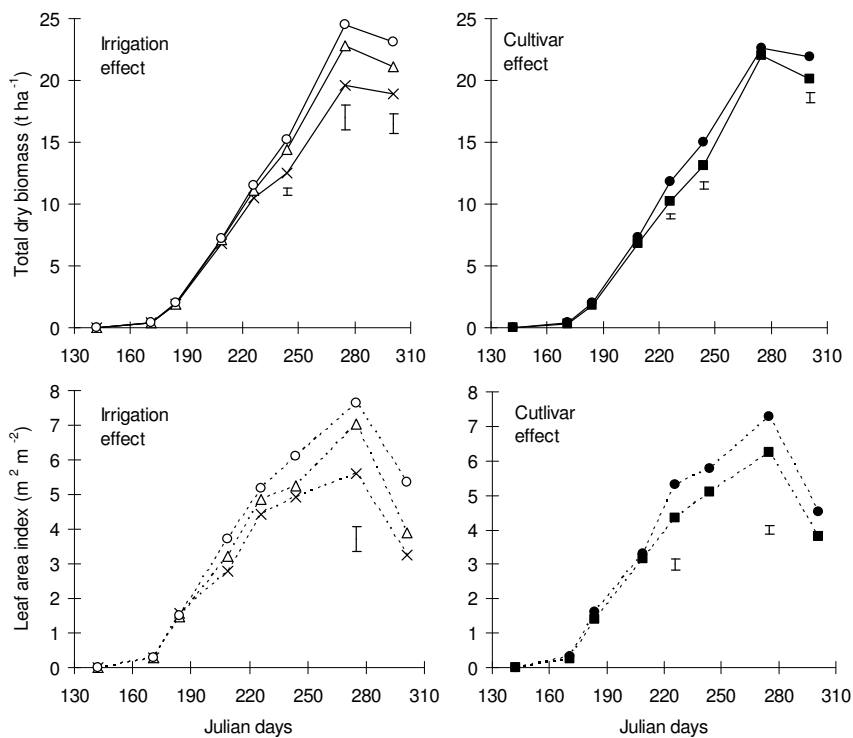
Figure 6.4.2: Total dry biomass (—) and leaf area index (- - -) as affected by three irrigation inputs (○: 100%, Δ: 50% and ×: 0% of ETm) and by two cultivars (■: Everglades 41, ●: Tainung 2). Within a panel, vertical bars (LSD at *P*<0.05) when visible indicate significant differences among irrigation inputs or between cultivars.
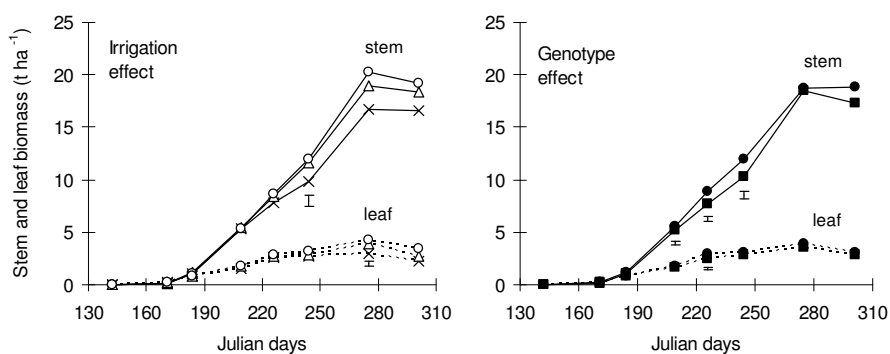
Figure 6.4.3: Stem (—) and leaf (-----) dry biomass as affected by three irrigation regimes (○: 100%, Δ: 50% and ×: 0% of ETm) and by two cultivars (■: Everglades 41, ●: Tainung 2). Within a panel, vertical bars (LSD at *P*<0.05) when visible indicate significant differences among irrigation inputs or between cultivars.

172

These LAI values were considered being maximum based on previous findings at the same site (Danalatos & Archontoulis, 2004; 2005). In contrast to our expectations, LAI increased further in September reaching values close to 7.5, most probably due to the effective rains falling at that time (Table 6.4.1). Specific leaf area index (SLA) remained close to 18.5 m^2 kg^{-1} for a large part of the growing season (June-August; data not shown) in all treatments ($P>0.05$).

Biomass production

As illustrated in Fig. 6.4.2, the growth and total biomass productivity were partially influenced by irrigation ($P<0.05$) with the I_3 plants to reach maximum growth rates of 254 kg ha^{-1} d^{-1} (from 209 to 226 JD) and 292 kg ha^{-1} d^{-1} (from 244 to 275 JD). Maximum yields were observed during flowering and were 19.6, 22.8 and 24.5 t ha^{-1} for I_1, I_2, I_3 plants, respectively. At flowering, stems comprised 83% of the total biomass (including petioles) and the leaves the remaining 17%. (Fig. 6.4.3). Stem and leaves dry weights were slightly affected by the different irrigation regimes but not statistically significant for the whole growing period (Figs. 6.4.2, 6.4.3). Significantly higher yield was found for the T2 than for E41 ($P<0.05$; Figs. 6.4.2, 6.4.3) with respect to total and stem dry weight. This might be attributed to the differences in the leaf shape between the two cultivars that allows light to penetrate deeper into T2 canopy than in E41. No differential response in leaf mass was obtained between the two genotypes ($P>0.05$; Fig. 6.4.3).

These biomass yields obtained in 2006 (Fig. 6.4.2) are among the highest that have ever been reported for the Mediterranean region (Manzanares *et al*., 1997; Quaranta *et al*., 2000; Alexopoulou *et al*., 2005). Based on previous results (Danalatos *et al*., 2006b), maximum yield under non-limited conditions at this site (Palamas) was 18–22 t ha^{-1}, whereas precipitation from September till 50% flowering was 32, 87, and 5 mm, for 2003, 2004 and 2005, respectively. In central Greece, the day length decreases substantially during September, and the crop responds qualitatively to the shortening days. Indeed flowering initiation was recorded at September 9th, but the duration of the flowering period was expanded to 38 days contrary to 25 days in previous years (Danalatos *et al*., 2006b).

The remarkable growth rates that were observed during September (average: 268 kg ha^{-1} d^{-1}) and the continuation of biomass accumulation by about 8 t ha^{-1} (average) are surprisingly high, considering the advanced development stage (Fig. 6.4.2). Calculating the relative growth rate (RGR) for this time period, it was found that the increase expressed per unit plant mass was relatively constant at 11 g kg^{-1} d^{-1} (Fig. 6.4.4).

Dissecting RGR into its components, it was found that this high growth rate was mainly attributed to the increase in the net assimilation rate (Fig. 6.4.4). This might have occurred due to a decrease in temperature (viz. from 26°C to 20°C) and in vapour pressure deficit, denoting lower C losses and higher C gain, through reduced respiration (dark and light mitochondrial respiration) and the absence of photosynthesis mid-day depression (Archontoulis *et al.*, 2006a, b). Temperature mostly affects the carbon losses, while the decrease in leaf to air vapour pressure deficit has an effect on the net carbon gain, due to absence of mid-day depression of the photosynthetic apparatus (Archontoulis *et al.*, 2006a). Amount and duration of sunlight decreased as well from August to September by about 32% (amount) and 2 h (duration), respectively, but they are considered adequate to obtain high assimilation rates.
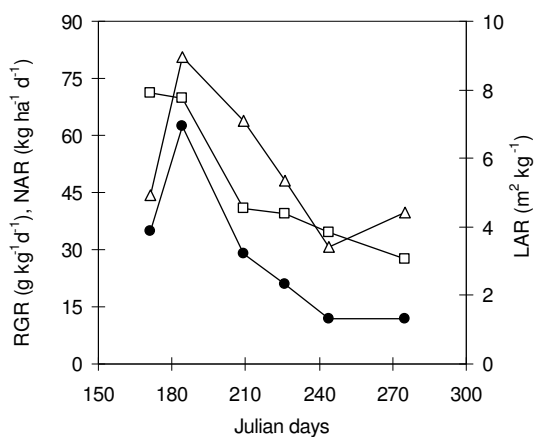
Figure 6.4.4: Relative growth rate (RGR, ●, left y-axis), Net assimilation rate (NAR, Δ, left y-axis) and Leaf area ratio (LAR, □, right y-axis) average values of all treatments (irrigation × cultivar) over the growing season of 2006 in central Greece.

On-farm yield

After completion of flowering, the biomass yield decreased (litter of leaves) irrespective of the various treatments, reaching an average value of ~21 t ha^{-1} at the end of October (Fig. 6.4.2) with ~75% plant moisture content. Two months later, the plant moisture content decreased further, while the on-farm yield harvested with a (maize) chopping machine was 15.4 t dry matter ha^{-1} (average values). The further decrease (27%) in biomass within these two months was attributed to: (i) the littering of the leaves; (ii) the stem maintenance respiration and (iii) the cutting height of the commercial machine (i.e. 25–35 cm above ground instead of 0–5 cm in the manual harvest).

Concluding remarks

This study confirms the high potential of the kenaf in central Greece and generally in the Mediterranean region. The present results of 2006 contribute significantly to the BioKenaf database due to peculiarity in the amount of precipitation that occurred during September and also due to the change in the plant arrangements. Cultivar Everglades 41 showed slightly lower yields, compared to cultivar Tainung 2. With respect to irrigation application, we believe that capillary rise in the studied soil strongly influenced yield and minimized the difference among different irrigation inputs. Lower plant density (13.5 instead of 18–28 pl. m^{-2}) due to longer row spacing distance (0.75 instead of 0.5 m) did not influence biomass productivity, denoting that kenaf can undertake a wide range of plant population densities without any yield costs.

Chapter 7

General discussion

Abstract

In Chapter 1 of this thesis it was argued that the acreage of energy crops is going to expand to meet the increasing demands for bioenergy and that there is a lack of experience and strong data to support this sector. In this context, we focused on biomass production aspects and we performed leaf–canopy–crop level studies to enhance our understanding and to support future cropping strategies for three Mediterranean bioenergy crops: sunflower, kenaf and cynara (Chapters 2–5). We also carried out agronomic research for inferences on the practicality of biomass production in Greece (Chapter 6). This Chapter 7 broadens the discussion of preceding chapters to the overall achievements and to issues that are related to the suitability of the tested crops. The following issues are discussed: (1) advances made in crop physiology; (2) agronomic aspects; (3) implication for crop modelling; and (4) future of the tested crops in the Mediterranean region.

Advances made in crop physiology

This section of the general discussion focuses on quantification of light interception by the canopy and on vertical distributions of light and nitrogen within canopies. It argues that leaf photosynthesis and respiration are central for modelling the crops and for interpreting biomass production in response to genotype × management × environment interactions.

Light interception, and light and nitrogen canopy profiles

Canopy light interception (= radiation × $1-\exp^{-(LAI \times K_L)}$) is fundamental for calculating canopy photosynthesis or radiation use efficiency (amount of dry matter produced per unit of light intercepted; Monteith, 1977), and therefore for assessments of crop productivity. Obviously, knowledge of K_L (the light extinction coefficient) is very important. This study brings new information on K_L for three bioenergy crops, paying particular attention to the effects of water stress – the major agricultural concern in the Mediterranean region (Katerji *et al*., 2008) – and to the effects of crop age and time of year (Chapter 4).

In general, K_L is affected by several factors including canopy structure and solar position, but also by the methodology through which it is assessed (Johnson *et al*., 2010). For instance, canopy structure might be affected by crop age (change in LAI; e.g. Zaffaroni & Schneiter, 1989; Lizaso *et al*., 2003), leaf thickness which affects light transitivity (Thornley, 2002), plant arrangement (e.g. Flénet *et al*. 1996; Maddonni *et al*., 2001), water and nitrogen availability (e.g. Sadras *et al*., 1991; Muchow, 1992), genotype (e.g. Madakadze *et al*., 1998), and growing environments (e.g. Rosenthal & Gerik, 1991; Kiniry *et al*., 1999). Also, K_L has been reported to change with daytime, day of year, location and solar beam direct/diffuse composition (Clegg *et al*., 1974; Sadras *et al*., 1991; Goudriaan & van Laar, 1994; Flénet *et al*., 1996; Anten, 1997; Sinclair, 2006; Evers *et al*., 2009).

For determining K_L, laborious and time consuming measurements are required and this explains why earlier studies on modelling used literature values of related species and why indirect approaches were developed for its assessment (e.g. leaf angle, plant geometry; Goudriaan, 1998; Sinoquet *et al*., 2000; Rosati *et al*., 2001; Pronk *et al*., 2003; Wang *et al*., 2007). In this study we used the traditional direct approach to derive K_L (Beer's law; Monsi and Saeki, 2005), but instead of measuring light penetration at different crop stages or at different crop heights at only one development stage, we applied a combined experimental protocol similar to Bertheloot *et al*. (2008).

It is commonly assumed in crop modelling that K_L does not change in relation to time or level of input of resources for growth. When we tested these assumptions, we found that under irrigated conditions K_L slightly changed over

time (P>0.05) but under water stress conditions K_L was always lower than under irrigated conditions and moreover decreased to even lower values as water stress prolonged (Fig. 4.4). Our findings and generalizations for sunflower and kenaf species (petiole-leaves) are not applicable to cereal crops (stem-leaves).

Another objective of this thesis was to estimate the nitrogen extinction coefficient (K_N). In general, K_N is less researched than the K_L parameter because it finds application in only a few crop models (e.g. GECROS). However, it is a significant parameter when leaf photosynthesis is related to leaf nitrogen (leaf anatomy × nitrogen availability; see Chapter 5) and when detailed methodologies are applied to scale up photosynthetic CO_2 fluxes from leaf to canopy levels (Leuning *et al.*, 1995; Anten, 1997; de Pury & Farquhar, 1997). In all crops studied, we found non-uniform distributions of leaf nitrogen within crop canopies only when LAI was ≥1.5 (Fig. 4.5) and that was particularly evident during mid-season. The highest values were always at the top (2.2–3.8 g N m^{-2}; Fig. 4.7g, h and i) and the lowest at the bottom of the canopy (around 1.0 g N m^{-2}); showing also that nitrogen distribution is somehow related to the light distribution (r^2>0.66; Fig. 4.8). However, observed leaf nitrogen extinction was less steep than the one that would maximize canopy photosynthesis ($K_N < K_L$), in line with many studies (e.g. Hirose & Werger, 1987; Anten *et al.*, 1995; Bertheloot *et al.*, 2008).

Leaf photosynthesis and respiration

Generally leaf-level studies (gas exchange rates) for energy crops are rare. For the species studied, some information existed for sunflower (e.g. Connor *et al.*, 1993), little for kenaf (Muchow, 1990; Ramachandra Reddy & Ramma Das, 2000; Cosentino *et al.*, 2004; Archontoulis et al., 2005, 2006a, 2006b) and none for cynara. Chapter 5 of this thesis fills this knowledge gap by providing comprehensive gas exchange data and analysis for sunflower, kenaf and cynara. The photosynthetic data were analyzed using the biochemical model of Farquhar, von Caemmerer & Berry (the FvCB model) for two reasons. Firstly, this model represents mechanistically the effects of elevated CO_2 and has the potential to accurately represent the effect of elevated temperature on photosynthesis and thus can easily assist studies on climate change (Yin & Struik, 2010). Secondly, the model provides understanding of the factors limiting photosynthesis (V_{cmax}, J_{max}, R_d). Although FvCB parameters are required by very detailed crop models (e.g., GECROS; Yin & van Laar, 2005), present findings can also feed simpler crop models such as SUCROS (Goudriaan & van Laar, 1994).

In this thesis the effects of CO_2 (at stomata cavity), irradiance, temperature and leaf nitrogen content on net assimilation rate were successfully quantified (r^2>0.91; Table 5.3; Fig. 5.10). Thus photosynthesis can be predicted under a wide range of climatic and management conditions. Impact of management was

reflected here by the leaf nitrogen content as this input parameter reflects well leaf dynamics (leaf age, rank; see Chapter 4). However, to further increase prediction of the present models and their application for practical purposes, new algorithms for CO_2 transfer resistance from atmosphere to stomatal cavity and/or to chloroplast level (e.g., Yin & Struik, 2009a) should be evaluated in the near future. The same holds for functions relating biochemical parameters to leaf water potential (e.g. Vico & Porporato, 2008).

An innovation of this thesis is that the FvCB model was parameterized from light response curves and not from CO_2 response curves as is common (e.g. Wise *et al.*, 2004; Yamori *et al.*, 2005). Although this perhaps is a matter of debate, earlier studies showed no apparent differences in model behaviour parameterized either from A_n–I_{inc} or A_n–C_i data (Niinements & Tenhunen, 1997; Wohlfahrt *et al.*, 1998). In addition, our approach bypasses current concerns about the appropriate method of fitting A_n–C_i curves (Ethier *et al.*, 2004; Sharkey *et al.*, 2007; Miao *et al.*, 2009; Patrick *et al.*, 2009; Su *et al.*, 2009; Gu *et al.*, 2010) and provides opportunities to reduce empiricism in crop models which is strongly needed (Müller *et al.*, 2005; Yin & Struik, 2010). Currently, most of the crop models use empirical algorithms to calculate leaf photosynthesis (van Ittersum *et al.*, 2003) and it is uncertain whether they can accurately predict the effect of climate change on crop production (Yin & Struik, 2009a). Our study provides an alternative means to derive such parameters from A_n–I_{inc} data that are widely available and commonly used in crop modelling.

A second innovation of this thesis is that it (among very few other studies) provided direct night time respiration measurements, underlying the high importance of respiration in carbon budgets (Valentini *et al.*, 2000). Moreover assumptions regarding the quantification of night respiration (R_n) and its discrimination from the day respiration (R_d) were assessed in Chapter 5. For instance, R_d is commonly fixed as 1% of V_{cmax} (Müller *et al.*, 2005; Niinemets & Tenhunen, 1997; de Pury & Farquhar, 1997; Medlyn *et al.*, 2002) or as 50% of R_n (Braune *et al.*, 2009; Wohlfahrt *et al.*, 1998; Yamori *et al.*, 2005; Kosugi *et al.*, 2003). In this study the ratio of R_d/V_{cmax} ranged from 0.57 to 1.03% (Table 5.3) and the ratio of R_d/R_n was approximately 72% for all tested crops (Fig. 5.5).

Insights in agronomic aspects

In this section biomass and seed yields obtained at the experimental site are discussed. Data accumulated during the experimental period (note: only a fraction of the available data is presented in this thesis) were combined with previous findings obtained at the same site, in order to arrive at a solid assessment of sunflower, kenaf and cynara productivity in central Greece (see Fig.

7.1). Biomass yields are explained in the light of new findings in crop physiology (Chapters 4 and 5).
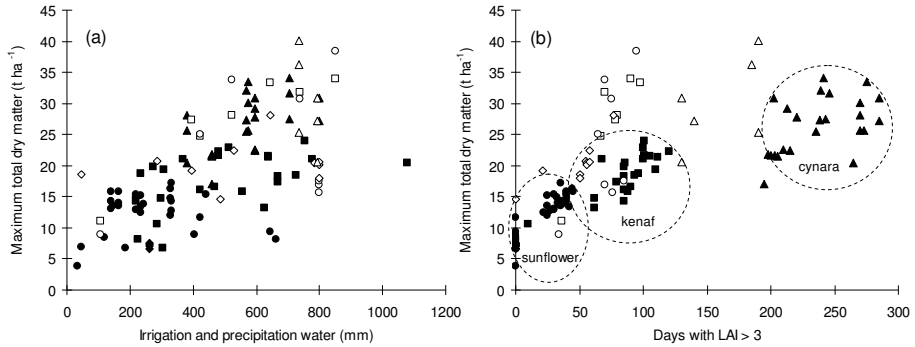
Figure 7.1: Maximum total dry biomass weight in relation to (a) total irrigation and precipitation water received during crop growth and (b) days with LAI > 3 for sunflower (●), kenaf (■), cynara (▲), rapeseed (♦), fibre sorghum (□), sweet sorghum (○), miscanthus (Δ), and maize (◊) crops grown in two experimental sites located in central Greece over the last decade (adapted from Archontoulis *et al.*, 2011b). Y-axis values refer to aboveground maximum total biomass including leaves, stalks and reproductive organs obtained during the growth cycle and not to biomass yield at the final harvest. This is because kenaf and other species, i.e. sorghum and miscanthus, do not reach physiological maturity in central Greece. Each set of data (n=112) refers to a specific combination of crop, genotype, plant density, sowing date, year of cultivation, location (soils with and without groundwater level), fertilization and irrigation input (for further details see Archontoulis *et al.*, 2011b). In panel b, rainwater (% of total water) comprised 85–100% for cynara and 25–35% for sunflower and kenaf. Data on rapeseed and C4 sorghum, maize and miscanthus are also given for comparison. For the perennials cynara and miscanthus yields beyond the second growth cycle were considered. For kenaf maximum productivities were observed during flowering.

Biomass and seed yields for cynara

The range of cynara final biomass yields found in this thesis (5–34 t ha^{-1} y^{-1}; Fig. 3.6) agrees well with reports from Italy (Foti *et al.*, 1999, Piscioneri *et al.*, 2000; Raccuia & Melilli, 2007a; Angelini *et al.*, 2009; Mandineo *et al.*, 2009; Ierna & Mauromicale, 2010), Spain (Fernández *et al.*, 2006 and references therein), and Portugal (Gominho *et al.*, 2011 and references therein). According to Fernández *et al.* (2006) the threshold precipitation and/or irrigation amount required by cynara to attain satisfactory yields (>15 t ha^{-1} y^{-1}) is 400 mm per season. In central Greece,

this amount ranged from 400 to 800 mm per season (Fig. 7.1a). Many of our experiments were carried out on aquic soils (Chapter 3), with large quantities of available water and this explains well the observed high biomass yields (Figs. 3.6 and 7.1). For instance, the importance of soil type (aquic vs. dry) on growth and biomass productivity of cynara was analyzed in Chapters 6.1 and 6.2.

Analyzing the factors determining biomass productivity, it was found that under appropriate management techniques (including crop establishment at high plant density; Chapter 3), cynara was able to maintain LAI values above 3 for most of its growth cycle (~250 days; Fig. 7.1b). Given also its high leaf photosynthetic capacity (~30 μmol CO_2 m^{-2} s^{-1}; Chapter 5) and its non-uniform distribution of leaf nitrogen that approaches the distribution of light within the crop canopy (Chapter 4), the crop was able to establish very high crop growth rates up to 320 kg ha^{-1} d^{-1} (Chapter 6.1 and Archontoulis *et al.*, 2011b). So far, there was no study to provide such crop physiological information to explain yield formation in cynara; most previous analyses were based on regressions of empirical yield vs. water (e.g. Fernández *et al.*, 2009).

Among factors affecting biomass productivity, three are considered most important for cynara: (1) adequate crop establishment at high plant density, (2) irrigation, and (3) nutrient supply. Higher plant densities not only help the crop to efficiently overcome initial competition with weeds (see Chapter 2 growth stages), but also, when soil fertility is sufficient, the crop can maintain more plants per unit area, increasing the seed/biomass ratio and the overall heating value of the crop biomass (see Chapter 3). Regarding irrigation and nitrogen fertilization, this thesis showed that in areas with no groundwater table or with low precipitation, applying irrigation during the stage BBCH 50–65 can significantly increase biomass and seed yields (Chapter 6.2). In areas with shallow groundwater table, the gain in biomass and seed yield was lower (Chapter 6.1 and unpublished data from 2008–2009). The range of attainable seed yields for cynara as well as an empirical model to predict seed yield under varying crop age, soil type, plant density, and levels of input of resources were extensively discussed in Chapter 3.

Sunflower seed yields

In central Greece sunflower was not cultivated until 2005, but later on due to favourable policies (Directive 2003/30/EC), farmers started to grow sunflower. Researchers tried to find the best management techniques and genotypes suitable for this environment. In this context, a number of experiments were carried out in central Greece that showed very promising results: high LAI values (see Fig. 7.1b); seed yields up to 5.5 t ha^{-1} (Danalatos *et al.*, 2004, 2005); very good seed oil

characteristics; and an energy output/input efficiency of 7.75:1 (Geronikolou *et al.*, 2004, 2005).

A typical productivity experiment in relation to irrigation and nitrogen fertilization for a new sunflower hybrid was analyzed in Chapter 6.3. Results obtained in this experiment (2006) also showed high seed yield with little response to water and nitrogen input application (Fig. 6.3.3). However, these promising results were not confirmed in later years (2007–2009; data not shown), most likely due to different hybrids used and also due to less favourable weather conditions, i.e. heat waves in 2007 and excessive droughts in 2008. For instance, in 2007 sunflower showed a strong response to applying irrigation with maximum LAI values of 2.9 for only a short period of time (Fig. 4.2j) and seed yields of 0.9 to 2.8 t ha^{-1} (Giannoulis *et al.*, 2008). In that year the extremely high temperature (> 40°C for several days) accelerated crop development rate and reduced the number of days available for growth, while leaf photosynthetic rate was also declined (Fig. 5.6), thus explaining the lower yields compared to those in 2006. In water stressed plants that difference was more evident. Actually, temperature measurements in attached leaves in the field verified this statement (data not shown). During day-time, irrigated plants had leaf temperatures approximately 6°C below air temperature, while water stressed plants had leaf temperatures only 1.5°C below air temperature. Importantly, the soil temperature of the dry plots was 8°C higher than the air temperature during day-time (note: LAI <1.5). Such data would be of great interest in crop models for precise determination of thermal time, while the large deviations found between canopy and air temperature bring new food for thought.

Seed yields in 2008 and in 2009 ranged from 0.7 to 3.4 t ha^{-1} in response to applying irrigation (data not shown). In view of increasing farmer income, the idea of planting sunflower just after the wheat harvest (end of June; Giannoulis *et al.*, 2008) was also tested within this study. However, this late sowing increased crop water demands and given also the high summer temperatures resulted in low yields, thus this idea rejected.

In short, among factors affecting sunflower productivity, the following are the most important for central Greece: (1) genotype, (2) early sowing to make use spring rainfalls (e.g. March–April), and (3) applying irrigation.

Kenaf biomass and stem yields

Unlike sunflower, kenaf is still not cultivated on a commercial basis in many Mediterranean sites due to lack of support from the fibre industry. Biomass productivities obtained in central Greece (Fig. 7.1; average stem/biomass ratio of 0.82) are in line with many findings from other sites (Amaducci *et al.*, 2000; Webber *et al.*, 2002; Alexopoulou *et al.*, 2005; Patanè & Sortino, 2010). Observed

high biomass yields is due to high leaf assimilation rates (Chapter 5) and because of long stay-green periods (LAI>3 for ~90 days; Fig. 7.1b). Like sunflower, kenaf growth during 2007 and 2008 showed the greatest response to water supply (7.4 to 20.7 t ha^{-1}; data not shown).

An innovation of this study was that kenaf planted in 75 cm row-to-row distances instead of the common 50 cm row-to-row distance (Danalatos & Archontoulis, 2010 and references therein). This was done in order to improve crop mechanization (note maize is also planted at 75 cm). Nevertheless, this change in plant arrangement, which was accompanied by a slight reduction in plant population density, did not affect biomass production. This is not surprising given that kenaf can compensate well across a wide range of plant densities (Muchow, 1979, Carberry & Muchow, 1992; Alexopoulou *et al.*, 2000).

In short, the most important factors that determine kenaf productivity in central Greece are: (1) sowing time, and (2) irrigation. The proper sowing period for kenaf (short day plant) in central Greece is during May.

The effect of nitrogen fertilization

In general, kenaf and sunflower crops showed little response to nitrogen fertilization (Chapters 6.3 and 6.4). Apparently, the crops' nitrogen requirements were satisfied from the high quantities of available nutrients present in the soil at the experimental site. Cynara showed higher response to nitrogen fertilization, most probably due to the larger amount of biomass that had to be sustained (Chapters 6.1 and 6.2). Nevertheless, nitrogen restoration schemes are necessary when the crops are to be grown at commercial scale for long periods. Based on the present findings, it was calculated that annually 88 to 97 kg N ha^{-1} is removed from the field when cropped to sunflower (seed yield ~ 3 t ha^{-1}) or kenaf (stem yield ~ 13 t ha^{-1}). In the case of cynara, the total nitrogen uptake rates may reach up to 300 kg N ha^{-1} (see Table 6.1.1; Fig. 6.2.5).

Knowledge of crop phenology

Knowledge of crop phenology is a prerequisite to efficient plant management practices and experimental treatments (e.g. weeding, irrigation, harvesting operations, etc.). Given that such information was not available for cynara, we defined and described in detail the growth stages of cynara using the worldwide reference BBCH coding system (Chapter 2). This code can be applied under all circumstances, irrespective of climate and genotype and provides precise start and end points of each stage.

So far, more than 30 important plant species including the model plant Arabidopsis have been described with the BBCH code, while the list is

continuously expanding (Hess *et al*., 1997; Meier, 1997; Boyers *et al*., 2001; Meier *et al*., 2009a). For sunflower the BBCH scale was developed in 1990 (Lancashire *et al*., 1991). For kenaf, although a BBCH scale does not exist yet, the development of the crop is very simple with two distinct phases (see detailed description by Carberry *et al*., 1992; Williams, 1994). General BBCH codes can also be applied when necessary (e.g. Finn *et al*., 2007). The BBCH code is particularly useful for farmers and researchers, but its numerical code (from 0 to 100) has no biological meaning and therefore cannot be used in modelling. Basically, the scale and the code have been designed so that the numerical value of the code increases as the plant develops.

Implications for crop modelling

As mentioned in Chapter 1 (section methodological framework), this thesis also aimed to provide specific data sets to parameterize the GECROS crop model (Yin & van Laar, 2005). GECROS requires a number of parameters related to photosynthesis, phenology, morphology, nitrogen content, and biomass composition. Many of these parameters have been defined or can be easily calculated from the existing data sets (e.g. SLA and maximum plant height). For instance, photosynthetic and respiration data (Chapter 5) along with the light and nitrogen extinction coefficients (Chapter 4), provide a complete set of parameters for computation of canopy photosynthesis. Crop morphology i.e. LAI development and leaf senescence, can be quantified based on the present findings and approaches developed by Yin *et al*. (2000, 2003a). Agronomic data accumulated all these years (including biomass and LAI curves; e.g. Chapter 6) can help to validate model predictions.

However, due to the nature of this thesis (viz. field study), parameters related to crop phenology are difficult to be quantified precisely (data analysis is in progress). Instead, supporting literature information regarding the phenology of our crops is given below.

For modelling crop phenology, both cardinal temperatures (base, optimum, ceiling temperatures) and parameters defining photoperiod sensitivity (for short or long day plants) are needed (Yin & van Laar, 2005). Usually thermal parameters are derived from growth chamber experiments where seed emergence or leaf elongation rate is evaluated under different temperature regimes and then estimates are used to describe plant developmental rate (Carberry & Abrecht, 1990; Carberry *et al*., 1992; Villalobos & Ritchie, 1992; Sadras & Villalobos, 1993; Villalobos *et al*., 1996; Lisson *et al*., 2000a; Timmermans *et al*., 2007). So far experimental evidence for the studied crops suggests a base temperature for plant growth of 4–7.2 °C for sunflower (Robinson, 1971; Kiniry *et*

al., 1992; Villalobos & Ritchie, 1992), 10–12 °C for kenaf (Angelini *et al*., 1998; Carberry & Abrecht, 1990) and 5.7–10 °C for cynara (Angelini *et al*., 2009; Virdis *et al*., 2009).

Parameters quantifying the response of development to photoperiod are commonly derived from analysis of reciprocal transfer (controlled) experiments (Lisson *et al*., 2000b; Yin *et al*., 2005; Yin, 2008) or, less accurately, from an analysis of field data (including different years and locations; Carberry *et al*., 1992; Williams, 1994; Patanè & Sortino, 2010). Recently, Amaducci *et al*. (2008) showed for hemp that all photo-thermal parameters (plant level) can be estimated from an appropriate analysis of large field data sets using optimization techniques. Kenaf is a typical short-day plant and combined thermal and photoperiodic parameters are needed for modelling (Carberry *et al*., 1992). For sunflower use of thermal parameters alone is sufficient to model crop phenology (Kiniry *et al*., 1992; Pereyra-Irujo & Aguirrezabal, 2007); nevertheless some modellers also included photoperiodic parameters (Steer *et al*., 1993; Villalobos *et al*., 1996). For cynara there is no relevant information yet. Virdis *et al*. (2009) found for globe artichoke (*Cynara cardunculus* var. *scolymus*), a species close to our species (*Cynara cardunculus* var. *altilis* DC), a negative correlation between leaf appearance rate and photoperiod (from 9.9 to 14.2 h; *P*<0.001), but no relation between flowering time and photoperiod (*P*>0.05). Others assessed cynara's phenology as a simple function of thermal time only (Angelini *et al*., 2009). Nevertheless whether or not cynara responds to photoperiod needs to be quantified in future (controlled) experiments.

Future of energy crops

Generally, whether to include energy crops in crop production systems or not depends on the factors summarised in Fig. 7.2. Currently, political decisions are quite favourable for the development of energy crops, while technology is still developing (e.g. harvesting machines, crop/fuel conversion chains). At farm level, the combination of biomass yield, production cost and market outlet availability are the most important criteria for a farmer to make the final decision about growing a crop. This thesis focused on the production aspects of energy crops (Chapters 2–6), while a generic view on the future energy targets, markets and crop/fuel chains was presented in Chapter 1. Production cost, product quality, heating value as well as alternatives to energy markets for the tested crops are briefly discussed below in order to have an overall picture of the crops' suitability for Greece.
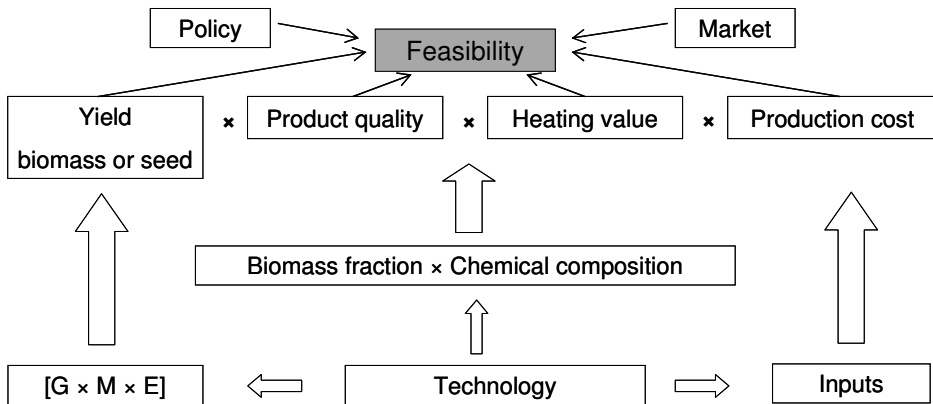
Figure 7.2: A simplified representation of the main factors determining the suitability of energy crops to be included in production systems. Arrows indicate direct effects (e.g. genotype on biomass yield) while the symbol "×" denotes interactions (e.g. product quality and heating value).

Production cost

The current uncertainty regarding oil and agro-chemical prices, subsidies and CAP reform makes any economic assessment of the suitability of energy crops quite risky and preliminary in nature. In this context, in order to have a solid view on the production costs of energy crops for a specific environment (Greece), we considered outputs from three different studies: (1) multi-farm mathematical modelling (Lychnaras & Schneider, 2011); (2) large-scale experimental plots (Skoulou *et al.*, 2011); and (3) long-term farm budgets (Panoutsou, 2007). Studies considered on-farm biomass yields (which are lower than experimental yields) and included harvesting operations, labour and farm rent in their cost estimations.

Results indicated that cynara is by far the most economically feasible crop for energy production in Greece (production cost of 28–42 € t^{-1}) and for non-irrigated lands the only viable option. Irrigation constitutes a large expense and this is the main reason for the superiority of cynara over other perennials like miscanthus, switchgrass, and giant reed (viz. summer crops; production cost of 40–100 € t^{-1}). Compared to C$_4$ miscanthus that is propagated by rhizomes, cynara is propagated by seeds, which further reduces the costs. Production costs for sunflower and kenaf were 2–3 times higher than those of cynara.

Quality of crop biomass and heating value

Quality of crop biomass is particularly important when biomass is combusted for heat and power generation. Ash content and mineral compositions characterize the product quality (high values associated with slagging, fouling and corrosion tendencies). In general wood biomass is superior to crop biomass in terms of quality. The ash content is also inversely related to heating value; with every 1% increase in ash content, the heating value is decreasing by 0.2 MJ kg^{-1} (Cassida *et al*., 2005). The heating value of the energy crops (entire biomass) ranges from 14 to 20 MJ kg^{-1} depending on biomass composition and partitioning over plant components (Encinar *et al*., 2000; Cassida *et al*., 2005; Fernández *et al*., 2006; Aho *et al*., 2008; Grammelis *et al*., 2008; Angelini *et al*., 2009; Mantineo *et al*., 2009; Vamvuka *et al*., 2009).

In literature, biomass quality data for energy crops are very variable because of different experimental protocols used (biomass partitioning, time of harvest, method of sampling, etc.). Particularly for cynara, there is ongoing discussion due to the large difference found among studies (i.e. ash content ranges from 4 to 17% dry weight; Encinar *et al*., 2000, 2002; Grammelis *et al*., 2008; Angelini *et al*., 2009; Vamvuka *et al*., 2009). Monti *et al*. (2008) studied six energy crops and found that cynara exhibited the highest ash and mineral contents, and miscanthus and switchgrass the lowest. On the other hand, Mantineo *et al*. (2009) found smaller differences in ash contents between cynara (5.5–8.2%) and giant reed (2.3–6.0%) and miscanthus (2.0–8.2%). In general, the mineral composition of the energy crops is characterized by high Cl and S contents and improvements should be made to avoid boiler corrosion (Monti *et al*., 2008).

Improved agricultural practices along with a better understanding of the crop behaviour are commonly suggested as requirements for improving product quality. For cynara, quantification of the growth stages with the BBCH system (Chapter 2) and determination of seed/head and head/biomass fractions (Chapter 3) can assist in that respect. Moreover, harvesting operations (Fernández *et al*., 2007b; Pari *et al*., 2009) should be improved to avoid biomass contamination by soil particles. Crops should be harvested as dry as possible in order to allow minerals to be re-mobilized from aboveground to belowground organs. Lastly during growth fertilization with KCl should be avoided while other conversion technologies like pyrolysis and gasification should be further explored (Fernández *et al*., 2006; Grammelis *et al*., 2008; Franco *et al*., 2009). Co-combusting cynara with coal showed good results (Aho *et al*., 2008).

Alternative cropping strategies for the tested crops

Crop species chosen for this study cover three major bio-applications: sunflower seeds for biodiesel; kenaf stems for paper, panels, building materials, adsorbents and textiles production; and cynara lignocellulosic biomass for electricity. However, there are many alternative cropping strategies to consider, which might be more profitable.

Supplementary to biodiesel production from sunflower seeds, the remaining press cake (seed residues after oil extraction) can be used for animal feed due to its high nutrition value (~20% protein concentration). Sunflower crop residues after seed threshing can also be used for bioenergy production to acquire additional farmer income and to increase total bioenergy production. Considering sunflower crop residues of ~ 6 t ha^{-1} (Figs. 6.3.3 and 6.3.4) and a heating value of 15 MJ kg^{-1}, additionally 90 GJ ha^{-1} can be produced. In this intensive scenario, in total 140 kg N ha^{-1} are removed from the field annually and the question arises whether exploitation of sunflower residues for energy is profitable for farmers and in conflict with sustainable soil management. This makes the question emerge: shall we focus on maximization or optimization of bioenergy production per cultivation system? Answers to these questions are highly variable. For instance, use of agri-residues is a sustainable option because it has few direct impacts on land use, but on the other hand, crop residues are also required to maintain soil organic matter and prevent erosion while their systematic removal can damage soil quality and reduce agronomic productivity (Blanco-Canqui & Lal, 2009; Lal, 2010; Neil, 2011).

Besides the production of valuable fibre products kenaf has two more important applications: forage feed and bioenergy. Webber (1993) and Webber *et al*. (2002) reported that kenaf can be used as a livestock feed because it has high protein yields, can be ensiled effectively and also it has satisfactory dry matter and protein digestibility (53 to 71%). The plant has high protein concentration in the dry biomass that can reach up to 23% under appropriate management techniques (planting density affecting leaf/stem ratio, time of harvest and multiple harvests per season; Webber 1993; Bhardwaj *et al*., 1995). Due to its high cellulose and hemicellulose contents (similar to fibre sorghum, hemp and maize; Amaducci *et al*., 2000) kenaf can be used for bioethanol production. By using second generation conversion technology, Zatta *et al* (2010) estimated that from 1 tonne of kenaf dry stem weight some 290 litres of ethanol can be produced. Kenaf can also be used for production of solid biofuels (agri-pellets or chips for heat and power production). Seed production from kenaf is also possible (16–22% oil:seed ratio; yields up to 3.5 t ha^{-1}; Webber *et al*., 2002; Patanè & Sortino, 2010), but seed production strategies in the Mediterranean region are strongly affected by the cultivar and latitude, due to the crop's photoperiod sensitivity.

Among the tested species, cynara is the crop with the most applications: (1) heat and power, (2) biodiesel, (3) bioethanol, (4) paper and other by-products, (5) forage feed, (6) pharmacological compounds and others less important applications (see review by Fernández *et al.*, 2006 and also Chapters 2, 3, 6.1 and 6.2). For forage feed the crop does not require industrial support or specific equipment for harvesting operations thus can be applied anywhere. Lastly, it should be added that after biodiesel production, cynara's press cake can also be used for animal feed (protein concentration of 18%; Chapter 3) or alternatively as organic fertilizer (Curt *et al.*, 2002) because cynara's press cake has a carbon:nitrogen ratio (C:N=13:1) close to soil humus (C:N=10:1).

Critical assessment of crops' suitability

Usually for assessing the suitability of energy crop cultivations an output:input balance study is performed (life cycle assessment; e.g. Venturi & Venturi, 2003). However, this index changes a lot with management practices, end product used in calculations (seed or whole biomass), size of the farm, assumptions made, etc. Such calculations are beyond the scope of this study and readers are referred to literature studies for further details (Venturi & Venturi, 2003; Hillier *et al.*, 2009; Mantineo *et al.*, 2009; Monti *et al.*, 2009; Rettenmaier *et al.*, 2010). Herein our purpose was to show the potential of the tested crops for various applications, the range of biomass production in response to management practices, and crop physiological data to explain biomass formation at any environment (crop level).

Based on data presented above, we depict some different views regarding the suitability of energy crops. From a farmer viewpoint, cynara is more preferable than sunflower and kenaf (and other energy crops) because it produces large amounts of biomass at low production costs. From an industrial viewpoint, cynara is not a first priority because presently the feedstock is of low quality. From an agronomic viewpoint, cynara is very interesting because of the perennial character, long stay-green periods, and because it can grow without irrigation. But, the annuals kenaf and sunflower have other benefits like positive rotation effects (e.g. Zegada-Lizarazu & Monti, 2011). Besides these generic views, the choice of a crop to grow for energy production depends also on particular circumstances of a specific region/farm, i.e. water availability, distance to the nearest processing plant, available equipment, etc. This thesis addressed all possible applications of the tested crops and provided adequate agronomic and crop physiological information to support any cultivation strategy.

Conclusions

This thesis provides essential information on phenology, agronomy and crop physiology of three (Mediterranean) bioenergy crops, sunflower, kenaf and cynara. Thus, it contributes to the general objective of gaining more insight into bioenergy production from crop species. Given that crops are still experimental or only cultivated at small scale in the Mediterranean region, data presented in this thesis can help farmers to design better cultural techniques (viz. information on water and nutrient input application, biomass yields, etc.), agronomists to better understand factors that determine biomass production (viz. information on light interception, leaf photosynthetic capacity), modellers to parameterize simulation models to predict potential, attainable and actual biomass production, and provide food for thought to scientists in the areas of genetics and logistics. This thesis prioritizes the perennial *Cynara cardunculus* as the most interesting crop for bioenergy production in the Mediterranean region and provides fundamental information on this crop (e.g. growth stages) to assist upcoming studies to better exploit its potential and to improve its biomass both quantitatively and qualitatively.

References

AEBIOM 2008. European Biomass Association – A pellet road map for Europe, November (http://www.aebiom.org/IMG/pdf/Pellet_Roadmap_final.pdf).

AEBIOM 2010. European Biomass Association, Biomass statistics – 2010 (http://www.aebiom.org/?cat=16).

Aho M, Gil A, Taipalea R, Vainikkaa P. 2008. A pilot-scale fireside deposit study of co-firing cynara with two coals in a fluidized bed. *Fuel* 87: 58–69.

AIR2–CT92–1089. 1999. *Cynara cardunculus* L. as New Crop for Marginal and Set-Aside Lands, September 1999 (EU project, summary report).

Albrizio R, Steduto P. 2005. Resource use efficiency of field-grown sunflower, sorghum, wheat and chickpea I. Radiation use efficiency. *Agriculture and Forest Meteorology* 130: 254–268.

Alexopoulou E, Christou M, Cosentino SL, Danalatos NG, Archontoulis SV, *et al.*, 2005. BioKenaf, a European Network for biomass production chain of kenaf. In: *Proceedings of the 14th European Biomass Conference*, Paris, France, p. 290–293.

Alexopoulou E, Christou M, Mardikis M, Chatziathanasiou A. 2000. Growth and yields of kenaf varieties in central Greece. *Industrial Crops and Products* 11: 163–172.

Amaducci S, Amaducci MT, Benati R, Venturi G. 2000. Crop yield and quality parameters of four annual fibre crops (hemp, kenaf, maize and sorghum) in the north of Italy. *Industrial Crops and Products* 11: 179–186.

Amaducci S, Colauzzi M, Bellocchi G, Venturi G. 2008. Modelling post-emergent hemp phenology (*Cannabis sativa* L.): Theory and evaluation. *European Journal of Agronomy* 28: 90–102.

Angelini LG, Ceccarini L, Nassi o Di Nasso N, Bonari E. 2009. Long-term evaluation of biomass production and quality of two cardoon (*Cynara cardunculus* L.) cultivars for energy use. *Biomass and Bioenergy* 33: 810–816.

Angelini LG, Macchia M, Ceccarini L, Bonari E. 1998. Screening of kenaf (*Hibiscus cannabinus* L.) genotypes for low temperature requirements during germination and evaluation of feasibility of seed production in Italy. *Field Crops Research* 59: 73–79.

Anten NPR. 1997. Modelling canopy photosynthesis using parameters determined from simple non-destructive measurements. *Ecological Research* 12: 77–88.

Anten NPR, Schieving F, Werger MJA. 1995. Patterns of light and nitrogen distribution in relation to whole canopy carbon gain in C_3 and C_4 mono- and dicotyledonous species. *Oecologia* 101: 504–513.

Archontoulis SV, Danalatos NG, Struik PC. 2009. Determination of *Cynara cardunculus* seed yield and harvest index. In: *Proceedings of the 17th European Biomass Conference*, Hamburg, Germany, p. 557– 561.

Archontoulis SV, Danalatos NG, Struik PC, Vos J, Yin X. 2008a. Agronomy of *Cynara cardunclulus* growing in an aquic soil in central Greece. In: *Proceedings of the International Conference on Agricultural Engineering*, June, Crete, Greece. Abstract in p.42; full paper 15 pp on CD.

Archontoulis SV, Danalatos NG, Yin X, Struik PC. 2008b. Leaf photosynthesis and respiration of *Cynara cardunculus*. In: *Proceedings of the 16th European Biomass Conference*, Valencia, Spain, p. 636–639.

Archontoulis SV, Struik PC, Danalatos NG. 2005. Leaf photosynthesis of kenaf (cv. Everglades 41) as affected by different light intensity and temperature regimes. In: *Proceedings of the 14th European Biomass Conference*, Paris, France, p. 414–417.

Archontoulis SV, Struik PC, Danalatos NG. 2006a. Kenaf dark respiration as affected by temperature and leaf position. In: *Proceedings of the International Conference on Information Systems, Sustainable Agriculture, Agro-environment and Food Technology*, Volos, Greece, p. 415–422.

Archontoulis SV, Struik PC, Danalatos NG. 2006b. Diurnal leaf gas exchange patterns of two kenaf genotypes at two leaf positions. In: *Proceedings of the International Conference on Information Systems, Sustainable Agriculture, Agro-environment and Food Technology*, p. 423–431.

Archontoulis SV, Struik PC, Vos J, Danalatos NG. 2010a. Phenological growth stages of *Cynara cardunculus*: codification and description according to the BBCH scale. *Annals of Applied Biology* 156: 253–270.

Archontoulis SV, Struik PC, Yin X, Bastiaans L, Vos J, Danalatos NG. 2010b. Inflorescence characteristics, seed composition, and allometric relationships predicting seed yields in the biomass crop *Cynara cardunculus*. *Global Change Biology–Bioenergy* 2: 113–129.

Archontoulis SV, Vos J, Yin X, Bastiaans L, Danalatos NG, Struik PC. 2011a. Temporal dynamics of light and nitrogen vertical distributions in canopies of sunflower, kenaf and cynara. *Field Crops Research* 122: 186–198.

Archontoulis SV, Struik PC, Yin X, Danalatos NG. 2011b. A comparative analysis of biomass production from seven energy crop species grown in a Mediterranean environment. In: *Proceedings of the 19th European Biomass Conference*, Berlin, Germany (*in press*).

Arcila-Pulgarin L, Buhr L, Bleiholder H, Hack H, Meier U, Wicke H. 2002. Application of the extended BBCH scale for the description of the growth stages of coffee (*Coffea* spp.). *Annals of Applied Biology* 141: 19–27.

Ardente F, Beccali M, Cellura M, Mistretta M. 2008. Building energy performance: A LCA case study of kenaf-fibres insulation board. *Energy and Buildings* 40: 1–10.

Atkin OK, Bruhn D, Hurry VM, Tjoelker MG. 2005. The hot and the cold: unravelling the variable response of plant respiration to temperature. *Functional Plant Biology* 32: 87–105.

Atwell B, Kriedemann P, Turnbull C. 1999. Plants in action. Adaptation in nature performance. Macmillan publishers Australia PTY LTD, p. 664.

Bange MP, Hammer GL, Rickert KG. 1997. Effect of specific leaf nitrogen on radiation use efficiency and growth of sunflower. *Crop Science* 37: 1201–1207.

Banse M, van Meijl H, Tabeu A, Woltjer G, Hellmann F, Verburg PH. 2011. Impacts of EU biofuel policies on world agricultural production and land use. *Biomass and Bioenergy* 35: 2385–2390.

Barlog P, Grzebisz W. 2004. Effects of timing and nitrogen fertilizer application on winter oilseed rape (*Brassica napus* L.). I. Growth dynamics and seed yield. *Journal of Agronomy and Crop Science* 190: 305–313.

Baum S, Weih M, Busch G, Kroiher F, Bolte A. 2009. The impact of Short Rotation Coppice plantations on phytodiversity. *Agriculture and Forestry Research* 3: 163–170.

Beale CV, Long SP. 1997. Seasonal dynamics of nutrient accumulation and partitioning in the perennial C_4–grasses *Miscanthus × giganteus* and *Spartina cynosuroides*. *Biomass and Bioenergy* 12: 419–428.

Benlloch-Gonzalez M, Fournier JM, Ramos J, Benlloch M. 2005. Strategies underlying salt tolerance in halophytes are present in *Cynara cardunculus*. *Plant Science* 168, 653–659.

Beringer T, Lucht W, Schaphoff S. 2011. Bioenergy production potential of global biomass plantations under environmental and agricultural constraints. *Global Chance Biology – Bioenergy* 3: 299–312.

Bernacchi CJ, Singsaas EL, Pimentel C, Portis AR, Long SP. 2001. Improved temperature response functions for models of Rubisco-limited photosynthesis. *Plant, Cell and Environment* 24: 253–259.

Bernacchi CJ, Portis AR, Nakano H, von Caemmerer S, Long SP. 2002. Temperature response of mesophyll conductance. Implications for the determination of Rubisco enzyme kinetics and for limitations to photosynthesis in vivo. *Plant Physiology* 130: 1992–1998.

Bernacchi CJ, Pimentel C, Long SP. 2003. In vivo temperature response functions of parameters required to model RuBP-limited photosynthesis. *Plant, Cell and Environment* 26: 1419–1430.

Berndes C, 2002. Bioenergy and water – the implication of large scale bioenergy production for water use and supply. *Global Environmental Change* 12: 253–271.

Bertheloot J, Martre P, Andrieu B. 2008. Dynamics of light and nitrogen distribution during grain filling within wheat canopy. *Plant Physiology* 148: 1707–1720.

Bhardwaj HL, Rangappa M, Webber CL. 1995. Potential of kenaf as a forage. In: Proceedings of the International Kenaf Association Conference, Irving, TX, USA, 7: 95–103.

Blanco-Canqui H, Lal R. 2009. Crop residue removal impacts on soil productivity and environmental quality. *Critical Reviews in Plant Sciences* 28: 139–163.

Bleiholder H, van den Boom T, Langelüddecke P, Stauss R. 1991. Codificación uniforme para los estadios fenológicos de las plantas cultivadas y de las malas hierbas. *Phytoma* 28: 1–4.

Bolstad PV, Mitchell K, Vose JM. 1999. Foliar temperature–respiration response functions for broad-leaved tree species in southern Appalachians. *Tree Physiology* 19: 871–878.

Boote KJ, Pickering NB. 1994. Modelling photosynthesis of row crop canopies. *HortScience* 29: 1423–1434.

Borrás L, Curá AJ, Otegui ME. 2002. Maize kernel composition and post-flowering source-sink ratio. *Crop Science* 42: 781–790.

Boundy B, Davis SC, Wright L, Badger PC, Perlack B. 2010. Biomass Energy Data Book 2010. US Department of Energy, pp. 230 (http://cta.ornl.gov/bedb).

Boyes DC, Zayed AM, Ascenzi R, McCaskill AJ, Hoffman NE, Davis KR, Görlach J. 2001. Growth Stage–Based Phenotypic Analysis of Arabidopsis: A Model for High Throughput Functional Genomics in Plants. *Plant Cell* 13: 1499–1510.

Braune H, Müller J, Diepenbrock W. 2009. Integrating effects of leaf nitrogen, age, and growth temperature into the photosynthesis-stomatal conductance model LEAFC3-N parameterized for barley (*Hordeum vulgare* L.). *Ecological Modelling* 220: 1599–1612.

Buckley TN, Adams MA. 2011. An analytical model of non-photorespiration CO_2 release in the light and dark in leaves of C3 species based on stoichiometric flux balance. *Plant, Cell and Environment* 34: 89–112.

Bunce JA. 2000. Acclimation of photosynthesis to temperature in eight cool and warm climate herbaceous C3 species: Temperature dependence of parameters of a biochemical photosynthesis model. *Photosynthesis Research* 63: 59–67.

Campbell JE, Lobell DB, Genova RC, Field CB. 2008. The global potential of bioenergy on abandoned agriculture lands. *Environmental Science and Technology* 42: 5791–5794.

Carberry PS, Abrecht DG. 1990. Germination and elongation of the hypocotyls and radicle of kenaf (*Hibiscus cannabinus*) in response to temperature. *Field Crops Research* 24: 227–240.

Carberry PS, Muchow RC. 1992. A simulation model for kenaf assisting fibre industry planning in northern Australia. II. Leaf area Development. *Australian Journal of Agricultural Research* 43: 1515–26.

Carberry PS, Muchow RC, Williams R, Sturtz JD, McCown RL. 1992. A simulation model for kenaf assisting fibre industry planning in northern Australia. I. General introduction and phenological model. *Australian Journal of Agricultural Research* 43: 1501–1513.

Carvalho IS, Miranda I, Pereira H. 2006. Evaluation of oil composition of some crops suitable for human nutrition. *Industrial Crops and Products* 24: 75–78.

Cassida KA, Muir JP, Hussey MA, Read JC, Venuto BC, Ocumpaugh WR. 2005. Biofuel component concentrations and yields of switchgrass in South central US environments. *Crop Science* 45: 682–92.

Charles-Edwards DA, Lawn RJ. 1984. Light interception by grain legume row crops. *Plant, Cell and Environment* 7: 247–251.

Christou M, Alexopoulou E, Panoutsou C, Monti A. 2010. Overview of the markets for the energy crops in EU-27. *Biofuels, Bioproducts and Biorefining* 4: 605–619.

Clegg MA, Biggs WW, Eastin JD, Maranville JW, Sullivan CY, 1974. Light transmission in field communities of sorghum. *Agronomy Journal* 66: 471–476.

Connor DJ, Hall AJ, Sardas VO. 1993. Effects of nitrogen content on the photosynthetic characteristics of sunflower leaves. *Australian Journal of Plant Physiology* 20: 251–263.

Connor DJ, Hernandez CG. 2009. Crops for biofuels: current status and prospects for the future. In: Howarth RW and Bringezu S (eds) Biofuels: Environmental Consequences and Interactions with Changing Land Use. *Proceedings of the Scientific Committee on Problems of the Environment* (SCOPE) *International Biofuels Project Rapid Assessment*, Gummersbach Germany. Cornell University, Ithaca NY, USA (http://cip.cornell.edu/biofuels/), p. 65–80.

Connor DJ, Sadras VO, Hall AJ. 1995. Canopy nitrogen distribution and the photosynthetic performance of sunflower crops during grain filling – a quantitative analysis. *Oecologia* 101: 274–281.

Cosentino SL, Patane C, Sanzone E, Copani V, Foti S. 2007. Effects of soil water content and nitrogen supply on the productivity of *Miscanthus × giganteus* Greef et Deu. in a Mediterranean environment. *Industrial Crops and Products* 25: 75–88.

Cosentino SL, Riggi E, D'Agosta G. 2004. Leaf photosynthesis in kenaf (*Hibiscus cannabinus* L.) in response to water stress. In: *Proceedings of the 2nd World Biomass Conference*, Roma, Italy, p. 374–376.

Crutzen PJ, Mosier AR, Smith KA, Winiwarter W. 2008. N_2O release from agro-biofuel production negates global warming reduction by replacing fossil fuels. *Atmospheric Chemistry and Physics* 8: 389–395.

Curt MD, Sanchez G. Fernandez J. 2002. The potential of *Cynara cardunculus* L. for seed oil production in a perennial cultivation system. *Biomass and Bioenergy* 23: 33–46.

Dalianis L, Panoutsou C, Dercas N. 1996. Spanish thistle artichoke, *Cynara cardunculus* L., under Greek conditions. In: *Proceedings of the 9th E.C. Conference Biomass for Energy and Industry* (Eds Chartier P, Ferrero GL, Henius UM, Hultberg S, Sachau J, Wiinblad M), Pergamon, Oxford, Vol. I, p. 663–668.

Danalatos NG. 2008. Changing roles: cultivating perennial weeds vs. conventional crops for bio-energy production. The case of *Cynara cardunculus*. In: *Proceedings of CTSI Clean Technology and Sustainable Industries Conference and Trade Show*. Boston, USA, p. 1–4.

Danalatos NG, Archontoulis SV. 2004. Potential growth and biomass productivity of kenaf under central Greek conditions: I. The influence of fertilization and irrigation. In: *Proceedings of the 2ⁿᵈ World Biomass Conference*, Roma, Italy, Vol. I, p. 323−326.

Danalatos NG, Archontoulis SV. 2005. Irrigation and N-fertilization effects on Kenaf growth and biomass productivity in central Greece. In: *Proceedings of International Conference on Industrial Crops and Rural Development*, Murcia, Spain, p. 879−888.

Danalatos NG, Archontoulis SV. 2009. Oilseed rape growth, biomass accumulation and seed yield as affected by variety and N-fertilization in a dry year in Greece. In: *Proceedings of the 17ᵗʰ European Biomass Conference*, Germany, p. 507–511.

Danalatos NG, Archontoulis SV. 2010. Growth and biomass productivity of kenaf (*Hibiscus cannabinus*) under different agricultural inputs and management practices in Greece. *Industrial Crops and Products* 32: 231–240.

Danalatos NG, Archontoulis SV, Geronikolou L, Papadakis G. 2004. Potential growth and productivity of three sunflower hybrids in a soil with aquic moisture regime in central Greek conditions. In: *Proceedings of the 2ⁿᵈ World Biomass Conference,* Roma, Italy, p. 315−318.

Danalatos NG, Archontoulis SV, Geronikolou L, Papadakis G. 2005. Biomass and seed yield of sunflower as alternative energy crop in Greece. In: *Proceedings of the 14ᵗʰ European Biomass Conference*, Paris, France, p. 308–311.

Danalatos NG, Archontoulis SV, Giannoulis K, Rozakis S. 2006a. Miscanthus and cardoon as alternative crops for solid fuel production in central Greece. In: *Proceedings of the International Conference on Information Systems, Sustainable Agriculture, Agro-environment and Food Technology,* Volos, Greece, p. 387−397.

Danalatos NG, Archontoulis SV, Mitsios I. 2007b. Potential growth and biomass productivity of *Miscanthus × giganteus* as affected by plant density and N-fertilization in central Greece. *Biomass and Bioenergy* 31: 145–152.

Danalatos NG, Archontoulis SV, Tsibukas K. 2009. Comparative analysis of sorghum vs. corn growing under optimum and water/nitrogen limited conditions in central Greece. In: *Proceedings of the 17ᵗʰ European Biomass Conference*, Germany, p. 538–544.

Danalatos NG, Gintsioudis II, Skoufogianni E, *et al.,* 2006b. Three years kenaf cultivation in central Greece: Assessment and future perspectives. In: *Proceedings of the International Conference, on Information Systems, Sustainable Agriculture, Agro-environment and Food technology*, Volos, Greece, p. 382−386.

Danalatos NG, Skoufogianni E, Giannoulis K, Archontoulis SV. 2007a. Responses of *Cynara cardunculus* to irrigation and N-fertilization in central Greece. *Proceedings of the 15ᵗʰ European Biomass Conference*, Berlin, Germany, p. 421–424.

De Fraiture C, Berndes G. 2009. Biofuels and water. In: *Proceedings of the Scientific Committee on Problems of the Environment* (SCOPE) *International Biofuels Project*

Rapid Assessment, Gummersbach, Germany. Cornell University, Ithaca NY, USA (http://cip.cornell.edu/biofuels/), p. 139-153.

Del Pozo A, Dennett MD. 1999. Analysis of the distribution of light, leaf nitrogen, and photosynthesis within the canopy of *Vicia faba* L. at two contrasting plant densities. *Australian Journal of Agricultural Research* 50: 183–189.

de Pury DGG, Farquhar GD. 1997. Simple scaling of photosynthesis from leaves to canopies without the errors of the big-leaf models. *Plant, Cell and Environment* 20: 537–557.

Dercas N, Liakatas A. 2007. Water and radiation effect on sweet sorghum productivity. *Water Resource Management* 21: 1585–1600.

De Vries BJ, van Vuuren DP, Hoogwijk M. 2007. Renewable energy sources: their global potential for the first-half of the 21st century at a global level: an integrated approach. *Energy Policy* 35: 2590–2610.

de Wit CT. 1992. Resource use efficiency in agriculture. *Agricultural Systems* 40: 125–151.

Dornburg V, Faaij A, Verweij P, Langeveld H, van de Ven G, *et al.*, 2008. Biomass assessment: global biomass potentials and their links to food, water, biodiversity, energy demand and economy. Climate change scientific assessment and policy analysis (WAB) programme. pp. 98.

Dreyer E, Le Roux X, Montpied P, Daudet AF, Masson F. 2001. Temperature response of leaf photosynthetic capacity in seedlings from seven temperate tree species. *Tree Physiology* 21: 223–232.

Duarte D, Figueiredo R, Pereira S, Pissarra J. 2006. Structural characterization of the sigma style complex of *Cynara cardunculus* (Asteraceae) and immunolocalization of cardosins A and B during floral development. *Canadian Journal of Botany* 84: 737–749.

Duer H, Christensen PO. 2010. Socio-economic aspects of different biofuels development pathways. *Biomass and Bioenergy* 34: 237–243.

EEA 2006. How much bioenergy can Europe produce without harming the environment? European Environment Agency, EEA Report 7/2006, pp. 72.

Either GJ, Livington NJ. 2004. On the need to incorporate sensitivity to CO_2 transfer conductance into the Farquhar–von Caemmerer–Berry leaf photosynthesis model. *Plant, Cell and Environment* 27: 137–153.

Encinar JM, González JF, González J. 2000. Fixed-bed pyrolysis of Cynara cardunculus L. Product yields and compositions. *Fuel Processing Technology* 68: 209–222.

Encinar JM, Gonzalez JF, Gonzalez J. 2002. Steam gasification of cynara cardunculus L.: Influence of variables. *Fuel Processing Technology* 75: 27–43.

Estienne P, Godard E. 1970. Climatologie. A. Collin editino, pp. 365.

EUR 21350, 2005. European Commission: Biomass – Green Energy for Europe report 2005, pp. 52.

EUR 2006. Sustainable bioenergy cropping systems for the Mediterranean. Proceedings of the Expert Consultation, European Commission, pp. 149.

Eurostat 2010. European Commission: Europe in figures – Eurostat yearbook 2010, pp. 667.

Evans JR. 1993. Photosynthetic acclimation and nitrogen partitioning within a lucerne canopy. I canopy characteristics. *Australian Journal Plant Physiology* 20: 55–67.

Evers JB, Huth NI, Renton M. 2009. Light extinction in spring wheat canopies in relation to crop configuration and solar angle. In: *Proceedings of plant growth modelling and application*. IEEE Computer Society, 107–110 (doi: 10.1109/PMA.2009.20)

Evers JB, Vos J, Yin X, Romero P, van der Putten PEL, Struik PC. 2010. Simulation of wheat growth and development based on organ-level photosynthesis and assimilate allocation. *Journal of Experimental Botany* 61: 2203–2216.

Fargione J, Hill J, Tilman D, Polasky S, Hawthorne P. 2008. Land clearing and the biofuel carbon debt. *Science* 319: 1235–1238.

Farquhar GD, von Caemmerer S. 1982. Modelling of photosynthetic response to environmental conditions. In: Lange OL, Nobel PS, Osmond CB, Ziegler H (eds). Physiological Plant Ecology II, Water relations and carbon assimilation. Encyclopaedia of Plant Physiology, New Series, Vol. 12 B, Springer Verlag, Berlin, p. 549–588.

Farquhar GD, von Caemmerer S, Berry JA. 1980. A biochemical model of photosynthetic CO_2 assimilation in leaves of C_3 species. *Planta* 149: 78–90.

Fernández J, Curt D. 2004. Low-cost biodiesel from Cynara oil. In: P*roceedings of the 2nd World Biomass Conference*, Roma, Italy, p. 10–14.

Fernández J, Curt M, Aguado PL. 2006. Industrial applications of *Cynara cardunculus* L. for energy and other uses. *Industrial Crops and Products* 24: 222–229.

Fernández J, Curt MD, Sanz M, Escudero A. 2007a. Biomass partitioning of cynara as a function of the plant height. In: *Proceedings of the 15th European Biomass Conference*, Berlin, Germany, p. 654–656.

Fernández J, Pari L, Muller MG, Marquez L, Fedrizzi M, Curt MD. 2007b. Strategies for the mechanical harvest of cynara. In: *Proceeding of the 15th European Biomass Conference*, Berlin, Germany, p. 657–664.

Fernández J, Hidalgo M, del Monte JP, Curt MD. 2005. *Cynara cardunculus* L. as a perennial crop for non-irrigated lands: yields and applications. *Acta Horticulturae* 681: 109–116.

Fernández J, Sanchez J, Esteban B, Checa M, Aguado PL, Curt MD, Romero L, Mosquera F. 2009. Potential lignocellulosic biomass production from dedicated energy crops in marginalized agricultural land of Spain. In: *17th European Biomass Conference*, Hamburg, Germany, p. 131–137.

Fernández-Moya V, Martinez-Force E, Garces R. 2005. Oils from improved high stearic acid sunflower seeds. *Journal of Agriculture and Food Chemistry* 53: 5326–5330.

Ferreira AM, Abreu FG. 2001. Description of development, light interception and growth of sunflower at two sowing dates and two densities. *Mathematics and Computers in Simulations* 56: 369–384.

Fischer G, Prieler S, van Velthuizen H, Lensink SM, Londo M, de Wit M. 2010a. Biofuels production potential in Europe: sustainale use of cultivated land and pastures. Part I. Land productivity potentials. *Biomass and Bioenergy* 34: 159–172.

Fischer G, Prieler S, van Velthuizen H, Berndes G, Faail A, Londo M, de Wit M. 2010b. Biofuels production potential in Europe: sustainale use of cultivated land and pastures. Part I. Land productivity potentials. *Biomass and Bioenergy* 34: 173–187.

Finn GA, Straszewski AE, Peterson V. 2007. A general growth stage key for describing trees and woody plants. *Annals of Applied Biology* 151: 127–131.

Flénet F, Kiniry JR, Board JE, Westgate ME, Reicosky DC. 1996. Row spacing effects on light extinction coefficients of corn, sorghum, soybean, and sunflower. *Agronomy Journal* 88: 185–190.

Flengmark P. 2000. Growing of hemp and *Bunias orientalis* as energy crops. In: Do energy crops have a future in Denmark? (Jorgensen, U. ed.) DJF report Markbrug nr. 29: 12–17.

Flexas J, Diaz-Espejo A, Berry JA, Cifre J, Galmes J, Kaldenhoff R, Medrano H, Ribas-Carbó M. 2007. Analysis of leakage in IRGA's leaf chambers of open gas exchange systems: quantification and its effects in photosynthesis parameterization. *Journal of Experimental Botany* 58: 1533–1543.

Flexas J, Ribas-Carbó M, Diaz-Espejo A, Galmes J, Medrano H. 2008. Mesophyll conductance to CO_2: current knowledge and future prospects. *Plant, Cell and Environment* 31: 602–621.

Foti S, Mauromicale G, Raccuia SA, Fallico B, Fanella F, Maccarone E. 1999. Possible alternative utilization of *Cynara* spp. I. Biomass, grain yield and chemical composition of grain. *Industrial Crops and Products* 10: 219–228.

Franco C, Lopes H, Pinto F, Andre R, Cabrita GI. 2009. Gasification study of Cynara cardunculus to produce hydrogen rich gas. In: *Processing of the 17th European Biomass Conference*, Hamburg, Germany, p. 629–634.

Galmes J, Medrano H, Flexas J. 2007. Photosynthetic limitation in response to water stress and recovery in Mediterranean plants with different growth forms. *New Phytologist* 175: 81–93.

Garcia-Carbonell S, Yague B, Bleiholder H, Hack H, Meier U, Agusti M. 2002. Phenological growth stages of the persimmon tree (*Diospyros kaki*). *Annals of Applied Biology* 141: 73–76.

Gastal F, Lemaire G. 2002. N uptake and distribution in crops: an agronomical and ecophysiological perspective. *Journal of Experimental Botany* 53: 789–799.

Gerbens-Leenes PW, Hoekstra A, van der Meer T. 2008. Water footprint of bio-energy and other primary energy carriers. Value of Water Research Report Series No. 29. UNESCO-IHE, Delft, the Netherlands.

Geronikolou L, Danalatos NG, Archontoulis SV, Kalavriotou P, Papadakis G. 2004. An experiment study of sunflower oil production in Greece to be used as an alternative fuel. In: *Proceedings of the 2nd World Biomass Conference*, Roma, Italy, p. 612−615.

Geronikolou L, Archontoulis SV, Danalatos NG, Papadakis G, Kyritsis S. 2005. Economic opportunity for seed oil production in S. Europe by new sunflower varieties and under new C.A.P. conditions. In: *Proceedings of the 14th European Biomass Conference*, Paris, France, p. 1917−1920.

Gherbin P, Monteleone M, Tarantino E. 2001. Five year evaluation on cardoon (*Cynara cardunculus* L. var. *altilis*) biomass production in a Mediterranean environment. *Italian Journal of Agronomy* 5: 11–19.

Giannoulis KD, Archontoulis SV, Bastiaans L, Struik PC, Danalatos NG, 2008. Growth and seed yield of sunflower as affected by sowing time, irrigation and N-fertilization in central Greece. In: *Proceedings of the International Conference on Agricultural Engineering*, Crete, Greece (paper 10 pp. on CD).

Gimenez C, Connor DJ, Rueda F. 1994. Canopy development, photosynthesis and radiation-use efficiency in sunflower in response to nitrogen. *Field Crops Research* 38: 5–27.

Gominho J, Lourenço A, Curt M, Fernandez J, Pereira H. 2009. Characterization of hairs and pappi from *Cynara cardunculus* capitula and their suitability for paper production. *Industrial Crops and Products* 29: 116–125.

Gominho J, Lourenco A, Palma P, Lourenco ME, Curt MD, Fernandez J, Pereira H. 2011. Large scale cultivation of *Cynara cardunculus* L. for biomass production– A case study. *Industrial Crops and Products* 33: 1–6.

González J, Pérez F, Fernández J, Lezaun JA, Rodríguez D, Perea F, Romero C, Ochoa MJ, García M. 2004. Study of Cynara cardunculus L. lignocelullosic biomass production in dry conditions. *Acta Horticulturae* 660: 221–227.

Goskoy AT, Demir AO, Turan ZM, Dagustu N. 2004. Response of sunflower (*Helianthus annuus* L.) to full and limited irrigation at different growth stages. *Field Crop Research* 87: 167–178.

Goudriaan J. 1979. A family of saturation type curves, especially in relation to photosynthesis. *Annals of Botany* 43: 783–785.

Goudriaan J. 1988. The bare bones of leaf angle distribution in radiation models for canopy photosynthesis and energy exchange. *Agricultural and Forest Meteorology* 43: 155–169.

Goudriaan J, van Laar HH. 1994. Modelling potential crop growth processes. Dordrecht, The Netherlands: Kluwer Academic Publishers.

Grammelis P, Malliopoulou A, Basinas P, Danalatos NG. 2008. Cultivation and characterization of *Cynara cardunculus* for solid biofuels production in the Mediterranean region. *International Journal Molecular Science* 9: 1241–1258.

Griffin KL, Turnbull M, Murthy R. 2002. Canopy position affects the temperature response of leaf respiration in Populus deltoids. *New Phytologist* 154: 609–619.

Gu L, Pallardy SG, Tu K, Law BE, Wullschleger SD. 2010. Reliable estimation of biochemical parameters from C3 leaf photosynthesis–intercellular carbon dioxide response curves. *Plant, Cell and Environment* 33: 1852–1874.

Haberl H, Beringer T, Bhattacharya SC, Erb K-H, Hoogwijk M. 2010. The global technical potential of bio-energy in 2050 considering sustainability constraints. *Current Opinion in Environmental Sustainability* 2: 1–10.

Hack H, Bleiholder H, Buhr L, Meier U, Schnock-Fricke E, Weber E, Witzenberger A. 1992. Einheitliche Codierung der phänologischen Entwicklungsstadien mono-und dikotyler Pflanzen - Erweiterte BBCH-Skala, Allgemein. *Nachrichtenblatt des Deutschen Pflanzenschutzdienstes,* 44, 265–270.

Hall AJ, Connor DJ, Sadras VO. 1995. Radiation-use efficiency of sunflower crops: effects of specific leaf nitrogen and ontogeny. *Field Crops Research* 41: 65–77.

Harley PC, Thomas RB, Reynolds JF, Strain BR. 1992. Modelling photosynthesis of cotton grown in elevated CO_2. *Plant, Cell and Environment* 15: 271–282.

Harper JL, Lovell PH, Moore KG. 1970. The shapes and size of seeds. *Annual Review of Ecology and Systematics* 1: 327–356.

Hastings A, Clifton-Brown J, Wattenbach M, Mitchell CP, Smith P. 2009. The development of MISCANFOR, a new Miscanthus crop growth model: towards more robust yield predictions under different climatic and soil conditions. *Global Change Biology – Bioenergy* 1: 154–170.

Hein KRG. 2005. Future energy supply in Europe – challenge and chances. *Fuel* 84: 1189–1194.

Heinimo J, Junginger M. 2009. Production and trading of biomass for energy – an overview of the global status. *Biomass and Bioenergy* 33, 1310–1320.

Hess M, Barralis G, Bleiholder H, Buhr L, Eggers T, Hack H, Stauss R. 1997. Use of the extended BBCH scale-general for the description of the growth stages of mono- and dicotyledonous weed species. *Weed Research* 37: 433–441.

Hikosaka K. 2005. Nitrogen partitioning in the photosynthetic apparatus of *Plantago asiatica* leaves grown under different temperature and light conditions: similarities and differences between temperature and light acclimation. *Plant Cell Physiology* 46: 1283–1290.

Hillier J, Whittaker C, Dailey G, Aylott M, Casella E, Richter GM, Riche A, Murphy R, Taylor G, Smith P. 2009. Greenhouse gas emissions from four bioenergy crops in England and Wales: Integrating spatial estimates of yield and soil carbon balance in life cycle analyses. *Global Change Biology – Bioenergy* 1: 267–281.

Hirose T, Werger MJA. 1987. Maximizing daily canopy photosynthesis with respect to the leaf nitrogen allocation pattern in the canopy. *Oecologia* 72: 520–526.

Hirose T, Ackerly DD, Traw MB, Ramseirer D, Bazz FA. 1997. CO_2 elevation, canopy photosynthesis and optimal leaf area index. *Ecology* 78: 2339–2350.

Jaggard KW, Q1 A, Ober ES. 2010. Possible change to arable crop yields by 2050. *Philosophical transaction of the Royal Society, Biological Science* 365: 2835–2851.

Johnson MV, Kiniry JR, Burson BL. 2010. Ceptometer deployment method affects measurement of fraction of intercepted photosynthetically active radiation. *Agronomy Journal* 102: 1132–1137.

Jorgensen U, Mortensen J. 2000. Combined energy crop production and groundwater protection. In: Do energy crops have a future in Denmark? (Jorgensen U. ed.) DJF rapport Markbrug no. 29: 97–104.

Jorgensen U, Schelde K. 2001. Energy crop water and nutrient use efficiency. Report for the International Energy Agency, IEA Bioenergy Task 17, Short Rotation Crops. Denmark, pp. 38.

Jossart JM. 2009. Overview of energy crops and their uses in Europe. Presentation in Pulawy, Poland, Energy crops creating markets for heat and electricity Conference, September (http://www.encrop.net/default.asp?sivuID=23643).

Jurginger M, M, Faaij A, Rosillo-Calle F, Wood J. 2006. The growing role of biofuels–opportunities, challenges, and pitfalls. *International Sugar Journal* 108: 618–629.

IEA 2010. Key World Energy statistics. International Energy Agency, pp. 84, (http://www.iea.org/textbase/nppdf/free/2010/key_stats_2010.pdf).

IEA Bioenergy 2009. Bieoenergy – A sustainable and reliable energy source: A review of status and prospects. Report, pp. 136, (http://www.ieabioenergy.com/DocSet.aspx?id=6506&ret=lib).

Ierna A, Mauromicale C. 2010. *Cynara cardunculus* L. genotypes as a crop for energy purposes in a Mediterranean environment. *Biomass and Bioenergy* 34: 754–760.

Ishikawa K, Onoda Y, Hikosaka K. 2007. Intraspecific variation in temperature dependence of gas exchange characteristics among *Plantago asiatica* ecotypes from different temperature regimes. *New Phytologist* 176: 356–364.

Kallivroussis L, Natsis A, Papadakis G. 2002. The energy balance of sunflower production for biodiesel in Greece. *Biosystems Engineering* 81: 347–354.

Karp A, Shield I. 2008. Bioenergy from plants and the sustainable yield challenge. *New Phytologist* 179: 15–32.

Katerji N, Mastrorilli M, Rana G. 2008. Water use efficiency of crops cultivated in the Mediterranean region: Review and analysis. *European Journal of Agronomy* 28: 493–507.

Kiniry JR, Blanchet R, Williams JR, Texier V, Jones, CA, Cabelguenne M. 1992. Sunflower simulation using the EPIC and ALMANAC models. *Field Crops Research* 30: 403–423.

Kiniry JR, Tischler CR, Van Esbroeck GA. 1999. Radiation use efficiency and leaf CO_2 exchange for diverse C_4 grasses. *Biomass and Bioenergy* 17: 95–112.

Kosugi Y, Shibata S, Kobashi S. 2003. Parameterization of the CO_2 and H_2O gas exchange of several temperate deciduous broadleaved trees at the leaf scale considering seasonal changes. *Plant, Cell and Environment* 26: 285–301.

Krasuska E, Cadorniga C, Tenorio JL, Testa G, Scordia D. 2010. Potential land availability for energy crops production in Europe. *Biofuels, Bioproducts and Biorefining* 4: 658–673.

Lal R. 2010. Managing soils for a warming earth in a food-insecure and energy-starved world. *Journal of Plant Nutrition and Soil Science* 173: 4–15.

Lancashire PD, Bleiholder H, Langeluddecke P, Stauss R, van den Boom T, Weber E, Witzenberger A. 1991. A uniform decimal code for growth stages of crops and weeds. *Annals of Applied Biology* 119: 561–601.

Lapola DM, Schaldach R, Alcamo J, *et al.*, 2010. Indirect land-use changes can overcome carbon savings from biofuels in Brazil. *Proceedings of the National Academy of Sciences* 107: 3388–3393.

Lemus R, Lal R. 2005. Bioenergy crops and carbon sequestration. *Critical Reviews in Plant Sciences* 24: 1–21.

Leuning R. 2002. Temperature dependence of two parameters in a photosynthetic model. Plant, Cell and Environment 25: 1205–1210.

Leuning R, Kelliher FM, de Pury DGG, Schulze ED. 1995. Leaf nitrogen, photosynthesis, conductance and transpiration: scaling from leaves to canopies. *Plant, Cell and Environment* 18: 1183–1200.

Lindquist JL, Arkebauer TJ, Walters DT, Cassman KG, Dobermann A. 2005. Maize radiation use efficiency under optimal growth conditions. *Agronomy Journal* 97: 72–78.

Lisson SN, Mendham NJ, Carberry PS. 2000a. Development of a hemp (Cannabis sativa L.) simulation model. 1. General introduction and the effect of temperature on the pre-emergent development of hemp. *Australian Journal of Experimental Agriculture* 40: 405–411.

Lisson SN, Mendham NJ, Carberry PS. 2000b. Development of a hemp (Cannabis sativa L.) simulation model. 2. The flowering response of two hemp cultivars to photoperiod. *Australian Journal of Experimental Agriculture* 40: 413–417.

Lizaso J, Batchelor WD, Westgate ME. 2003. A leaf area model to simulate cultivar-specific expansion and senescence of maize leaves. *Field Crops Research* 80: 1–17.

Lopez-Bellido RJ, Lopez-Bellido L, Castillo JE, Lopez-Bellido FJ. 2003. Nitrogen uptake by sunflower as affected by tillage and soil residual nitrogen in a wheat-sunflower rotation under rainfed Mediterranean conditions. *Soil and Tillage Research* 72: 43–51.

Losavio N, Ventrella D, Lamascese N, Vonella AV. 1999. Growth, water and radiation use efficiency of kenaf (*Hibiscus cannabinus*) cultivated in the Mediterranean conditions. In: *Proceedings of the 4th Biomass Conference of the Americas* "Biomass a growth opportunity in green energy and value-added products", Oakland, California, p. 155–160.

Lötscher M, Stroh K, Schnyder H. 2003. Vertical leaf nitrogen distribution in relation to nitrogen status in grassland plants. *Annals of Botany* 92: 679–688.

Lychnaras V, Scheider UA. 2011. Multi-farm economic analysis of perennial energy crops in central Greece, taking into account the CAP reform. *Biomass and Bioenergy* 35: 700–715.

Maccarone E, Fallico B, Fanella F, Mauromicale G, Raccuia SA, Foti S. 1999. Possible alternative utilization of *Cynara* spp. II. Chemical characterization of their grain oil. *Industrial Crops and Products* 10: 229–237.

Madakadze IC, Coulman BE, Peterson P, Stewart KA, Samson R, Smith DL. 1998. Leaf area development, light interception, and yield among switchgrass populations in a short-season area. *Crop Science* 38: 827−834.

Maddonni GA, Chelle M, Drouet JL, Andrieu B. 2001. Light interception of contrasting azimuth canopies under square and rectangular plant spatial distributions: simulations and crop measurements. *Field Crops Research* 70: 1–13.

Magar SB, Pelkonen P, Tahvanainen L, Toivonen R, Toppinen A. 2011. Growing trade of bioenergy in the EU: Public acceptability, policy harmonization, European standards and certification needs. *Biomass and Bioenergy* 35: 3318–3327.

Makino A, Nakano H, Mae T. 1994. Effects of growth temperature on the responses of Ribulose-1.5-bisphosphate carboxylase, electron transport components, and sucrose synthesis enzymes to leaf nitrogen in rice, and their relationships to photosynthesis. *Plant Physiology* 105: 1231–1238.

Makino A, Sato T, Nakano H, Mae T. 1997. Leaf photosynthesis, plant growth and nitrogen allocation in rice under different irradiances. *Planta* 203: 390–398.

Mantineo M, D'Agosta GM, Copani V, Patanè C, Cosentino SL. 2009. Biomass yield and energy balance of three perennial crops for energy use in the semi-arid Mediterranean environment. *Field Crops Research* 114: 204–213.

Manzanares M, Tenorio JL, Eyerbe L. 1997. Sowing time, cultivar, plant population and application of N fertilizer on kenaf in Spain's central Plateu. *Biomass and Bioenergy* 12: 263–271.

Manzanares M, Tenorio JL, Manzanares P, Ayere L. 1993. Yield and development of kenaf (*Hibiscus cannabinus*) crop in relation to water supply and intercepted radiation. *Biomass and Bioenergy* 5: 337–345.

Medlyn BE, Dreyer E, Ellsworth D, Forstreuter M, *et al.*, 2002a. Temperature response of parameters of a biochemically based model of photosynthesis. II. A review of experimental data. *Plant, Cell and Environment* 25: 1167–1179.

Medlyn BE, Loustau D, Delzon S. 2002b. Temperature response of parameters of a biochemically based model of photosynthesis. I. Seasonal changes in mature maritime pine (*Pinus pinaster* Alt.). *Plant, Cell and Environment* 25: 1155–1165.

Meier U. 1997. BBCH–Monograph. Growth stages of plants - Entwicklungsstadien von Pflanzen – Estadios de las plantas – Développement des Plantes. Blackwell Wissenschaftsverlag, Berlin und Wien, p 622.

Meier U, Bheiholder H, Brumme H, Mehring B, Proll T, Wiegand J. 2009b. Phenological growth stages of roses (*Rosa* sp.): Codification and description according to the BBCH scale. *Annals of Applied Biology* 154: 231–238.

Meier U, Bleiholder H, Buhr L, Feller C, Hack H, *et al.*, 2009a. The BBCH system to coding the phenological growth stages of plants – history and publications–. *Journal für Kulturpflanzen* 61: 41–52.

Melillo JM, Reilly JM, Kicklighter DW *et al.*, 2009. Indirect emissions from biofuels: how important? *Science* 326: 1397–1399.

Menichetti E, Otto M. 2009. Energy balance and greenhouse gas emissions of biofuels from a life-cycle perspective. In: *Proceedings of the Scientific Committee on Problems of the Environment* (SCOPE) *International Biofuels Project Rapid Assessment*, Gummersbach Germany. Cornell University, Ithaca NY, USA, (http://cip.cornell.edu/biofuels/), p. 81–109.

Miao Z, Xu M, Lathrop JR, Wange Y. 2009. Comparison of the *A*–*Cc* curve fitting methods in determining maximum ribulose 1·5-bisphosphate carboxylase/oxygenase carboxylation rate, potential light saturated electron transport rate and leaf dark respiration. *Plant, Cell and Environment* 32: 109–122.

Milroy SP, Bange MP, Sadras VO. 2001. Profiles of leaf nitrogen and light in reproductive canopies of cotton (*Cossypium hirsutum*). *Annals of Botany* 87: 325–333.

Monsi M, Saeki T. 2005. On the factor light in plant communities and its importance for matter production. *Annals of Botany* 95: 549–567.

Monteith JL. 1977. Climate and the efficiency of crop production in Britain. *Philosophical Transactions of the Royal Society*, London, B. 281: 227–294.

Monti A, Di Virgilio N, Venturi G. 2008. Mineral composition and ash content of six major energy crops. Biomass and Bioenergy 32: 216–223.

Monti A, Fazio S, Venturi G. 2009. Cradle-to-farm gate life cycle assessment in perennial energy crops. *European Journal of Agronomy* 31: 77–84.

Muchow RC. 1979. Effects of plant population and season on kenaf (*Hibiscus cannabinus* L.) grown under irrigation in tropical Australia. II. Influence on growth parameters and yield prediction. *Field Crops Research* 2: 67–76.

Muchow RC. 1990. Effect of leaf nitrogen and water regime on the photosynthetic capacity of kenaf (*Hibiscus cannabinus*) under field conditions. *Australian Journal of Agricultural Research* 41: 845–852.

Muchow RC. 1992. Effect of water and nitrogen supply on radiation interception and biomass accumulation of kenaf (*Hibiscus cannabinus*) in a semi-arid tropical environment. *Field Crops Research* 28: 281–293.

Mueller SA, Anderson JE, Wallington TJ. 2011. Impact of biofuel production and other supply and demand factors on food price increase in 2008. *Biomass and Bioenergy* 35: 1623–1632.

Müller J, Braune H, Diepenbrock W. 2008. Photosynthesis–stomatal conductance model LEAFC3-N: specification for barley, generalised nitrogen relations and aspects of model application. *Functional Plant Biology* 35: 797–810.

Müller J, Wernecke P, Diepenbrock W. 2005. LEAFC3–N: a nitrogen sensitive extension of the CO_2 and H_2O gas exchange model LEAFC3 parameterized

and tested for winter wheat (*Triticum aestivum* L.). *Ecological Modelling* 183: 183–210.

Neill C. 2011. Impacts of crop residue management on soil organic matter stocks: A modelling study. *Ecological Modelling* 222: 2751–2760.

Niinemets Ü. 2010. A review of light interception in plants stands from leaf to canopy in deferent plant functions types and in species with varying shade tolerance. *Ecological Research* 25: 693–714.

Niinemets Ü, Ellsworth D, Lukjanova A, Tobias M. 2001. Site fertility and the morphological and photosynthetic acclimation of *Pinus sylvestris* needles to light. *Tree Physiology* 21: 1231–1244.

Niinemets Ü, Tenhunen JD. 1997. A model separating leaf structural and physiological effects on carbon gain along light gradients for the shade-tolerant species *Acer saccharum*. *Plant, Cell and Environment* 20: 845–865.

Nilsson D, Bernesson S, Hansson P-A. 2011. Pellets production from agricultural raw materials–A systems analysis. *Biomass and Bioenergy* 35: 679–689.

O'Connell M, O'Leary GJ, Whitfield DM, Connor DJ. 2004. Interception of photosynthetically active radiation and radiation-use efficiency of wheat, field pea and mustard in a semi-arid environment. *Field Crops Research* 85: 111–124.

Ohlrogge J, Allen D, Berguson B, DellaPenna D, Scachar-Hill Y, Stymne S. 2009. Driving on Biomass. *Science* 34: 1019–1020.

Ow FL, Griffin KL, Whitehead D, Walcroft AS, Turnbull M. 2008. Thermal acclimation of leaf respiration but not photosynthesis in *Populus deltoides × nigra*. *New Phytologist* 178: 123–134.

Ozdemir ED, Hardtlein M, Eltrop L. 2009. Land substitution effects of biofeul side products and implication on the land are required for EU 2020 biofuels targets. *Energy Policy* 37: 2986–2996.

Panoutsou C. 2007. Socio-economic impacts of energy crops for heat generation in Northern Greece. *Energy Policy* 35: 6046–6059.

Pari L, Civitaresa V, Assirelli A, del Guidice A. 2009. Prototype for cynara cardunculus capitula thressing and biomass windrowing. In: *Proceedings of the 17th European Biomass Conference*, Hamburg, Germany, p. 262–267.

Passioura JB. 2002. Review: Environmental biology and crop improvement. *Functional Plant Biology* 29: 537–546.

Patanè C, Sortino O. 2010. Seed yield in kenaf (*Hibiscus cannabinus* L.) as affected by sowing time in south Italy. *Industrial Crops and Products* 32: 381–388.

Patric LD, Ogle K, Tissue DT. 2009. A hierarchical Bayesian approach for estimation of photosynthetic parameters of C_3 plants. *Plant, Cell and Environment* 32: 1695–1709.

Pereyra-Irujo GA, Aguirrezábal LAN. 2007. Sunflower yield and oil quality interactions and variability: Analysis through a simple simulation model. *Agricultural and Forest Meteorology* 143: 252–265.

Piscioneri I, Sharma N, Baviello G, Orlandini S. 2000. Promising industrial energy crop, *Cynara cardunculus*: a potential source for biomass production and alternative energy. *Energy Conversion and Management* 41: 1091–1105.

Ploschuk EL, Slafer GA, Ravetta DA. 2005. Reproductive allocation of biomass and nitrogen in annual and perennial *Lesquerella* crops. *Annals of Botany* 96: 127–135.

Pons TL, Flexas J, von Caemmerer S, Evans JR, Genty B, Ribas-Carbo M, Brugnoli E. 2009. Estimating mesophyll conductance to CO_2: methodology, potential errors, and recommendations. *Journal of Experimental Botany* 60: 2217–2234.

Pons TL, Jordi W, Kuiper D. 2001. Acclimation of plants to light gradients in leaf canopies: evidence for a possible role for cytokinins transported in the transpiration stream. *Journal of Experimental Botany* 52: 1563–1574.

Pons TL, Welschen RAM. 2002. Overestimation of respiration rates in commercially available clamp-on leaf chambers. Complications with measurement of net photosynthesis. *Plant, Cell and Environment* 25: 1367–1372.

Poorter H, Evans JR. 1998. Photosynthetic nitrogen-use efficiency of species that differ inherently in specific leaf area. *Oecologia* 116: 26–37.

Proctor JTA, Dorais M, Bleiholder H, Willis A, Hack H, Meier V. 2003. Phenological growth stages of North Americal ginseng (*Panax quinquefolius*). *Annals of Applied Biology* 143: 311–317.

Pronk AA, Goudriaan J, Stilma E, Challa H. 2003. A simple method to estimate radiation interception by nursery stock conifers: a case study of eastern white cedar. *Netherlands Journal of Agricultural Sciences* 51: 279–295.

Quilhó T, Gominho J, Pereira H. 2004. Anatomical characterization and variability of the thistle *Cynara cardunculus* in view of pulping potential. *IAWA Journal* 25: 217–230.

Quaranta E, Belocchi A, Bottazzi P, Monotti M, Del Pino AM, Desiderio E. 2000. Limited water supply on kenaf (*Hibiscus cannabinus* L.) in central Italy. *Italian Journal of Agronomy* 4: 1–9.

Raccuia SA, Cavallaro V, Melilli MG. 2004. Intraspecific variability in *Cynara cardunculus* L. var. sylvestris Lam. Sicilian populations Seed germination under salt and moisture stresses. *Journal of Arid Environments* 56: 107–116.

Raccuia SA, Melilli MG. 2004. Genetic variation for assimilate accumulation and translocation in Cynara spp. *Acta Horticulturae* 660: 241–248.

Raccuia SA, Melilli MG. 2007a. Biomass and grain oil yields in *Cynara cardunculus* L. genotypes grown in a Mediterranean environment. *Field Crop Research* 101: 187–197.

Raccuia SA, Melilli MG. 2007b. Plant architecture and biomass partitioning variation as affected by plant density in *Cynara cardunculus* L. var. *sylvestris* Lam. *Acta Horticulturae* 730: 149–155.

Ragauskas AJ, Williams CK, Davison BH *et al.*, 2006. The path forward for biofuels and biomaterials. *Science* 311: 484–489.

Ramachandra Reddy A, Rama Das VS. 2000. Photosynthesis and kinetic characteristics of rubisco in *Hibiscus cannabinus* L. *Indian Journal of Experimental Biology 38*: 841–844.

Ragwitz M, Schleich J, Huber C, Resch G, Faber T, Voogt M, Coenraads R, Cleijne H, Bodo P. 2005. FORRES 2020: Analysis of the renewable energy sources evolution up to 2020. Final report. (http://www.eeg.tuwien.ac.at/eeg. tuwien.ac.at_pages/research/downloads/PR_30_FORRES_summary.pdf).

Rawson HM, Dunstone RL, Long MJ, Begg JE. 1984. Canopy development, light interception and seed production in sunflower as influenced by temperature and radiation. *Australian Journal Plant Physiology* 11: 255–265.

Reich PB, Walters MB, Ellsworth DS, Vose JM, Volin JC, Gresham C, Bowman WD. 1998. Relationships of leaf dark respiration to leaf nitrogen, specific leaf area and leaf life-span: A test across biomes and functional groups. *Oecologia* 114: 471–482.

Rettenmaier N, Köppen S, Gärtner SO, Reinhardt GA. 2010. Life cycle assessment of selected future energy crops for Europe. *Biofuels, Bioproducts and Biorefining* 4: 620–636.

Rinaldi M. 2001. Application of EPIC model for irrigation scheduling of sunflower in southern Italy. *Agricultural Water Management* 49: 185–196.

Rinaldi M, Losavio N, Flagella Z. 2003. Evaluation and application of the OILCROP-SUN model for sunflower in southern Italy. *Agricultural Systems* 78: 17–30.

Robinson RG. 1971. Sunflower phenology, year, variety, and date of planting effects on day and growing degree-day summations. *Crop Science* 11: 635–638.

Romo-Fernandez LM, Lopez-Pujalte C, Bote VPG, Anegon FM. 2011. Analysis of Europe's scientific production on renewable energies. *Renewable Energy* 36: 2529–2537.

Rosati A, Badeck FW, Dejong TM. 2001. Estimating canopy light interception and absorption using leaf mass per unit leaf area in Solanum melongena. *Annals of Botany* 88: 101–109.

Rosenthal WD, Gerik TJ. 1991. Radiation use efficiency among cotton cultivars. *Agronomy Journal* 83: 655–658.

Ruffo ML, Garcia FO, Bollero GA, Fabrizzi K, Ruiz RA. 2003. Nitrogen balance approach to sunflower fertilization. *Communications in Soil Science and Plant Analysis* 34: 2645–2657.

Ruiz RA, Maddonni GA. 2006. Sunflower seed weight and oil concentration under different post-flowering source-sink ratios. *Crop Science* 46: 671–680.

Sadras VO. 2007. Evolutionary aspects of the trade-off between seed size and number in crops. *Field Crops Research* 100: 125–138.

Sadras VO, Hall AJ, Connor DJ. 1993. Light-associated nitrogen distribution profile in flowering canopies of sunflower (*Helianthus annuus* L.) altered during grain growth. *Oecologia* 95: 488–494

Sadras VO, Villalobos FJ. 1993. Floral initiation, leaf initiation and leaf appearance in sunflower. *Field Crops Research* 33: 449–457.

Sadras VO, Whitfield DM, Connor DJ. 1991. Regulation of evapotranspiration, and its partitioning between transpiration and soil evaporation by sunflower crops: a comparison between hybrids of different stature. *Field Crops Research* 28: 17–37.

Sage RF, Rearcy RW. 1987. The nitrogen use efficiency of C_3 and C_4 plants. II. Leaf nitrogen effects on the gas exchange characteristics of *Chenopodium album* L. and *Amaranthus retroflexus* L. *Plant Physiology* 84: 959–963.

Saidur R, Abdelaziz EA, Mekhilef S. 2011a. A review on electrical and thermal energy for industries. Renewable and Sustainable Energy Reviews 15: 2073–2086.

Saidur R, Abdelaziz EA, Demirbas A, Hossain MS, Mekhilef S. 2011b. A review on biomass as a fuel for boilers. *Renewable and Sustainable Energy Reviews* 15: 2262–2289.

Sands PJ. 1995. Modelling canopy production. I. Optimal distribution of photosynthetic resources. *Australian Journal Plant Physiology* 22: 593–601.

Sartori F, Lal R, Ebinger MH, Parrish DJ. 2006. Potential soil carbon sequestration and CO_2 offset by dedicated energy crops in the USA. *Critical Reviews in Plant Sciences* 25: 441–472.

Sassenrath-Cole GF. 1995. Dependence of canopy light distribution on leaf and canopy structure for two cotton (*Gossypium*) species. *Agricultural and Forest Meteorology* 77: 55–72.

Schneiter AA, Miller JF. 1981. Description of sunflower growth stages. *Crop Science* 85: 901–903.

Schultz HR. 2003. Extension of a Farquhar model for limitation of leaf photosynthesis induced by light environment, phenology and leaf age in grapevines (*Vitis vinifera* cv. White Riesling and Zinfabdel). *Functional Plant Biology* 30: 673–687.

Searchinger TD, Heimlich R, Dong F, *et al.*, 2008. Use of US croplands for biofuels increases greenhouse gases through emissions from land-use change. *Science* 319: 1238–1540.

Searle SY, Thomas S, Griffin KL, Horron T, Kornfeld, Yakir D, Hurry V, Turnbull MH. 2011. Leaf respiration and alternative oxidase in field-grown alpine grasses to natural changes in temperature and light. *New Phytologist* 189: 1027–1039.

Semere T, Slater F. 2007. Ground flora, small mammal and bird species diversity in miscanthus (*Miscanthus_giganteus*) and reed canary-grass (*Phalaris arundinacea*) fields. *Biomass and Bioenergy* 31: 20–29.

Sharkey TD. 1985. Photosynthesis in intact leaves of C3 plants: physics, physiology and rate limitations. *Botanical Review* 51: 53–105.

Sharkey TD, Bernacchi CJ, Farquhar GD, Singass EL. 2007. Fitting photosynthetic carbon dioxide response curves for C_3 leaves. *Plant, Cell and Environment* 30: 1035–1040.

Sharp RE, Matthews MA, Boyer JS. 1984. Kok effect and the quantum yield of photosynthesis. Light partially inhibits dark respiration. *Plant Physiology* 75: 95–101.

Shiraiwa T, Sinclair TR. 1993. Distribution of nitrogen among leaves in soybean canopies. *Crop Science* 33: 804–808.

Silim SN, Ryan N, Kubien DS. 2010. Temperature of photosynthesis and respiration in *Populus balsamifera* L.: acclimation versus adaptation. *Photosynthesis Research* 104: 19–30.

Sims REH, Hastings A, Schlamadinger B, Taylor G, Smith P. 2006. Energy crops: current status and future prospects. *Global Change Biology* 12: 2054–2076.

Sinclair TR. 2006. A reminder of the limitations in using Beer's law to estimate daily radiation interception by vegetation. *Crop Science* 46: 2343–2347.

Sinclair TR, Horie T. 1989. Leaf nitrogen, photosynthesis, and crop radiation use efficiency: a review. *Crop Science* 29: 90–98.

Sinoquet H, Rakocevic M, Varlet-Grancher C. 2000. Comparison of models for daily light partitioning in multispecies canopies. *Agricultural and Forest Meteorology* 101: 251–263.

Skoulou V, Mariolis N, Zanakis G, Zabaniotou A. 2011. Sustainable management of energy crops for intergrated biofuels and green energy production in Greece. *Renewable and Sustainable Energy Reviews* 15: 1928–1936.

Smith JM, Froment MA. 1998. A growth stage key for winter linseed (*Linum usitatissimum*). *Annals of Applied Biology* 133: 297–306.

Sonnante G, Pibnone D, Hammer K. 2007. The domestication of artichoke and cardoon: From Roman times to the genomic age. A review. *Annals of Botany* 100: 1095–1100.

Steer BT, Milroy SP, Kamona RM. 1993. A model to simulate the development, growth and yield of irrigated sunflower. *Field Crops Research* 32: 83–99.

Su Y, Zhu G, Miao Z, Feng Q, Chang Z. 2009. Estimation of parameters of a biochemically based model of photosynthesis using a genetic algorithm. *Plant, Cell and Environment* 32: 1710–1723.

Thornley JHM. 2002. Instantaneous canopy photosynthesis: analytical expressions for sun and shade leaves based on exponential light decay down the canopy and an acclimated non-rectangular hyperbola for leaf photosynthesis. *Annals of Botany* 89: 451–458.

Tilman D, Hill J, Lehman C. 2006. Carbon-negative biofuels from low-input high-diversity grassland biomass. *Science* 314: 1598–1600.

Timmermans BGH, Vos J, van Nieuwburg J, Stomph TJ, van der Putten PEL. 2007. Germination rates of Solanum sisymbriifolium: temperature response models, effects of temperature fluctuations and soil water potential. *Seed Science Research* 17: 221–231.

Trudgill DL, Honek A, van Straalen NM. 2005. Thermal time – concepts and utility. *Annals of Applied Biology* 146: 1–14.

Tuck G, Glendining MJ, Smith P, House JI, Wattenbach M. 2006. The potential distribution of bioenergy crops in Europe under present and future climate. *Biomass and Bioenergy* 30: 183–197.

Turnbull MH, Whitehead D, Tissue DT, Schuster WSF, Brown KL, Griffin KL. 2003. Scaling foliar respiration in two contrasting forest canopies. *Functional Ecology* 17: 101–114.

Tuzet A, Perrier A, Leuning R. 2003. A coupled model of stomatal conductance, photosynthesis and transpiration. *Plant, Cell and Environment* 26: 1097–1116.

USDA 1975. Soil taxonomy. Basic system of soil classification for making and interpreting soil surveys. Agricultural Handbook, Washington, DC, vol. 466, pp. 754.

Valentini R, Matteucci G, Dolman AJ, *et al.,* 2000. Respiration as the main determinant of carbon balance in European forests. *Nature* 404: 861–865.

Valladares F, Pugnaire FI. 1999. Tradeoffs between irradiance capture and avoidance in semi-arid environments assessed with a crown architecture model. *Annals of Botany* 83: 459–469.

Vamvuka D, Topouzi V, Sfakiotakis S, Pentari D, Chistou M. 2009. Production yield and combustion characteristics of cardoon grown as a potential feedstock for energy application in Greece. In: *Proceedings of the 17th European Biomass Conference*, Hamburg, Germany, p. 1269–1272.

Van Dam J, Faaij APC, Lewandowski I, Fischer G. 2008. Biomass production potentials in Central and Eastern Europe under different scenarios. *Biomass and Bioenergy* 31: 345–366.

van Ittersum MK, Leffelaar PA, van Keulen H, Kropff MJ, Bastiaans L, Goudriaan J. 2003. On approaches and applications of the Wageningen crop models. *European Journal of Agronomy* 18: 201–234.

van Keulen H. 1982. Graphical analysis of annual crop response to fertiliser application. *Agricultural Systems* 9: 113–126.

van Oosterom EJ, Borrell AK, Chapman SC, Broad IJ, Hammer GL. 2010. Functional dynamics of the nitrogen balance in sorghum: I. N demand of vegetative plant parts. *Field Crop Research* 115: 19–28.

van Vliet AJH, de Groot RS, Bellens Y, *et al.,* 2003. The European Phenology Network. *International Journal of Biometeorology* 47: 202–212.

Vega CRC, Sadras VO, Andrade FH, Uhart SA. 2000. Reproductive allometry in soybean, maize and sunflower. *Annals of Botany* 85: 461–468.

Venturi P, Venturi G. 2003. Analysis of energy comparison for crops in European agricultural systems. *Biomass and Bioenergy* 25: 235–255.

Vico G, Porporato A. 2008. Modelling C_3 and C_4 photosynthesis under water-stressed conditions. *Plant Soil* 313: 187–203.

Villalobos FJ, Hall AJ, Ritchie JT, Orgaz F. 1996. OILCROP-SUN: A development, growth, and yield model of the sunflower crop. *Agronomy Journal* 88: 403–415.

Villalobos FJ, Ritchie JT. 1992. The effect of temperature on leaf emergence rates of sunflower genotypes. *Field Crops Research* 29: 37–46.

Virdis A, Motzo R, Giunta F. 2009. Key phenological events in globe artichoke (*Cynara cardunculus* var. *scolymus*) development. *Annals of Applied Biology* 155: 419–429.

von Caemmerer S, Farquhar GD. 1981. Some relationships between the biochemistry of photosynthesis and the gas exchange of leaves. *Planta* 153: 376–387.

von Caemmerer S, Farquhar G, Berry J. 2009. Biochemical model of C_3 photosynthesis. In: Laisk A, Nebal L and Govindjee (eds), Photosynthesis in silico: Understanding Complexity from Molecules to Ecosystems. Springer Science+Business Media BV, pp. 209–230.

Vos J. 1997. The nitrogen response of potato (*Solanum tuberosum* L.) in the field: nitrogen uptake and yield, harvest index and nitrogen concentration. *Potato Research* 40: 237–248.

Vos J. 2009. Nitrogen responses and nitrogen management in potato. *Potato Research* 52: 305–317.

Vos J, Evers JB, Buck-Sorlin GH, Andrieu B, Chelle M, de Visser PHB. 2010. Functional–structural plant modelling: a new versatile tool in crop science. *Journal of Experimental Botany* 61: 2101–2115.

Wang W-M, Li Z-L, Su H-B. 2007. Comparison of leaf angle distribution functions: Effects on extinction coefficient and fraction of sunlit foliage. *Agricultural and Forest Meteorology* 143: 106–122.

Warren CR. 2004. The photosynthetic limitation posed by internal conductance to CO_2 movement is increased by nutrient supply. *Journal of Experimental Botany* 55: 2313–2321.

Webber CL. 1993. Crude protein and yield components of six kenaf cultivars as affected by crop maturity. *Industrial Crops and Products* 2: 27–31.

Webber CL, Bhardwaj HL, Bledsoe VK. 2002. Kenaf Production: Fiber, Feed, and Seed. In: Trends in new crops and new uses. 2002. Janick J, Whipkey A (eds). ASHS Press, Alexandria, VA, p. 327–339.

White VA, Holt JS. 2005. Competition of artichoke thistle (*Cynara cardunculus*) with native and exotic grassland species. *Weed Science* 53: 826–833.

Williams RL. 1994. Genetic variation of the control of flowering in kenaf with emphasis on the ambiphotoperiodic response of cultivar Guatemala 4. *Industrial Crops and Products* 2: 161–170.

Wilson KB, Baldocchi DD, Hanson PJ. 2000. Spatial and seasonal variability of photosynthetic parameters and their relationship to leaf nitrogen in a deciduous forest. *Tree Physiology* 20: 565–578.

Wilson KB, Baldocchi DD, Hanson PJ. 2001. Leaf age affects the seasonal pattern of photosynthetic capacity and net ecosystem exchange of carbon in a deciduous forest. *Plant, Cell and Environment* 24: 571–583.

Wise MA, Calvin KV, Thomson AM, *et al*. 2009. The implications of limiting CO2 concentrations for agriculture, land use, land use change emissions and bioenergy. *Science* 324: 1183–1186.

Wise RR, Olson AJ, Schrader SM, Sharkey TD. 2004. Electron transport is the functional limitation of photosynthesis in field-grown Pima cotton plants at high temperature. *Plant, Cell and Environment* 27: 717–724.

Wohlfahrt G, Bahn M, Haufner E, Horak I, Michaeler W, Rottmar K, Tappeiner U, Cerbusca A. 1999. Inter-specific variation of the biochemical limitation to photosynthesis and related leaf traits of 30 species from mountain grassland ecosystems under different land use. *Plant, Cell and Environment* 22: 1281–1296.

Wohlfahrt G, Bahn M, Horak I, Tappeiner U, Cerbusca A. 1998. A nitrogen sensitive model of leaf carbon dioxide and water vapour gas exchange: application to 13 key species from differently managed mountain grassland ecosystems. *Ecological Modelling* 113: 179–199.

Wright GC, Hammer GL. 1994. Distribution of nitrogen and radiation use efficiency in peanut canopies. *Australian Journal of Agricultural Research* 45: 565–74.

Wullschleger SD. 1993. Biochemical limitations to carbon assimilation in C_3 plants – a retrospective analysis of the A/C_i curves from 109 species. *Journal of Experimental Botany* 44: 907–920.

Yamori W, Evans JR, von Caemmerer S. 2010. Effects of growth and measurement light intensities on temperature dependence of CO_2 assimilation rate in tobacco leaves. *Plant, Cell and Environment* 33: 332–343.

Yamori W, Nogughi K, Terashima I. 2005. Temperature acclimation of photosynthesis in spinach leaves: analyses of photosynthetic components and temperature dependencies of photosynthetic partial reactions. *Plant, Cell and Environment* 28: 536–547.

Yin X. 2008. Analysis of reciprocal-transfer experiments to estimate the length of phases having different responses to temperature. *Annals of Botany* 101: 603–611.

Yin X, Goudriaan J, Lantinga EA, Vos J, Spiertz JHJ. 2003b. A flexible sigmoid function of determinate growth. *Annals of Botany* 91: 361–371.

Yin X, Lantinga EA, Schapendonk AHCM, Zhong X. 2003a. Some quantitative relationships between leaf area index and canopy nitrogen content and distribution. *Annals of Botany* 91: 893–903.

Yin X, Schapendonk ADHCM, Kroff M, van Oijen M, Bindraban PS. 2000. A Generic equation for nitrogen-limited leaf area index and its application in crop growth models for predicting leaf senescence. *Annals of Botany* 85: 579–585.

Yin X, Struik PC, Tang J, Qi C, Liu T. 2005. Model analysis of flowering phenology in recombinant inbred lines of barley. *Journal of Experimental Botany* 56: 959–965.

Yin X, Struik PC. 2009a. C_3 and C_4 photosynthesis models: An overview from the perspective of crop modelling. *NJAS–Wageningen Journal of Life Sciences* 57: 27–38.

Yin X, Struik PC. 2009b. Theoretical reconsiderations when estimating the mesophyll conductance to CO_2 diffusion in leaves of C_3 plants by analysis of combined gas exchange and chlorophyll fluorescence measurements. *Plant, Cell and Environment* 32: 1513–1524.

Yin X, Struik PC. 2010. Modelling the crop: from system dynamics to systems biology. *Journal of Experimental Botany* 61: 2171–2183.

Yin X, Struik PC, Romero P, Harbinson J, Evers JB, van den Putten PEL, Vos J. 2009. Using combined measurements of gas exchange and chlorophyll fluorescence to estimate parameters of a biochemical C_3 photosynthesis model: a critical appraisal and a new integrated approach applied to leaves in a wheat (*Triticum aestivum*) canopy. *Plant, Cell and Environment* 32: 448–464.

Yin X, Sun Z, Struik PC, Gu J. 2011. Evaluating a new method to estimate the rate of leaf respiration in the light by analysis of combined gas exchange and chlorophyll fluorescence measurements. *Journal of Experimental Botany* 62: 3489–3499.

Yin X, van Laar HH. 2005. Crop System Dynamics. An Ecophysiological Simulation Model for Genotype-by-environment Interactions. Wageningen Academic Publishers, Wageningen, The Netherlands, pp. 153.

Yin X, van Oijen M, Schapendonk AHCM. 2004. Extension of a biochemical model for the generalized stoichiometry of electron transport limited C_3 photosynthesis. *Plant, Cell and Environment* 27: 1211–1222.

Yuan JS, Tiller KH, Al-Ahmad H, Stewart NR, Stewart Jr NC. 2008. Plants to power: bioenergy to fuel the future. *Trends in Plant Science* 13: 421–429.

Yusuf NNAN, Kamarudin SK, Yaakub Z. 2011. Overview on the current trends in biodiesel production. *Energy Conversion and Management* 52: 2741–2751.

Zadoks JC, Chang TT, Konzak CF. 1974. A decimal code for the growth stages of cereals. *Weed Research* 14: 415–421.

Zaffaroni E, Schneiter AA. 1989. Water-use efficiency and light interception of semidwarf and standard-height sunflower hybrids grown in different row arrangements. *Agronomy Journal* 81: 831–836.

Zatta A, di Virgilio N, Vecchi A, Monti A. 2010. Hemp and Kenaf: Potential feedstocks for second generation bioethanol in south Europe. Presentation available at: http://ccgconsultinginc.com/Documents/Track%204-%20alessandro%20zatta.pdf

Zegada-Lizarazu W, Elbersen HW, Cosentino S, Zatta A, Alexopoulou E, Monti A. 2010. Agronomic aspects of future energy crops in Europe. *Biofuels, Bioproducts and Biorefining* 4: 674–691.

Zegada-Lizarazu W, Monti A. 2011. Energy crops in rotation. A review. *Biomass and Bioenergy* 35: 12–25.

Zuibillaga MM, Aristi JP, Lavado RS. 2002. Effect of phosphorus and nitrogen fertilization on sunflower (*Helianthus annuus* L.) nitrogen uptake and yield. *Journal of Agronomy and Crop Science* 188: 267–274.

Summary

Energy production from plants is a "hot" research topic worldwide, driven by concerns about energy and food security and climate change. In 2005, bioenergy provided 10% to total primary energy worldwide, while its potential has been estimated to be three to ten times higher, indicating that plants are grossly underexplored. Forest trees and wood residues are the major source of bioenergy (~68%), but this source has reached a near saturation point. Energy crops, the main source for transport bio-fuels, currently contribute a small proportion (~3%) to total bioenergy, but the proportion is bound to grow over the next few decades, in the EU to 10% by 2020.

Options to increase bioenergy production from agricultural crops include increasing area and/or yields and employing more efficient conversion technologies. Prerequisite to all these options is a good knowledge of the crops. However, it is generally recognized that in spite of the fast bioenergy growth worldwide, there is a lack of strong experimental data and field experience to support this growth. This limitation is particularly noticeable for the agronomy and crop physiology of new energy crops. Such information is needed for the farmers, breeders, researchers, and modellers to allow them to better evaluate future agricultural land uses, and genetics to improve biomass quantity and quality. Obviously data sets from different regions with different soil-climatic conditions and on different cropping systems should be created.

In line with this general objective, this thesis provides essential information on phenology, agronomy and crop physiology of three (Mediterranean) bioenergy crops: *Helianthus annuus* (sunflower), *Hibiscus cannabinus* (kenaf) and *Cynara cardunculus* (cynara). Among several candidate species, we have chosen the above because these crops cover a wide range of bio-industrial applications, fit into different cropping strategies (short or long growing periods, cultivation with or without irrigation, etc.) and previous studies have shown promising results in terms of biomass productivity. For these species we identified important knowledge gaps and performed a series of field experiments to fill these gaps and to generate quantitative parameters to feed crop growth models. These gaps together with an update about bioenergy production are provided in the introduction chapter (**Chapter 1**) of this thesis. Then, in the following five chapters (**Chapters 2–6**) research results gained in the experimental phase of the study are presented. In the final chapter (**Chapter 7**) the overall contribution of this study is discussed.

Chapter 2 presents the phenological growth stages of *Cynara cardunculus* L. (var. *altilis* DC.) based on the BBCH scale and its associated decimal code. Basically,

the scale and the code have been designed so that the numerical value of the code increases from 0 to 100 as the plant develops. Nine principal growth stages were defined and each principal stage was subdivided into secondary growth stages. Descriptive keys with illustrations and a practical use of the scale were proposed. This scale can be used by anyone involved in the production of cynara and it can be applied under all circumstances, irrespectively of the rate of development that varies among regions and varieties. Additionally, this code provides precise start and end points of each development stage, which are essential in studies on the effect of temperature on development rate. The most important BBCH stages that require particular attention by the farmers and researchers are: (a) stages 00–15: proper time for sowing according to climate of each production area and mechanical weed control during the first year; (b) principal stages 4–6: the crop can be harvested for forage feed; and (c) principal stages 5–7: crop nutrients requirements maximised.

Chapter 3 provides comprehensive information on *Cynara cardunculus* seed and biomass productivity from 16 field experiments varying in crop age and environmental × management conditions in Greece. We present a robust and easily applicable methodology to estimate seed yield overcoming problems arising from the compound structure of the crop's inflorescences. Indeed, within a plant or a unit area the heads of cynara are variable in terms of size, number, maturity and position on the plant, while within a head, seeds (achenes) are positioned at the base of the head (receptacle) surrounded by hairs (pappus) and bracts (erect spines). By measuring two simple inflorescence traits, total weight (HW) and number (HN) of all seed bearing heads per unit area, the seed yield (SY) per unit area could be estimated as: $SY = 0.43 \cdot HW - 2.9 \cdot HN$. This model was tested against current and published data from Italy and proved to be valid under variable management practices (e.g. plant arrangements) and environmental conditions (r^2=0.93). Attainable cynara seed yields ranged from 1.9 to 4.8 t ha^{-1} yr^{-1}, on dry soils and on soils with shallow ground water level. The corresponding biomass yields ranged from 13 to 27 t ha^{-1} yr^{-1}, respectively. During the first cropping cycle, seed and biomass yields were 57–80% lower than in subsequent cycles. The variation in seed yield was sufficiently explained by the analyses of head-weight distribution (small, medium and large heads) and variability of seed/head weight ratio at head level. Seed quality characteristics such as oil (23%) and protein (19%) concentration was rather invariant through different seed sizes (range: 26–56 mg seed^{-1}) as well as growing environments, meaning that under Greek conditions, these fixed values can be used to estimate seed oil and protein yields.

Chapter 4 provides information at canopy level and shows spatial-temporal dynamics of leaf area index (LAI), specific leaf area (SLA), nitrogen concentration (N_{conc}), and the specific leaf nitrogen content (SLN) in relation to water availability for all tested species. Two very important parameters for crop modelling, the light (K_L) and nitrogen (K_N) extinction coefficients, were determined. Sunflower, kenaf and cynara had morphologically contrasting canopies in terms of leaf area and mass

distribution along the stem, with the largest fractions of the leaf mass and area in well-developed crops being allocated at the middle, top and bottom of the canopy, respectively. We paid particular attention to the effects of water stress and to temporal aspects in order to test the common assumption used in crop modelling that K_L does not change in relation to time or level of water application. Measurements on leaf mass implemented at different crop stages and at different insertion heights within crop canopies and light and nitrogen distributions were quantified by the Beer's law (exponential model). Results indicated that within a year, K_L did not change significantly over the studied period in all irrigated crops, but differences in K_L were significant between years for sunflower and kenaf (sunflower: 0.74 vs. 0.89; kenaf: 0.62 vs. 0.71), but not for cynara (0.77). K_L estimates were always lower (–48 to –65%) in water-stressed sunflower and kenaf crops than in crops with abundant water because of the reduction in leaf angle. These results should be taken into account, when simulating water-limited biomass production for these crops. Vertical SLN distributions were found in canopies when LAI was above 1.5 m² m⁻². These distributions were significantly correlated with the cumulative LAI from the top (r^2=0.75–0.81), providing parameters to upscale photosynthesis from leaf to canopy levels. Vertical SLN distributions followed species-specific patterns over the crop cycle and generally showed a strong association with light distributions (r^2 > 0.66; sunflower and kenaf).

Chapter 5 deals with leaf photosynthesis and respiration. Based on large data sets (*in situ* leaf gas exchange measurements during day and night over three years) and optimization techniques we parameterized the C_3 leaf photosynthesis model of Farquhar, von Caemmerer and Berry (FvCB) and an empirical night respiration model for sunflower, kenaf and cynara. We studied in detail the effects of temperature and leaf nitrogen because these factors had a great impact on estimates of maximum carboxylation rate and maximum electron transport rate. In total, we assessed 16 parameters per crop including four parameters characterising Rubisco limitation, six parameters characterising electron transport limitation, two parameters characterising the degree to which light inhibits leaf respiration, three parameters for night respiration, and the minimum leaf nitrogen required for photosynthesis. Model predictions were tested against independent data sets and results indicated that current models are robust, with good prediction ability (r^2>0.91) under different levels of intercellular CO_2 concentration, light, temperature and leaf nitrogen. Under ambient atmospheric CO_2 concentration, optimum temperature, saturated light and leaf nitrogen, all tested species showed maximum leaf net assimilation rate of ca 33 µmol CO_2 m⁻² s⁻¹. Among tested crops, the perennial cynara has long annual growth cycles (~ 10 months) and therefore we further investigated seasonal acclimation effects on photosynthesis and respiration for this crop. It was observed significant seasonal effects on electron transport rate (e.g. on parameters associated with the conversion efficiency of light into electron transport) and night

respiration (e.g. parameters related to activation energy). These effects were incorporated into the model, further improving predictions. In the light of current trends for parallel increases in food and energy production from crop species in the context of climate change and the need to feed crop models with photosynthetic parameters, we summarized existing information for five major cash crops (wheat, barley, cotton, tobacco and grape) and we assessed how conservative FvCB parameters were among crop species including bioenergy crops. Lastly, in this chapter we proposed an alternative method (alternative to the common analysis based on relationships between net photosynthesis and intercellular CO_2 concentration) to derive FvCB parameters from analysis of relationships between net photosynthesis and incoming radiation, which might generate opportunities to reduce empiricism in crop models by using readily available data on net photosynthesis and incoming radiation.

Chapter 6 deals with the agronomy of the tested energy crops in central Greece. In **Chapters 6.1 and 6.2** we report growth, seed and biomass productivity for cynara from two experimental sites. In both sites, cynara developed very high LAI values (up to 10 m^2 m^{-2}) and maintained LAI values above 3 for most of the growing period (~8 months). Irrigation and N-fertilization application during the period of maximum increase in biomass (cf. May–June or BBCH 5–6) had a positive effect on biomass and seed production. This effect was particularly evident at the dry site (e.g. 50% increase in seed yield). The nitrogen use efficiency for cynara (above-ground biomass) was ~ 120 kg dry matter kg^{-1} N taken up, similar among sites. In contrast, nitrogen uptake rates differed substantially among sites: from 60 to 180 (dry site) and from 170 to 300 (wet site) kg N ha^{-1}. Given that the weather conditions and the management practises were similar among sites, it can be inferred that the higher productivity of cynara at the wet site was mainly due to the higher amount of nitrogen taken up by the crop.

In **Chapter 6.3** we investigate biomass and seed yield of a new sunflower hybrid and assess the economic viability of sunflower in central Greece. The results indicated high seed yields (up to 4.7 t ha^{-1}) with little response to irrigation and N-fertilization during 2006, most likely due to soil type and favourable effective precipitations occurring at the site. However, these promising findings were not confirmed in later years (Chapter 7) due to weather extremes and different hybrids used. In central Greece, sunflower completes its cycle within 3 months providing many cultivation options to the farmers, e.g. early sowing to make use of spring rainfalls. Construction of sunflower farm budgets indicated that profits made by cultivating sunflower (2006) were lower compared to profits made by cultivating cotton in this area. Taking into account CAP reforms and the unstable environment regarding oil prices, material prices and selling prices, we concluded that sunflower cultivation in this area can be economically feasible and can therefore be a very good option for increasing the country's biodiesel production, in line with the EU targets.

Chapter 6.4 shows productivity data for two kenaf cultivars (Tainung 2 and Everglades 41) in relation to irrigation water. This study was conducted in year 2006 within the frame of the BioKenaf project, but instead of planting kenaf at row-to-row distance of 50 cm, kenaf was planted at 75 cm (similar to maize) in an effort to improve mechanization of the crop. We found a significant effect of irrigation on total dry biomass and plant height, although the absolute differences among treatments were relatively small (10–20%). Tainung 2 had slightly higher values in all measured growth parameters compared to Everglades 41. On average, the crop reached a final height of 3.9 m, a maximum LAI of 7.5 m^2 m^{-2}, while SLA was around 18.5 m^2 kg^{-1}. The crop reached maximum yields of 19.6, 22.8 and 24.5 t ha^{-1} under no-, moderate- and full irrigation, respectively (average values of two cultivars). These yields were comparable or superior to yields obtained in previous years in central Greece, indicating no effect of changing plant arrangement in biomass production.

Chapter 7 broadens the discussion of the proceeding chapters to the overall achievements of this thesis. We highlight the advances made in crop physiology and agronomy, the progress made towards modelling these species using simulation models, and lastly we critically assess the future of the tested crops in Greece taking into account many issues that are related to the suitability of the tested crops. We concluded that among the tested crops *Cynara cardunculus* is the best option for bioenergy production in the Mediterranean region and we suggested options to improve the crop's biomass quantity and quality.

Samenvatting

De productie van energie uit biomassa is wereldwijd een populair onderzoeksthema. Zorgen omtrent zekerheid van energie- en voedselvoorziening en klimaatsverandering dragen in belangrijke mate bij aan deze populariteit. In 2005 bestond wereldwijd 10% van de totale primaire energie uit bio-energie. Schattingen laten zien dat bio-energie hieraan in potentie 3 tot 10 maal meer zou kunnen bijdragen. Dat wil zeggen dat momenteel de bijdrage van planten sterk wordt onderbenut. Bos en houtresten zijn belangrijke bronnen van bio-energie (ongeveer 68%), maar deze bron kan niet veel meer groeien. Energiegewassen, de belangrijkste bron van biobrandstoffen voor transport, dragen momenteel slechts in geringe mate (ongeveer 3%) bij aan de totale bio-energie, maar dit aandeel zal de komende decennia gaan stijgen, in de EU naar verwachting tot 10% in 2020.

Om de productie van energie met behulp van landbouwgewassen te laten stijgen, kan het areaal of de productiviteit per hectare worden vergroot of kunnen de conversietechnologieën efficiënter worden gemaakt. Voor al deze drie mogelijkheden is een goede kennis omtrent de gewassen vereist. Het is echter gemeengoed, dat er, ondanks de snelle en wereldwijde groei van bio-energie, gebrek is aan goede experimentele data en praktische ervaring om deze groei te ondersteunen. Deze beperking doet zich vooral gelden op het gebied van de agronomie en de gewasfysiologie van nieuwe energiegewassen. Boeren, veredelaars en onderzoekers (en dan vooral de onderzoekers die met groeimodellen werken) hebben behoefte aan zulke informatie om in staat te worden gesteld de hoeveelheid en kwaliteit van de geproduceerde biomassa te verbeteren en toekomstig landbouwkundig landgebruik te evalueren. Uiteraard is het daarbij nodig datasets te genereren gebaseerd op verschillende regio's met diverse bodem- en klimaatcondities en met verschillende teeltsystemen.

Overeenkomstig deze algemene doelstelling verschaft dit proefschrift essentiële informatie over de fenologie, agronomie en gewasfysiologie van drie (Mediterrane) bio-energiegewassen, te weten zonnebloem (*Helianthus annuus*), kenaf (*Hibiscus cannabinus*) en kardoen (*Cynara cardunculus*). Uit een breed assortiment zijn juist deze gewassen gekozen, omdat de soorten een grote verscheidenheid aan bio-industriële toepassingen vertegenwoordigen, maar ook passen in diverse teeltstrategieën (korte of lange groeiduur, teelt met en zonder irrigatie, enz.) en omdat eerdere studies hadden aangetoond dat deze gewassen veelbelovend zijn betreffende hun biomassaproductiviteit. Voor deze gewassen hebben we de belangrijkste kennisleemten geïdentificeerd en hebben we een serie veldproeven uitgevoerd om deze kennisleemten op te vullen, maar ook om datasets te genereren

waarmee groeimodellen gevoed konden worden. In het inleidend hoofdstuk (**Hoofdstuk 1**) van het proefschrift worden deze leemten in de kennis gepresenteerd en wordt een actueel overzicht gegeven over de bestaande kennis omtrent bio-energieproductie. Vervolgens worden in de volgende vijf hoofdstukken (**Hoofdstukken 2–6**) de onderzoeksresultaten gepresenteerd van de experimentele fase van de studie. Ten slotte wordt in een afsluitend hoofdstuk (**Hoofdstuk 7**) bediscussieerd wat deze studie uiteindelijk heeft opgeleverd.

 Hoofdstuk 2 presenteert de fenologische groeistadia van *Cynara cardunculus* L. (var. *altilis* DC.) gebaseerd op de BBCH schaal en de daarmee verbonden decimale code. De schaal en de codes werden in principe zo ontworpen dat gedurende de ontwikkeling van de plant de numerieke code voor de verschillende stadia toeneemt van 0 tot 100. Er zijn negen primaire groeistadia en elk primair stadium wordt onderverdeeld in secundaire groeistadia. Beschrijvende sleutels met illustraties en een toelichting voor het praktische gebruik van de schaal werden voorgesteld. De schaal is nuttig voor iedereen die betrokken is bij de teelt van kardoen en kan worden toegepast onder alle omstandigheden, ongeacht de snelheid van ontwikkeling, die immers kan variëren naar gelang de teeltomstandigheden of het ras. Bovendien beschrijft deze code de precieze aanvang en eindpunt van elk ontwikkelingsstadium, momenten die essentieel zijn in studies omtrent het effect van temperatuur op ontwikkelingssnelheid. De belangrijkste BBCH stadia, die vooral aandacht behoeven van de onderzoeker en de teler, zijn: (a) stadia 00–15: juiste tijdstip van zaai gebaseerd op het klimaat van elk productiegebied en mechanische onkruidbestrijding gedurende het eerste teeltjaar; (b) primaire stadia 4–6: het gewas kan worden geoogst als ruwvoer; en (c) primaire stadia 5–7: maximale behoefte van het gewas aan voedingsstoffen.

 Hoofdstuk 3 verschaft uitgebreide informatie over de productiviteit van *Cynara cardunculus* in termen van zaad en biomassa, verzameld in 16 veldproeven met verschillende gewasleeftijd en combinaties van omgeving en teelttechniek in Griekenland. We presenteren een robuuste en eenvoudig toepasbare methode om de zaadopbrengst te schatten. Met deze methode kunnen problemen overwonnen worden die voortkomen uit de samengestelde structuur van de bloeiwijzen van kardoen. Inderdaad zijn binnen een plant en binnen een oppervlakte-eenheid de hoofden van kardoen variabel in termen van grootte, aantal, rijpheid en positie aan de plant. In een bloemhoofd zijn de dopvruchten (de achenen) ingeplant in de bloembodem en omgeven door haren (pappus) en schutbladen (in de vorm van erecte doornen). Door twee eenvoudige eigenschappen van de bloeiwijze te meten voor alle zaaddragende hoofden per oppervlakte-eenheid, te weten het totale gewicht (HW) en het aantal hoofden (HN) kon de zaadopbrengst per oppervlakte-eenheid (SY) adequaat worden voorspeld via de formule SY = 0.43 HW – 2.9·HN. Dit model werd getest met behulp van eigen data en gepubliceerde gegevens uit Italië. Het model bleek valide te zijn onder diverse teeltomstandigheden (bijv.

verschillende plantverbanden) en omgevingscondities (r^2=0.93). Haalbare opbrengsten van kardoenzaad varieerden van 1.9 tot 4.8 t ha^{-1} j^{-1}, op respectievelijk droge gronden en op gronden met een ondiep grondwaterniveau. De corresponderende biomassa-opbrengsten varieerden van 13 tot 27 t ha^{-1} j^{-1}. Gedurende de eerste gewascyclus lagen de zaad- en biomassa-opbrengsten 57–80% lager dan in de daaropvolgende cycli. De variatie in zaadopbrengst werd in voldoende mate verklaard op basis van analyses van de gewichtsverdeling van de hoofden (kleine, middelgrote en grote hoofden), en de variabiliteit in de gewichtsverhouding zaad:hoofd per hoofd. Eigenschappen betreffende de zaadkwaliteit, zoals oliegehalte (23%) en eiwitgehalte (19%), waren tamelijk constant, zowel voor verschillende zaadgroottes (spreiding: 26–56 mg zaad^{-1}) als voor groeicondities. Dit betekent dat onder Griekse omstandigheden deze vaste waarden kunnen worden gebruikt om de olie- en eiwitopbrengst van het zaad te schatten.

Hoofdstuk 4 verschaft informatie over het bladerdek en laat zien hoe de bebladeringsindex (LAI), de specifieke bladoppervlakte (SLA), de stikstofconcentratie (N_{conc}) en de specifieke stikstofhoeveelheid in het blad (SLN) veranderen in ruimte en tijd onder invloed van beschikbaarheid van water voor alle drie de onderzochte soorten. Twee voor gewasmodellering zeer belangrijke parameters werden bepaald, te weten de extinctiecoëfficiënten van licht (K_L) en stikstof (K_N). Zonnebloem, kenaf en kardoen hebben morfologisch contrasterende bladerdekken in termen van de verdeling van bladoppervlakte en bladmassa langs de stengel. In goed ontwikkelde gewassen bleken de grootste fracties van bladmassa en bladoppervlakte zich in het midden (bij zonnebloem), aan de top (bij kenaf) of in de onderste helft (bij kardoen) van het gewas te bevinden. Speciale aandacht werd besteed aan de effecten van droogte en tijd om de in gewasmodellering algemeen gangbare aanname te toetsen dat K_L niet verandert onder invloed van het niveau van watervoorziening of de tijd. Data omtrent bladmassa werden verzameld in verschillende gewasstadia en op verschillende planthoogten binnen het gewas; ook de licht- en stikstofverdeling werden gekwantificeerd met de Wet van Beer (exponentieel model). Resultaten toonden aan dat voor geïrrigeerde gewassen, gedurende de onderzochte periode, de K_L binnen één jaar niet significant veranderde. De verschillen in K_L tussen jaren waren echter significant voor zonnebloem en kenaf (zonnebloem 0.74 vs. 0.89; kenaf: 0.62 vs. 0.71), maar niet voor kardoen (kardoen: 0.77). Geteeld onder droogte-stress waren de schattingen voor K_L in zonnebloem en kenaf altijd lager (–48 tot –65%) dan in de gewassen geteeld met overvloedig water, omdat onder droogte de bladhoek afnam. Deze resultaten dienen in acht te worden genomen bij het simuleren van water-gelimiteerde biomassaproductie van deze gewassen. Verticale SLN gradiënten werden waargenomen in bladerdekken bij LAI-waarden hoger dan 1.5 m^2 m^{-2}. Deze gradiënten waren significant gecorreleerd aan de cumulatieve LAI (gerekend van boven naar beneden) (r^2=0.75–0.81). Deze verbanden leveren parameters op waarmee de fotosynthese van blad naar

gewasniveau kan worden opgeschaald. De verticale SLN gradiënten waren gewasspecifiek en vertoonden in het algemeen een sterk verband met de lichtgradiënten ($r^2 > 0.66$; zonnebloem en kenaf).

Hoofdstuk 5 behandelt de bladfotosynthese en ademhaling. Op basis van grote datasets (*in situ* gasuitwisseling van het blad gedurende de dag en de nacht over 3 jaren) en optimalisatietechnieken, werden het model van Farquhar, von Caemmerer en Berry (FvCB) voor C_3-bladfotosynthese en een empirisch model voor de nachtelijke ademhaling voor de gewassen zonnebloem, kenaf en kardoen geparametriseerd. De effecten van temperatuur en bladstikstof werden in detail bestudeerd omdat deze factoren een grote invloed hadden op de schattingen van de maximale snelheden van carboxylatie en elektronentransport. In totaal werden per gewas 16 parameters bepaald, waaronder vier parameters die de Rubiscolimitering karakteriseren, zes parameters die de elektronentransportlimitering karakteriseren, twee parameters die de mate karakteriseren waarin licht de bladademhaling beperkt, drie parameters voor de nachtelijke ademhaling, en de minimale hoeveelheid bladstikstof benodigd voor fotosynthese. De modelvoorspellingen werden getest tegen onafhankelijke datasets en de resultaten gaven aan dat de huidige modellen robuust waren, met een goed voorspellend vermogen ($r^2 > 0.91$) onder verschillende niveaus van intercellulaire CO_2-concentratie, licht, temperatuur en bladstikstof. Onder normale omgevingsconcentratie van CO_2, optimale temperatuur, en bij het verzadigingsniveau van licht en bladstikstof vertoonden alle geteste soorten een maximale netto fotosynthese van het blad van circa 33 µmol CO_2 m^{-2} s^{-1}. Van de geteste soorten had het meerjarige gewas kardoen een lange jaarlijkse groeicyclus (~ 10 maanden) en daarom werden de effecten van acclimatie gedurende het seizoen op de fotosynthese en de ademhaling van dit gewas nader onderzocht. Er bleken significante seizoenseffecten te bestaan voor elektronentransportsnelheid (bijv. op parameters die betrekking hebben op de conversie-efficiëntie van licht naar elektronentransport) en nachtelijke ademhaling (bijv. op parameters met betrekking tot de activeringsenergie). Deze effecten werden in het model ingebouwd om zodoende de kwaliteit van de voorspellingen te verbeteren. Met het oog op de huidige trend om tegelijkertijd, in de context van klimaatsverandering, de voedsel- en energieproductie van gewassen te verhogen en gezien de noodzaak om gewasmodellen te voeden met fotosynthese-gelieerde parameters werd de bestaande informatie voor vijf belangrijke marktgewassen (te weten tarwe, gerst, katoen, tabak en druif) samengevat. Met behulp van deze informatie werd vastgesteld hoe stabiel de FvCB parameters zijn voor verschillende soorten gewassen, inclusief gewassen geteeld voor bio-energie. Ten slotte werd in dit hoofdstuk een aanvullende methode voorgesteld om, naast de normale analyse (gebaseerd op het verband tussen netto-fotosynthese en intercellulaire CO_2 concentratie), de FvCB parameters af te leiden van een analyse van het verband tussen netto-fotosynthese en inkomende straling. Deze alternatieve methode kan aanleiding zijn om de mate van empirie in

gewasgroeimodellen te verkleinen via het benutten van eenvoudig beschikbare data betreffende de netto-fotosynthese en de inkomende straling.

Hoofdstuk 6 gaat over de agronomie van de geteste energiegewassen in centraal Griekenland. In de **hoofdstukken 6.1** en **6.2** wordt gerapporteerd over de groei, zaadproductie en biomassaproductie van kardoen op twee proeflocaties. Op beide locaties ontwikkelde kardoen zeer hoge LAI-waarden (tot 10 m^2 m^{-2}) en werden voor het overgrote deel van het groeiseizoen (~8 maanden) LAI-waarden hoger dan 3 m^2 m^{-2} gehandhaafd. Irrigatie en N-bemesting gedurende de periode van maximale toename van de biomassa (mei–juni of BBCH 5–6) hadden een positief effect op biomassa- en zaadproductie. Dit effect was vooral zichtbaar op de droge locatie (bijv. 50% toename in zaadopbrengst). De stikstofgebruiksefficiëntie voor kardoen (op basis van bovengrondse biomassa) was ~ 120 kg droge stof per kg opgenomen N, zonder grote verschillen tussen de locaties. Daarentegen verschilden de opgenomen hoeveelheden stikstof tussen de locaties aanzienlijk: van 60 tot 180 (droge locatie) en van 170 tot 300 (natte locatie) kg N ha^{-1}. Aangezien de weersomstandigheden en de teelttechniek vergelijkbaar waren voor de locaties moet de hogere productiviteit van kardoen op de natte locatie vooral te danken zijn geweest aan de grotere hoeveelheid door het gewas opgenomen stikstof.

In **Hoofdstuk 6.3** werden de biomassa- en zaadproductie van een nieuwe zonnebloemhybride onderzocht en werd nagegaan in hoeverre de zonnebloemteelt economisch haalbaar is in centraal Griekenland. Er werden hoge zaadopbrengsten bereikt (tot 4.7 t ha^{-1}) met in 2006 weinig respons op irrigatie en stikstofbemesting, zeer waarschijnlijk vanwege het bodemtype en de gunstige neerslag op de betreffende locatie in dat jaar. In latere jaren konden deze veelbelovende resultaten echter niet worden bevestigd (Hoofdstuk 7), vanwege weersextremen en het gebruik van andere hybriden. In centraal Griekenland voltooit de zonnebloem zijn groeicyclus binnen 3 maanden. Deze korte groeiduur biedt de boeren veel ruimte om de teelttechniek aan te passen, bijvoorbeeld door te kiezen voor een vroege zaai om op die manier te profiteren van de voorjaarsregens.

Saldoberekeningen gaven aan dat in dit gebied het telen van zonnebloem in 2006 minder opleverde dan de teelt van katoen. Gezien de CAP-hervormingen en het onstabiele klimaat betreffende de prijzen van olie, hulpmiddelen en landbouwproducten werd geconcludeerd dat de teelt van zonnebloem economisch haalbaar kan zijn en dat deze teelt dus een goede optie is om daarmee de biodieselproductie van Griekenland te verhogen, binnen de doelstellingen van het EU beleid.

Hoofdstuk 6.4 geeft productiviteitcijfers voor twee kenafrassen (Tainung 2 en Everglades 41) in relatie tot beregening. Deze studie werd in 2006 uitgevoerd in het kader van het BioKenaf project. In een poging de mechanisatie van het gewas te verbeteren, werd kenaf, in plaats van in een rijafstand van 50 cm, geplant in een rijafstand van 75 cm (net als bij maïs). We vonden een significant effect van

beregening op de totale droge biomassa en op planthoogte, hoewel de absolute verschillen tussen behandelingen relatief klein (10–20%) waren. Tainung 2 had iets hogere waarden voor alle gemeten groeiparameters dan Everglades 41. Gemiddeld bereikte het gewas een uiteindelijke hoogte van 3.9 m, een maximale LAI van 7.5 m^2 m^{-2}, terwijl de SLA ongeveer 18.5 m^2 kg^{-1} was. Het gewas bereikte maximale opbrengsten van 19.6, 22.8 and 24.5 t ha^{-1} voor, respectievelijk, geen, matige en volle beregening (gemiddelde waarden voor de twee rassen). Deze opbrengsten waren vergelijkbaar met of zelfs hoger dan de opbrengsten zoals die in voorafgaande jaren in Griekenland werden gehaald. Dit resultaat suggereert dat de aanpassing in plantverband geen effect had op biomassaproductie.

Hoofdstuk 7 tilt de discussie uit de voorafgaande hoofdstukken naar de algehele verworvenheden van dit proefschrift. Het hoofdstuk benadrukt de vooruitgang die is geboekt aangaande de gewasfysiologie en agronomie van de behandelde gewassen en de vooruitgang in het modelleren van de groei van deze gewassen. Daarnaast wordt in dit hoofdstuk de toekomst van deze gewassen in Griekenland kritisch geëvalueerd, daarbij rekening houdend met de vele aspecten die de geschiktheid van deze gewassen bepalen. Er wordt geconcludeerd dat, van de geteste gewassen, kardoen de beste optie is voor bio-energieproductie in het Mediterrane gebied. Ten slotte worden mogelijkheden gesuggereerd om de hoeveelheid en kwaliteit van de door dit gewas geproduceerde biomassa te verbeteren.

Curriculum vitae

Sotiris Archontoulis was born on 29 June 1980 in Karditsa, Greece. He completed his basic education in 1998 and few moths later he entered as a student at the University of Thessaly, department of Agriculture, Greece. In 2004, he obtained a 5-yr BSc diploma in Agronomy. Then he moved to the Netherlands and in 2006, he obtained his MSc degree in Crop Science (Wageningen University). Few months later, he enrolled to the PhD program of the Wageningen University. The main subjects in his PhD research were studies in phenology, agronomy, crop physiology and modelling of three bioenergy crops. In general, his research interest is to understand growth dynamics of bioenergy crops and to explore their production potential through simulation crop models. So far he has worked with the following crops: miscanthus, cynara, sunflower, kenaf, rapeseed sorghum fibre, sorghum sweet, sorghum sudan, maize, wheat, cotton, and he investigated opportunities for energy production from different plant fractions and assessed genotype × environment × management interactions on biomass production. He has participated as a research assistant or researcher in four R&D Projects, and he has written five publications in double refereed international journal (one more submitted), forty one papers in proceedings of International Conferences and one booklet on energy crops (guide on how to cultivate energy crops: cynara, sunflower and sorghum).

Publication list

Papers published or to be published in refereed journals

Archontoulis SV, Yin X, Vos J, Danalatos NG, Struik PC. 2011. Leaf photosynthesis and respiration of three bioenergy crops in relation to temperature and leaf nitrogen: How conservative are biochemical model parameters among crop species? Submitted for publication. (this thesis)

Archontoulis SV, Vos J, Yin X, Bastiaans L, Danalatos NG, Struik PC. 2011. Temporal dynamics of light and nitrogen vertical distributions in canopies of sunflower, kenaf and cynara. *Field Crops Research* 122: 186–198. (this thesis)

Archontoulis SV, Struik PC, Yin X, Bastiaans L, Vos J, Danalatos NG. 2010. Inflorescence characteristics, seed composition, and allometric relationships predicting seed yields in the biomass crop *Cynara cardunculus*. *Global Change Biology–Bioenergy* 2: 113–129. (this thesis)

Archontoulis SV, Struik PC, Vos J, Danalatos NG. 2010. Phenological growth stages of *Cynara cardunculus*: codification and description according to the BBCH scale. *Annals of Applied Biology* 156: 253–270. (this thesis)

Danalatos NG, **Archontoulis** SV. 2010. Growth and biomass productivity of kenaf (*Hibiscus cannabinus*) under different agricultural inputs and management practices in Greece. *Industrial Crops and Products* 32: 231–240.

Danalatos NG, **Archontoulis** SV, Mitsios I. 2007. Potential growth and biomass productivity of Miscanthus × giganteus as affected by plant density and N-fertilization in central Greece. *Biomass and Bioenergy* 31: 145–152.

Selected papers published in Proceedings of International Conferences

Archontoulis SV, Struik PC, Yin X, Danalatos NG. 2011. A comparative analysis of biomass production from seven energy crop species grown in a Mediterranean environment. In: *Proceedings of the 19th European Biomass Conference*, Berlin, Germany (*in press*).

Tsitsibikou N, Dichala O, **Archontoulis** SV, Bartzialis D, Tzortzios S, Danalatos NG, Struik PC. 2011. Sorghum and maize biomass, protein, and bioethanol yields in a semi-arid environment of central Greece. In: *Proceedings of the 19th European Biomass Conference*, Berlin, Germany (*in press*).

Archontoulis SV, Struik PC, Vos J, Danalatos NG. 2010. Maize and sorghum biomass and protein accumulation under adequate and limited supply of water and nitrogen in Greece. In: *Proccedings of the XIth European Conference of Agronomy*, Monepellier, France, p. 569–570.

Archontoulis SV, Danalatos NG, Struik PC, Batzogiannis D, Savas V. 2010. The effect of nitrogen fertilization and supplemental irrigation on seed and biomass productivity of *Cynara cardunculus* growing in a semi-arid environment in central Greece. In: *Proceedings of the 18th European Biomass Conference*, Lyon, France p. 273–279. (this thesis)

Danalatos NG, **Archontoulis** SV, Tsibukas K. 2009. Comparative analysis of sorghum vs. corn growing under optimum and water/nitrogen limited conditions in

central Greece. In: *Proceedings of the 17th European Biomass Conference*, Hamburg, Germany, p. 538–544.

Danalatos NG, **Archontoulis** SV. 2009. Oilseed rape growth, biomass accumulation and seed yield as affected by variety and N-fertilization in a dry year in Greece. In: *Proceedings of the 17th European Biomass Conference*, Hamburg, Germany, p. 507–511.

Archontoulis SV, Danalatos NG, Yin Y, Struik PC. 2008. Leaf photosynthesis and respiration of *Cynara cardunculus*. In: *Proceedings of the 16th European Biomass Conference*, Valencia, Spain, p. 636–639.

Giannoulis KD, **Archontoulis** SV, Bastiaans L, Struik PC, Danalatos NG. 2008. Potential growth and seed yield of sunflower as affected by sowing time, irrigation and N-fertilization in central Greece. In: *Proceedings of the International Conference on Agricultural Engineering*, Crete, Greece, pp.10 in CD.

Danalatos NG, Gintsioudis II, **Archontoulis** SV. 2008. Evaluation and application of the biokenaf model for kenaf production in south Europe. In: *Proceedings of the International Conference on Agricultural Engineering*, Crete, Greece, p. 8 in CD.

Archontoulis SV, Danalatos NG, Struik PC. 2007. Irrigation effects on the growth and biomass productivity of two kenaf genotypes on aquic soils of central Greece. In: *Proceedings of the 15th European Biomass Conference*, Berlin, Germany, p. 409–412 (this thesis)

Danalatos NG, **Archontoulis** SV, Giannoulis K, Rozakis S. 2006. Miscanthus and cardoon as alternative crops for solid fuel production in central Greece. In: *Proceedings of the International Conference on Information Systems, Sustainable Agriculture, Agro-environment and Food Technology*, Volos, Greece, p. 387–397.

Danalatos NG, Gintsioudis II, **Archontoulis** SV. 2006. Biokenaf: A crop growth simulation model for kenaf under Greek conditions. In: *Proceedings of the International Conference on Information Systems, Sustainable Agriculture, Agro-environment and Food Technology*, Volos, Greece, p. 373−381.

Archontoulis SV, Struik PC, Danalatos NG. 2006. Diurnal leaf gas exchange rates of two kenaf genotypes at two leaf positions. In: *Proceedings of the International Conference on Information Systems, Sustainable Agriculture, Agro-environment and Food Technology*, Volos, Greece, p. 423−431.

Geronikolou L, **Archontoulis** SV, Danalatos NG, Papadakis G, Kyritsis S. 2005. Economic opportunity for seed oil production in S. Europe by new sunflower varieties and under new C.A.P. Conditions. In: *Proceedings of the 14th European Biomass Conference*, Paris, France, p. 1917−1920

Danalatos NG, **Archontoulis** SV, Geronikolou L, Papadakis G. 2005. Irrigation and N-fertilization effects on growth and productivity of three sunflower hybrids in an aquic soil in central Greece. In: *Proceedings of the International Conference on Industrial Crops and Rural Development*, Murcia, Spain, p 129−138.

Danalatos NG, **Archontoulis** SV. 2004. Potential growth and biomass productivity of kenaf under central Greek conditions: II. the influence of variety, sowing time and plant density. In: *Proceedings of the 2nd World Biomass Conference*, Roma, Italy, p. 319−322.

PE & RC PhD Education Certificate

With the educational activities listed below the PhD candidate has complied with the educational requirements set by the C.T. de Wit Graduate School for Production Ecology and Resource Conservation (PE&RC) which comprises of a minimum total of 32 ECTS (= 22 weeks of activities)

Review of literature (4.2 ECTS)
- Bio-energy sources and options to increase bio-energy production from plant species (2011)

Writing of project proposal (7 ECTS)
- Growth dynamics of Mediterranean bioenergy crops (2006)

Post-graduate courses (3.7 ECTS)
- Basic and advance statistics; PE&RC, Wageningen (2007)
- Soil ecology; PE&RC, Wageningen (2007)
- Working with dynamic crop models; ESA conference, Montpellier, France (2010)

Laboratory training and working visits (2.8 ECTS)
- Working visit at Bio-pellet and Murek association; Austria (2007)
- Working visit at 2nd World Bio-Energy Exhibition; Fieracricola, Verona, Italy (2008)
- Working visit at SIMA exhibition: new developments in bioenergy; Paris, France (2009)

Deficiency, refresh, brush-up courses (1.1 ECTS)
- Designing sustainable cropping systems; CSA (2010)

Competence strengthening / skills courses (3.1 ECTS)
- PhD Competence assessment; PE&RC (2007)
- Training: regulation for managing large scale "demonstration" bioenergy cultivations in Greece; University of Thessaly (UTH), Greece (2007/2008)
- Training: regulation for developing agricultural movies related to the cultivation of energy crops; National Agricultural Research Foundation (N.AG.RE.F, AG.E.P.R.I.), Greece, 2008

PE & RC Annual meetings, seminars and the PE&RC weekend (1.65 ECTS)
- How to write a world-class paper; Library WUR, Wageningen (2010)
- PE&RC Weekend (2010)
- PE&RC Day; WUR, Wageningen (2010, 2011)

Discussion groups / local seminars / other scientific meetings (5.4 ECTS)
- Sustainable Energy Crops for Thessaly Plain; CERETETH Research Institute; Karditsa, Greece (2007)
- Energy Crops; GREENBOX and Agrenda agricultural newspaper; Larissa, Greece (2007)
- Renewable Energy Sources; Technical Chamber of Greece, Larissa, Greece (2007)
- Crops for energy production; Lab of Agronomy and Applied Crop Physiology, UTH, Greece (2008–2009)
- Frontier literature in plant physiology (FLOP) (2010–2011)

International symposia, workshops and conferences (14.6 ECTS)
- 15th European Biomass Conference; Berlin, Germany (2007)
- 16th European Biomass Conference; Valencia, Spain (2008)
- International Conference on Agricultural Engineering; Crete, Greece (2008)
- 17th European Biomass Conference; Hamburg, Germany (2009)
- 11th European Conference for Agronomy; Montpellier, France (2010)
- 18th European Biomass Conference; Lyon, France (2010)
- 19th European Biomass Conference; Berlin, Germany (2011)

Courses in which the PhD candidate has worked as a teacher; 5 days
- Research methods in crop science; CSA, WUR (2011)

Supervision of 4 MSc students; 32 days
- Sunflower growth and seed yield
- Sorghum and maize protein yields
- Cynara leaf area vertical profiles
- Cynara seed/head ratio

Funding